In vitro Evaluation of Cytotoxicity caused by Carbamazepine and its Metabolites in Association to Carbamazepine-induced Hypersensitivity Reactions

Thesis submitted in accordance with the requirements of the

University of Liverpool

for the degree of Doctor in Philosophy

by

Philippe Theodor Marlot

19.12.2014

Declaration

I hereby declare that this thesis is the result of my own work and has not been published for any other degree.

……..

Philippe Theodor Marlot

Acknowledgements

I would like to thank Prof Munir Pirmohamed for the opportunity to be part of his research group during the time of my PhD. I also want to thank him and Dr Ana Alfirevic for being my supervisors. I appreciate the guidance received as well as the time invested by them. Besides my many flaws, they never lost their patience with me. I would also like to thank Angela Foxcroft for managing the administrative part of the project so that my focus could be on my work. I want to thank Dr Amy Mercer, Dr Xiaoli Meng and Dr James Maggs for helping me with parts of my work by showing me certain techniques.

I would like to extend my deepest gratitude to Prof Ivan Rusyn for allowing me to carry out experiments as part of my placement in his research group at the University of North Carolina at Chapel Hill. In this context, I also have to thank Nour Abdo as my partner in crime during that time. I also thank all the friends I made during the time which made my experience in the USA unforgettable.

I thank Dr Steffen Rädisch for his company and friendship during the whole time of our PhD in Liverpool. Without him this time would have only been merely half as enjoyable.

A big thank you to all my colleagues and fellow students of the Wolfson Centre. There are far too many to list them all here but you know who you are guys. A very special thank you is needed for all the nurses, who took the endless number of blood samples I needed. I also thank the many volunteers that had to suffer through it. I am very grateful to Dr Eunice Zhang for the help and advice she gave me. Also thank you Gurpreet and Karen for keeping me company in the final stages of my PhD.

Last but in no way least is the gratitude I give to my family, especially my mother. She supported me throughout my whole academic studies and encouraged me in the seemingly unbearable moments, I faced during that time.

Table of Contents

Abbreviations

9-AC	9-Acridinecarboxaldehyde
ABC	Abacavir
ACN	Acetonitrile
ADR	Adverse drug reaction
AGEP	Acute generalised exanthematous pustulosis
ANCOVA	Analysis of covariance
ANOVA	Analysis of variance
ATP	Adenosine triphosphate
BSA	Bovine serum albumin
Caspase	Cysteine aspartase
CBZ	Carbamazepine
CBZE	Carbamazepine-10,11 epoxide
CO_2	Carbone dioxide
CytB	Cytochalasin B
CYP	Cytochrome P450 enzyme
DHR	Drug-induced hypersensitivity reaction
DMSO	Diemethyl sulfoxide
DNA	Deoxyribonucleic acid
dNTP	Deoxynucleoside triphosphate
DP	Desolvation potential
DRESS	Drug reaction with eosinophilia and systemic symptoms

DUOX1	Dual oxidase 1
EC10	Effective concentration 10
EP	Entrance potential
FA	Formic acid
FACS	Fluorescent activated cell sorting
FCS	Fetal calve serum
FDA	Food and Drug Administration
FITC	Fluorescein isothiocyanate
GSH	Glutathione
GSTPi	Glutathione s-transferase π
GWAS	Genome-wide association study
HBSS	Hanks Balanced Salt Solution
HEPES	Hydroxyethyl piperazineethanesulfonic acid
HLA	Human leukocyte antigen
HPLC	High performance liquid chromatography
HSA	Human serum albumin
LC-MS/MS	Liquid chromatography tandem mass spectrometry
MAF	Minor allele frequency
MAGWAS	Multivariate ANCOVA genome-wide association software
MeOH	Methanol
MHC	Major histocompatibility complex
MMP	Mitochondrial membrane permeabilisation
MPE	Maculopapular exanthema

MTT	3-(4,5-Dimethylthiazol-2-yl)-2,5-diphenyltetrazolium
NADPH	Nicotinamide adenine dinucleotide phosphate
NAL	N-acetyl-lysine
NHS	National Health Service
PBMC	Peripheral blood mononuclear cell
PBS	Phosphate buffered saline
PCR	Polymerase chain reaction
PI	Propidium iodide
PS	Phosphatidylserine
qHTS	quantitative high-throughput screening
RNA-seq.	Ribonucleic acid sequencing
RPM	Revolutions per minute
RPMI	Roswell Park Memorial Institute
SJS	Steven Johnson syndrome
SNP	Single nucleotide polymorphism
STS	Staurosporin
TFA	Trifluoroacetic acid
TCR	T cell receptor
TEN	Toxic epidermal necrolysis
TMRE	Tetramethylrhodamine, ethyl ester, perchlorate
WHO	World Health Organisation
Z-VAD-FMK	Carbodenzoxy-valyl-alanyl-(O-methyl)-fluoromethylketone

Publications

Oral presentation

N. Abdo, **P. T. Marlot**, M. Pirmohamed, D. Shea, F. Wright, I. Rusyn: *In Vitro* Screening For Inter-Individual and Population Variability in Toxicity of Pesticide Mixtures. Superfund Research Program Annual Meeting, 2013

P. T. Marlot, N. Abdo, I. Rusyn, A. Alfirevic, M. Pirmohamed: Genome-wide analysis of the inter-individual variability in *in vitro* cell viability on exposure to carbamazepine and its metabolites. Pharmacology, British Pharmacological Society, 2013.

N. Abdo, **P. T. Marlot**, M. Pirmohamed, D. Shea, F. Wright, I. Rusyn: Utilizing Human Population Based *In Vitro* Model to Investigate Pesticide and Drug/Metabolite Pairs. Society of Toxicology annual meeting, 2014.

Poster presentation

P. T. Marlot, A. Alfirevic, M. Pirmohamed: Evaluation of cytotoxicity caused by 9-acridinecarboxaldehyde. CESAR annual meeting 2013.

Abstract

Carbamazepine (CBZ), an anticonvulsant and mood-stabilising drug, is known to cause delayed type hypersensitivity reactions. These reactions occur only in a minority of patients treated with the drug, but often result in severe clinical outcomes. Although an association between CBZ-induced hypersensitivity reactions and HLA alleles has been demonstrated, the underlying mechanism(s) of toxicity are poorly understood.

Cell death caused by CBZ and one of its metabolites, 9-acridinecarboxaldehyde (9-AC) was investigated. CBZ did not show cytotoxic effects in concentrations ranging from sub-therapeutic to supra-therapeutic. By contrast, 9-AC caused apoptosis in the lymphoblastoid cell line (50µM and 24 hours of exposure) and primary PBMCs (50 µM and 2 hours of exposure). PBMCs from 20 CBZ-naïve individuals showed significant inter-individual variability in the susceptibility to the cytotoxic effect of 9-AC.

To further investigate the observed inter-individual variability, 331 immortalised lymphoblast cell lines of unrelated individuals from 4 populations were exposed to CBZ, CBZ-10,11 epoxide or 9-AC and cell viability was measured after 24 hour exposure. Considerable inter-individual variability in the cytotoxic response was observed for all three compounds. The genome wide association study (GWAS) revealed two genetic polymorphisms in dual oxidase 1 (DUOX1) and RP11-354|13.2 that were linked to cell toxicity at low concentrations of all three compounds.

A SNP in DUOX1 was investigated further because of its biological plausibility. Genotyping of 153 patients did not show an association between this SNP and CBZ-induced hypersensitivity in Caucasians. Due to the higher than normal frequency of the DUOX1 variant in non-Caucasian patients (20%), the involvement of DUOX1 in the predisposition to CBZ-induced hypersensitivity reactions in non-Caucasians could not be excluded.

To elucidate how T cell activation occurs in CBZ-induced hypersensitivity reactions, the protein binding capability of CBZ and two of its metabolites, CBZ-10,11 epoxide (CBZE) and 9-AC, to human serum albumin and glutathione S-transferase π was assessed. Only CBZE was found to bind covalently to these proteins. For 9-AC, no covalent products were observed but an indication of reversible binding was detected.

Finally, newly developed genotyping methods for HLA-A*31:01 were investigated in comparison to sequence based typing. The methods were based on SSP-PCR. One of the methods showed exact accordance with the current gold standard but PCR failed to amplify the gene of interest and the control gene in considerable amount of samples (13.1%), while the second SSP-PCR typing method showed less reliability.

In conclusion, the mechanisms of CBZ hypersensitivity has been investigated using a number of approaches designed to elucidate bioactivation of the drug, and how cytotoxicity links with genetic factors. The genomic approach may have the potential to identify novel biomarkers, but needs further studies with larger sample size.

Chapter 1
General Introduction

1.1 Adverse Drug Reactions

Despite recent advances in science, adverse drug reactions (ADRs) still present a major clinical problem for modern medicine. ADRs can range from a mild skin rash to a severe life threatening systemic reaction, which affects multiple organs. ADRs can result in prolonged hospitalisation, which increases costs, and are a great concern to national health services [1]. A meta-analysis of data from the USA before 1990 extrapolated the number of deaths caused by ADRs to more than 100 000, making ADRs the fifth most common cause of death in hospitals [2]. Although this study was criticised for the heterogeneity of the data included and the methodology used [3], it still underlines the importance of understanding and preventing ADRs. A review from 2008 of over 25 studies conducted in the United Kingdom, revealed that out of 106 586 hospital admissions, 2 143 were related to ADRs, representing 5.3% of all hospital admissions.[4]. The cost of admissions to hospital due to ADRs was estimated to reach approximately £466m per year in the UK alone [1]. ADRs are also of great concern for pharmaceutical industry since they are the most common reason for withdrawal of marketed drugs [5]. Although ADRs are widespread, the underlying mechanisms are poorly understood and there are only a few genetic biomarkers available to predict a patient's risk for developing ADRs.

1.1.1 Definition of adverse drug reactions

The World Health Organisation defines ADRs as 'any response to a drug which is noxious, unintended, and occurs at doses normally used for prophylaxis, diagnosis, or therapy…' [6]. This definition excludes effects resulting from overdose and misuse and multiple attempts have been made to bring forth a more precise definition for ADRs. In this thesis, the definition by Edwards and Aronson will be used, which states that an ADR is 'an apparently harmful or unpleasant reaction, resulting from an intervention related to the use of medicinal product, which predicts hazard from future

administration and warrants prevention or specific treatment, or alteration or the dosage regimen, or withdrawal of the product.' [7]

1.1.2 Classification of adverse drug reactions

ADRs can be divided into different types: type A, B, C, D, E, and F. The precise determination of an ADR allows for appropriate management and prevention of further harm to the patient. Misdiagnosing ADRs can lead to fatal consequences for the patient. Several classification systems have been developed. Two of these will be discussed in this introduction.

1.1.2.1 Classification of ADRs by Rawlins and Thompson

The classification of ADRs by Rawlins and Thompson is the predominant model utilised in clinics and throughout literature [8]. The classification has been modified over the years as the understanding of molecular mechanisms of ADRs has improved. In this classification system, the ADRs are divided into the following groups according to their dose dependence.

Type A

Type A (augmented or 'ON TARGET' ADRs) is the most common form accounting for over 80% of all ADRs [9]. Their outcome is related to the known pharmacology of the drug and the toxic effects occur as a result of an overreaction of the body to the drug, which can be avoided by adjustment of the dose.

Type B

Type B, also named "bizarre", or 'OFF TARGET' ADRs, are less common (20%) [9]. They are also called idiosyncratic drug reactions as the reaction is not connected to the known pharmacological characteristics of the drug.

These ADRs are often more serious and account for many drug-induced deaths. A typical clinical feature is the lack of a clear dose-dependent relationship; the reactions can be observed at any dose within the therapeutic window. Type B ADRs generally do not have a high incidence rate and the risk factors for developing type B reactions are mostly unknown.

Other Types

Type A and B reactions were established to divide ADRs into dose-related and non-dose-related reactions. Over the years, this system left some ADRs, such as osteoporosis due to corticosteroid treatment, unclassified as they could not be placed into one of these two categories. Therefore, further categories were introduced to the ones proposed by Rawlins and Thompson, and should be briefly mentioned here for completeness of the current terminology [7, 10].

- Type C, or chronic ADRs, are less common. They are related to the cumulative dose of the drug. The best known example is hepatotoxicity caused by paracetamol [11].
- Type D, or delayed ADRs, are also uncommon but are usually related to the drug dose and occur a while after treatment with the drug, such as teratogenesis and carcinogenesis. Foetal hydantoin syndrome seen in children whose mothers were treated with phenytoin (an anticonvulsant) during pregnancy is an example [12].
- Type E, or end of use ADRs, are also uncommon. They occur soon after the drug treatment has been stopped. Such reactions can be observed after the withdrawal of opiate therapy [7].
- Type F, or failure ADRs, are common and dose-related. They can be caused by drug-drug interactions. An example of such reactions is the decreased effectiveness of oral contraceptives during treatment with antibiotics [13].

1.1.2.2 Dose relatedness, timing, and patient susceptibility

An alternative to the Rawlins and Thompson's classification is the dose relatedness, timing, and patient susceptibility (DoTS) system developed by Aronson and Ferner [14]. One of the advantages is that it was developed much later and with greater knowledge of ADRs. The issue with this system is its rare utilisation as it has not been widely established in the clinic or in literature.

Similar to the Rawlins and Thompson's model, the DoTS system categorises ADRs by the dose at which they occur and is based on supratherapeutic doses (toxic effect), standard therapeutic doses, and subtherapeutic doses.

Timing is subdivided into time dependent and time independent reactions. Time dependent reactions are further sub-divided into rapid, first dose, early, intermediate, late, and delayed reactions while time independent reactions can occur during any time of treatment.

The last category is susceptibility. It divides patients into different risk groups depending on known factors associated with higher risk for ADRs. Known factors that increase the susceptibility of a patient include age, gender, disease state, exogenous factors, genetic variation and chemical properties of the drug involved.

1.1.3 Risk factors for adverse drug reactions

Certain risk factors, such as age, gender, disease state, environmental factors, genetic variation, and chemical properties, have been associated with ADRs in different populations with different drugs.

The risk for most ADRs increases with age [15] but there are ADRs with a higher incidence in infants such as the liver injury caused by valproic acid [16]. Gender can also influence risk as many ADRs are more likely to occur in women [17-19]. Viral infections, especially HIV and herpes simplex virus, also increase the risk of ADRs [20-25]. The stage of the disease has also been shown to be important for the prediction of a patient's risk [26-30]. The

chemical properties of a drug are also considered important for the prediction of the risk of ADRs [31].

Furthermore, genetic variation can influence the risk of an ADR. Single nucleotide polymorphisms (SNPs) are the most common genetic variants and are known to increase risk of ADRs caused by certain drugs. SNPs associated with ADRs have been identified in genes across the human genome. These genes can be related to the pharmacology of the drug or apparently unrelated to the known pharmacology of the drug [32].

The first group of genes are responsible for the pharmacokinetics of ADR-causing drugs, including phase I and II metabolism genes, drug transporters, ion channels or receptors. A well-known example are the polymorphic genes that encodes the enzymes N-acetyltransferase type 1 and 2 (NAT-1, NAT-2) responsible for the detoxification of arylamine and hydrazine metabolites. SNPs in these genes cause amino acid substitutions in the protein sequence, which reduce their enzymatic activity [33]. It has been shown that the polymorphisms in these genes have clinical implications for the metabolism of drugs such as isoniazid and sulphonamides [34]. It has been reported that slow acetylators suffer from more side effects of certain drugs (e.g. dapsone and procainamide) while isoniazid treatment may fail in fast acetylators [35].

The second group of genes are mainly involved in the immune response (immunogenic genes). An increasing number of studies have shown a strong association between human leukocyte antigen (HLA) alleles and drug hypersensitivity reactions, which may allow prediction of ADRs (see Tab. 1.1) [36]. HLAs play an important role in the antigen presentation to T cells and two associations between HLA alleles and ADRs will be discussed in more detail in section 1.4.4.1 and 1.7.3 of this chapter.

Table 1.1: HLA-associated cutaneous drug-induced hypersensitivity reactions

Drug class	Drug	HLA allele	Adverse reaction	Reference
Antibiotic	Aminopenicillin	A2, DRw52	DRESS	[37]
	Dapsone	B*13:01	DRESS	[38]
Antiretroviral	Abacavir	B*57:01	DRESS	[39, 40]
	Efavirenz	DRB1*01	Skin rash	[41]
	Nevirapine	DRB1*01:01	DRESS	[42]
		C*04:01 (Malawian)	SJS/TEN	[43]
Antieplieptic	Carbamazepine	B*15:02 (Asian)	SJS/TEN	[44, 45]
		A*31:01 (Caucasian, Japanese)	MPE, DRESS, SJS/TEN	[46, 47]
	Lamotrigine	B*15:02	SJS/TEN	[48]
	Phenytoin	B*15:02	SJS/TEN	[45, 48]

DRESS: Drug rash with eosinophilia and systemic symptoms, SJS: Steven Johnson Syndrome, TEN: toxic epidermal necrolysis, MPE: maculopapular exanthema

1.2 Drug-induced Hypersensitivity Reactions

Drug-induced hypersensitivity reactions (DHRs) are a form of idiosyncratic or type B ADRs that can be observed in susceptible patients. DHRs can be subdivided into allergic (immune-mediated) and pseudo-allergic (non-immune-mediated) reactions. The majority of DHRs appear to be immune mediated and this work will focus on immune mediated DHRs [49].

DHRs do not show an observable dose-response relationship and are therefore considered dose independent [49]. The common understanding is that DHRs may occur at concentrations, well below therapeutic levels [50].

Another characteristic of most DHRs is the delayed onset of clinical symptoms, varying from one day to several weeks before the first manifestations [49, 51]. Symptoms of DHRs appear much quicker when the patient is re-challenged by the drug, consistent with the immune nature of the reactions [52, 53].

As DHRs only occur in a small minority of patients treated with the drug, they are rarely seen in phase I-III clinical trials and often only manifest in post-marketing surveillance (Phase IV). Currently there are very few animal models that can be used to study DHRs [54-56]. DHRs present a major clinical problem as well as being the main reason for post-marketing drug withdrawal. Although the risk-benefit ratio of a drug associated with DHRs is difficult to assess, withdrawal of the drug would protect a minority, it also means denial of an otherwise safe, and maybe more efficient, drug to the majority of people. As the safety and drug efficacy to all patients is the main concern, it is important to study and understand the mechanisms of DHRs and thus find markers to distinguish between patients who will benefit and those who will suffer from the unwanted effects of a drug.

1.2.1 Classifications of hypersensitivity reactions

According to Coombs and Gell, DHRs can be categorised, into four groups: type I, type II, type III and type IV reactions [57]. This system represents a sub classification of type B reactions in the system described by Rawlins and Thompson and is based on the mechanism of the immune response involved (see figure 1.1). This system has been utilised and has proven useful in clinical practice [58].

Some drugs have the ability to act as haptens. By binding covalently to host proteins, they form immunogenic complexes that elicit an immune response. In the case of type I hypersensitivity reactions, immunoglobulin (Ig) E, binds the hapten and the resulting complex promotes the activation of mast cells and basophils. Upon activation, these innate immune cells release a number of factors, such as histamine, leukotrienes, prostaglandins, and cytokines, which induce vasodilation, bronchoconstriction, vascular permeability, mucus production, and eosinophil recruitment [59]. The clinical features of an IgE-mediated reaction can vary in severity from a mild skin rash to lethal anaphylaxis.

Type II reactions are mainly IgG-mediated. In these reactions the hapten-carrier complex consisting of IgG and the drug coats target host cells and leads to sequestration of blood cells by the reticuloendothelial system in the liver and spleen through complement-receptor binding [59]. Alternatively, the hapten-carrier complex can activate the classical complement pathway and lead to cell lysis through complement-fixing immune complex formation. Clinical features, such as haemolytic anaemia, granulocytopenia and thrombocytopenia can be observed in type II hypersensitivity reactions.

Type III DHRs are similar to type II in the formation of immune complexes via IgG. Compared to type II, type III DHRs derive from an excessive formation of immune complexes, which are deposited in the basement membrane of blood vessels. Clinical manifestations of type III reactions include serum sickness and vasculitis [59].

Type IV DHRs are T cell mediated reactions and are also referred to as delayed-type hypersensitivity reactions. T helper and cytotoxic T cells involved in the type IV DHRs can orchestrate different forms of inflammation, which leads to different clinical manifestations. Based on the subset of T cells involved in the delayed-type DHR, the type IV reactions are sub-divided into four classes: type IV a, type IV b, type IV c, and type IV d (see Tab.1.2) [60].

The focus of this thesis is on the effect of the drug carbamazepine (CBZ) on inducing type IV reactions, which is discussed in more detail in section 1.7.3.

Table 1.2: Classification of type IV hypersensitivity reactions

	Type IV a	Type IV b	Type IV c	Type IV d
Type of T cells	T helper cells type 1	T helper cells type 2	Cytotoxic T cells	T cells
Pathological mechanism	Monocytic inflamation	Eosinophilic inflamation	Keratinocytes / hepatocytes death mediated by T cells	Neurophilic inflamation
Clinical manifestation	Eczema	MPE	Bullous exanthema (SJS, TEN), MPE and DRESS	Pustular exanthema (AGEP), SJS, TEN and MPE

MPE: maculopapular exanthema, SJS: Steven Johnson Syndrome, TEN: toxic epidermal necrolysis, AGEP: acute generalised exanthematous pustulosis, DRESS: drug rash with eosinophilia and systemic symptoms (adapted from Posadas and Pichler 2007 [60])

In type IV a reactions, T helper 1 cells release cytokines (e.g. interleukin (IL)-2, interferon-γ, and lymphotoxin-α) that activate macrophages and other phagocytes and increase their phagocytic activity [60, 61]. In addition, the T helper 1 cells stimulate the production of complement fixing antibodies (IgM and IgG) by plasma B cells and are pivotal in maintaining a proinflammatory response.

In type IV b reactions, T helper 2 cells secret cytokines (e.g. IL-4, IL-10, and IL-13) that increase antibody titres and regulate the antibody class switch from IgG to IgE the production of IgE and IgG production in plasma B cells. Furthermore, T helper 2 cells regulate the deactivation of macrophages, and the response of mast cells and eosinophil granulocytes [60, 61].

Type IV c reactions are mediated by cytotoxic T cells that act as effector cells. They migrate to tissues and can destroy tissue cells by lysing them or by inducing apoptosis [60]. The cytotoxic effects of cytotoxic T cells are triggered either by the recognition of non-self antigens presented by HLA class I on the surface of target host cells or though antibody-depended cellular cytotoxicity (ADCC) [62].

Type IV d involves antigen driven T cells coordinating neutrophilic inflammation. T cells recruit neutrophilic leucocytes through the release of the chemokine interleukin 8 and prevent the apoptosis of these leucocytes through white blood cell growth factors (granulocyte-macrophage colony-stimulating factors) [63]. A typical example for this is sterile inflammation of the skin, such as in acute generalised exanthematous pustulosis (AGEP).

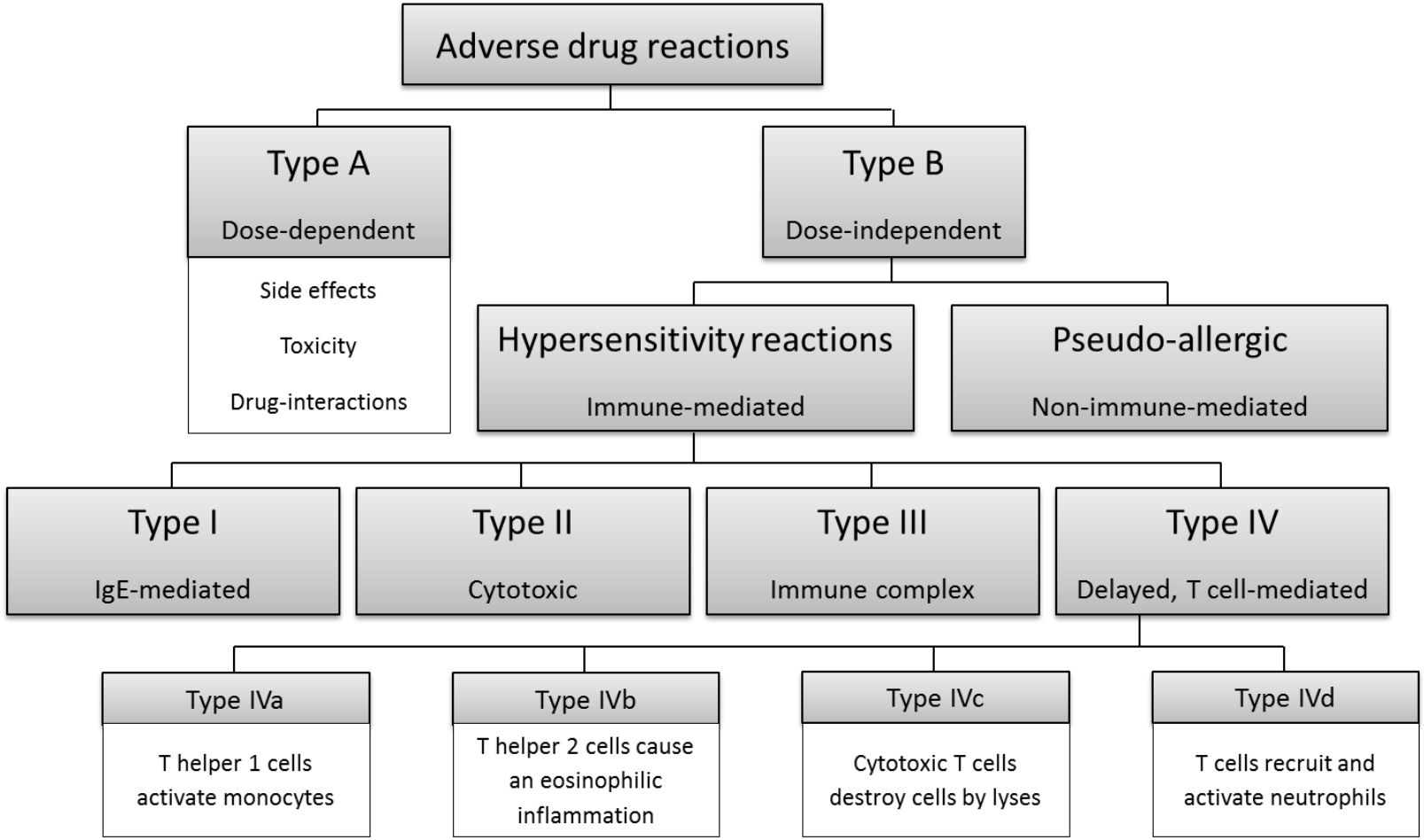

Figure 1.1: Overview for the classification of adverse drug reactions

Classification after Rawlins and Thompson including the sub classification of type B reactions proposed by Coombs and Gell.

1.2.2 Clinical manifestations of cutaneous drug reactions

DHRs can occur in almost any tissue or organ of the body including skin, liver, and blood [52] with skin being most commonly affected and accounting for 2-3% of hospitalised ADR patients [64-68].

Manifestations of cutaneous DHRs vary from mild rashes, which require treatment cessation, to severe blistering forms, which can require intensive care and have a high mortality rate. The clinical manifestations caused by a specific drug can vary between patients [52]. The different forms of cutaneous DHRs show distinct clinical characteristics [51] and include maculopapular exanthema (MPE), acute generalised exanthematous pustulosis (AGEP), Steven Johnson Syndrome (SJS) and toxic epidermal necrolysis (TEN).

The most common cutaneous reaction observed in DHRs is MPE, which accounts for 31-95% of all cutaneous DHRs [65, 66, 69]. The symptoms are usually observed during the first two weeks after the start of treatment and disappear after the treatment is discontinued [70, 71]. Initial manifestations include isolated patches of faint, pink or red macules. These then develop into maculopapular rashes in the extremities with moderate to severe itching and can be accompanied by fever.

AGEP is less common, with an incidence rate between 1-5 per million each year [72, 73]. Typical characteristics for AGEP are small, numerous pustules arising widely spread all over the skin [63]. Symptoms appear within the first week of treatment [74]. The mortality rate from AGEP is approximately 5% without appropriate clinical treatment [71].

The most severe blistering skin reactions caused by drugs are SJS and TEN. SJS and TEN are considered to be forms of the same spectrum of skin reaction. The incidence rate is estimated between 1:100 000 and 1:1 000 000, which makes them a very rare form of cutaneous DHRs [75]. The two forms are distinguished from each other by the percentage of skin detachment observed in the patient [76]. SJS is associated with up to 10% of skin detachment whereas TEN is associated with 30% or more of skin

detachment. Between 10-30% skin blistering is called SJS/TEN overlap syndrome. These reactions occur during the first eight weeks of treatment. After the first observed symptoms, the rash develops quite rapidly and withdrawal of the drug does not always stop the progression [52]. The most important clinical prognostic factors for the patient are percentage of skin detachment, age, and underlying disease. The mortality rate for SJS is 13%, for SJS/TEN overlap syndrome 21%, and for TEN ~30% [77].

Drug rash with eosinophilia and systemic symptoms (DRESS) is a severe DHR. Different terminologies are used in literature for drug reactions involving different organs, such as hypersensitivity syndrome (HSS) or drug-induced hypersensitivity syndrome (DIHS) [78-80]. In this work this reaction will be referred to as DRESS. Clinical symptoms of DRESS usually occur two to eight weeks after the start of drug treatment and often include a combination of different symptoms including high fever, skin rash, and lymph-node swelling. In addition, multiple organs are involved including liver, kidneys, lungs, and heart, resulting in pneumonitis, lymphadenopathy, hepatitis, and nephritis [52]. The liver is the most commonly involved organ [81] and DRESS can lead to liver failure, which is the most common cause of death in DRESS with a 10% mortality rate [51]. DRESS can be easily misdiagnosed as an acute viral infection. This is due to the level of activated T-cells and virus specific antibodies in the blood which can be similar to those seen for viral infections [82-85]. The underlying mechanism of DRESS is poorly understood but it has been proposed that activated T cells cause the tissue damage [86].

1.3 Immune system

Multicellular organisms employ the immune system to defend themselves from pathogens and cancers. To fulfil this protective function, the immune system has evolved complex mechanisms enabling it to distinguish between self- and non-self-structures. Upon the detection of non-self-structures the immune system responds either with tolerance or an immune response through its two arms, namely the innate and the adaptive immune system. The innate immune system provides a fast response to structures common in many pathogens, such as specific glycolipid or certain forms of nucleic acid. Since the recognition repertoire of the innate immune system is limited, some pathogens have evolved to evade the innate immune response. In comparison the adaptive immune system is slower, however, it has a vast variety of highly specific antibodies and receptors that is achieved through a complex gene rearrangement allowing it to adapt to the ever changing pathogens [87].

1.3.1 Innate immune system

The innate immune system is the first line of defence of the organism and consists of physical barriers (e.g., skin, mucus, low pH) and effector immune cells and molecules. The innate immune responses are mediated by phagocytic cells (macrophages, monocytes, neutrophils and dendritic cells), mast cells, basophils and eosinophils [88] which are triggered by patterns associated with pathogens [87, 89, 90].

The recognition of pathogen-associated molecular patterns (PAMPs) by innate immune cells and the alternative and lectin complement pathways plays a crucial role in the initiation of the innate immune response [91]. PAMPs are conserved molecules, only associated with pathogens such as bacteria (e.g. lipopolysaccharide, flagellin, peptidoglycan and bacterial DNA), viruses (e.g. single- or double-stranded viral DNA and RNA), fungi (e.g. glucan) and parasites (e.g. chitin). PAMPs are detected by pathogen

recognition receptors (PRRs), such as toll-like receptors, which can be found in soluble form (e.g. complement) or expressed on the membrane of phagocytic cells such as macrophages and neutrophils [92, 93]. The binding of soluble PRRs to PAMPs results in the lysis of the pathogen, for example as a result of the activation of the alternative and lectin complement pathways [87]. The activation of the complement system leads to the formation of pores in the membrane of the pathogen and it subsequent lysis.

Binding of membrane bound PRRs to PAMPs leads to the engulfment and phagocytosis of the pathogen, the release of inflammatory mediators and activation of the adaptive immune responses.

PRRs can also detect damage-associated patterns (DAMPs). DAMPs, such as heat shock proteins, high-mobility group box 1 proteins, adenosine triphosphate, uric acid and cellular DNA, are released by the loss of membrane integrity of a host cell, which can be caused by rupture of the cell through physical damage or through certain pathways of cell death such as necrosis [94, 95]. Similar to the detection of PAMPs, recognition of DAMPs by PRRs results in the activation of the adaptive immune system through the release of pro-inflammatory mediators, by basophils, eosinophils, mast cells, natural killer cells (NK) [88, 94, 96].

The cytotoxic NK cells belong to the innate arm of the immune system. However, in contrast to the other innate immune cells, they recognise malfunctioning host cells, such as cancer or virus infected cells, by the abnormal expression of HLA class I molecules on the cell surface and induce their apoptosis [97].

The dendritic cells (DCs) play a central role in the immune response. They absorb extracellular components through phagocytosis and pinocytosis and display antigens on their surface, thus turning into antigen-presenting cells (APCs) [88]. The APCs then initiate the activation of the adaptive immune system and therefore play an important role in the crosstalk between the innate and the adaptive immune systems.

1.3.2 Adaptive immune system

The adaptive immune system is more specific in its response but requires time before activation, during which the innate immune system keeps the pathogens at bay. The highly specialised cells of the adaptive immune system can be divided into two groups, namely cells involved in the humoral response (B-cells) and cells involved in the cell-mediated immune response (T cells) [98]. Like the cells of the innate immune system, they are derived from hematopoietic stem cells of the bone marrow, but maturate through distinct differentiation pathways in either the bone marrow (B cells) or thymus (T cells) [99-101]. The B and T cells can be activated and must be carefully controlled to prevent damage to healthy cells, while dealing with pathogens or malfunctioning host cells [87]. The B and T lymphocytes express specific B or T cell receptors on their cell membrane which can bind complementary antigens thus leading to their activation.

B cells detect antigens through B cell receptors which represent membrane bound antibodies. Upon recognition of pathogenic structures, B cells transform into plasma cells mostly under the influence of an activated T helper cell [102]. The differentiated plasma cells then produce and secrete soluble antibodies which can then bind to an antigen and thus mark it for digestion by phagocytic cells. Furthermore, antibodies specifically bound to an antigen can activate the classical complement pathway or stimulate antibody-dependent cytotoxicity (ADCC) carried out by NK, neutrophils and monocytes [103].

In contrast to B cells, the T cells are incapable of detecting foreign antigens directly: they require a presentation of antigens by APCs such as dendritic cells, macrophages, neutrophils and B cells. These phagocytes internalise and process the pathogenic proteins into peptides (epitopes) for presentation on the HLA class II. T helper lymphocytes express an antigen specific T cell receptor (TCR), which interacts with the peptides presented on the HLA at the surface of APCs. If the peptide is recognised as non-self, the T cells are activated [87, 104-107]. This results in proliferation and differentiation of a particular set of T cell into effector T cells.

The TCR is a heterodimer anchored in the outer membrane of T cells consisting of two polypeptides linked via disulphide bonds. The majority of the TCR polypeptides are highly variable α and β chains. Each of these chains is composed of four domains, namely, the N-terminal variable region, the constant region, a hydrophobic transmembrane domain followed by the cytoplasmic tail [108]. The variable region is responsible for the antigen recognition. Specific peptide recognition is achieved through gene rearrangement during gene expression. This process results in a variety of genes, which would not be possible to be encoded for in the genome. The naïve T cells undergo two selection processes in the thymus to ensure their functionality [88]. The first of these is a positive selection which selects for T cells capable of detecting self-peptides on HLA molecules. This is followed by a negative selection during which apoptosis is induced in T lymphocytes interacting too strongly with the self-peptides. This selection prevents the induction of autoimmune reactions initiated by T cells [109].

The T lymphocytes can be grouped into two functionally different types depending on the cluster of differentiation (CD) expressed on their surface. The function of the CD molecules is to recognise HLA molecules and assist during the TCR recognition of epitopes presented by HLA [87]. T cells expressing CD4 only detect epitopes presented by HLA class II molecules on APCs and are called T helper cells. These T cells mediate the activation of other innate and adaptive immune cells by secreting a variety of cytokines. As mentioned earlier (section 1.2.1), depending on the cytokines released, the T helper cells can be further subdivided into Th1 and Th2 which regulate the function of different immune cells. T cells expressing CD8 interact with HLA class I molecules and are referred to as cytotoxic T cells. These T lymphocytes are capable of killing infected cells by inducing apoptosis.

1.4 Major histocompatibility complex

The MHC is located on the short arm of chromosome 6 (6p21.3) and more than 220 genes that regulate innate and adaptive immune functions are encoded in this region [110, 111]. MHC encodes transmembrane glycoproteins expressed on the surface of every nucleated cell in the human body and possess an immunoglobulin-like region for the presentation of endogenous and exogenous peptides to T cells [112].

The MHC was first described in 1936 when it was found that antigenic molecules in the blood of mice are responsible for the rejection of transplanted tumours [113]. It was later discovered that similar antigenic structures are present on the cell surface of human leukocytes which is why human MHC molecules were named HLAs in humans [114].

1.4.1 Classification and structure

The MHC molecules are divided into three major classes, MHC I, MHC II and MHC III, based on their molecular structure and function. The first two classes of MHCs present peptide fragments to T cells and subcategorised into HLA-A, HLA-B and HLA-C for MHC I and HLA-DQ, HLA-DP and HLA-DR for MHC II. The HLA genes are generally inherited in blocks, one block from each progenitor, called haplotypes. These haplotypes are co-dominantly expressed in the individual. Frequencies of these haplotypes show large variability in different ethnicities [115]. MHC III genes encode proteins of the complement system and inflammatory cytokines including tumour necrosis factor α and heat shock proteins. These are however, not membrane proteins and have no role in the antigen presentation. A diagram of the MHC region depicting the three gene clusters is shown in figure 1.2.

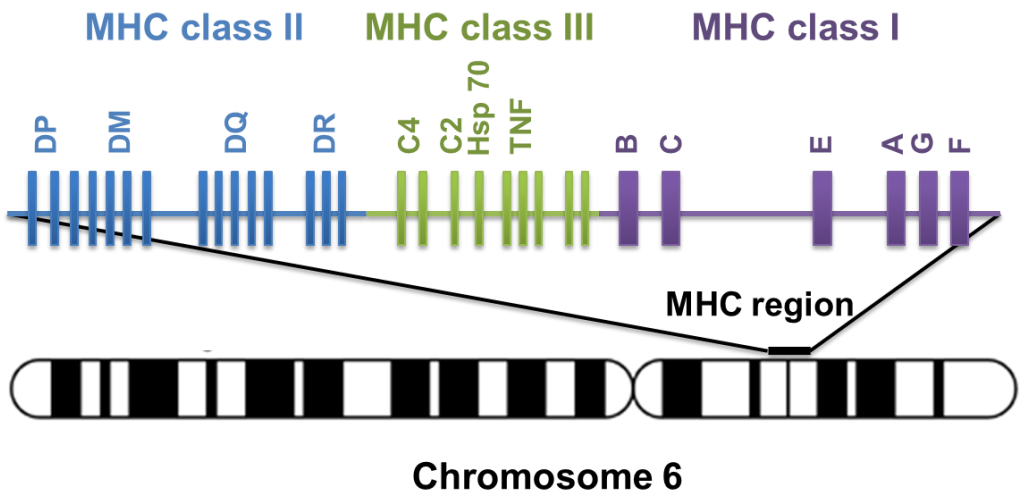

Figure 1.2: Localisation of genes in major histocompatibility complex (MHC) region (adapted from Klein and Sato, 2000 [112])

Class I and class II HLA molecules are related structurally and functionally and are expressed as glycosylated membrane bound heterodimers. Although HLA class I and HLA class II molecules share a number of functional similarities , differences exist in the source of protein fragments they present as well as in the subset of T cells they present these peptides to [116].

The HLA class I molecule consists of a 45 kDa α subunit (heavy chain), which is encoded by the HLA class I gene, and a 12 kDa β2-microglobulin polypeptide (light chain) encoded on chromosome 15 [117]. The polymorphic α chain contains three extracellular domains (α1, α2 and α3), a transmembrane region and a cytoplasmic tail. The α1 and α2 domains form the peptide-binding groove of HLA class I molecules, which presents 8 to 11 amino acids long peptide fragments [118]. HLA class I molecules can be found on the surfaces of all nucleated cells in the body. The peptides they present derive from the cytosolic antigen processing [119].

In contrast, HLA class II molecules are only expressed on APCs and the 12 to 25 amino acids long peptides fragments they present derive from the endocytic antigen processing [120]. The HLA class II molecule consists of a 33 kDa α chain and a 28 kDa β chain [117]. The each of the chains consists of two extracellular domains (α1 and α2 or β1 and β2), a transmembrane

region and a cytoplasmic tail. The peptide-binding groove is formed by α1 and β2 domains [112].

1.4.2 Polymorphism and nomenclature

The HLA genes are highly polymorphic, with a large number of HLA alleles reported and with the HLA-B locus being the most polymorphic [121, 122]. In the case of HLA class I alleles, single nucleotide polymorphisms (SNPs) that distinguish the different alleles located in the second and third exon and are most commonly typed, as these parts code for the antigen-binding groove of the HLA protein. For HLA class II, SNPs in the second exon are routinely typed, since most of these SNPs are non-synonymous and lead to changes in the amino acid sequence as well as in the peptide-binding groove [122].

The determination of HLA polymorphisms or HLA typing has evolved significantly since the first discovery of HLA antigens in human blood [114]. The first method used for HLA typing was based on serology utilising antibodies directed against HLA molecules on the cell surface [123]. Since then, the application of DNA-based methods increased the repertoire of available methods, especially after the discovery of sequence-based typing which applies PCR or next generation sequencing technology [124].

Due to the large number of known HLA alleles, systematic nomenclature has been introduced. The standardised nomenclature system was established in 1968 by the International Histocompatibility Working Group (IHW) [125]. This system is still used today and constantly maintained and updated by the WHO Nomenclature Committee for Factors of the HLA System [126].

The HLA allele name consists of the name of the gene locus followed by an asterisk and a number that identifies the gene variant (see Fig. 1.3). The identification number of the gene variant can consist of four fields, which are separated by colons. The first field identifies the type of allele and corresponds to the serological type in most cases. The next field is the subtype of the HLA allele. The field is assigned in sequential order, which allows the incorporation of further alleles. The third field describes

synonymous mutations while the last field identifies mutations in the non-coding regions. The identification number of the gene variant can be followed by an optional letter describing the expression status of the allele.

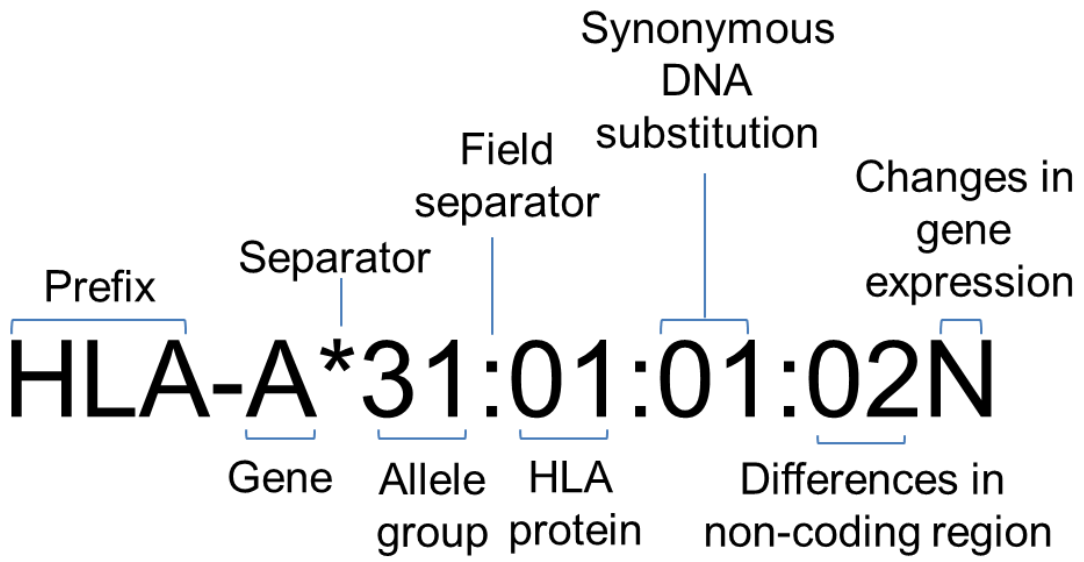

Figure 1.3: Nomenclature of HLA alleles

1.4.3 Antigen processing and presentation

As mentioned earlier (section 1.3.1), APCs play a central role in the activation of the adaptive immune response by engulfing, processing and presenting extracellular antigens on HLA class II to T helper cells in the lymph nodes [87].

HLA class I molecules present intracellular epitopes that are degraded in the cytosol by the proteasome. During this cytosolic (endogenous) antigen processing, the peptide fragments are translocated into the endoplasmic reticulum (ER) by a transporter associated with antigen processing (TAP). The peptides are then mounted onto HLA class I molecules by the peptide loading complex in the ER. After the formation of a stable peptide-HLA complex, the HLA class I complexes are released from the ER and proceed

through the Golgi apparatus to the surface of the cell for antigen presentation to cytotoxic T lymphocytes [127].

In contrast to HLA class I, HLA class II complexes present extracellular antigens. In the endocytic (exogenous) antigen processing, extracellular proteins are internalised by phagocytosis in endosomes. The endosomes merge with lysosomes to form the phagolysosome. The acidic conditions within this structure promote the activation of proteases, which digest proteins in the phagolysosome into peptide fragments. After the fragmentation of the proteins, the phagolysosome merges with vesicles containing HLA class II molecules and the peptide fragments are mounted on the HLA molecules [127]. The newly formed peptide-HLA complexes are then transported to the cell surface. The HLA class II α and β chain molecules are assembled in the ER and bind a third protein (invariant chain) that temporarily occupies the peptide-binding groove [128]. HLA class II molecules binding the invariant chain are transported to late phagolysosomes, where the invariant chain is degraded by proteases to a short peptide, class II-associated invariant chain peptide (CLIP). A chaperon, HLA-DM, alters the structure of HLA class II molecule, which results in the exchange of CLIP for a peptide fragment derived from the protein digestion in the phagolysosome [129].

Dividing the antigen processing pathways for HLA class I and class II in exclusively intracellular and extracellular proteins is a simplified model of the processes found in living cells. The process of cross-presentation has been described after it was shown that epitopes derived from extracellular proteins can be presented on HLA class I molecules, while HLA class II molecules presented intracellular epitopes through the fusion of autophagosome and vesicles containing HLA class II molecules [130, 131].

The HLA class I complexes are more restrictive during the protein loading due to the closed confirmation of the binding groove. The ends of the peptide-binding groove interact with the free N and C termini of the peptides, which limits the length of the presented peptide [132]. HLA class II complexes do not have this length restriction as the peptide-binding possess

open ends [133, 134]. The length of the peptide on HLA class II results from the peptide processing of proteases. The peptide-binding groove of a HLA complexe stabilises the peptide through a series of interactions with the peptide backbone and limited interactions with particular side chains of the peptide. Two or more residues (anchor residues) of the peptide dock in pockets of the peptide-binding cleft and ensure the correct positioning of the peptide in the HLA peptide-binding groove [135].

1.4.4 HLA associations with adverse drug reactions

HLA alleles play a key role during the activation of T cells thus initiating immune responses. The importance of the HLA in the pathogenesis of various diseases has been demonstrated by associations between HLA alleles and autoimmune disease, infectious disease and cancer [136]. However, the precise mechanism of pathogenesis in most diseases remains unknown. Furthermore, most of these diseases have multifactorial etiology, including environment, life style, and genetics, which complicates matters even further.

More and more discoveries of HLA associations with hypersensitivity reactions caused by various drugs are being reported, suggesting that HLA molecules may be of crucial importance in at least some drug-induced hypersensitivity reactions [137]. However, it is not clear however, what role HLA molecules have in the pathogenesis of drug-induced hypersensitivity reactions. Furthermore, the fact that HLA molecules are found to be associated with specific phenotypes of hypersensitivity reactions caused by a certain drug and the HLA molecule varying between different populations complicates the analysis of their role [137].

1.4.4.1 Abacavir

An overview of drug-induced hypersensitivity reactions with known association to HLA alleles is shown in table 1.1. Abacavir (ABC) will be discussed in more detail as an example of how the knowledge has advanced after the discovery of HLA associations and drug hypersensitivity.

ABC is a nucleoside analogue reverse transcriptase inhibitor and acts as an antiretroviral drug used for the treatment of human immunodeficiency virus (HIV). One of the most common side effects of the drug is ABC-induced hypersensitivity, manifesting in about 70% of the patients through a mild or moderate skin rash. More serous forms of ABC-induced hypersensitivity reactions, such as DRESS, can be observed in 5-8% of patients treated with the drug [36]. The symptoms of DRESS include fever, gastrointestinal manifestations and internal organ involvement. Two independent research groups have found a strong association between HLA-B*57:01 and ABC-induced DRESS [39, 40]. Utility of pre-treatment HLA-B*57:01 testing for reducing the incidence of hypersensitivity reactions in individuals prescribed ABC has been demonstrated in a randomised controlled clinical trial conducted in Australia [36]. Further research revealed the presence of activated $CD8^+$ T lymphocytes in the skin of patients who had suffered from ABC-induced hypersensitivity [138]. Additionally, a T-cell response could be triggered in T cells derived from patients as well as from ABC-naïve healthy volunteers carrying the HLA-B*57:01 allele [139]. The T cell response was found to be HLA-B*57:01 restricted, as even highly similar HLA types were unable to induce T cell activation in the presence of ABC.

The mechanism of T cell activation caused by ABC has been discovered recently by three groups who independently reported an interaction of ABC with certain amino acids within the binding groove of HLA-B*57:01 [140-142]. ABC seems to bind in a non-covalent fashion to one pocket of HLA-B*57:01. The preference of the peptide mounted on the HLA molecule during the antigen processing is altered through this occupation of one of the pockets in the peptide-binding groove. The new peptides preferred for presentation possess smaller residues in the position where the peptide interacts with the

F-pocket. Based on this observation, a new mechanism for drug mediated T cell activation was proposed, the so called “altered self-peptide hypothesis” (discussed in section 1.5.3).

Screening for HLA-B*57:01 in patients before the start of ABC therapy was shown to reduce the incidence of ABC-induced hypersensitivity and also was proven to be cost effective [143]. Therefore pharmacogenetic testing for HLA-B*57:01 in patients is recommended by both the US Food and Drug Administration and the European Medicine Agency before the start of treatment. ABC is an example for the success of personalised medicine, where the discoveries made in the laboratory are transferred into health care to the bedside of the patient.

1.5 T cell activation in hypersensitive reactions

The activation of T cells plays an important role in the initiation of an adaptive immune response. Two signals are required for the full activation of T cells. The first signal involves the presentation of peptides on HLA molecules by APCs. T cells interact with the peptide-HLA complexes through the TCR and co-receptors such as CDs [87]. Mature T cells possess either the co-receptor CD4 or CD8 for the interaction with HLA class II or HLA class I molecules, respectively. During the recognition, the TCR binds directly to the peptide presented, while the co-receptors interact with the HLA-molecule to stabilise the TCR-peptide-HLA complex. This process is termed “signal 1” and in instances where signal 1 is generated alone, the induction of immune tolerance will occur [144].

The second signal (signal 2) derives from the detection of primal and feedback danger signals in the organism [144]. Primal danger signals consist of two subclasses: (i) exogenous and (ii) endogenous danger signals. Exogenous danger signals are molecules produced by pathogens (PAMPs), while endogenous danger signals are molecules released by cells that undergo stress or abnormal cell death (DAMPs) (see section 1.3.1). The detection of primal danger signals by resting APCs results in the activation of APCs, which trigger T cell activation through the presentation of costimulatory signals [95, 145]. For example, immature DCs express low levels of HLA class II and costimulatory molecules, while surveying the tissue for danger signals. Through the detection of exogenous or endogenous danger signals, DCs become activated and turn into APCs with increased expression of HLA class II and costimulatory molecules (e.g. B7, OX40L and 4-1BBL) [146]. The activated DCs then migrate to the lymph nodes where they prime naïve T cells.

Feedback danger signals are proinflammatory cytokines (e.g. IL-2, interferon-γ, or TNF α), which are secreted by activated cells of the immune system [147]. The detection of feedback danger signals increases the presentation of costimulatory signals on the surface of APCs. The

costimulatory signals, such as B7, on APCs can interact with CD28 on T cells. The interaction of the costimulatory molecules in the presence of signal 1 results in the full activation of T cells by amplifying the signalling cascade triggered through TCR-peptide-HLA interaction, thereby promoting antigen-specific T cell proliferation, differentiation and survival as well as cytokine production [148].

The TCR forms a complex with two CD3 heterodimers (CD3εγ and CD3εδ) and one CD3 homodimer (CD3ζ) for the activation of intrinsic cell signalling pathways [87]. Each of the dimers possesses two intracellular tyrosine-based activation motifs (ITAMs). Upon binding of TCR to the antigen and either CD4 or CD8 to the HLA molecule, associated Src family kinases, proto-oncogene tyrosine-protein kinase (Fyn) and lymphocyte-specific protein tyrosine kinase (Lck), become activated and phosphorylate tyrosines in the ITAMs [149]. Phosphorylated ITAMs recruit zeta-chain-associated protein kinase 70 (ZAP-70), which becomes activated through the phosphorylation by Lck. ZAP-70 phosphorylates the linker for activation of T cells (LAT) and LAT in turn activates transcription factors through the Ras-Erk and phosphoinositide 3-kinase (PI3K) pathways [150]. The PI3K pathway activates nuclear factor kappa-light-chain-enhancer of activated B cells (NF-κB) and Ca^{2+} flux from the ER, which both result in the transcription of genes related to T cell proliferation and effector function [151]. The costimulatory signalling (e.g. from B7 bound to CD28) intensifies PI3K signalling and increases the expression of pro-survival genes [148].

The isolation of drug-specific T cells from blood and tissue of hypersensitivity patients clearly showed that T cells are involved in delayed hypersensitivity reactions [83, 152]. The above described mechanism of T cell activation requires the processing of large molecules, with a mass greater than 1 000 Da. Drug molecules are too small and would only become immunogenic after interacting with larger molecules such as proteins [49, 153, 154]. Therefore the hapten hypothesis has been developed as a model to explain how drugs can be involved in the activation of T cells through covalent binding to proteins. Several other models of T-cell activation which

do not involve covalent binding of drugs to proteins, have been proposed recently, and will be discussed below.

1.5.1 Hapten hypothesis

The first model to describe the activation of T cells by drugs was the hapten hypothesis. A hapten is a small exogenous molecule, which as such is unable to initiate an immune response. Only through covalent binding to larger endogenous molecules, such as proteins, can haptens become immunogenic. In 1935, Landsteiner and Jacobs formulated this hypothesis after they showed in experiments that small molecules (< 1 000 Da) can induce skin rashes in guinea pigs by binding to proteins [155]. In their experiments, Landsteiner and Jacobs showed that reactive molecules of dinitrochlorobenzene can cause T cell activation. They demonstrated *in vitro* that the compound used in the experiments could modify proteins. From these observations, they hypothesised that small, reactive molecules (haptens) can modify proteins and through this trigger an immune response. It was later proven that covalent binding of haptens to proteins is required for T cell recognition [156].

The observation that metabolites but not the parent drug can bind to proteins and act as haptens lead to the introduction of the term pro-hapten [157]. This bioactivation of the pro-hapten would occur predominantly in the liver through cytochrome P450 but can also take place in the skin or in blood, however, at a lower rate [60, 158]. If these hapten metabolites are not detoxified, they can damage the metabolising host cell, activate the immune system, and form protein adducts, which are also capable of evoking an immune response [52]. The haptenization of proteins can lead to the formation of anti-drug antibodies as the hapten-modified proteins can be also processed by the antigen-presenting machinery of APCs to haptenised peptides, which are then displayed to T cells [100]. The hapten hypothesis is depicted in figure 1.4.

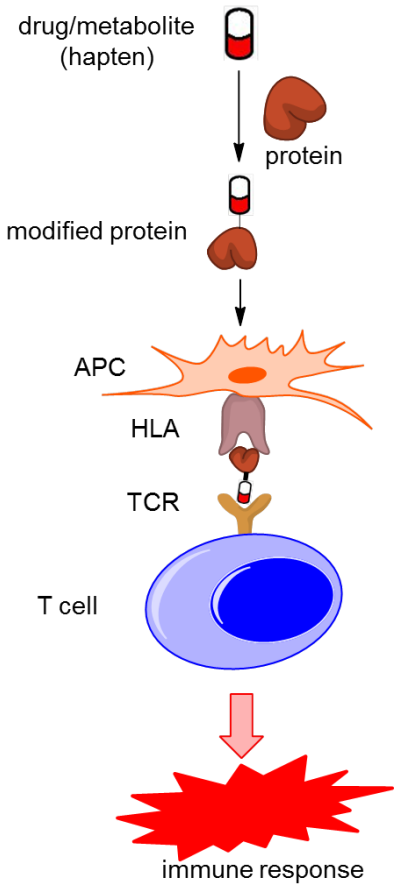

Figure 1.4: Hapten hypothesis

A reactive drug or metabolite binds covalently to an endogenous peptide. The hapten-modified protein is taken up, processed and presented on the human leukocyte antigen (HLA) by an antigen presenting cell (APC). This can then be recognised by a T cell through the T cell receptor (TCR), which leads to an immune reaction (adapted from Uetrecht, 2007 [49]).

Examples of drugs acting as haptens are β-lactam antibiotics, such as penicillin, which covalently bind to lysine residues of many proteins, including serum albumin. It has been shown that anti-penicillin antibodies and penicillin-conjugate specific T cells are found in the serum of hypersensitive patients [52].

Sulfamethoxazole (SMX) is an example of a prohapten. SMX is metabolised by cytochrome P450 in the liver to SMX hydroxylamine. This hydroxylamine can then undergo autooxidation resulting in nitroso-SMX, which is highly reactive and reacts with the cysteine residues of various proteins [52].

1.5.2 Pharmacological Interaction Concept

The observation of T cell activation by drugs that are not capable of forming adducts with peptides, led to the proposal of an alternative theory that focuses on the pharmacological interaction of drugs with immune receptors (p-i) [159, 160]. In contrast to the hapten hypothesis where reactive drugs form covalent bonds with proteins, it has been proposed that chemically inert drugs directly interact with TCR or HLA molecules through non-covalent bonds, such as electric, van der Waals, hydrophobic, and hydrogen bonding forces, thus leading to the activation of T cells. The T cell activation is thought to result from previously primed effector cells and memory T cells, which possess a lower activation threshold [159]. The p-i concept is supported by experimental evidence showing that T cells could be activated via a HLA-dependent mechanism in the presence of glutaraldehyde-fixed APCs and nonreactive drugs [161, 162]. These chemically fixed APCs are unable of processing proteins for antigen presentation, which suggests that the drug interacts with the peptides on HLA molecules of APCs. Additionally, T cell activation, measured through visualisation of calcium influx, after the exposure to the drug occurred too fast for antigen processing and presentation to have taken place [161, 163]. Figure 1.5 depicts the mechanism of the p-i concept.

Drugs found to activate drug-specific T cells include carbamazepine, lamotrigine, lidocaine, and sulfamethoxazole [83, 162-164]. Experiments with T cells isolated from SMX-hypersensitivity patients showed that the cells were activated by the parent drug, SMX, as well as the metabolites, suggesting that both mechanisms (the hapten and p-i hypothesis) are important in the development of SMX-induced hypersensitivity [165]. T cells isolated from SMX hypersensitivity patients reacted only to the parent drug in the presence of APCs [163]. It was also shown that covalently SMX-modified peptides mounted on HLA molecules did not activate SMX-specific T cells [166]. Recent modelling of SMX and TCR interaction revealed a possible site for interaction [167]. This suggests that the peptide is not involved in the HLA binding and activation of SMX-modified TCR.

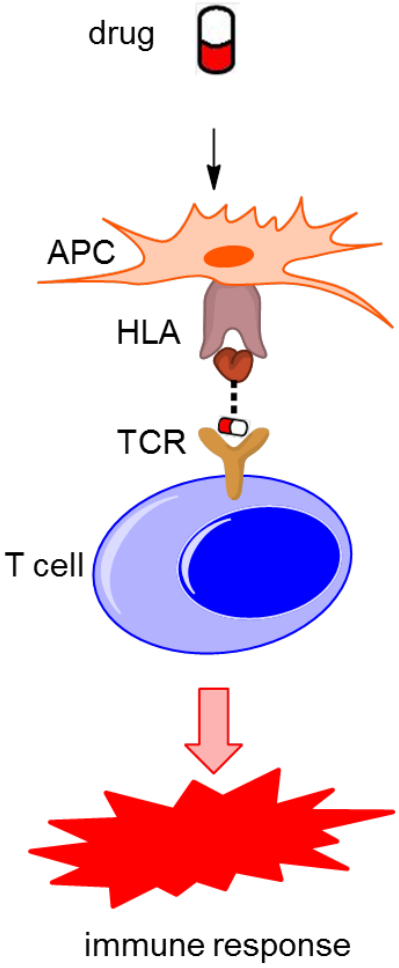

Figure 1.5: Pharmacological interaction (p-i) hypothesis

A chemically inert drug binds in a reversible manner to the peptide presented on the human leukocyte antigen (HLA). This modified peptide is recognised as a non-self structure by T cell receptor (TCR) of a T cell, triggering an immune response (adapted from Bharadwaj *et al.*, 2012 [168]).

1.5.3 Altered self-peptide hypothesis

The discovery of the mechanism of ABC-induced hypersensitivity reaction resulted in the postulation of a novel hypothesis, the altered self-peptide hypothesis [141]. The antiviral drug ABC causes hypersensitivity reactions in patients expressing HLA-B*57:01 [40, 169]. It was shown that ABC interacts with a specific pocket in HLA molecule, changing the configuration of the groove and resulting in the presentation of different self-peptides by HLA-B*57:01 [140-142]. The different self-peptide presented by the APCs activates cytotoxic $CD8^+$ T cells, which mediate the clinical manifestation of the ABC hypersensitivity syndrome.

Based on this observation the hypothesis states that drug molecules bind in a non-covalent fashion to pockets within the binding groove of HLA molecules. This interaction changes the shape and the chemical properties of the pocket, altering the repertoire of self-peptides presented by the affected HLA molecule, thus resulting in the presentation of different peptides. These new HLA complexes do not take part in the negative selection of T cells in the thymus. Therefore, the self-peptides which can only bind to the HLA molecule in the present of the drug are capable of activating T cells, which presents a mechanism of drug-induced autoimmunity since the recognised protein is not modified. Another example of a drug interacting with the binding groove of HLA is CBZ [140]. It was shown that CBZ can occupy a certain pocket in HLA*B-15:02, which alters the presented peptide. The altered self-peptide hypothesis is schematically illustrated in figure 1.6.

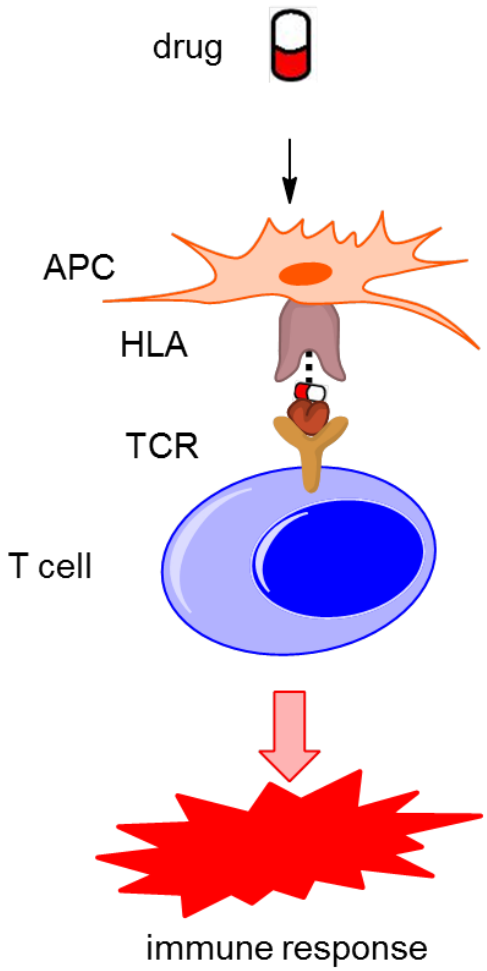

Figure 1.6: Altered self-peptide hypothesis

A drug binds to the binding groove of the human leukocyte antigen (HLA) in a reversible manner. This changes the properties of the pocket resulting in the binding of novel peptides. These peptides are recognised by the T cell receptor and trigger an immune response (adapted from Bharadwaj *et al.*, 2012 [168]).

1.5.4 Danger Hypothesis

The danger hypothesis was proposed in 1994 and is based on the observation that the activation of T cells requires more than one signal [170]. It has been shown that at least two signals are necessary for triggering T cell activation [171]. As discussed at the beginning of this section, the recognition of non-self peptides presented on HLA molecules by T cells via the TCR is termed signal 1 and alone this signal results in immune tolerance [172].

The second signal is derived from the interaction of various costimulatory molecules on the surface of APCs (e.g. B7) and the receptors on T cells (e.g. CD28) and leads to proliferation, differentiation, and survival of the T lymphocytes [173]. Signal 2 on APCs is modulated by the detection of PAMPs and DAMPs [95, 145]. The first model to describe costimulatory signalling for T cell activation assumed that the signals derive from pathogens (PAMPs) [174]. The danger model added another source for costimulatory signals, which are derived from cells of the body (DAMPs) [170]. In the danger model, the detection of non-self structures is not the important signal that triggers an immune response. Only the simultaneous presence of danger signal initiates the full activation of T cells [175].

According to the danger hypothesis drugs require costimulatory signals to activate naïve T cells. Reactive drugs or metabolites, which cause cellular damage, function as antigenic stimuli (see 1.5.1 hapten hypothesis) and also lead to the presence of danger signals, which are detected by APCs and result in the full activation of naïve T cells [154, 176]. Depending on the damaged tissue as a source of danger signals, the hypothesis could explain the localised occurrence of DHRs phenotypes [49]. This theory also explains why not all reactive drugs or metabolites cause hypersensitivity as not all reactive drugs cause cellular damage, thus avoiding the release of danger signals [49]. Alternative sources for danger signals are ongoing infections, such as HIV and herpes simplex virus, as seen for certain drugs [20, 21]. The principle of the danger hypothesis is shown in figure 1.7.

It has been shown that ABC, amoxicillin and metabolites of SMX can lead to danger signalling [177-179]. For ABC, it was found that the redistribution of heat shock proteins in APCs is induced by the drug and that this redistribution is accompanied by the expression costimulatory molecules on the surface of APCs [177].

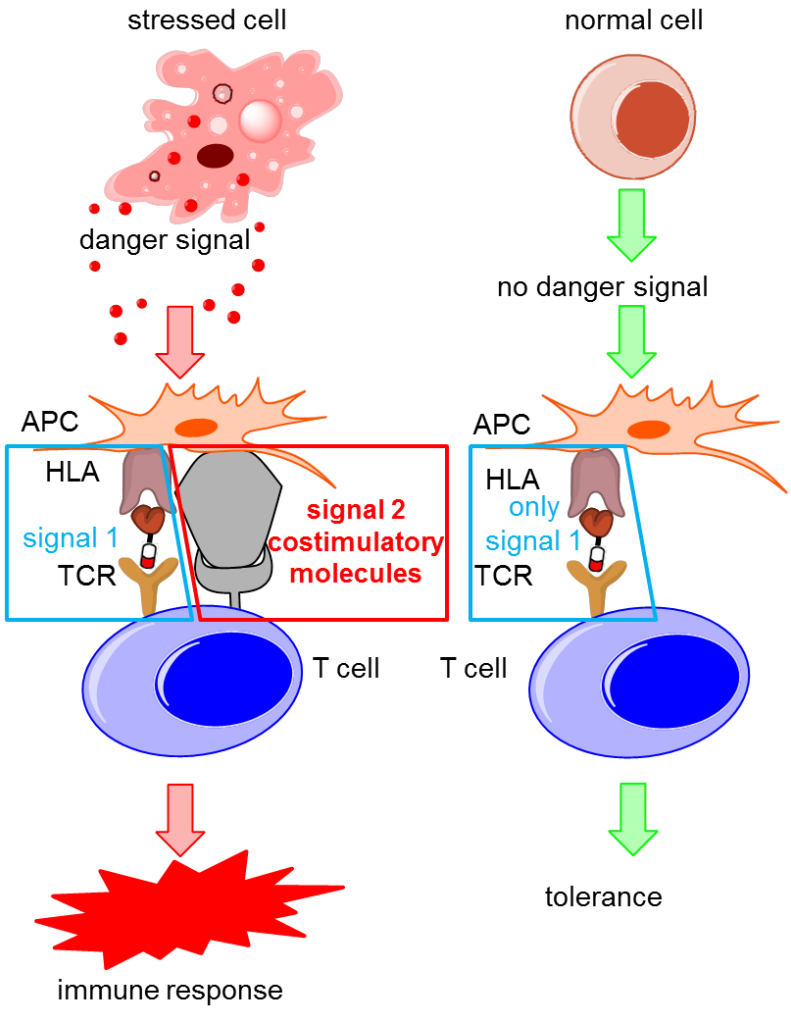

Figure 1.7: Danger hypothesis

Signal 1 occurs as described above for the hapten hypothesis (see Fig. 1.4). Signal 2 is present on the surface of antigen presenting cells (APCs) after the detection of danger such as infection or tissue damage. Only if both signals are present on the surface of the APC will the T cell be activated, resulting in an immune response. The absence of the second signal results in tolerance (adapted from Uetrecht, 2007 [49]).

1.6 Cell Death

To maintain and ensure the functioning of tissues, the body needs to renew cells as well as dispose of infected, malfunctioning or old cells. Different modes of cell death have been described [180]. The best known forms of cell death are apoptosis and necrosis. Due to different definitions for these cell death pathways, the Society of Toxicologic Pathologists formed a committee on the Nomenclature of Cell Death, which first made recommendations for the definition and use of the terms apoptosis and necrosis [181]. This committee later included other forms of cell death and provided definitions and recommendations for the newly discovered cell death pathways [180, 182]. In the beginning, the cell death pathways were defined by morphological changes observed during the cell death. In 2012, the committee proposed a change of the definitions from the system based on morphological characteristics to a system based on functional aspects (quantifiable biochemical properties) [183]. The two main advantages of the new system are: (1) the observed effect is quantifiable and (2) the interpretation of the results is not dependent on the experimenter. According to the definition on functional aspects, cell death pathways can be classified as accidental or regulated, with programmed cell death presenting a subcategory of regulated cell death. The biochemical properties, which define the cell death pathway include, enzymes activated during the process and immunological characteristics. The enzymes activated during cell death include proteases and nucleases. The definition based on the immunological characteristics focuses on whether the death of the cell results in an immune reaction in the surrounding tissue or not [184].

The most important forms of cell death for the work carried out in this thesis are apoptosis and necrosis, which will be discussed in greater detail. Other cell death pathways will be mentioned in brief.

1.6.1 Apoptosis

Apoptosis plays an important role during the development of organs and tissues and is essential for maintaining the functionality of an organism [185-187]. For example, apoptosis is the central process leading to the elimination of activated immune cells and termination of the immune response [188]. During bacterial or viral infections, the apoptosis of infected cells acts as a defensive mechanism as it destroys the pathogen and the source of pathogen production. Apoptosis is a highly regulated process and does not disturb the surrounding tissue.

Morphological characteristics of apoptosis include detachment from neighbouring cells, shrinkage of the cell, condensation of chromatin, fragmentation of the nucleus, membrane blebbing resulting in the shedding of apoptotic bodies, and phagocytosis of the apoptotic bodies [189]. A important feature of apoptotic cell death is that the process does not cause inflammation (immunologically silent) [190].

Apoptosis was first described as programmed cell death by Currie in 1972 [189]. In mammals, there are two major pathways by which apoptosis can be initiated in response to a variety of signals. These apoptotic pathways are the extrinsic (death receptor) and the intrinsic (mitochondrial) pathway. The extrinsic apoptotic pathway is initiated by extrinsic signals such as the binding of death-inducing ligands to death receptors on the cell surface. In contrast, the intrinsic pathway is activated through intrinsic signals, such as DNA damage, and the mitochondria play a central role [191].

The activation of the extrinsic pathway is initiated by the binding of death-inducing ligands to death receptors. These receptors belong to the tumour necrosis factor (TNF) receptor family, such as the TNF receptor, TNF-related apoptosis-inducing ligand receptor and Fas receptor. These receptors are involved also in other cellular processes, including proliferation and differentiation [192]. The best studied pathway is the Fas pathway, which also plays an important role in immune responses. For example, the elimination of infected cells by cytotoxic T cells as well as the deletion of activated T cells after an immune response is mediated via the Fas pathway

[193]. After Fas ligand binding, activated Fas receptors trimerize and a death-inducing signalling complex (DISC) is formed [194]. The trimerization allows Fas-associated death domain adaptor proteins to be recruited, through interactions between the death domains of the adaptor proteins and DISC. The adaptor proteins contain death effector domains, which bind procaspase-8 and -10 [195]. Caspase-8 is the main initiator in the Fas signalling of apoptosis. The clustering in the death-inducing complex composed of Fas, Fas-associated death domain and procaspase-8 leads to the cleaving of prodomain in procaspase-8, its dimerization, and the release of the active caspase. The activated caspase-8 subsequently initiates a caspase cascade reaction which leads to the activation of the executioner caspase. Additionally, caspase 8 cleaves Bcl-2-homology 3-only protein, a member of the protein family responsible for controlling apoptosis via the mitochondrial apoptosis [196], and thus also initiates the mitochondrial apoptotic pathway [197, 198].

The activation of caspase is an important indication for apoptosis as the caspase cascade orchestrates various processes [199]. Active caspase can be detected as early as 10-15 min. after triggering apoptosis by the extrinsic pathway [200, 201]. There are 14 different caspases known in mammals which all share important features. Caspases are expressed as inactive proenzymes consisting of a prodomain followed by a large and a small subunit. Cleaving of the prodomain and dimerization of caspase result in its activation. All caspases cleave substrates at an Asp-XXX motif and their catalytic triad consists of Cys285, His237 and a carbonyl group at residue 177 [202]. The 14 caspases can be divided into three groups based on their function. The first group consists of inflammatory caspases and includes caspase-1, -4, -5, -11, -12, -13, and -14. These caspases are involved in inflammation rather than apoptosis. The second group represents the initiator caspases and contains caspase-2, -8, -9, and -10. These caspases have long prodomains, which contain motifs that allow their recruitment to the complexes formed during the initiation of the apoptosis. Caspase-8 and -10 are the initiator caspases in the extrinsic pathway and possess a death effector domain [203]. This domain is needed for the interaction and

activation by the death-inducing signalling complex. Caspase-2 and -9 are involved in the initiation of the intrinsic pathway and their prodomain contains a caspase activation and recruitment domain, responsible for the interaction and activation by the apoptosome [204]. The last group of caspases are the apoptotic effector caspases and includes caspase-3, -6, and -7. Experiments with caspase-3 knockout mice suggest that caspase-3 is the most important of the executioner caspases, while caspase-6 and -7 appear to be rather redundant [205-207]. Their prodomain is short and they are generally activated by initiator caspases. After activation, they cleave multiple cellular substrates including apoptotic regulators, structural proteins, proteins involved in DNA repair, and regulators of the cell cycle [208]. DNases, such as the DNA fragmentation factor 45 kD subunit, are cleaved by caspase and thus activated, which results in the DNA fragmentation in the nucleus [209, 210]. The activation of pro-apoptotic kinases results in the formation of apoptotic bodies [211], which is supported by the cleaving of the structural proteins, such as fodrin and gelsolin (actin filament network) [212, 213]. The inactivation of DNA repair mechanisms serves the purpose of saving energy needed for the completion of apoptosis, while cleaving cell cycle regulators promotes apoptotic signalling [214].

The mitochondria are the main regulator of the intrinsic pathway of apoptosis. The most important event in the intrinsic pathway is the permeabilisation of the mitochondrial membrane (MMP), which is controlled by members of the B cell lymphoma-2 (Bcl-2) protein family. Through MMP, pro-apoptotic molecules are released while the essential functionality of mitochondria is lost, and thus production of energy within the cell is impossible [215]. The members of the Bcl-2 protein family belong either to the pro-survival (e.g. Bcl-2) or the pro-apoptotic group (e.g. Bax and Bak). Proteins of the Bcl-2 family are expressed in the cell and localised in the membrane of mitochondria and endoplasmic reticulum [216]. Members of the pro-survival group can inhibit apoptosis by neutralising members of the pro-apoptotic group. The proportion of anti- to pro-apoptotic proteins is important for the survival and the susceptibility to intrinsic apoptosis of the cell [217]. Various stimuli, such as DNA damage or cytotoxic insult, can trigger the

transcription of pro-apoptotic Bcl-2 proteins inside the cell inducing the intrinsic apoptotic pathway. Upon the detection of DNA damage for example, p53 regulates the transcription of Bax [218]. The higher proportion of pro-apoptotic Bcl-2 proteins (e.g. Bax and Bak) in the outer membrane of the mitochondria induces the formation of pores in the outer membrane, resulting in its permeabilisation, and the initiation of apoptosis. The permeabilisation of mitochondria leads to the release of cytochrome c into the cytosol [215]. In the presence of ATP, cytochrome c binds to apoptosis protease activating factor 1, which leads to the formation of the apoptosome [219]. The apoptosome then recruits procaspase-9 that becomes activated and forms dimers. Caspase-9 cleaves and activates the executioner caspases.

Besides the mitochondria, the endoplasmic reticulum (ER) can also initiate the intrinsic apoptotic pathway. The ER hosts mechanisms, which control and ensure that proteins are folded in the right confirmation. Oxidative stress and chemical toxicity can lead to misfolded proteins, which have to be unfolded. To prevent accumulation of unfolded proteins and to refold them, the protein synthesis is decreased, chaperons and folding catalysts are induced, and ER-associated protein degradation is activated to eliminate possible aggregates [220, 221]. If these countermeasures do not resolve the problem of misfolded proteins, cell death is initiated by calcium ions release from the ER [222]. The released calcium ions are then taken up by the mitochondria, resulting in cytochrome c release, which in turn increases the release of calcium ions by the ER. The cytochrome c release leads to the formation of the apoptosome, resulting in the activation of the executioner caspases. It has been shown that ER-mediated apoptosis plays a pathogenic role in neurodegenerative disorders such as Alzheimer’s disease and Parkinson’s disease [223].

The clearance of apoptotic bodies through phagocytosis before these lose membrane integrity and cellular content leaks into the surrounding tissue, is important to prevent an immune response in the surrounding tissue. This also presents a protective mechanism from potentially cytotoxic or pathogenic contents by preventing them from spreading further in the body [224]. The process of this clearance itself is also important for the prevention

of an immune response, as during the consummation of apoptotic cells, phagocytes release anti-inflammatory mediators, including transforming growth factor β, interleukin-10 and prostaglandin E_2, while the release of pro-inflammatory mediators such as TNF α is inhibited [225]. The migration of phagocytes to the site of apoptosis is accomplished through attraction signals. Apoptotic cells secrete chemo-attractants, such as lysophosphatidylcholine, which lead to the migration of monocytes and macrophages to the apoptotic cells. After the migration, the phagocytes recognise and consume the apoptotic cells via the so called ‘eat-me’ signal [226]. The apoptotic cell undergoes surface changes during apoptosis. Early on during apoptosis, phosphatidylserine (PS), which is normally localised on the inner side of the outer membrane, is exposed on the cell surface. PS can be found in discrete patches on the outer membrane and present the ‘eat-me’ signal [227]. Bridging molecules from the serum, such as β2 glycoprotein I, serum protein S, and growth arrest-specific 6, bind to PS exposed on the outer membrane and link the apoptotic cell to phagocytes, which leads to uptake and phagocytosis [228].

1.6.2 Necrosis

Necrosis was long considered an accidental and uncontrolled pathway of cell death [229]. According to this theory, necrosis happens as a result of the inability of the cell to undergo apoptosis [230] or as a result of physical or chemical damage [231, 232]. Growing evidence changed the few of necrosis being only accidental and suggests that a regulated, caspase-independent pathway of cell death with the morphologic characteristics of necrosis exists, which contributes to the development of the body as a backup mechanism of cell death [233].

The controlled form of necrosis was named necroptosis. It was first observed in cells in which the caspase cascade was inhibited, but where TNF α and Fas ligand were found to cause cell death [234, 235]. In *in vitro* experiments utilising caspase inhibitors, such as Carbobenzoxy-valyl-alanyl-aspartyl-(O-methyl)-fluoromethylketone (Z-VAD-FMK), cells have been shown to die via

an organised pathway displaying morphological characteristics resembling necrosis [236, 237]. Even though the precise mechanism of necroptosis is not completely understood, it is clear that receptor-interacting protein kinase (RIPK) 1 and 3 play an important role [238]. During extrinsic apoptosis, the formed death-inducing signalling complex activates caspase-8, which then cleaves RIPK1 and leads to the activation of the executioner caspases thus resulting in apoptosis. During the absence of caspase-8 activity, RIPK1 is not cleaved and forms a complex with the death-inducing signalling complex and procaspase-8. This complex recruits RIPK3 and is called necrosome. Mixed lineage kinase domain-like (MLKL) protein is phosphorylated by the necrosome and activates a protein phosphatase located in the mitochondria, which then inactivates a dynamin-related GTPase and leads to mitochondrial fragmentation [239]. It was also observed that MLKL transfers to the cell membrane where it activates non-voltage-sensitive ion channels, which results in an increased concentration of calcium ions in the cell [240]. Calcium ion overload leads to the opening of large nonselective pores in the mitochondria, which results in the rupture of the mitochondria. Furthermore, calcium ion overload activates phospholipases, proteases, and neuronal nitric oxide synthase, which all contribute to the execution of necroptosis [241].

Necrosis can be best distinguished from apoptosis through the morphology of the cell during the process (see Fig. 1.8). Characteristics include swelling of the cell, dysfunction of mitochondria, and rupture of the cellular membrane. In contrast to apoptosis, no DNA degradation is observed. The cell rupture leads to the leakage of cellular content into the extracellular space and act as DAMPs, which causes inflammation in the surrounding tissue [242]. Necrosis of a cell disturbs the function of the surrounding cells greatly and can even force them to undergo cell death.

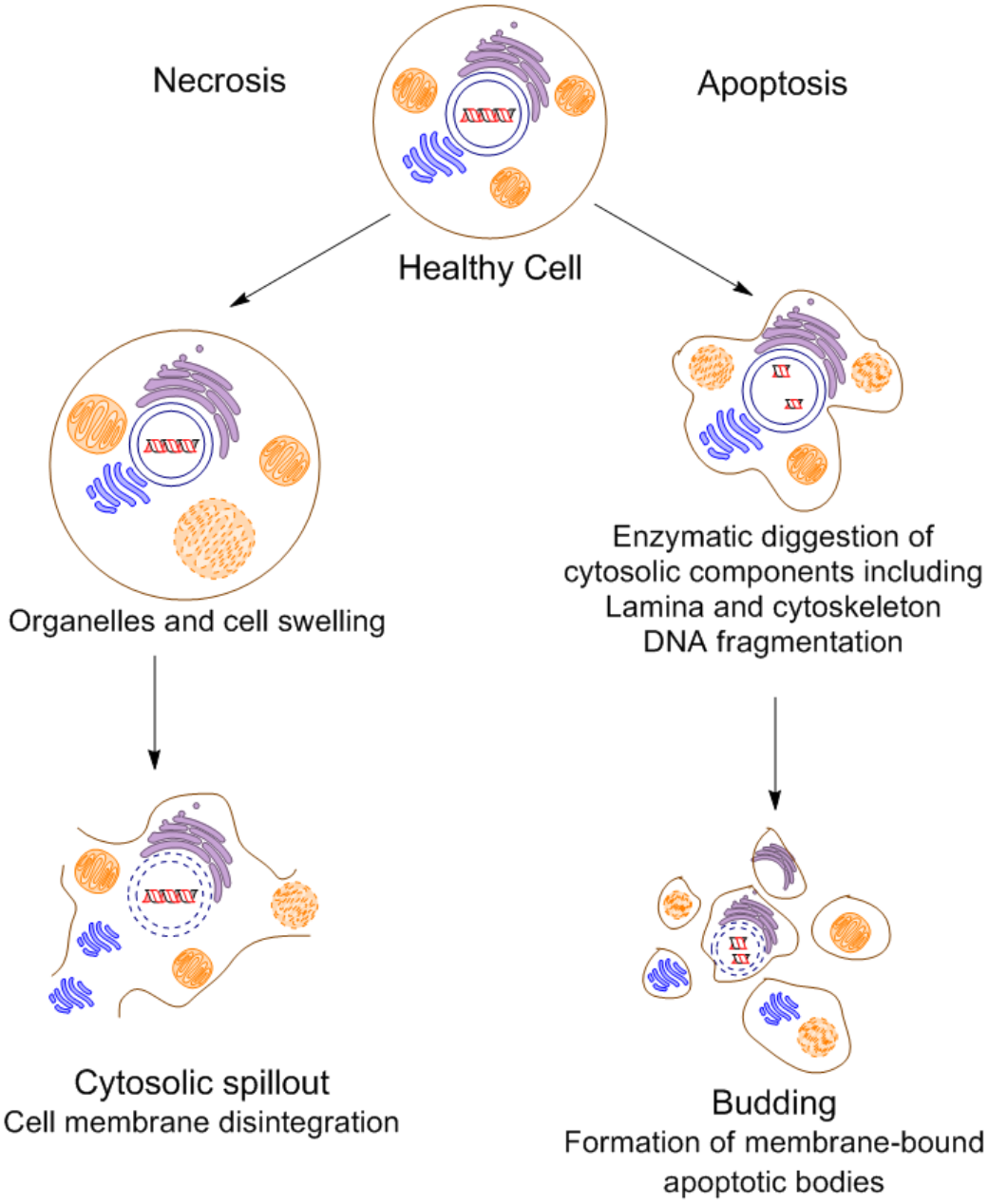

Figure 1.8: Cell death. Difference between apoptosis and necrosis

Necrosis: after the initial cell damage, the cell and the organelles start swelling. In mitochondria this can lead to the loss of membrane integrity and the release of cytochrome c. Further swelling of the cell will lead to cell rapture and cause the spillage of cytosolic content into the extracellular space which leads to inflammation in the surrounding tissue. **Apoptosis:** Triggered either through extrinsic or intrinsic pathway which leads to the activation of caspases, which in turn causes the digestion of cytosolic components, including the cytoskeleton, and the fragmentation of the DNA. This is followed by budding where apoptotic bodies containing components of cell are formed out of the cell membrane. During the whole process the integrity of the membrane is maintained and no inflammation occurs in the surrounding tissue.

1.6.3 Other cell death pathways

Autophagy is a cellular mechanism with the purpose to dismantle and recycle proteins and organelles. At normal levels, autophagy ensures the function of the cell by digestion of malfunctioning proteins or organelles [243]. It is still debated whether autophagy alone is the cause of cell death or accompanies apoptosis or necrosis. However, it has been shown that increased levels or incomplete autophagy can lead cell death [244]. Mammalian target of rapamycin (mTOR) plays a central role in autophagy. Upon inhibition of mTOR, an autophagosome, a double membrane vesicle, is formed around the organelle or protein and is transported to a lysosome [245]. The lysosome and the autophagosome merge and the engulfed structure is degraded. In the case of autophagic cell death, the mitochondria release cytochrome c through pores formed by Bax and Bak. In contrast to apoptosis, the formation of pores is mediated either by products of the autophagy related genes or by proteases, leaked out of the lysosome [246, 247].

Mitotic catastrophe has been defined as another cell death pathway, which can happen during or shortly after unsuccessful mitosis. It has been mainly observed in cells display micronuclei or multiple nuclei after mitosis [248]. This feature is seen as the main difference between mitotic catastrophe, and apoptosis and necrosis [249]. However, the cell death that occurs after unsuccessful mitosis activates pathways for apoptosis or necrosis and shows morphological characteristics of either of these processes [250]. These observations suggest that mitotic catastrophe is a different way of triggering either apoptosis or necrosis.

In the last two decades many new cell death pathways have been discovered [251-254]. However, further research is required to determine whether these are novel cell death pathways or different modes of already known pathways as they exhibit similar morphological characteristics [180].

Anoikis was first described in 1994 [255]. It describes an apoptotic response as a result of the loss of cell-cell interaction. The molecular cascade initiated in anoikis is triggered by the lack of signalling that normally derives from interaction between neighbouring cells within the tissue [256, 257]. It is important to point out, that the cell death is executed by the same mechanism as intrinsic apoptosis.

Entosis describes a cell death mechanism in which cells can be found engulfed in cells that are not phagocytes and was previously described as ‘cell cannibalism’ [253, 258, 259]. It was shown that the downregulation of proteins needed for the formation of junctions between the cells lead to the engulfment of cells [260]. After the engulfment, entosis progresses following a non-apoptotic pathway, thus distinguishing entosis from anoikis [253, 261].

Parthanatos has been introduced as a cell death pathway mediated by DNA damage-responsive enzymes. Under normal physiological conditions of mild DNA damage, these enzymes interact with the DNA repair enzymes to restore DNA [262]. Extensive activation of DNA repair enzymes leads to several toxic effects in the cell including energy depletion and MMP [263-265]. Due to the energy depletion, parthanatos is a caspase-independent programmed cell death pathway.

Pyroptosis is a caspase-1 dependent form of cell death, which exhibits morphological characteristics of apoptosis and necrosis [266]. One necrotic characteristic of pyroptosis is the formation of pores in the cell membrane, which results in the rupture of the cell. Apoptotic characteristics include MMP and DNA fragmentation. Pyroptosis is triggered by the recognition of PAMPs through toll-like receptors or DAMPs through NOD-like receptors. This leads to the formation of a large signalling complex referred to as inflammasome [267]. The inflammasome activates procaspase-1, which is the main caspase in the execution of pyroptosis. Activated caspase-1 forms pores in the plasma membrane of the cell, which leads to water influx and the lysis of the cell [268].

Netosis is a cell death mode that can be only observed in granulocytes. Granulocytic cells undergoing netosis show vast vacuolisation of the

cytoplasm, and fast chromatin decondensation as well as degradation of cellular membranes leading to the formation of neutrophil extracellular traps [269]. It was shown that inhibitors of apoptosis and programmed necrosis do not prevent netosis, suggesting that a different mechanism for the execution is involved [270].

Cornification describes a physiological cell death pathway that only appears in keratinocytes [269]. Through cornification, the stratum corneum is formed. The stratum corneum is a layer of dead keratinocytes containing various proteins and lipids needed for different characteristics of the skin including structural stability, mechanical resistance, elasticity and hydrophobia. Experiments suggested that caspase-14 plays an important role in the process of cornification [271].

1.7 Carbamazepine

CBZ is one of the most commonly prescribed drugs for the treatment of epilepsy in patients with partial and generalised seizures. It is also prescribed for the treatment of neuropathic pain syndromes or as a mood stabiliser in bipolar disorders [272, 273].

It was first synthesised in the late 1950s in Switzerland. The synthesis was first described by Schindler in 1954 [274] and its antiepileptic effect was discovered by Theobald and Kunz in 1963 [275].

The chemical name of CBZ according to the International Union of Pure and Applied Chemistry (IUPAC) is either 5*H*-dibenzo[b,f]azepine-5-carboxamide or 5-carbamyl-5H-dibenzo[b,f]azepine. It is a derivative of iminostilbene and has a tricyclic structure [276]. The antiepileptic properties derive from the carbamyl group in the 5-position as 5*H*-dibenzo[b,f]azepine and its derivatives show only modest antiepileptic activity. This antiepileptic activity is further enhanced by the double bond at the 10 and 11 position.

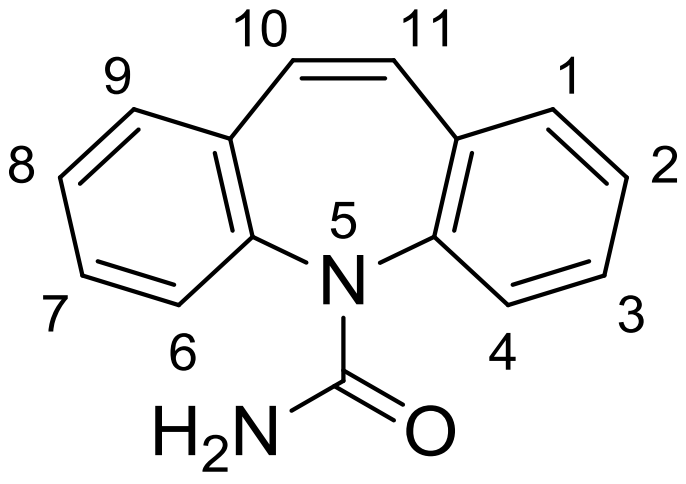

Figure 1.9: Chemical structure of carbamazepine

The mechanism of action for CBZ is not well understood. The many functions that have been discovered can be divided into two general mechanisms [277]:

1. Effects on neuronal ion channels
2. Effect on synaptic and postsynaptic transmission

The antiepileptic effect is believed to result from effects on neuronal ion channels. It reduces high-frequency repetitive firing of action potentials which occur during seizures by stabilising the inactive state of the voltage-gated sodium channels. This decreases the sodium influx into the neuron and makes the neurons less likely to prolong the action potential shortly after another one has been prolonged [278].

1.7.1 Pharmacokinetics

CBZ is slowly absorbed in the digestive tract. The reason for this is the rate with which CBZ dissolves in the gastrointestinal fluid, due to its nonpolar structure, which also increases its gastrointestinal transit time.

Peak plasma concentration is reached between four to eight hours after administration but it has been reported that in some cases, peak plasma concentration was only observed after as long as 26 hours [279]. Absolute bioavailability of CBZ is hard to determine because of the lack of an injectable formulation. The estimate however, ranges from 75% to 85%. After absorption, CBZ is distributed rapidly in all tissues and 73%-81% of CBZ in blood is bound to proteins, including albumin [280, 281].

CBZ is extensively metabolised *in vivo* with more than 30 known metabolites of CBZ many of which also have antiepileptic activity [282, 283]. CBZ is mainly metabolised in the liver by CYP enzymes. The main metabolic pathway is the oxidation of the double bond at the 10 and 11 position. This results in an epoxide, CBZ-10,11 epoxide [284]. The main CYP isoform involved is CYP 3A4 [285]. CBZ induces its own metabolism by increasing the activity of CYP 3A4 [286]. Up to 50% of CBZ-10,11 epoxide can be found

in plasma compared to concentrations of CBZ. The epoxide is then hydrolysed to a dialcohol, CBZ-10,11 diol. This diol is then conjugated and excreted by renal clearance.

Different metabolic pathways have been described, which include a hypothesised arene oxide and a ring contraction of CBZ (see Fig. 1.10). The hypothetical arene oxide is highly reactive and has not been found *in vivo* [287]. Detoxification products have been found in rat bile that can only be explained with an arene oxide intermediate [288]. The structure is then further metabolised. This results in a single or a double alcohol group at one of the benzene rings. The single alcohol can be further metabolised into iminoquinone, via iminostilbene, before being excreted. The dialcohol gets transformed into a quinone.

Another metabolic pathway leads to a ring contraction, catalysed by the myeloperoxidase. This reaction is assumed to take place predominantly in the blood. The ring contraction results in an acridine structure, which is then conjugated and excreted [289].

The half-life of CBZ ranges from 18 to 55 hours. As CBZ induces its own metabolism by increasing the activity of CYP 3A4, the half-life on long term treatment decreases to 5 to 6 hours. The half-life for the main metabolite CBZ-10,11 epoxide is six to seven hours, and therefore much shorter than that of CBZ.

Because of the auto-induction of CBZ, treatment is normally started with a lower daily dose of 100 to 200 mg to avoid toxic effects. It is then adjusted according to the response and plasma concentration of the patient. The therapeutic dose ranges from 4 to 15 µg/ml plasma concentration.

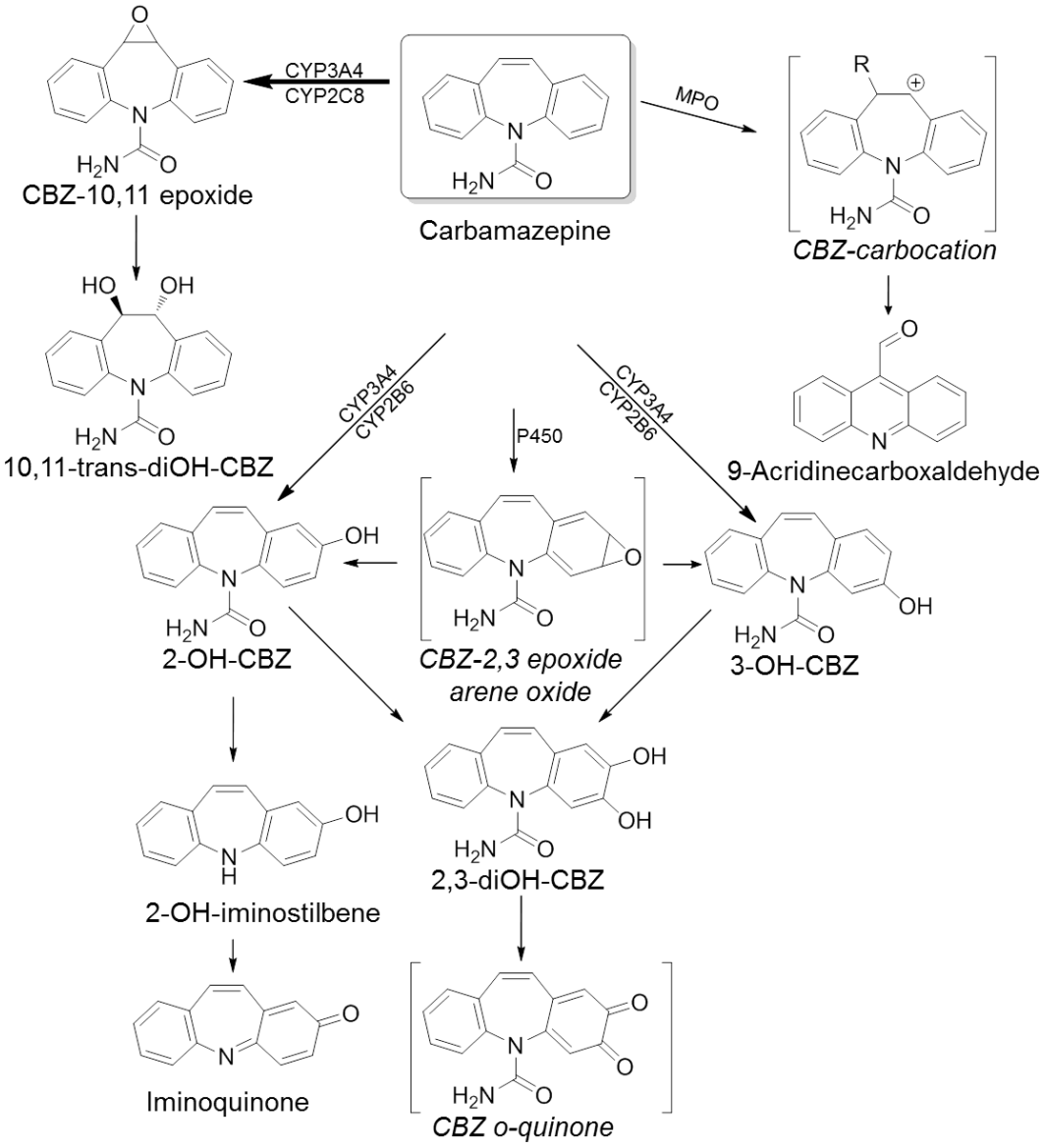

Figure 1.10: Metabolism of carbamazepine

Carbamazepine (CBZ) is extensively metabolised. This is a brief overview of several pathways. The main pathway, via the CBZ-10,11 epoxide to the CBZ-10,11 dialcohol, is catalysed by cytochrome P450 (CYP). In addition, the pathway via the single alcohol group on the benzene ring or the theoretical arene oxide is catalysed by CYP. These alcohols can be further metabolised to the 2,3-dialcohol of CBZ, which can then be transformed into CBZ quinone. The 2-alcohol of CBZ can be metabolised into iminoquinone via an iminostilbene alcohol.

1.7.2 Carbamazepine-induced adverse effects

Patients treated with CBZ can suffer from several adverse effects, which could be dose-dependent and dose-independent. CBZ also causes teratogenic effects during pregnancy [290].

Dose-dependent CBZ-induced toxicity can commonly be observed during the start of treatment within hours after administering a dose. The symptoms include blurred vision, dizziness, nausea, ataxia, sedation, and diplopia. Higher concentrations are associated with reduction in alertness and diminished pain sensation. The effects are reversible by dose reduction. During acute intoxication, seizures, impairment of consciousness, coma and death can be observed [291-293]. For this reason, treatment is started at a low dose and then continuously increased until the desired level is reached.

1.7.3 Hypersensitivity reactions

The dose-independent side effects are less frequent. They include skin rashes and abnormal organ function, mostly seen in the liver [294, 295]. Mild skin rashes are the most common form of hypersensitivity reactions and can be observed in up to 10% of patients treated with CBZ [296]. These can develop into severe CBZ-induced hypersensitivity reactions. The most severe forms comprise SJS, TEN and DRESS as described under the clinical manifestations of cutaneous drug reactions (see section 1.2.2). DRESS associated with rash, fever, eosinophilia and internal organ involvement, generally occurs during the first eight weeks of therapy with an estimated frequency of 4 in 10 000 [80, 297]. The most severe skin reactions SJS and TEN occur in Caucasians rarely with an estimated frequency of 1 in 10 000 [298]. In Han Chinese, the occurrence of SJS and TEN is roughly ten-fold higher [299]. These severe DHRs often cannot be predicted and require close monitoring of the patient.

1.7.3.1 Pharmacogenetics

CBZ-induced hypersensitivity reactions were thought to have a genetic origin. This theory was supported by reports of hypersensitivity reactions observed in members of the same family and in monozygotic twins [300]. These studies have suggested that reactive metabolites of CBZ, such as arene oxides, cause cytotoxicity and thus trigger an immune response. Case reports supported that the DHRs of CBZ have a genetic association and that genetic polymorphisms in metabolising enzymes might be involved [300, 301]. For example, a case report demonstrated that a patient that had developed DHRs during treatment with CBZ possessed a less active form of an epoxide hydroxylase which is necessary for the metabolism of CBZ epoxide to the CBZ diol [302]. Therefore studies have focused on genetic differences in metabolising enzymes, particularly enzymes involved in the detoxification of CBZ such as microsomal epoxide hydroxylase, glutathione transferase, catechol-O-methyl transferase, and quinone reductase [300]. However, the results failed to show any association [303, 304]. Furthermore, antibodies against CYP isoforms involved in the metabolism of CBZ have been detected in patients with DHRs [305]. This observation led to the suggestion that reactive metabolites of CBZ bind to CYP enzymes, act as haptens and activate the adaptive immune system as per the hapten hypothesis. However, a genetic association between isoforms of CYP and CBZ-induced hypersensitivity reactions has not been found [44, 306].

The first evidence of an association between genetic polymorphism in genes with immune function in epileptic patients on CBZ was found by Pirmohamed and colleagues [307]. They showed that a polymorphism in TNF α at position 308 together with HLA-DR3 and HLA-DQ2 increased the risk of Caucasian patients developing DRESS but not of any other forms of DHRs.

A major breakthrough was the identification of an association between particular HLA alleles and specific clinical phenotypes observed in patients suffering from CBZ-induced hypersensitivity reactions. In 2004, a strong association between CBZ-induced SJS/TEN and HLA-B*15:02 in Han Chinese has been reported [44]. All patients, which had suffered from SJS or

TEN were carriers of the HLA allele while it was only present in 3% of CBZ tolerant patients and in 8.6% of healthy volunteers [44]. The association was also found in other Southeast Asian populations, including Indians, Malaysians, and Thai [45, 308-310]. Other studies showed that HLA-B*15:02 is only associated with CBZ-induced SJS/TEN and not with other forms of CBZ-induced hypersensitivity reactions, including MPE and DRESS [306, 311]. The association between HLA-B*15:02 and DHRs was not found in Europeans, possibly due to the low frequency of the HLA-B*15:02 allele in Caucasians [312]. Due to the evidence for a strong association between HLA-B*15:02 and SJS/TEN, genetic testing for this allele is recommended by the regulatory committees in patients with Asian ancestry before the start of CBZ therapy [313].

Recently an association was discovered between HLA-A*31:01 and all clinical phenotypes of CBZ-induced hypersensitivity reaction. This association was found by two independent research groups in Japan and Europe [46, 314]. In Europeans, the presence of HLA-A*31:01 increased the risk of developing ADRs from 5 to 26%, while the absence decreased the risk from 5 to 3.8%. In Japanese patients, HLA-A*31:01 was found in 60% of the patients who had suffered from DHRs. It has been reported that this HLA allele is also associated with CBZ-induced MPE in Han Chinese [306]. Based on the evidence, the association of HLA-A*31:01 and CBZ-induced hypersensitivity reactions is included in the label of the drug [315].

1.7.3.2 Functional studies

The clinical phenotypes of CBZ-induced hypersensitivity reactions led to the assumption that these DHRs are immune-mediated. The detection of CBZ-specific T cells in patients with CBZ-induced hypersensitivity reactions supported the hypothesis [152, 316]. The discovery of the above mentioned genetic association suggests a direct involvement of specific HLA alleles in presenting CBZ to cytotoxic T cells, leading to a T cell mediated immune response.

The role of HLA-B*15:02 in the role of CBZ-induced SJS in patients has been well studied and described: the immune reaction is mediated by cytotoxic T cells, which interact with HLA-B*15:02 [317, 318]. One *in vitro* study showed that CBZ activated drug-specific T cells directly, without the need of drug metabolism [164]. It was also shown that the parent drug CBZ does not modify peptides presented by the HLA [319]. Furthermore, T cell stimulation by CBZ in the presence of chemically fixed APCs, incapable of antigen processing, has been demonstrated [316]. All these observations led to the assumption that CBZ interacts with HLA or the TCR, thus activating the cytotoxic T cells, as described in the p-i concept. Recently, it has been shown that CBZ binds directly but non-covalently to HLA-B*15:02 [317]. Computer modelling revealed that the 5-carboxamide group on the tricyclic ring of CBZ is responsible for the interaction and identified three possible sites for interaction in the binding grove of HLA-B*15:02. These findings are supported by another study in which the non-covalent binding of CBZ to HLA-B*15:02 was also observed [140]. Furthermore, the analysis of the peptides mounted on HLA-B*15:02 in the presence of CBZ showed a change towards peptides with increased hydrophobicity. This shift in preferred self-peptides in the presence of CBZ implies that drug-specific T cell stimulation occurs according to the altered self-peptide hypothesis.

1.8 Aims of Thesis

Case reports of patients suffering from CBZ-induced hypersensitivity reactions have found an involvement the adaptive immune system in DHRs. Additionally, experimental findings have shown strong evidence for an association between HLA class I genes and CBZ-induced DHRs. The discovery that CBZ changes the self-peptide repertoire by binding in the grove of HLA-B*15:02 shows that the altered self-peptide hypothesis is important during CBZ-induced hypersensitivity reactions [140]. It has been observed, that memory T cells have a lower threshold for activation and therefore do not require costimulatory signals for their activation [320, 321]. However, a considerable amount of patients carrying the risk allele do not suffer from hypersensitivity reactions when treated with CBZ. These experiments have used drug-specific T cells from hypersensitive patients. Therefore, the mechanism of drug-specific T cell formation in patients remains unclear. Furthermore, the discovery of antibodies against CBZ in sera of hypersensitive and tolerant patients suggests that other factors are necessary for the activation of T cells [322-325].

Following this observation, other possible mechanism for the formation of drug-specific T cells *in vitro* were investigated in this work, not only considering the parent drug CBZ but also metabolites of the drug.

The aims of this work were to:

1. Explore the involvement of the mechanism defined by the danger hypothesis in the induction of CBZ-induced hypersensitivity reactions by investigating the possible release of danger signals by cells exposed to CBZ and one of its metabolites.
2. Investigate the capability of CBZ and its metabolites to covalently modify proteins, leading to the formation of potentially immunogenic peptides, as described in the hapten hypothesis or signal 1 according to the danger hypothesis.

3. Discover new biomarkers for the assessment of a patient’s risk to suffer from CBZ-induced hypersensitivity reactions by finding genetic association with susceptibility of drug-caused toxicity and verifying these biomarkers in patient samples.
4. Validate different newly developed methods for HLA-A*31:01-typing and their possible application for patient screening in hospital.

1.9 References

1. Pirmohamed, M., et al., *Adverse drug reactions as cause of admission to hospital: prospective analysis of 18 820 patients.* BMJ, 2004. **329**(7456): p. 15-9.
2. Lazarou, J., B.H. Pomeranz, and P.N. Corey, *Incidence of adverse drug reactions in hospitalized patients: a meta-analysis of prospective studies.* JAMA, 1998. **279**(15): p. 1200-5.
3. Kvasz, M., et al., *Adverse drug reactions in hospitalized patients: A critique of a meta-analysis.* MedGenMed, 2000. **2**(2): p. E3.
4. Kongkaew, C., P.R. Noyce, and D.M. Ashcroft, *Hospital admissions associated with adverse drug reactions: a systematic review of prospective observational studies.* Ann Pharmacother, 2008. **42**(7): p. 1017-25.
5. Arnaiz, J.A., et al., *The use of evidence in pharmacovigilance. Case reports as the reference source for drug withdrawals.* Eur J Clin Pharmacol, 2001. **57**(1): p. 89-91.
6. *International drug monitoring: the role of national centres. Report of a WHO meeting.* World Health Organ Tech Rep Ser, 1972. **498**: p. 1-25.
7. Edwards, I.R. and J.K. Aronson, *Adverse drug reactions: definitions, diagnosis, and management.* Lancet, 2000. **356**(9237): p. 1255-9.
8. Rawlins, M.D. and J.W. Thompson, *Mechanism of adverse drug reactions*, in *Textbook of adverse drug reactions*. 1991, Oxford University. p. 18-45.
9. Thien, F.C., *3. Drug hypersensitivity.* Med J Aust, 2006. **185**(6): p. 333-8.
10. Royer, R.J., *Mechanism of action of adverse drug reactions: an overview.* Pharmacoepidemiol Drug Saf, 1997. **6 Suppl 3**: p. S43-50.
11. Hawkins, L.C., J.N. Edwards, and P.I. Dargan, *Impact of restricting paracetamol pack sizes on paracetamol poisoning in the United Kingdom: a review of the literature.* Drug Saf, 2007. **30**(6): p. 465-79.
12. Adab, N., et al., *Common antiepileptic drugs in pregnancy in women with epilepsy.* Cochrane Database Syst Rev, 2004(3): p. CD004848.
13. DeRossi, S.S. and E.V. Hersh, *Antibiotics and oral contraceptives.* Dent Clin North Am, 2002. **46**(4): p. 653-64.
14. Aronson, J.K. and R.E. Ferner, *Joining the DoTS: new approach to classifying adverse drug reactions.* BMJ, 2003. **327**(7425): p. 1222-5.
15. Williamson, J. and J.M. Chopin, *Adverse reactions to prescribed drugs in the elderly: a multicentre investigation.* Age Ageing, 1980. **9**(2): p. 73-80.
16. Dreifuss, F.E., et al., *Valproic acid hepatic fatalities: a retrospective review.* Neurology, 1987. **37**(3): p. 379-85.
17. Sharma, V.K., G. Sethuraman, and A. Minz, *Stevens Johnson syndrome, toxic epidermal necrolysis and SJS-TEN overlap: a retrospective study of causative drugs and clinical outcome.* Indian J Dermatol Venereol Leprol, 2008. **74**(3): p. 238-40.
18. Barranco, P. and M.C. Lopez-Serrano, *General and epidemiological aspects of allergic drug reactions.* Clin Exp Allergy, 1998. **28 Suppl 4**: p. 61-2.
19. Schopf, E., et al., *Toxic epidermal necrolysis and Stevens-Johnson syndrome. An epidemiologic study from West Germany.* Arch Dermatol, 1991. **127**(6): p. 839-42.
20. Khambaty, M.M. and S.S. Hsu, *Dermatology of the patient with HIV.* Emerg Med Clin North Am, 2010. **28**(2): p. 355-68, Table of Contents.
21. Shiohara, T., M. Inaoka, and Y. Kano, *Drug-induced hypersensitivity syndrome (DIHS): a reaction induced by a complex interplay among herpesviruses and antiviral and antidrug immune responses.* Allergol Int, 2006. **55**(1): p. 1-8.

22. Descamps, V., et al., *Association of human herpesvirus 6 infection with drug reaction with eosinophilia and systemic symptoms.* Arch Dermatol, 2001. **137**(3): p. 301-4.
23. Bayard, P.J., T.G. Berger, and M.A. Jacobson, *Drug hypersensitivity reactions and human immunodeficiency virus disease.* J Acquir Immune Defic Syndr, 1992. **5**(12): p. 1237-57.
24. Mitsuyasu, R., J. Groopman, and P. Volberding, *Cutaneous reaction to trimethoprim-sulfamethoxazole in patients with AIDS and Kaposi's sarcoma.* N Engl J Med, 1983. **308**(25): p. 1535-6.
25. Pullen, H., N. Wright, and J.M. Murdoch, *Hypersensitivity reactions to antibacterial drugs in infectious mononucleosis.* Lancet, 1967. **2**(7527): p. 1176-8.
26. Pirmohamed, M. and B.K. Park, *HIV and drug allergy.* Curr Opin Allergy Clin Immunol, 2001. **1**(4): p. 311-6.
27. Atkin, P.A. and G.M. Shenfield, *Medication-related adverse reactions and the elderly: a literature review.* Adverse Drug React Toxicol Rev, 1995. **14**(3): p. 175-91.
28. Harb, G.E. and M.A. Jacobson, *Human immunodeficiency virus (HIV) infection. Does it increase susceptibility to adverse drug reactions?* Drug Saf, 1993. **9**(1): p. 1-8.
29. Petri, M. and J. Allbritton, *Antibiotic allergy in systemic lupus erythematosus: a case-control study.* J Rheumatol, 1992. **19**(2): p. 265-9.
30. Lang, D.M., et al., *Increased risk for anaphylactoid reaction from contrast media in patients on beta-adrenergic blockers or with asthma.* Ann Intern Med, 1991. **115**(4): p. 270-6.
31. Riedl, M.A. and A.M. Casillas, *Adverse drug reactions: types and treatment options.* Am Fam Physician, 2003. **68**(9): p. 1781-90.
32. Park, B.K., M. Pirmohamed, and N.R. Kitteringham, *Idiosyncratic drug reactions: a mechanistic evaluation of risk factors.* Br J Clin Pharmacol, 1992. **34**(5): p. 377-95.
33. Evans, D.A., K.A. Manley, and K.V. Mc, *Genetic control of isoniazid metabolism in man.* Br Med J, 1960. **2**(5197): p. 485-91.
34. Summerscales, J.E. and P.D. Josephy, *Human acetyl CoA:arylamine N-acetyltransferase variants generated by random mutagenesis.* Mol Pharmacol, 2004. **65**(1): p. 220-6.
35. Shenfield, G.M., *Genetic polymorphisms, drug metabolism and drug concentrations.* Clin Biochem Rev, 2004. **25**(4): p. 203-6.
36. Pavlos, R., S. Mallal, and E. Phillips, *HLA and pharmacogenetics of drug hypersensitivity.* Pharmacogenomics, 2012. **13**(11): p. 1285-306.
37. Romano, A., et al., *Delayed hypersensitivity to aminopenicillins is related to major histocompatibility complex genes.* Ann Allergy Asthma Immunol, 1998. **80**(5): p. 433-7.
38. Zhang, F.R., et al., *HLA-B*13:01 and the dapsone hypersensitivity syndrome.* N Engl J Med, 2013. **369**(17): p. 1620-8.
39. Hetherington, S., et al., *Genetic variations in HLA-B region and hypersensitivity reactions to abacavir.* Lancet, 2002. **359**(9312): p. 1121-2.
40. Mallal, S., et al., *Association between presence of HLA-B*5701, HLA-DR7, and HLA-DQ3 and hypersensitivity to HIV-1 reverse-transcriptase inhibitor abacavir.* Lancet, 2002. **359**(9308): p. 727-32.
41. Vitezica, Z.G., et al., *HLA-DRB1*01 associated with cutaneous hypersensitivity induced by nevirapine and efavirenz.* AIDS, 2008. **22**(4): p. 540-1.
42. Martin, A.M., et al., *Predisposition to nevirapine hypersensitivity associated with HLA-DRB1*0101 and abrogated by low CD4 T-cell counts.* AIDS, 2005. **19**(1): p. 97-9.

43. Carr, D.F., et al., *Association of human leukocyte antigen alleles and nevirapine hypersensitivity in a Malawian HIV-infected population.* Clin Infect Dis, 2013. **56**(9): p. 1330-9.
44. Chung, W.H., et al., *Medical genetics: a marker for Stevens-Johnson syndrome.* Nature, 2004. **428**(6982): p. 486.
45. Locharernkul, C., et al., *Carbamazepine and phenytoin induced Stevens-Johnson syndrome is associated with HLA-B*1502 allele in Thai population.* Epilepsia, 2008. **49**(12): p. 2087-91.
46. McCormack, M., et al., *HLA-A*3101 and carbamazepine-induced hypersensitivity reactions in Europeans.* N Engl J Med, 2011. **364**(12): p. 1134-43.
47. Kashiwagi, M., et al., *Human leukocyte antigen genotypes in carbamazepine-induced severe cutaneous adverse drug response in Japanese patients.* J Dermatol, 2008. **35**(10): p. 683-5.
48. Hung, S.I., et al., *Common risk allele in aromatic antiepileptic-drug induced Stevens-Johnson syndrome and toxic epidermal necrolysis in Han Chinese.* Pharmacogenomics, 2010. **11**(3): p. 349-56.
49. Uetrecht, J., *Idiosyncratic drug reactions: current understanding.* Annu Rev Pharmacol Toxicol, 2007. **47**: p. 513-39.
50. Rawlins, M.D., *Clinical pharmacology. Adverse reactions to drugs.* Br Med J (Clin Res Ed), 1981. **282**(6268): p. 974-6.
51. Hausmann, O., B. Schnyder, and W.J. Pichler, *Drug hypersensitivity reactions involving skin.* Handb Exp Pharmacol, 2010(196): p. 29-55.
52. Uetrecht, J. and D.J. Naisbitt, *Idiosyncratic adverse drug reactions: current concepts.* Pharmacol Rev, 2013. **65**(2): p. 779-808.
53. Pirmohamed, M., *Pharmacogenetics of idiosyncratic adverse drug reactions.* Handb Exp Pharmacol, 2010(196): p. 477-91.
54. Ng, W., et al., *Animal models of idiosyncratic drug reactions.* Adv Pharmacol, 2012. **63**: p. 81-135.
55. Nierkens, S. and R. Pieters, *Murine models of drug hypersensitivity.* Curr Opin Allergy Clin Immunol, 2005. **5**(4): p. 331-5.
56. Uetrecht, J., *Role of animal models in the study of drug-induced hypersensitivity reactions.* AAPS J, 2005. **7**(4): p. E914-21.
57. Gell, P.G.H. and R.R.A. Coombs, *Clinical Aspects of Immunology*. 1963, Oxford: Blackwell.
58. Pichler, W.J., *Delayed drug hypersensitivity reactions.* Ann Intern Med, 2003. **139**(8): p. 683-93.
59. Schnyder, B. and W.J. Pichler, *Mechanisms of drug-induced allergy.* Mayo Clin Proc, 2009. **84**(3): p. 268-72.
60. Posadas, S.J. and W.J. Pichler, *Delayed drug hypersensitivity reactions - new concepts.* Clin Exp Allergy, 2007. **37**(7): p. 989-99.
61. Spellberg, B. and J.E. Edwards, Jr., *Type 1/Type 2 immunity in infectious diseases.* Clin Infect Dis, 2001. **32**(1): p. 76-102.
62. Clemenceau, B., et al., *Effector memory alphabeta T lymphocytes can express FcgammaRIIIa and mediate antibody-dependent cellular cytotoxicity.* J Immunol, 2008. **180**(8): p. 5327-34.
63. Britschgi, M., et al., *T-cell involvement in drug-induced acute generalized exanthematous pustulosis.* J Clin Invest, 2001. **107**(11): p. 1433-41.
64. Crowson, A.N., T.J. Brown, and C.M. Magro, *Progress in the understanding of the pathology and pathogenesis of cutaneous drug eruptions : implications for management.* Am J Clin Dermatol, 2003. **4**(6): p. 407-28.
65. Bigby, M., *Rates of cutaneous reactions to drugs.* Arch Dermatol, 2001. **137**(6): p. 765-70.
66. Hunziker, T., et al., *Comprehensive hospital drug monitoring (CHDM): adverse skin reactions, a 20-year survey.* Allergy, 1997. **52**(4): p. 388-93.

67. Bigby, M., et al., *Drug-induced cutaneous reactions. A report from the Boston Collaborative Drug Surveillance Program on 15,438 consecutive inpatients, 1975 to 1982.* JAMA, 1986. **256**(24): p. 3358-63.
68. Arndt, K.A. and H. Jick, *Rates of cutaneous reactions to drugs. A report from the Boston Collaborative Drug Surveillance Program.* JAMA, 1976. **235**(9): p. 918-23.
69. Apaydin, R., et al., *Drug eruptions: a study including all inpatients and outpatients at a dermatology clinic of a university hospital.* J Eur Acad Dermatol Venereol, 2000. **14**(6): p. 518-20.
70. Valeyrie-Allanore, L., B. Sassolas, and J.C. Roujeau, *Drug-induced skin, nail and hair disorders.* Drug Saf, 2007. **30**(11): p. 1011-30.
71. Roujeau, J.C., *Clinical heterogeneity of drug hypersensitivity.* Toxicology, 2005. **209**(2): p. 123-9.
72. Leclair, M.A., B. Maynard, and C. St-Pierre, *Acute generalized exanthematous pustulosis with severe organ dysfunction.* CMAJ, 2009. **181**(6-7): p. 393-6.
73. Sidoroff, A., et al., *Acute generalized exanthematous pustulosis (AGEP)--a clinical reaction pattern.* J Cutan Pathol, 2001. **28**(3): p. 113-9.
74. Zlotnik, A. and O. Yoshie, *Chemokines: a new classification system and their role in immunity.* Immunity, 2000. **12**(2): p. 121-7.
75. Chan, H.L., et al., *The incidence of erythema multiforme, Stevens-Johnson syndrome, and toxic epidermal necrolysis. A population-based study with particular reference to reactions caused by drugs among outpatients.* Arch Dermatol, 1990. **126**(1): p. 43-7.
76. Mockenhaupt, M., *The current understanding of Stevens-Johnson syndrome and toxic epidermal necrolysis.* Expert Rev Clin Immunol, 2011. **7**(6): p. 803-13; quiz 814-5.
77. Downey, A., et al., *Toxic epidermal necrolysis: review of pathogenesis and management.* J Am Acad Dermatol, 2012. **66**(6): p. 995-1003.
78. Pirmohamed, M., et al., *Phenotype standardization for immune-mediated drug-induced skin injury.* Clin Pharmacol Ther, 2011. **89**(6): p. 896-901.
79. Carroll, M.C., et al., *Drug-induced hypersensitivity syndrome in pediatric patients.* Pediatrics, 2001. **108**(2): p. 485-92.
80. Knowles, S.R., L.E. Shapiro, and N.H. Shear, *Anticonvulsant hypersensitivity syndrome: incidence, prevention and management.* Drug Saf, 1999. **21**(6): p. 489-501.
81. Amante, M.F., et al., *Dress syndrome and fulminant hepatic failure induced by lamotrigine.* Ann Hepatol, 2009. **8**(1): p. 75-7.
82. Naisbitt, D.J., et al., *Hypersensitivity reactions to carbamazepine: characterization of the specificity, phenotype, and cytokine profile of drug-specific T cell clones.* Mol Pharmacol, 2003. **63**(3): p. 732-41.
83. Naisbitt, D.J., et al., *Characterization of drug-specific T cells in lamotrigine hypersensitivity.* J Allergy Clin Immunol, 2003. **111**(6): p. 1393-403.
84. Masaki, T., et al., *Human herpes virus 6 encephalitis in allopurinol-induced hypersensitivity syndrome.* Acta Derm Venereol, 2003. **83**(2): p. 128-31.
85. Arakawa, M., et al., *Allopurinol hypersensitivity syndrome associated with systemic cytomegalovirus infection and systemic bacteremia.* Intern Med, 2001. **40**(4): p. 331-5.
86. Picard, D., et al., *Drug reaction with eosinophilia and systemic symptoms (DRESS): a multiorgan antiviral T cell response.* Sci Transl Med, 2010. **2**(46): p. 46ra62.
87. Murphy, K., et al., *Immunobilogy*. 8th ed. 2012, New York: Garland Science.
88. Delves, P.J. and I.M. Roitt, *The immune system. First of two parts.* N Engl J Med, 2000. **343**(1): p. 37-49.

89. Medzhitov, R. and C. Janeway, Jr., *Innate immune recognition: mechanisms and pathways.* Immunol Rev, 2000. **173**: p. 89-97.
90. Janeway, C.A., Jr., *Approaching the asymptote? Evolution and revolution in immunology.* Cold Spring Harb Symp Quant Biol, 1989. **54 Pt 1**: p. 1-13.
91. Khan, N., et al., *Manipulation of costimulatory molecules by intracellular pathogens: veni, vidi, vici!!* PLoS Pathog, 2012. **8**(6): p. e1002676.
92. Kumar, H., T. Kawai, and S. Akira, *Pathogen recognition in the innate immune response.* Biochem J, 2009. **420**(1): p. 1-16.
93. Matzinger, P., *Friendly and dangerous signals: is the tissue in control?* Nat Immunol, 2007. **8**(1): p. 11-3.
94. Bianchi, M.E., *DAMPs, PAMPs and alarmins: all we need to know about danger.* J Leukoc Biol, 2007. **81**(1): p. 1-5.
95. Oppenheim, J.J., et al., *Alarmins initiate host defense.* Adv Exp Med Biol, 2007. **601**: p. 185-94.
96. Kono, H. and K.L. Rock, *How dying cells alert the immune system to danger.* Nat Rev Immunol, 2008. **8**(4): p. 279-89.
97. Terunuma, H., et al., *Potential role of NK cells in the induction of immune responses: implications for NK cell-based immunotherapy for cancers and viral infections.* Int Rev Immunol, 2008. **27**(3): p. 93-110.
98. Herzenberg, L.A., *B-1 cells: the lineage question revisited.* Immunol Rev, 2000. **175**: p. 9-22.
99. Engel, I. and C. Murre, *Disruption of pre-TCR expression accelerates lymphomagenesis in E2A-deficient mice.* Proc Natl Acad Sci U S A, 2002. **99**(17): p. 11322-7.
100. Greenbaum, S. and Y. Zhuang, *Regulation of early lymphocyte development by E2A family proteins.* Semin Immunol, 2002. **14**(6): p. 405-14.
101. Schebesta, M., B. Heavey, and M. Busslinger, *Transcriptional control of B-cell development.* Curr Opin Immunol, 2002. **14**(2): p. 216-23.
102. Mitchison, A., *Latent help to and from H-2 antigens.* Eur J Immunol, 1992. **22**(1): p. 123-7.
103. Tamm, A. and R.E. Schmidt, *IgG binding sites on human Fc gamma receptors.* Int Rev Immunol, 1997. **16**(1-2): p. 57-85.
104. Behrens, G., et al., *Helper T cells, dendritic cells and CTL Immunity.* Immunol Cell Biol, 2004. **82**(1): p. 84-90.
105. Ho, I.C. and L.H. Glimcher, *Transcription: tantalizing times for T cells.* Cell, 2002. **109 Suppl**: p. S109-20.
106. Abbas, A.K., K.M. Murphy, and A. Sher, *Functional diversity of helper T lymphocytes.* Nature, 1996. **383**(6603): p. 787-93.
107. Zinkernagel, R.M. and P.C. Doherty, *Restriction of in vitro T cell-mediated cytotoxicity in lymphocytic choriomeningitis within a syngeneic or semiallogeneic system.* Nature, 1974. **248**(5450): p. 701-2.
108. Rudolph, M.G., R.L. Stanfield, and I.A. Wilson, *How TCRs bind MHCs, peptides, and coreceptors.* Annu Rev Immunol, 2006. **24**: p. 419-66.
109. Turner, S.J., et al., *Structural determinants of T-cell receptor bias in immunity.* Nat Rev Immunol, 2006. **6**(12): p. 883-94.
110. Horton, R., et al., *Gene map of the extended human MHC.* Nat Rev Genet, 2004. **5**(12): p. 889-99.
111. Beck, S., et al., *Complete sequence and gene map of a human major histocompatibility complex.* Nature, 1999. **401**(6756): p. 921-923.
112. Klein, J. and A. Sato, *The HLA system. First of two parts.* N Engl J Med, 2000. **343**(10): p. 702-9.
113. Gorer, P.A., *The detection of a hereditary antigenic difference in the blood of mice by means of human group A serum.* Journal of Genetics, 1936. **32**(1): p. 17-31.
114. Dausset, J., *[Iso-leuko-antibodies].* Acta Haematol, 1958. **20**(1-4): p. 156-66.

115. Choo, S.Y., *The HLA system: genetics, immunology, clinical testing, and clinical implications.* Yonsei Med J, 2007. **48**(1): p. 11-23.
116. Deng, L., et al., *A structural basis for antigen recognition by the T cell-like lymphocytes of sea lamprey.* Proc Natl Acad Sci U S A, 2010. **107**(30): p. 13408-13.
117. Kindt, T.J., B.A. Osborne, and R.A. Goldsby, *Kuby Immunology*. 2006: W. H. Freeman & Company.
118. Speir, J.A., et al., *Two different, highly exposed, bulged structures for an unusually long peptide bound to rat MHC class I RT1-Aa.* Immunity, 2001. **14**(1): p. 81-92.
119. Neefjes, J., et al., *Towards a systems understanding of MHC class I and MHC class II antigen presentation.* Nat Rev Immunol, 2011. **11**(12): p. 823-36.
120. Rammensee, H.G., *Chemistry of peptides associated with MHC class I and class II molecules.* Curr Opin Immunol, 1995. **7**(1): p. 85-96.
121. Robinson, J., et al., *The IMGT/HLA database.* Nucleic Acids Res, 2013. **41**(Database issue): p. D1222-7.
122. Vandiedonck, C. and J.C. Knight, *The human Major Histocompatibility Complex as a paradigm in genomics research.* Brief Funct Genomic Proteomic, 2009. **8**(5): p. 379-94.
123. McCluskey, J., C. Kanaan, and M. Diviney, *Nomenclature and serology of HLA class I and class II alleles.* Curr Protoc Immunol, 2003. **Appendix 1**: p. Appendix 1S.
124. Erlich, H., *HLA DNA typing: past, present, and future.* Tissue Antigens, 2012. **80**(1): p. 1-11.
125. Gourraud, P.A., et al., *Nomenclature for HLA microsatellites.* Tissue Antigens, 2007. **69 Suppl 1**: p. 210-3.
126. Marsh, S.G., *Nomenclature for factors of the HLA system, update June 2014.* Tissue Antigens, 2014. **84**(3): p. 342-5.
127. Blum, J.S., P.A. Wearsch, and P. Cresswell, *Pathways of antigen processing.* Annu Rev Immunol, 2013. **31**: p. 443-73.
128. Romagnoli, P. and R.N. Germain, *The CLIP region of invariant chain plays a critical role in regulating major histocompatibility complex class II folding, transport, and peptide occupancy.* J Exp Med, 1994. **180**(3): p. 1107-13.
129. Pos, W., et al., *Crystal structure of the HLA-DM-HLA-DR1 complex defines mechanisms for rapid peptide selection.* Cell, 2012. **151**(7): p. 1557-68.
130. Joffre, O.P., et al., *Cross-presentation by dendritic cells.* Nat Rev Immunol, 2012. **12**(8): p. 557-69.
131. Munz, C., *Antigen Processing for MHC Class II Presentation via Autophagy.* Front Immunol, 2012. **3**: p. 9.
132. Matsumura, M., et al., *Emerging principles for the recognition of peptide antigens by MHC class I molecules.* Science, 1992. **257**(5072): p. 927-34.
133. Mohan, J.F. and E.R. Unanue, *A novel pathway of presentation by class II-MHC molecules involving peptides or denatured proteins important in autoimmunity.* Mol Immunol, 2013. **55**(2): p. 166-8.
134. Stern, L.J., et al., *Crystal structure of the human class II MHC protein HLA-DR1 complexed with an influenza virus peptide.* Nature, 1994. **368**(6468): p. 215-21.
135. Falk, K., et al., *Allele-specific motifs revealed by sequencing of self-peptides eluted from MHC molecules.* Nature, 1991. **351**(6324): p. 290-6.
136. Trowsdale, J., *The MHC, disease and selection.* Immunol Lett, 2011. **137**(1-2): p. 1-8.
137. Wei, C.Y., M.T. Lee, and Y.T. Chen, *Pharmacogenomics of adverse drug reactions: implementing personalized medicine.* Hum Mol Genet, 2012. **21**(R1): p. R58-65.

138. Phillips, E.J., et al., *Utility of patch testing in patients with hypersensitivity syndromes associated with abacavir.* AIDS, 2002. **16**(16): p. 2223-5.
139. Chessman, D., et al., *Human leukocyte antigen class I-restricted activation of CD8+ T cells provides the immunogenetic basis of a systemic drug hypersensitivity.* Immunity, 2008. **28**(6): p. 822-32.
140. Illing, P.T., et al., *Immune self-reactivity triggered by drug-modified HLA-peptide repertoire.* Nature, 2012. **486**(7404): p. 554-8.
141. Norcross, M.A., et al., *Abacavir induces loading of novel self-peptides into HLA-B*57: 01: an autoimmune model for HLA-associated drug hypersensitivity.* AIDS, 2012. **26**(11): p. F21-9.
142. Ostrov, D.A., et al., *Drug hypersensitivity caused by alteration of the MHC-presented self-peptide repertoire.* Proc Natl Acad Sci U S A, 2012. **109**(25): p. 9959-64.
143. Phillips, E. and S. Mallal, *Successful translation of pharmacogenetics into the clinic: the abacavir example.* Mol Diagn Ther, 2009. **13**(1): p. 1-9.
144. Gallucci, S. and P. Matzinger, *Danger signals: SOS to the immune system.* Curr Opin Immunol, 2001. **13**(1): p. 114-9.
145. Miyake, K., *Innate immune sensing of pathogens and danger signals by cell surface Toll-like receptors.* Semin Immunol, 2007. **19**(1): p. 3-10.
146. Smith-Garvin, J.E., G.A. Koretzky, and M.S. Jordan, *T cell activation.* Annu Rev Immunol, 2009. **27**: p. 591-619.
147. Watts, T.H., *TNF/TNFR family members in costimulation of T cell responses.* Annu Rev Immunol, 2005. **23**: p. 23-68.
148. Acuto, O. and F. Michel, *CD28-mediated co-stimulation: a quantitative support for TCR signalling.* Nat Rev Immunol, 2003. **3**(12): p. 939-51.
149. Nel, A.E., *T-cell activation through the antigen receptor. Part 1: signaling components, signaling pathways, and signal integration at the T-cell antigen receptor synapse.* J Allergy Clin Immunol, 2002. **109**(5): p. 758-70.
150. Gorentla, B.K. and X.P. Zhong, *T cell Receptor Signal Transduction in T lymphocytes.* J Clin Cell Immunol, 2012. **2012**(Suppl 12): p. 5.
151. Morris, G.P. and P.M. Allen, *How the TCR balances sensitivity and specificity for the recognition of self and pathogens.* Nat Immunol, 2012. **13**(2): p. 121-8.
152. Mauri-Hellweg, D., et al., *Activation of drug-specific CD4+ and CD8+ T cells in individuals allergic to sulfonamides, phenytoin, and carbamazepine.* J Immunol, 1995. **155**(1): p. 462-72.
153. Holt, M.P. and C. Ju, *Mechanisms of drug-induced liver injury.* AAPS J, 2006. **8**(1): p. E48-54.
154. Pirmohamed, M., et al., *The danger hypothesis--potential role in idiosyncratic drug reactions.* Toxicology, 2002. **181-182**: p. 55-63.
155. Landsteiner, K. and J. Jacobs, *Studies on the Sensitization of Animals with Simple Chemical Compounds.* J Exp Med, 1935. **61**(5): p. 643-56.
156. Ortmann, B., et al., *Synthetic peptides anchor T cell-specific TNP epitopes to MHC antigens.* J Immunol, 1992. **148**(5): p. 1445-50.
157. Chipinda, I., J.M. Hettick, and P.D. Siegel, *Haptenation: chemical reactivity and protein binding.* J Allergy (Cairo), 2011. **2011**: p. 839682.
158. Siest, G., et al., *Transcription factor and drug-metabolizing enzyme gene expression in lymphocytes from healthy human subjects.* Drug Metab Dispos, 2008. **36**(1): p. 182-9.
159. Adam, J., W.J. Pichler, and D. Yerly, *Delayed drug hypersensitivity: models of T-cell stimulation.* Br J Clin Pharmacol, 2011. **71**(5): p. 701-7.
160. Pichler, W.J., *Direct T-cell stimulations by drugs--bypassing the innate immune system.* Toxicology, 2005. **209**(2): p. 95-100.

161. Zanni, M.P., et al., *HLA-restricted, processing- and metabolism-independent pathway of drug recognition by human alpha beta T lymphocytes.* J Clin Invest, 1998. **102**(8): p. 1591-8.
162. Schnyder, B., et al., *Direct, MHC-dependent presentation of the drug sulfamethoxazole to human alphabeta T cell clones.* J Clin Invest, 1997. **100**(1): p. 136-41.
163. Depta, J.P., et al., *Drug interaction with T-cell receptors: T-cell receptor density determines degree of cross-reactivity.* J Allergy Clin Immunol, 2004. **113**(3): p. 519-27.
164. Wu, Y., et al., *Activation of T cells by carbamazepine and carbamazepine metabolites.* J Allergy Clin Immunol, 2006. **118**(1): p. 233-41.
165. Castrejon, J.L., et al., *Stimulation of human T cells with sulfonamides and sulfonamide metabolites.* J Allergy Clin Immunol, 2010. **125**(2): p. 411-418 e4.
166. Burkhart, C., et al., *Non-covalent presentation of sulfamethoxazole to human CD4+ T cells is independent of distinct human leucocyte antigen-bound peptides.* Clin Exp Allergy, 2002. **32**(11): p. 1635-43.
167. Pichler, W.J., D.J. Naisbitt, and B.K. Park, *Immune pathomechanism of drug hypersensitivity reactions.* J Allergy Clin Immunol, 2011. **127**(3 Suppl): p. S74-81.
168. Bharadwaj, M., et al., *Drug hypersensitivity and human leukocyte antigens of the major histocompatibility complex.* Annu Rev Pharmacol Toxicol, 2012. **52**: p. 401-31.
169. Mallal, S., et al., *HLA-B*5701 screening for hypersensitivity to abacavir.* N Engl J Med, 2008. **358**(6): p. 568-79.
170. Matzinger, P., *Tolerance, danger, and the extended family.* Annu Rev Immunol, 1994. **12**: p. 991-1045.
171. Curtsinger, J.M., et al., *Inflammatory cytokines provide a third signal for activation of naive CD4+ and CD8+ T cells.* J Immunol, 1999. **162**(6): p. 3256-62.
172. Danese, S., M. Sans, and C. Fiocchi, *The CD40/CD40L costimulatory pathway in inflammatory bowel disease.* Gut, 2004. **53**(7): p. 1035-43.
173. Sharpe, A.H., *Mechanisms of costimulation.* Immunol Rev, 2009. **229**(1): p. 5-11.
174. Janeway, C.A., Jr., *The immune system evolved to discriminate infectious nonself from noninfectious self.* Immunol Today, 1992. **13**(1): p. 11-6.
175. Seguin, B. and J. Uetrecht, *The danger hypothesis applied to idiosyncratic drug reactions.* Curr Opin Allergy Clin Immunol, 2003. **3**(4): p. 235-42.
176. Li, J. and J.P. Uetrecht, *The danger hypothesis applied to idiosyncratic drug reactions.* Handb Exp Pharmacol, 2010(196): p. 493-509.
177. Martin, A.M., et al., *Immune responses to abacavir in antigen-presenting cells from hypersensitive patients.* AIDS, 2007. **21**(10): p. 1233-44.
178. Sanderson, J.P., et al., *Sulfamethoxazole and its metabolite nitroso sulfamethoxazole stimulate dendritic cell costimulatory signaling.* J Immunol, 2007. **178**(9): p. 5533-42.
179. Rodriguez-Pena, R., et al., *Potential involvement of dendritic cells in delayed-type hypersensitivity reactions to beta-lactams.* J Allergy Clin Immunol, 2006. **118**(4): p. 949-56.
180. Kroemer, G., et al., *Classification of cell death: recommendations of the Nomenclature Committee on Cell Death 2009.* Cell Death Differ, 2009. **16**(1): p. 3-11.
181. Levin, S., et al., *The nomenclature of cell death: recommendations of an ad hoc Committee of the Society of Toxicologic Pathologists.* Toxicol Pathol, 1999. **27**(4): p. 484-90.

182. Kroemer, G., et al., *Classification of cell death: recommendations of the Nomenclature Committee on Cell Death.* Cell Death Differ, 2005. **12 Suppl 2**: p. 1463-7.
183. Galluzzi, L., et al., *Molecular definitions of cell death subroutines: recommendations of the Nomenclature Committee on Cell Death 2012.* Cell Death Differ, 2012. **19**(1): p. 107-20.
184. Galluzzi, L., et al., *Essential versus accessory aspects of cell death: recommendations of the NCCD 2015.* Cell Death Differ, 2015. **22**(1): p. 58-73.
185. Baehrecke, E.H., *How death shapes life during development.* Nat Rev Mol Cell Biol, 2002. **3**(10): p. 779-87.
186. Roach, H.I. and N.M. Clarke, *Physiological cell death of chondrocytes in vivo is not confined to apoptosis. New observations on the mammalian growth plate.* J Bone Joint Surg Br, 2000. **82**(4): p. 601-13.
187. Barkla, D.H. and P.R. Gibson, *The fate of epithelial cells in the human large intestine.* Pathology, 1999. **31**(3): p. 230-8.
188. Elmore, S., *Apoptosis: a review of programmed cell death.* Toxicol Pathol, 2007. **35**(4): p. 495-516.
189. Kerr, J.F., A.H. Wyllie, and A.R. Currie, *Apoptosis: a basic biological phenomenon with wide-ranging implications in tissue kinetics.* Br J Cancer, 1972. **26**(4): p. 239-57.
190. Krysko, D.V. and P. Vandenabeele, *From regulation of dying cell engulfment to development of anti-cancer therapy.* Cell Death Differ, 2008. **15**(1): p. 29-38.
191. Green, D.R., et al., *Ten years of publication in cell death.* Cell Death Differ, 2004. **11**(1): p. 2-3.
192. Baud, V. and M. Karin, *Signal transduction by tumor necrosis factor and its relatives.* Trends Cell Biol, 2001. **11**(9): p. 372-7.
193. Rashedi, I., et al., *Autoimmunity and apoptosis--therapeutic implications.* Curr Med Chem, 2007. **14**(29): p. 3139-51.
194. Kischkel, F.C., et al., *Cytotoxicity-dependent APO-1 (Fas/CD95)-associated proteins form a death-inducing signaling complex (DISC) with the receptor.* EMBO J, 1995. **14**(22): p. 5579-88.
195. Peter, M.E. and P.H. Krammer, *The CD95(APO-1/Fas) DISC and beyond.* Cell Death Differ, 2003. **10**(1): p. 26-35.
196. Youle, R.J. and A. Strasser, *The BCL-2 protein family: opposing activities that mediate cell death.* Nat Rev Mol Cell Biol, 2008. **9**(1): p. 47-59.
197. Li, H., et al., *Cleavage of BID by caspase 8 mediates the mitochondrial damage in the Fas pathway of apoptosis.* Cell, 1998. **94**(4): p. 491-501.
198. Luo, X., et al., *Bid, a Bcl2 interacting protein, mediates cytochrome c release from mitochondria in response to activation of cell surface death receptors.* Cell, 1998. **94**(4): p. 481-90.
199. Zhivotovsky, B., *Caspases: the enzymes of death.* Essays Biochem, 2003. **39**: p. 25-40.
200. Los, M., et al., *Requirement of an ICE/CED-3 protease for Fas/APO-1-mediated apoptosis.* Nature, 1995. **375**(6526): p. 81-3.
201. Ghavami, S., et al., *Apoptosis and cancer: mutations within caspase genes.* J Med Genet, 2009. **46**(8): p. 497-510.
202. Stennicke, H.R. and G.S. Salvesen, *Caspases - controlling intracellular signals by protease zymogen activation.* Biochim Biophys Acta, 2000. **1477**(1-2): p. 299-306.
203. Varfolomeev, E.E., et al., *Targeted disruption of the mouse Caspase 8 gene ablates cell death induction by the TNF receptors, Fas/Apo1, and DR3 and is lethal prenatally.* Immunity, 1998. **9**(2): p. 267-76.

204. Kuida, K., et al., *Reduced apoptosis and cytochrome c-mediated caspase activation in mice lacking caspase 9.* Cell, 1998. **94**(3): p. 325-37.
205. Zheng, T.S., et al., *Deficiency in caspase-9 or caspase-3 induces compensatory caspase activation.* Nat Med, 2000. **6**(11): p. 1241-7.
206. Woo, M., et al., *Essential contribution of caspase 3/CPP32 to apoptosis and its associated nuclear changes.* Genes Dev, 1998. **12**(6): p. 806-19.
207. Kuida, K., et al., *Decreased apoptosis in the brain and premature lethality in CPP32-deficient mice.* Nature, 1996. **384**(6607): p. 368-72.
208. Degterev, A., M. Boyce, and J. Yuan, *A decade of caspases.* Oncogene, 2003. **22**(53): p. 8543-67.
209. Enari, M., et al., *A caspase-activated DNase that degrades DNA during apoptosis, and its inhibitor ICAD.* Nature, 1998. **391**(6662): p. 43-50.
210. Sakahira, H., M. Enari, and S. Nagata, *Cleavage of CAD inhibitor in CAD activation and DNA degradation during apoptosis.* Nature, 1998. **391**(6662): p. 96-9.
211. Rudel, T. and G.M. Bokoch, *Membrane and morphological changes in apoptotic cells regulated by caspase-mediated activation of PAK2.* Science, 1997. **276**(5318): p. 1571-4.
212. Kothakota, S., et al., *Caspase-3-generated fragment of gelsolin: effector of morphological change in apoptosis.* Science, 1997. **278**(5336): p. 294-8.
213. Rao, L., D. Perez, and E. White, *Lamin proteolysis facilitates nuclear events during apoptosis.* J Cell Biol, 1996. **135**(6 Pt 1): p. 1441-55.
214. Nahle, Z., et al., *Direct coupling of the cell cycle and cell death machinery by E2F.* Nat Cell Biol, 2002. **4**(11): p. 859-64.
215. Green, D.R. and G. Kroemer, *The pathophysiology of mitochondrial cell death.* Science, 2004. **305**(5684): p. 626-9.
216. Korsmeyer, S.J., *Regulators of cell death.* Trends Genet, 1995. **11**(3): p. 101-5.
217. Danial, N.N. and S.J. Korsmeyer, *Cell death: critical control points.* Cell, 2004. **116**(2): p. 205-19.
218. Schuler, M. and D.R. Green, *Mechanisms of p53-dependent apoptosis.* Biochem Soc Trans, 2001. **29**(Pt 6): p. 684-8.
219. Riedl, S.J. and G.S. Salvesen, *The apoptosome: signalling platform of cell death.* Nat Rev Mol Cell Biol, 2007. **8**(5): p. 405-13.
220. Patil, C. and P. Walter, *Intracellular signaling from the endoplasmic reticulum to the nucleus: the unfolded protein response in yeast and mammals.* Curr Opin Cell Biol, 2001. **13**(3): p. 349-55.
221. Travers, K.J., et al., *Functional and genomic analyses reveal an essential coordination between the unfolded protein response and ER-associated degradation.* Cell, 2000. **101**(3): p. 249-58.
222. Breckenridge, D.G., et al., *Regulation of apoptosis by endoplasmic reticulum pathways.* Oncogene, 2003. **22**(53): p. 8608-18.
223. Verkhratsky, A. and E.C. Toescu, *Endoplasmic reticulum Ca(2+) homeostasis and neuronal death.* J Cell Mol Med, 2003. **7**(4): p. 351-61.
224. Voll, R.E., et al., *Immunosuppressive effects of apoptotic cells.* Nature, 1997. **390**(6658): p. 350-1.
225. Grimsley, C. and K.S. Ravichandran, *Cues for apoptotic cell engulfment: eat-me, don't eat-me and come-get-me signals.* Trends Cell Biol, 2003. **13**(12): p. 648-56.
226. Schlegel, R.A. and P. Williamson, *Phosphatidylserine, a death knell.* Cell Death Differ, 2001. **8**(6): p. 551-63.
227. Ishimoto, Y., et al., *Promotion of the uptake of PS liposomes and apoptotic cells by a product of growth arrest-specific gene, gas6.* J Biochem, 2000. **127**(3): p. 411-7.

228. Lauber, K., et al., *Clearance of apoptotic cells: getting rid of the corpses.* Mol Cell, 2004. **14**(3): p. 277-87.
229. Skulachev, V.P., *Bioenergetic aspects of apoptosis, necrosis and mitoptosis.* Apoptosis, 2006. **11**(4): p. 473-85.
230. Los, M., et al., *Activation and caspase-mediated inhibition of PARP: a molecular switch between fibroblast necrosis and apoptosis in death receptor signaling.* Mol Biol Cell, 2002. **13**(3): p. 978-88.
231. Vandenabeele, P., et al., *The role of the kinases RIP1 and RIP3 in TNF-induced necrosis.* Sci Signal, 2010. **3**(115): p. re4.
232. Wyllie, A.H., J.F. Kerr, and A.R. Currie, *Cell death: the significance of apoptosis.* Int Rev Cytol, 1980. **68**: p. 251-306.
233. Oppenheim, R.W., et al., *Programmed cell death of developing mammalian neurons after genetic deletion of caspases.* J Neurosci, 2001. **21**(13): p. 4752-60.
234. Vercammen, D., et al., *Inhibition of caspases increases the sensitivity of L929 cells to necrosis mediated by tumor necrosis factor.* J Exp Med, 1998. **187**(9): p. 1477-85.
235. Vercammen, D., et al., *Dual signaling of the Fas receptor: initiation of both apoptotic and necrotic cell death pathways.* J Exp Med, 1998. **188**(5): p. 919-30.
236. Vandenabeele, P., T. Vanden Berghe, and N. Festjens, *Caspase inhibitors promote alternative cell death pathways.* Sci STKE, 2006. **2006**(358): p. pe44.
237. Van Noorden, C.J., *The history of Z-VAD-FMK, a tool for understanding the significance of caspase inhibition.* Acta Histochem, 2001. **103**(3): p. 241-51.
238. He, S., et al., *Receptor interacting protein kinase-3 determines cellular necrotic response to TNF-alpha.* Cell, 2009. **137**(6): p. 1100-11.
239. Wang, Z., et al., *The mitochondrial phosphatase PGAM5 functions at the convergence point of multiple necrotic death pathways.* Cell, 2012. **148**(1-2): p. 228-43.
240. Cai, Z., et al., *Plasma membrane translocation of trimerized MLKL protein is required for TNF-induced necroptosis.* Nat Cell Biol, 2014. **16**(1): p. 55-65.
241. Kroemer, G., L. Galluzzi, and C. Brenner, *Mitochondrial membrane permeabilization in cell death.* Physiol Rev, 2007. **87**(1): p. 99-163.
242. Proskuryakov, S.Y., V.L. Gabai, and A.G. Konoplyannikov, *Necrosis is an active and controlled form of programmed cell death.* Biochemistry (Mosc), 2002. **67**(4): p. 387-408.
243. Mizushima, N., *Autophagy: process and function.* Genes Dev, 2007. **21**(22): p. 2861-73.
244. Aki, T., A. Nara, and K. Uemura, *Cytoplasmic vacuolization during exposure to drugs and other substances.* Cell Biol Toxicol, 2012. **28**(3): p. 125-31.
245. Jung, C.H., et al., *ULK-Atg13-FIP200 complexes mediate mTOR signaling to the autophagy machinery.* Mol Biol Cell, 2009. **20**(7): p. 1992-2003.
246. Terman, A., et al., *Mitochondrial turnover and aging of long-lived postmitotic cells: the mitochondrial-lysosomal axis theory of aging.* Antioxid Redox Signal, 2010. **12**(4): p. 503-35.
247. Betin, V.M. and J.D. Lane, *Caspase cleavage of Atg4D stimulates GABARAP-L1 processing and triggers mitochondrial targeting and apoptosis.* J Cell Sci, 2009. **122**(Pt 14): p. 2554-66.
248. Castedo, M., et al., *Cell death by mitotic catastrophe: a molecular definition.* Oncogene, 2004. **23**(16): p. 2825-37.
249. Takai, H., et al., *Aberrant cell cycle checkpoint function and early embryonic death in Chk1(-/-) mice.* Genes Dev, 2000. **14**(12): p. 1439-47.
250. Vakifahmetoglu, H., M. Olsson, and B. Zhivotovsky, *Death through a tragedy: mitotic catastrophe.* Cell Death Differ, 2008. **15**(7): p. 1153-62.

251. Gilloteaux, J., et al., *Cancer cell necrosis by autoschizis: synergism of antitumor activity of vitamin C: vitamin K3 on human bladder carcinoma T24 cells.* Scanning, 1998. **20**(8): p. 564-75.
252. Gilmore, A.P., *Anoikis.* Cell Death Differ, 2005. **12 Suppl 2**: p. 1473-7.
253. Overholtzer, M., et al., *A nonapoptotic cell death process, entosis, that occurs by cell-in-cell invasion.* Cell, 2007. **131**(5): p. 966-79.
254. Andrabi, S.A., T.M. Dawson, and V.L. Dawson, *Mitochondrial and nuclear cross talk in cell death: parthanatos.* Ann N Y Acad Sci, 2008. **1147**: p. 233-41.
255. Frisch, S.M. and H. Francis, *Disruption of epithelial cell-matrix interactions induces apoptosis.* J Cell Biol, 1994. **124**(4): p. 619-26.
256. Mailleux, A.A., et al., *BIM regulates apoptosis during mammary ductal morphogenesis, and its absence reveals alternative cell death mechanisms.* Dev Cell, 2007. **12**(2): p. 221-34.
257. Reginato, M.J., et al., *Integrins and EGFR coordinately regulate the pro-apoptotic protein Bim to prevent anoikis.* Nat Cell Biol, 2003. **5**(8): p. 733-40.
258. Matarrese, P., et al., *Xeno-cannibalism as an exacerbation of self-cannibalism: a possible fruitful survival strategy for cancer cells.* Curr Pharm Des, 2008. **14**(3): p. 245-52.
259. Mormone, E., et al., *Genotype-dependent priming to self- and xeno-cannibalism in heterozygous and homozygous lymphoblasts from patients with Huntington's disease.* J Neurochem, 2006. **98**(4): p. 1090-9.
260. Lai, Y., et al., *Silencing the Metallothionein-2A gene induces entosis in adherent MCF-7 breast cancer cells.* Anat Rec (Hoboken), 2010. **293**(10): p. 1685-91.
261. Fiorentini, C., et al., *Activation of rho GTPases by cytotoxic necrotizing factor 1 induces macropinocytosis and scavenging activity in epithelial cells.* Mol Biol Cell, 2001. **12**(7): p. 2061-73.
262. Jeggo, P.A., *DNA repair: PARP - another guardian angel?* Curr Biol, 1998. **8**(2): p. R49-51.
263. Andrabi, S.A., et al., *Poly(ADP-ribose) (PAR) polymer is a death signal.* Proc Natl Acad Sci U S A, 2006. **103**(48): p. 18308-13.
264. Yu, S.W., et al., *Apoptosis-inducing factor mediates poly(ADP-ribose) (PAR) polymer-induced cell death.* Proc Natl Acad Sci U S A, 2006. **103**(48): p. 18314-9.
265. Yu, S.W., et al., *Mediation of poly(ADP-ribose) polymerase-1-dependent cell death by apoptosis-inducing factor.* Science, 2002. **297**(5579): p. 259-63.
266. Bergsbaken, T., S.L. Fink, and B.T. Cookson, *Pyroptosis: host cell death and inflammation.* Nat Rev Microbiol, 2009. **7**(2): p. 99-109.
267. von Moltke, J., et al., *Recognition of bacteria by inflammasomes.* Annu Rev Immunol, 2013. **31**: p. 73-106.
268. Fink, S.L. and B.T. Cookson, *Caspase-1-dependent pore formation during pyroptosis leads to osmotic lysis of infected host macrophages.* Cell Microbiol, 2006. **8**(11): p. 1812-25.
269. Fuchs, T.A., et al., *Novel cell death program leads to neutrophil extracellular traps.* J Cell Biol, 2007. **176**(2): p. 231-41.
270. Remijsen, Q., et al., *Neutrophil extracellular trap cell death requires both autophagy and superoxide generation.* Cell Res, 2011. **21**(2): p. 290-304.
271. Denecker, G., et al., *Caspase-14 protects against epidermal UVB photodamage and water loss.* Nat Cell Biol, 2007. **9**(6): p. 666-74.
272. Ettinger, A.B. and C.E. Argoff, *Use of antiepileptic drugs for nonepileptic conditions: psychiatric disorders and chronic pain.* Neurotherapeutics, 2007. **4**(1): p. 75-83.
273. Spina, E. and G. Perugi, *Antiepileptic drugs: indications other than epilepsy.* Epileptic Disord, 2004. **6**(2): p. 57-75.

274. Schindler, W. and F. Haefliger, *Ueber Derivate des Iminodibenzyls.* Helvetica Chimica Acta, 1954. **37**(2): p. 472-483.
275. Schatzenberger, A.F. and C.B. Nemeroff, *Textbook of Psychopharmacology*. 2005: American Psychiatric Press, Inc.
276. Kutt, H., *Antiepileptic Drugs*. 3rd ed. 1989, New York: Raven.
277. Post, R.M., S.R. Weiss, and D.M. Chuang, *Mechanisms of action of anticonvulsants in affective disorders: comparisons with lithium.* J Clin Psychopharmacol, 1992. **12**(1 Suppl): p. 23S-35S.
278. Rogawski, M.A. and W. Loscher, *The neurobiology of antiepileptic drugs.* Nat Rev Neurosci, 2004. **5**(7): p. 553-64.
279. Wilder, B.J., *Pharmacokinetics of valproate and carbamazepine.* J Clin Psychopharmacol, 1992. **12**(1 Suppl): p. 64S-68S.
280. Rawlins, M.D., et al., *Distribution and elimination kinetics of carbamazepine in man.* Eur J Clin Pharmacol, 1975. **8**(2): p. 91-6.
281. Hooper, W.D., et al., *Plasma protein binding of carbamazepine.* Clin Pharmacol Ther, 1975. **17**(4): p. 433-40.
282. Lertratanangkoon, K. and M.G. Horning, *Metabolism of carbamazepine.* Drug Metab Dispos, 1982. **10**(1): p. 1-10.
283. Leeder, J.S., *Mechanisms of idiosyncratic hypersensitivity reactions to antiepileptic drugs.* Epilepsia, 1998. **39 Suppl 7**: p. S8-16.
284. Frigerio, A. and P.L. Morselli, *Carbamazepine: biotransformation.* Adv Neurol, 1975. **11**: p. 295-308.
285. Kerr, B.M., et al., *Human liver carbamazepine metabolism. Role of CYP3A4 and CYP2C8 in 10,11-epoxide formation.* Biochem Pharmacol, 1994. **47**(11): p. 1969-79.
286. Pirmohamed, M., et al., *An investigation of the formation of cytotoxic, protein-reactive and stable metabolites from carbamazepine in vitro.* Biochem Pharmacol, 1992. **43**(8): p. 1675-82.
287. Gerson, W.T., et al., *Anticonvulsant-induced aplastic anemia: increased susceptibility to toxic drug metabolites in vitro.* Blood, 1983. **61**(5): p. 889-93.
288. Madden, S., J.L. Maggs, and B.K. Park, *Bioactivation of carbamazepine in the rat in vivo. Evidence for the formation of reactive arene oxide(s).* Drug Metab Dispos, 1996. **24**(4): p. 469-79.
289. Eichelbaum, M., et al., *Plasma kinetics of carbamazepine and its epoxide metabolite in man after single and multiple doses.* Eur J Clin Pharmacol, 1975. **8**(5): p. 337-41.
290. Rosa, F.W., *Spina bifida in infants of women treated with carbamazepine during pregnancy.* N Engl J Med, 1991. **324**(10): p. 674-7.
291. Stremski, E.S., et al., *Pediatric carbamazepine intoxication.* Ann Emerg Med, 1995. **25**(5): p. 624-30.
292. Gillham, R.A., et al., *Cognitive function in adult epileptic patients established on anticonvulsant monotherapy.* Epilepsy Res, 1990. **7**(3): p. 219-25.
293. Ronnberg, J., S. Samuelsson, and B. Soderfeldt, *Memory effects following carbamazepine monotherapy in patients with complex partial epilepsy.* Seizure, 1992. **1**(4): p. 247-53.
294. Uetrecht, J.P., *New concepts in immunology relevant to idiosyncratic drug reactions: the "danger hypothesis" and innate immune system.* Chem Res Toxicol, 1999. **12**(5): p. 387-95.
295. Park, B.K., M. Pirmohamed, and N.R. Kitteringham, *Role of drug disposition in drug hypersensitivity: a chemical, molecular, and clinical perspective.* Chem Res Toxicol, 1998. **11**(9): p. 969-88.
296. Marson, A.G., et al., *The SANAD study of effectiveness of carbamazepine, gabapentin, lamotrigine, oxcarbazepine, or topiramate for treatment of partial epilepsy: an unblinded randomised controlled trial.* Lancet, 2007. **369**(9566): p. 1000-15.

297. Gogtay, N.J., S.B. Bavdekar, and N.A. Kshirsagar, *Anticonvulsant hypersensitivity syndrome: a review.* Expert Opin Drug Saf, 2005. **4**(3): p. 571-81.
298. Yip, V., et al., *SEVERE HYPERSENSITIVITY TO ANTIEPILEPTIC DRUGS: BRITISH NEUROLOGICAL SURVEILLANCE UNIT (BNSU).* Journal of Neurology, Neurosurgery & Psychiatry, 2013. **84**(11): p. e2.
299. Hung, S.-I., W.-H. Chung, and Y.-T. Chen, *HLA-B genotyping to detect carbamazepine-induced Stevens-Johnson syndrome: implications for personalizing medicine.* Personalized Medicine, 2005. **2**(3): p. 225-237.
300. Edwards, S.G., et al., *Concordance of primary generalised epilepsy and carbamazepine hypersensitivity in monozygotic twins.* Postgrad Med J, 1999. **75**(889): p. 680-1.
301. Strickler, S.M., et al., *Genetic predisposition to phenytoin-induced birth defects.* Lancet, 1985. **2**(8458): p. 746-9.
302. Calligaris, L., et al., *Carbamazepine hypersensitivity syndrome triggered by a human herpes virus reactivation in a genetically predisposed patient.* Int Arch Allergy Immunol, 2009. **149**(2): p. 173-7.
303. Gaedigk, A., S.P. Spielberg, and D.M. Grant, *Characterization of the microsomal epoxide hydrolase gene in patients with anticonvulsant adverse drug reactions.* Pharmacogenetics, 1994. **4**(3): p. 142-53.
304. Green, V.J., et al., *Genetic analysis of microsomal epoxide hydrolase in patients with carbamazepine hypersensitivity.* Biochem Pharmacol, 1995. **50**(9): p. 1353-9.
305. Leeder, J.S., et al., *Human anti-cytochrome P450 antibodies in aromatic anticonvulsant-induced hypersensitivity reactions.* J Pharmacol Exp Ther, 1992. **263**(1): p. 360-7.
306. Hung, S.I., et al., *Genetic susceptibility to carbamazepine-induced cutaneous adverse drug reactions.* Pharmacogenet Genomics, 2006. **16**(4): p. 297-306.
307. Pirmohamed, M., et al., *TNFalpha promoter region gene polymorphisms in carbamazepine-hypersensitive patients.* Neurology, 2001. **56**(7): p. 890-6.
308. Then, S.M., et al., *Frequency of the HLA-B*1502 allele contributing to carbamazepine-induced hypersensitivity reactions in a cohort of Malaysian epilepsy patients.* Asian Pac J Allergy Immunol, 2011. **29**(3): p. 290-3.
309. Mehta, T.Y., et al., *Association of HLA-B*1502 allele and carbamazepine-induced Stevens-Johnson syndrome among Indians.* Indian J Dermatol Venereol Leprol, 2009. **75**(6): p. 579-82.
310. Chang, C.C., et al., *Association of HLA-B*1502 allele with carbamazepine-induced toxic epidermal necrolysis and Stevens-Johnson syndrome in the multi-ethnic Malaysian population.* Int J Dermatol, 2011. **50**(2): p. 221-4.
311. Aihara, M., *Pharmacogenetics of cutaneous adverse drug reactions.* J Dermatol, 2011. **38**(3): p. 246-54.
312. Alfirevic, A., et al., *HLA-B locus in Caucasian patients with carbamazepine hypersensitivity.* Pharmacogenomics, 2006. **7**(6): p. 813-8.
313. Ferrell, P.B., Jr. and H.L. McLeod, *Carbamazepine, HLA-B*1502 and risk of Stevens-Johnson syndrome and toxic epidermal necrolysis: US FDA recommendations.* Pharmacogenomics, 2008. **9**(10): p. 1543-6.
314. Ozeki, T., et al., *Genome-wide association study identifies HLA-A*3101 allele as a genetic risk factor for carbamazepine-induced cutaneous adverse drug reactions in Japanese population.* Hum Mol Genet, 2011. **20**(5): p. 1034-41.
315. Chung, W.H., S.I. Hung, and Y.T. Chen, *Genetic predisposition of life-threatening antiepileptic-induced skin reactions.* Expert Opin Drug Saf, 2010. **9**(1): p. 15-21.

316. Wu, Y., et al., *Generation and characterization of antigen-specific CD4+, CD8+, and CD4+CD8+ T-cell clones from patients with carbamazepine hypersensitivity.* J Allergy Clin Immunol, 2007. **119**(4): p. 973-81.
317. Wei, C.Y., et al., *Direct interaction between HLA-B and carbamazepine activates T cells in patients with Stevens-Johnson syndrome.* J Allergy Clin Immunol, 2012. **129**(6): p. 1562-9 e5.
318. Nassif, A., et al., *Toxic epidermal necrolysis: effector cells are drug-specific cytotoxic T cells.* J Allergy Clin Immunol, 2004. **114**(5): p. 1209-15.
319. Yang, C.W., et al., *HLA-B*1502-bound peptides: implications for the pathogenesis of carbamazepine-induced Stevens-Johnson syndrome.* J Allergy Clin Immunol, 2007. **120**(4): p. 870-7.
320. Kannan, A., et al., *Signal transduction via the T cell antigen receptor in naive and effector/memory T cells.* Int J Biochem Cell Biol, 2012. **44**(12): p. 2129-34.
321. Boesteanu, A.C. and P.D. Katsikis, *Memory T cells need CD28 costimulation to remember.* Semin Immunol, 2009. **21**(2): p. 69-77.
322. Igarashi, M., et al., *Immunosuppressive factors detected during convalescence in a patient with severe serum sickness induced by carbamazepine.* Int Arch Allergy Immunol, 1993. **100**(4): p. 378-81.
323. Igarashi, M., et al., *An immunodominant haptenic epitope of carbamazepine detected in serum from patients given long-term treatment with carbamazepine without allergic reaction.* J Clin Immunol, 1992. **12**(5): p. 335-40.
324. Horneff, G., H.G. Lenard, and V. Wahn, *Severe adverse reaction to carbamazepine: significance of humoral and cellular reactions to the drug.* Neuropediatrics, 1992. **23**(5): p. 272-5.
325. Hosoda, N., et al., *Anticarbamazepine antibody induced by carbamazepine in a patient with severe serum sickness.* Arch Dis Child, 1991. **66**(6): p. 722-3.

Chapter 2

Evaluation of cytotoxicity caused by carbamazepine and its metabolite 9-acridinecarboxaldehyde *in vitro*

2.1 Introduction

Carbamazepine (CBZ) is extensively metabolised in the human body. Different studies have found more than 30 metabolites of CBZ *in vivo* (see section 1.7.1 in the general introduction). Phase I metabolism takes place mainly in the liver. Highly reactive metabolites would therefore react with proteins in the liver. Furst and colleagues found that metabolism of CBZ can take place in human blood [1]. This metabolism was shown to result in reactive metabolites for other drugs [2-4].

Peripheral blood mononuclear cells (PBMCs) are the main component of the blood and consist of T cells, B cells, and macrophages. They play an important role in the induction of a response from the immune system. PBMCs also express metabolic enzymes although to a lesser extent than liver cells [5].

Previous work, using a cytotoxicity assay with an *in vitro* metabolising system [6], found that cells from CBZ-hypersensitive patients are more susceptible to cytotoxic metabolites of CBZ, than cells from CBZ-tolerant patients [7-9]. The underlying mechanism of these observations has not been further investigated. The findings support the hypothesis of CBZ-induced hypersensitivity reactions being the result of an imbalance in the detoxification process. Tissue damage caused by cytotoxic metabolites could result in the presence of danger signal and together with other protein bound metabolites lead to an immune responses.

There are many assays available to investigate cell death. The difficulty is finding assays that are specific to the mode of the cell death being investigated. This is because of the overlap of some phenomena occurring during the different types of cell death [10].

Cell death assays can be divided into two distinct groups. The first is to measure the morphological changes and therefore the cell death directly. These include staining for intracellular proteins and use of vital dyes such as

Trypan blue. The other group is measuring cell death in an indirect manner such as the degree of cell attachment for adherent growing cell lines or loss of metabolic functions as in the MTT assay.

Apoptosis manifests generally through shrinkage of the cell followed by the condensation of the chromatin, activation of cysteine aspartases (caspases), fragmentation of the chromosomal DNA as well as nuclear fragmentation before the blebbing of apoptotic bodies [11]. These apoptotic bodies are then cleared by phagocytes *in vivo* [12]. Cells undergoing necrosis show different morphological and pathological characteristics during the process. The common morphological features that can be observed include swelling of organelles, condensation of chromatin and an increase in the cell volume which results in the rupture of the cell. Due to this, cell membrane integrity is not maintained, as in the case of apoptosis, and the cell contents leak into the surrounding tissue [13]. In contrast to apoptosis, necrosis has been regarded as accidental cell death, but recent findings revealed a regulated form of necrosis, necroptosis [14].

The discovery of the two different cell death mechanisms led to increased investigations of the mechanistic differences involved in both pathways. This resulted in a large expansion of the methods used to distinguish between the two. It was found that the activation of caspases, mitochondrial membrane permeabilisation (MMP), DNA fragmentation and the exposure of phosphatidylserine (PS) on the cell surface are characteristic of apoptosis [12]. Nevertheless, these characteristics can also occur during other physiological states of the cell. These can include other modes of cell death but also in states that do not lead to the death of the cell [15-21]. Due to these findings, apoptotic cell death is commonly determined by the results of at least two different assays [22].

Universal assays for the measurement of apoptosis detect morphological changes typical for apoptosis in the cell. This includes the detection of DNA fragmentation such as the terminal deoxynucleotidyl transferase-mediated dUTP nick-end labelling (TUNEL) [20]. Other assays measure pathway-

specific processes such as the activation of the caspase cascade, exposure of phosphatidylserine (PS) on the surface of the cell or MMP [17, 20, 23, 24].

The factors found to be specifically characteristic of necroptosis but not necrosis include activation of receptor-interacting protein kinase 1 and 3, metabolic burst with overproduction of reactive oxygen species, MMP and lysosomal membrane permeabilisation [13].

Experimental findings suggest an involvement of the adaptive immune system in CBZ-induced DHRs. Although, as described in the general introduction (see 1.7.3.1), there is strong evidence for associations between HLA alleles and CBZ-induced DHRs, many carriers of risk alleles do not suffer from DHRs. This suggests that there may be other, as yet undetermined, factors responsible for CBZ-induced DHRs. Still, many aspects of the pathogenesis of CBZ-induced DHRs are poorly understood, such as the sensitisation of hypersensitive patient. The hypothesis behind the work in this chapter was that the drug or its metabolite can damage cells, which results in the release of costimulatory signals for the activation of T cells, as described by the danger hypothesis (see general introduction 1.5.4). Therefore, the aim was to determine whether cells exposed to the drug and its metabolite, die via an apoptotic or necrotic pathway.

2.2 Material and Methods

2.2.1 Chemicals

CBZ (TOCRIS bioscience, Bristol, UK) and 9-acridinecarboxaldehyde (9-AC, Life Chemicals, Braunschweig, Germany) were used in the cell death assays. A 20 mM stock solution was made for each compound using methanol (MeOH, Sigma-Aldrich Co, Poole, UK) as a solvent.

Staurosporine and cytochalasin B (STS, CytB, Sigma-Aldrich Co.) were used as apoptotic and necrotic positive controls in the assays.

Carbobenzoxy-valyl-alanyl-aspartyl-(O-methyl)-fluoromethylketone (Z-VAD-FMK) from Enzo Life Sciences Inc. (Exeter, UK) was used as a broad caspase inhibitor in the measurement of cellular caspase activation.

2.2.2 Cell line and culture medium

CCRF-CEM cells (ATCC CCL-19), a T lymphoblastoid cell line derived from a four year old female Caucasian with acute lymphoblastic leukaemia, were used. CCRF-CEM cells were cultured at 37°C (5% CO_2) in RPMI-1640 with 10% (v/v) foetal calf serum (FCS) and 2 mM L-glutamine obtained from Invitrogen Ltd (Paisley, UK).

2.2.3 Peripheral blood mononuclear cell isolation

PBMCs were isolated from fresh heparinised venous blood taken from CBZ-naïve healthy volunteers. The isolation was conducted by centrifugation on Lymphoprep® density gradient (Axis-Shield, Dundee, UK). Blood was placed on top of Lymphoprep® and centrifuged at 600 g for 15 min (Heraeus Megafuge 11R, Thermo Fisher Scientific Inc., Loughborough, UK). During this step, the blood was divided into three components (see Fig. 2.1). The

erythrocytes aggregate and sediment to the bottom of the tube. The next layer consists of the Lymphoprep®. Above the layer of Lymphoprep® were the PBMCs and on top of them, plasma was found [25]. The layer of PBMCs was collected and washed twice with Hanks' balanced salt solution (HBSS, Invitrogen Ltd, Paisley, UK).

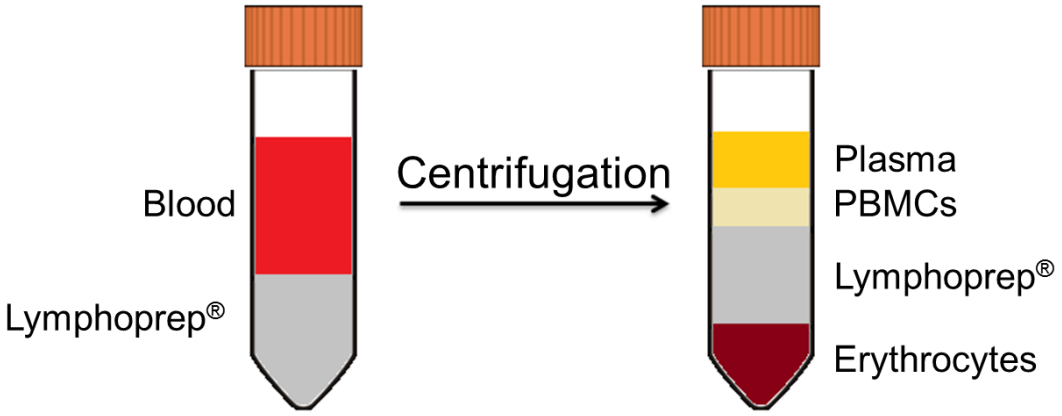

Figure 2.1: Blood separation over density gradient

The resulting pellet of PBMCs was resuspended in HBSS buffered with 15 mM HEPES (pH 7.5). Isolated PBMCs were counted and viability measured using the Trypan blue exclusion method [26]. Only samples with a viability ≥ 90% were used for the experiments. The cell count was adjusted to the required concentration using media.

2.2.4 Cell death assays

The adjusted cell suspension was then placed into wells of the plate. Compound dilutions were prepared out of the stock solution. The dilutions were made using methanol. 5 µl of these concentrations were then added to 495 µl of media. The same volume of the diluted compounds was added to the wells with plated cells. The methanol concentration in each sample was less than 1%. The resulting final concentrations for the assay were 0, 10, 50,

100 and 200 µM. For the 0 µM concentration, pure methanol was added to media before being added to the cell suspension.

The cells were then incubated for either 2 or 24 hours. In case of the 2 hour incubation, the cells were centrifuged after 2 hours, the compound containing medium was removed and replaced with drug free medium before placing the cells back in the incubator for the rest of the 24 hours.

2.2.4.1 Measuring cell viability using MTT

In this assay, 3-(4,5-dimethylthiazol-2-yl)-2,5-diphenyltetrazolium bromide (MTT, Sigma-Aldrich Co.) was transformed by dehydrogenases in cells into its purple formazan form. The absorption was then measured to calculate the amount of living cells in the sample with the amount of formazan formed proportional to the amount of living cells in the sample [27].

The concentration of cells was adjusted to 500 x 10^5 cells/ml. 50 µl of cell suspension was added into each well of a clear flat bottom 96 well plate.

Compound dilutions were prepared as described above. 50 µl of these were added to the plated cell suspension. Each concentration of each compound was plated in triplicate.

24 hours after the start of the incubation, 20 µl of MTT solution (5 mg MTT in 1 ml HBSS) was added to each well and the plate was incubated in the dark for 2 hours. 100 µl of lysis buffer (50% v/v Dimethylformamide, 20% w/v sodium dodecyl sulphate in dH_2O) was added to each well. The plate was incubated for at least 4 hours in the dark at 37°C. The absorbance was then measured at 595 nm using a plate reader (DTX 880 Multimode Detector, Beckman Coulter Ltd., High Wycombe, UK).

From the absorbance (A_{595}), the cell viability was calculated using the following formula:

$$Cell\ viability\ [\%]\ = \left(\frac{\sum A_{595,Sample} - \sum A_{595,Blank}}{\sum A_{595,Control}}\right) \times 100$$

The data were expressed as the mean with the error bars representing the standard deviation (SD) of the mean from three independent experiments.

2.2.4.2 Measurement of Mitochondrial Depolarisation using TMRE

Tetramethylrhodamine, ethyl ester, perchlorate (TMRE, Sigma-Aldrich Co.) is a fluorescent dye. It can accumulate in mitochondria when the membrane is not depolarised. The loss of fluorescence was measured in cells by flow cytometry. The depolarisation of the mitochondrial membrane is accompanied by the death of the cell [28].

Cell concentration was adjusted to 1 x 10^6 cells/ml. 500 µl of cell suspension was added into each well of a clear flat bottom 12 well plate.

The different concentrations were prepared as described above. 500 µl of the dilution was added into wells with cells. An apoptotic control STS was used at a final concentration of 4 µM [29].

24 hours after the start of the incubation, cells were washed 2 times with HBSS. After the second wash, pellets were dissolved with 500 µl of 50 nM TMRE in HBSS. Samples were then incubated at 37°C in the dark. Samples were measured in the fluorescence activated cell sorting machine (BD FACSCanto™, Becton Dickinson, Oxford, UK). An unstained sample was used for adjustment of the forward and side scatter. The data were analysed using Cyflogic software. It was gated for the cell population to remove debris. From this population, the gating was conducted to derive the percentage of cells with depolarised mitochondria (see Fig. 2.2). The data were expressed

as the mean and the error bars represented the SD of the mean from three independent experiments.

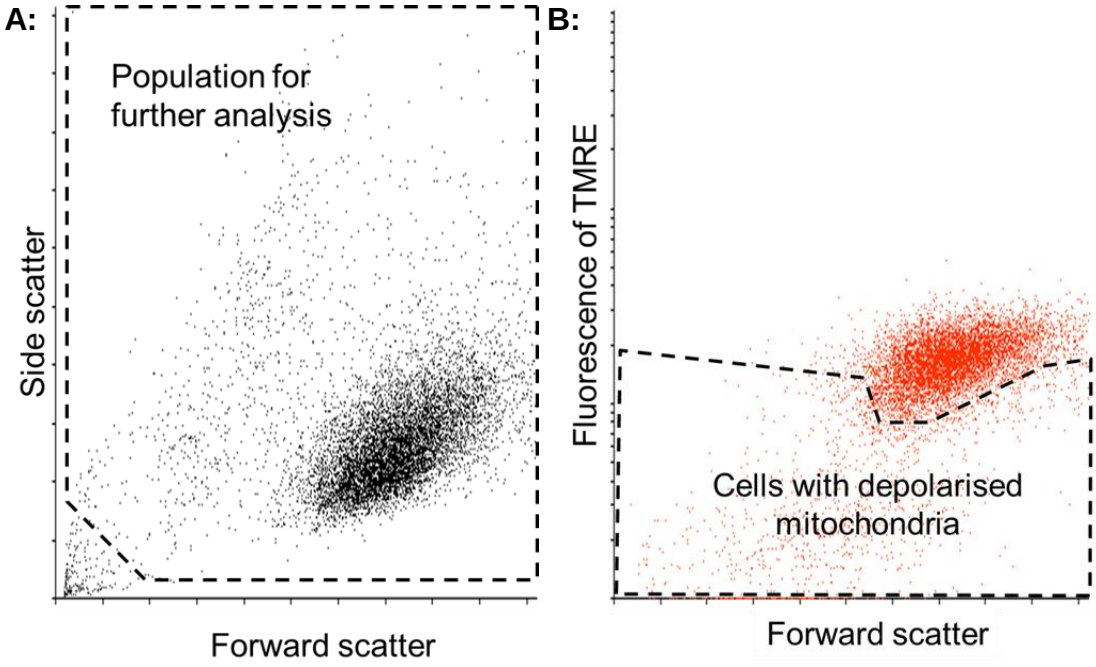

Figure 2.2: Gating for the analysis of depolarised mitochondria.

Plot A shows the forward against side scatter. To remove the debris for further analysis, only events in the area surrounded with the dashed line were selected and analysed further. Plot B shows the forward scatter against red fluorescence. Events in the area surrounded with the dashed line were identified as cells with depolarised mitochondria, due to their lack of red fluorescence.

2.2.4.3 Measurement of apoptotic and necrotic cells

Annexin-V-Fluorescein (Roche, Burgess Hill, UK) is a conjugate of Annexin V and a fluorescent dye. Annexin V binds to PS that is only present on the outer membrane of a cell, if this cell is undergoing apoptosis. Propidium iodide (PI, Roche) is a fluorescent dye that can bind to DNA. PI cannot penetrate the membrane of a living cell and therefore, it only binds to the DNA of necrotic cells as these cells have lost cell membrane integrity [30].

Cell concentration was adjusted to 1 x 10^6 cells/ml and 500 µl of cell suspension was added into each well of a clear flat bottom 12 well plate. The different concentrations were prepared as described above. 500 µl of the dilutions were added to wells with cells. STS (4 µM final concentration) and CytB (50 µM final concentration) were used as apoptotic and necrotic positive controls respectively [31].

24 hours after the start of the incubation, the samples were prepared as described in the manual of the Annexin-V-FLUOS Staining Kit from Roche [32]. A master mix of Annexin-V-Fluorescein and PI was prepared and 100 µl of it were added to each sample plus 400 µl of incubation buffer. Samples were then incubated for 15 minutes at room temperature. 500 µl of incubation buffer from the kit was added to the samples before measuring it in the fluorescence activated cell sorting machine (BD FACSCanto™, Becton Dickinson). An unstained sample was used for the adjustment of the forward and side scatter. Two single stained samples, either staurosporine and Annexin-V-Fluorescein or cytochrome B and PI were used for compensation. The data were analysed using Cyflogic software, gating for the cells to remove debris. From this population, gating was conducted to derive the percentage apoptotic and necrotic cells (see Fig. 2.3). Results were expressed as the mean and the error bars represent the SD of the mean from three independent experiments.

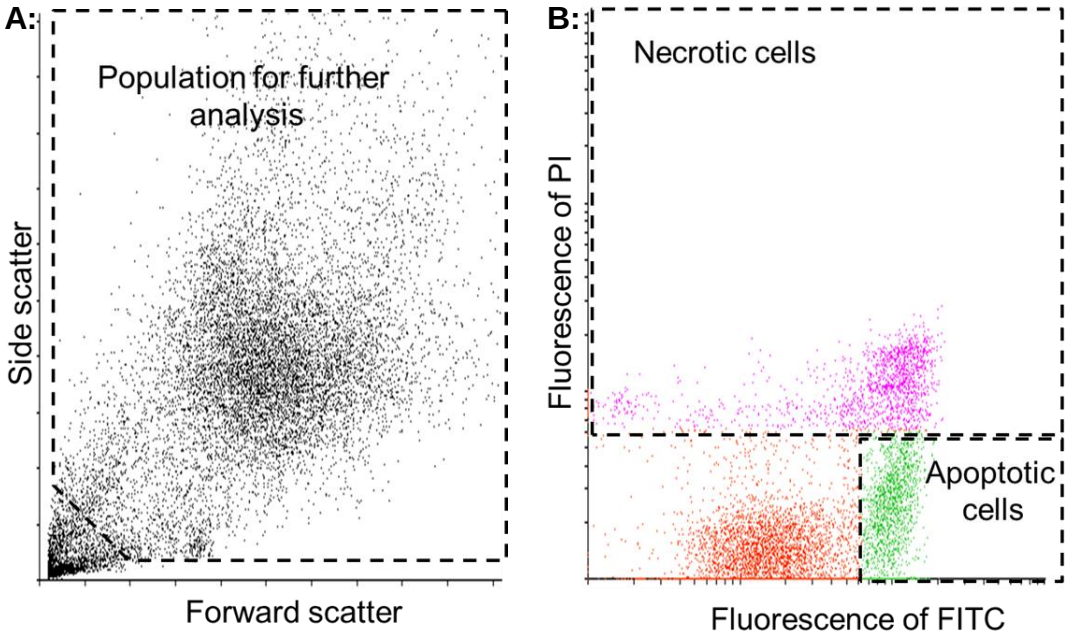

Figure 2.3: Gating for the measurement of apoptotic and necrotic cells

Plot A shows the forward and side scatter. To remove the debris for further analysis, only events in the area surrounded with the dashed line were selected and analysed further. Plot B shows the green fluorescence against red fluorescence after compensation. Events in the upper area surrounded with the dashed line were considered necrotic cells. Events in the lower right area surrounded with the dashed line were considered apoptotic cells.

2.2.4.4 Measurement of caspase activation

The Caspase-Glo® 3/7 assay (Promega) was used to detect caspase activation. In this assay, a mixture of a luminogenic substrate for caspase 3 and 7, luciferase, and cell lysis buffer is added to the samples. The substrate is then be cleaved by activated caspase 3 or 7. Luciferase can then generate a luminescent signal from the fragment. The amount of luminescence measured is proportional to the activated caspase in the sample.

Cell concentration was adjusted to 1 x 10^6 cells/ml. 50 µl of cell suspension was added into each well of a clear flat bottom 96 well plate. Compound dilutions were prepared as described above. 50 µl of these were added to the plated cell suspension. Staurosporine was used as an apoptotic control. Z-VAD-FMK was used as a broad caspase inhibitor [33]. Z-VAD-FMK (50

µM) was added together with 50 µM 9-AC to determine if the effect was reversible. Each concentration of compounds was plated in triplicate.

24 hours after the start of the incubation, samples were mixed and 50 µl of sample was added into separate wells of a white flat bottom 96 well plate. 50 µl of the freshly prepared reagent were added to each well. Contents were mixed for 30 seconds at 300 rpm using a plate shaker. Plates were then incubated for 2h at 37°C in the dark. The luminescence was measured using a plate reader (DTX 880 Multimode Detector, Beckman Coulter Ltd.).

From the luminescence measured, the value for the blank sample (medium, reagent) was subtracted and the mean of all three replicates for that concentration calculated. The results are expressed as the mean and the error bars represent the SD of the mean from three independent experiments.

2.2.3 Statistical analysis

Data were statistically analysed using one-way ANOVA with a Dunnet's post-hoc test. The different compound concentrations were compared with the untreated control.

2.3 Results

To investigate the role of cell death, different cell death assays were used after exposing CCRF-CEM cells or PBMCs, of CBZ-naïve volunteers, to CBZ and 9-AC, a metabolite of CBZ.

2.3.1 Evaluation in CCRF-CEM cell line

For the assessment of a toxic effect in CCRF-CEM cells, the MTT assay, a cell viability assay, was conducted after exposing the cell line to different concentrations of CBZ and 9-AC.

For CBZ overall, no cytotoxic effect was observed (see Fig. 2.4). The only exception to this was a statistically significant decrease in cell viability of CCRF-CEM cells after 2 hour exposure to the lowest concentration (10 µM) in the experiments which may be artefactual. In the 24 hour exposure a dose-dependent decrease in cell viability could be observed but the effect was not statistically significant except for the highest concentration (200 µM).

9-AC in comparison showed a dose-dependent effect after a 2 hour exposure (see Fig. 2.4 A). This effect was found to be statistically significant. The cytotoxic effect was also observed after a 24 hour exposure. Here the effect was more significant compared to the 2 hour exposure (see Fig. 2.4 B).

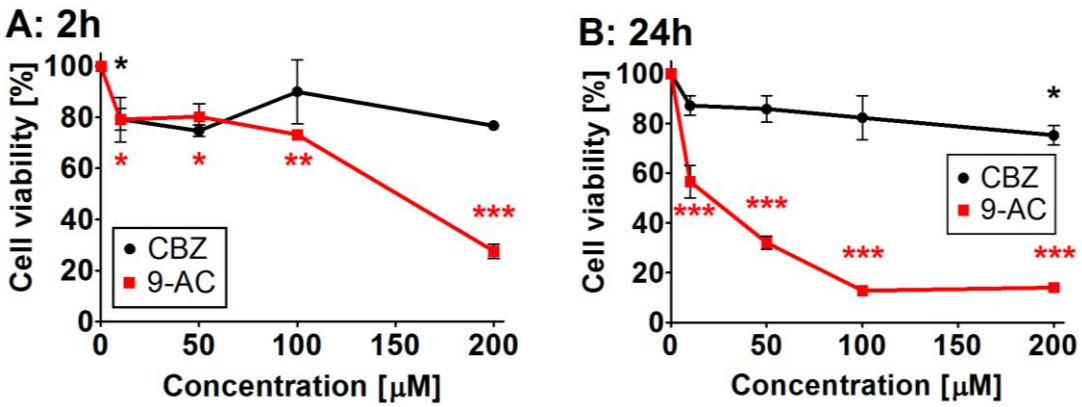

Figure 2.4: Cell viability in CCRF-CEM cells after exposure to compounds

CCRF-CEM cells were exposed to different concentrations of CBZ and 9-AC for 2 (**A**) and 24 (**B**) hours. 24 hours after the start of the incubation, MTT solution and lysis buffer were added and absorbance was measured (n=3, error bars: standard deviation of the mean, and p-value: *: <0.05-0.01, **: <0.01-0.001, ***: <0.001).

After the finding of cytotoxicity caused by 9-AC, further investigation was undertaken. MMP was assessed using TMRE for staining mitochondria.

CCRF-CEM cells exposed to CBZ did not show an increase in the number of cells with MMP (see Fig. 2.5).

CCRF-CEM cells exposed to 9-AC for 2 hours showed a small increase in cells with depolarised mitochondria. By contrast, cells exposed for 24 hours to 9-AC showed a statistically significant increase in the number of cells in which the mitochondrial membrane was depolarised (see Fig.2.5).

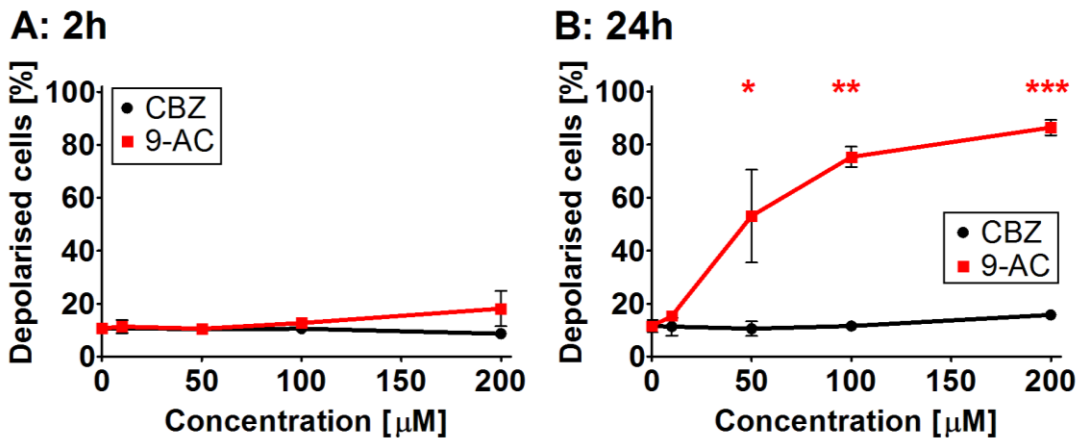

Figure 2.5: MMP in CCRF-CEM cells after exposure to compounds

CCRF-CEM cells were exposed to different concentrations of compounds for 2 (**A**) and 24 (**B**) hours. Cells were stained with TMRE 24 hours after start of incubation and fluorescence measured using flow cytometer. % shows amount of cells with MMP in whole population (n=3, error bars: standard deviation of the mean, and p-value: *: <0.05-0.01, **: <0.01-0.001, ***: <0.001).

This provided evidence of an apoptotic pathway involved in the cytotoxic effect caused by 9-AC. To validate that evidence, the percentage of cells exposing PS on the cell surface while possessing an intact cell membrane was determined.

In the Annexin V and PI experiment, a small increase in dead CEM cells was observed after exposure to CBZ but only at the highest concentration (200 µM) over 24 hours (see Fig. 2.6).

For 9-AC, as observed in the previous experiments, there was a dose-dependent cytotoxic effect observable after just 2 hours of exposure of CEM cells (see Fig. 2.6 A). After exposure of cells for 24 hours, the percentage of dead cells was statistically significant. The amount of apoptotic and necrotic cells increased with the amount of drug in the media. More apoptotic cells were found than the necrotic cells. Only for the highest concentration were more necrotic cells detected than apoptotic (see Fig. 2.6 B).

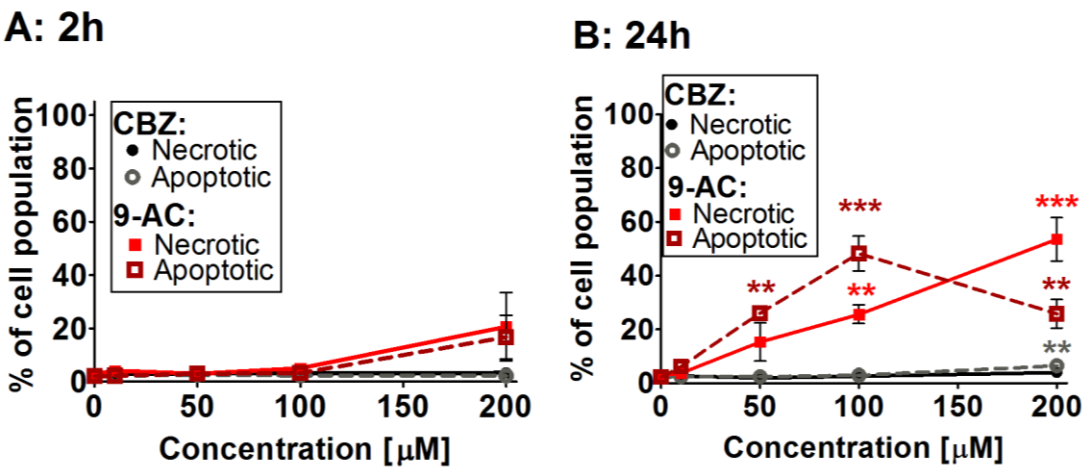

Figure 2.6: Apoptotic and necrotic cells in CCRF-CEM cells after exposure

CCRF-CEM cells were exposed to different concentrations of CBZ and 9-AC for 2 (**A**) and 24 (**B**) hours. Cells were stained with Annexin V and PI 24 hours after the start of the incubation and fluorescence measured in flow cytometer. Percentage gives the amount of different stained cells in comparison to the whole population (n=3, error bars: standard deviation of the mean, and p-value: *: <0.05-0.01, **: <0.01-0.001, ***: <0.001).

In the caspase activation assay, CCRF-CEM cells exposed to CBZ showed no increase in the activation of caspase except for the highest concentration and at 24 hours exposure (see Fig. 2.7). Cells exposed to 9-AC showed a significant increase in caspase activation. This effect was observable at the 50 µM concentration and 2 hour exposure (see Fig. 2.7 A). After the exposure of the cells for 24 hours, at the highest concentration, the cells showed a drastic drop in caspase activity. The amount of active caspase dropped below the caspase activity of unexposed cells.

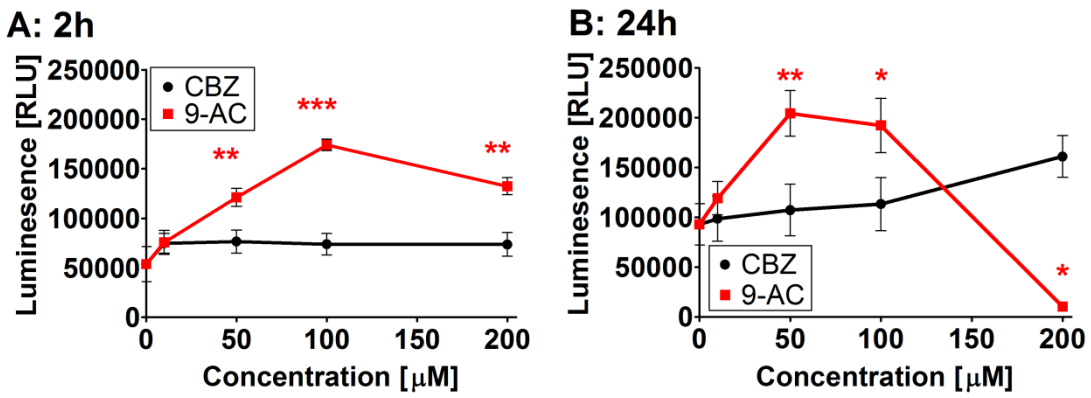

Figure 2.7: Caspase activity in CCRF-CEM cell line after exposure to compounds

CCRF-CEM cells were exposed to different concentrations of CBZ and 9-AC for 2 (**A**) and 24 (**B**) hours. 24 hours after the start of the incubation, the assay was stopped by adding reagent and luminescence was measured (n=3, error bars: standard deviation of the mean, and p-value: *: <0.05-0.01, **: <0.01-0.001, ***: <0.001).

Samples treated with 9-AC and Z-VAD-FMK (caspase inhibitor) showed a drop in caspase activity (see Fig. 2.8). The utilisation of the caspase inhibitor showed the dependence of the observed apoptosis upon caspase activation.

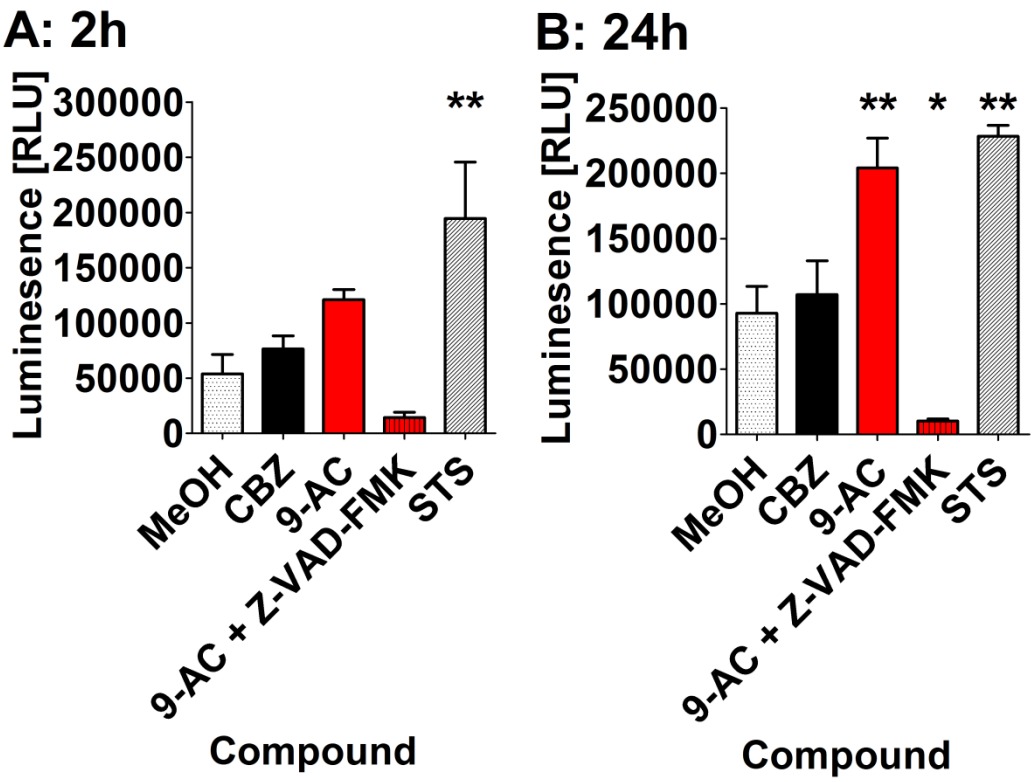

Figure 2.8: Caspase activity in CCRF-CEM cell line after exposure to single concentration of compounds

CCRF-CEM cells were exposed to 50 µM of CBZ and 9-AC, 50 µM 9-AC plus 50 µM Z-VAD-FMK, and 4 µM of STS for 2 (**A**) and 24 (**B**) hours. 24 hours after the start of the incubation, the assay was stopped by adding reagent and luminescence was measured (n=3, error bars: standard deviation of the mean, and p-value: *: <0.05-0.01, **: <0.01-0.001, ***: <0.001).

2.3.2 Evaluation of cytotoxicity in PBMCs

The finding that 9-AC caused apoptosis was demonstrated in a T lymphoblastoid cell line. The effect of 9-AC was further assess in primary cells, for which PBMCs from CBZ-naïve volunteers were used.

As shown in the T lymphoblastoid cell line, PBMCs treated with CBZ showed only a non-significant decrease in cell viability. The exception to this was the highest concentration of CBZ (200 µM) after a 24 hour exposure (see Fig. 2.9 B).

By contrast, cells exposed to 9-AC showed a dose-dependent decrease in cell viability. This effect was observable at both 2 and 24 hours. This decrease was found to be statistically significant starting from 50 µM for the 2 hour exposure and from 100 µM for the 24 hour exposure (see Fig. 2.9).

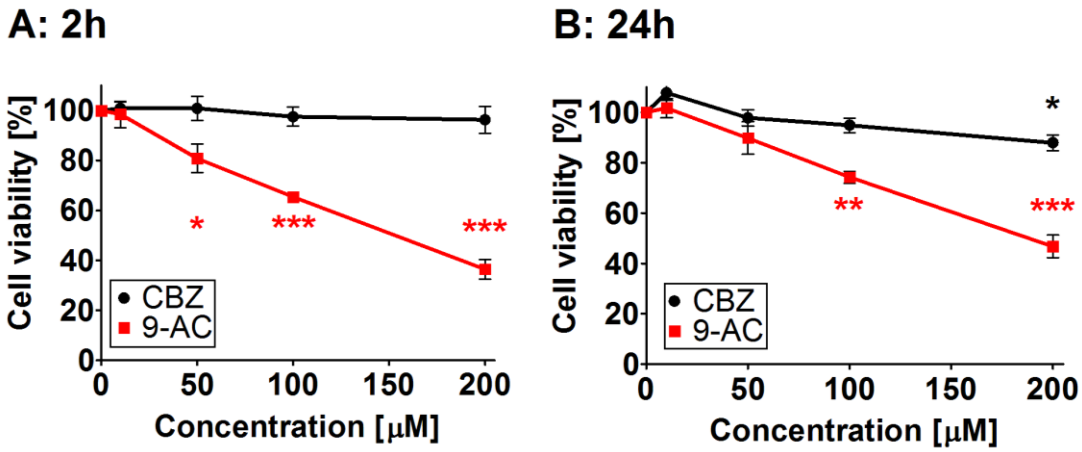

Figure 2.9: Cell viability in PBMCs after exposure to compounds

PBMCs were exposed to different concentrations of compounds for 2 (**A**) and 24 (**B**) hours. After 24 hours of incubation, MTT solution and lysis buffer were added and absorbance was measured (n=3, error bars: standard deviation of the mean, and p-value: *: <0.05-0.01, **: <0.01-0.001, ***: <0.001).

Following this observation, the MMP of PBMCs exposed to the compounds was assessed. Therefore cells were stained with TMRE after exposure to the compounds. A high percentage of PBMCs with MMP were observed in the control samples.

Cells exposed to CBZ for 2 or 24 hours did not show an increase in the number of cells with MMP. Cells exposed to 9-AC showed a dose-dependent increase in cells with MMP (Fig. 2.10).

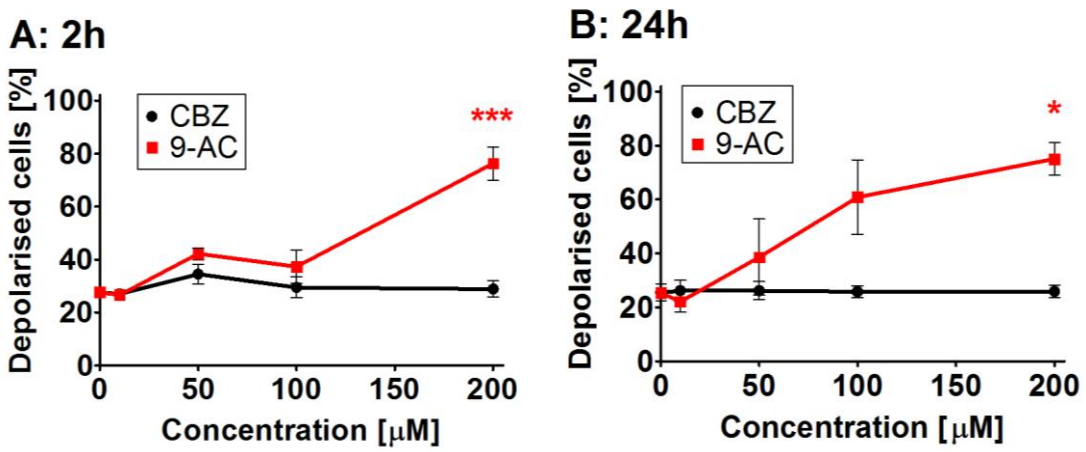

Figure 2.10: MMP in PBMCs after exposure to compounds

PBMCs were exposed to different concentrations of compounds for 2 (**A**) and 24 (**B**) hours. PBMCs were stained with TMRE 24 hours after start of incubation. Cells with MMP were expressed as percentage of whole population (n=3, error bars: standard deviation of the mean, and p-value: *: <0.05-0.01, **: <0.01-0.001, ***: <0.001).

To further investigate the nature of the cytotoxic effect, the amount of cells presenting PS on the cell surface, while the cell membrane is still intact, was assessed. The data from the flow cytometric analysis did not show precise populations of apoptotic and necrotic cells, which made the interpretation difficult (Fig. A2.1 in the appendix). A high percentage of cells showing signs of cell death, were found in the unexposed samples. Nevertheless it distinguished between dead and living cells.

The percentage of cells showing signs of cell death did not increase when exposed to CBZ. For 9-AC, the number of PBMCs, showing signs of cell death, rose with the increase in concentration (see Fig. 2.11).

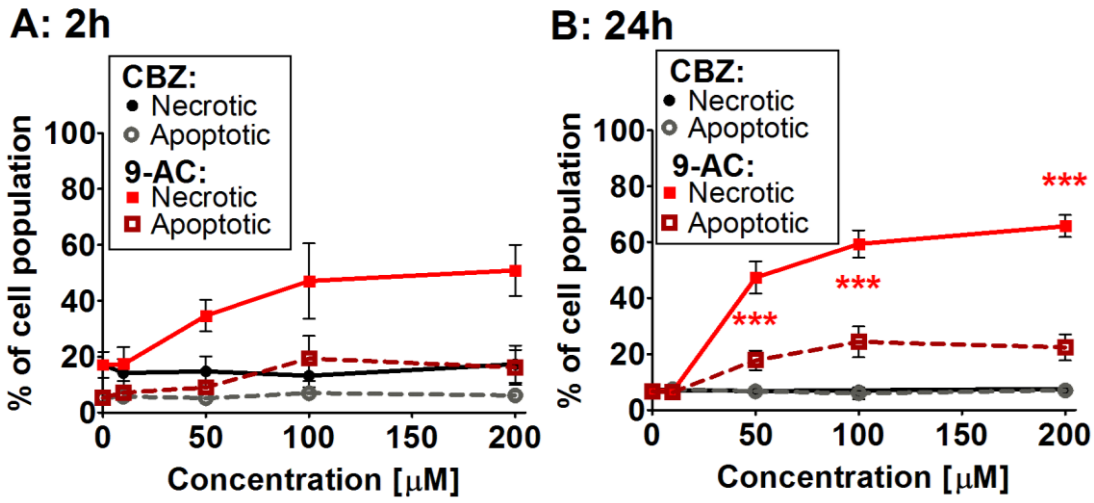

Figure 2.11: Apoptotic and necrotic cells in PBMCs after exposure

PBMCs were exposed to different concentrations of compounds for 2 (**A**) and 24 (**B**) hours. PBMCs were stained with Annexin V and PI 24 hours after the start of the incubation and fluorescence measured in flow cytometer. Percentage gives the amount of different stained cells in comparison to the whole population (n=3, error bars: standard deviation of the mean, and p-value: *: <0.05-0.01, **: <0.01-0.001, ***: <0.001).

Since the previous assay only confirmed that the cells were dying but could neither support nor dismiss the possibility of apoptosis or necrosis, the caspase activation assay was utilised. This assay can provide clear evidence of either apoptosis or necrosis since it has been shown to be cell type-independent [34].

The activity of caspase did not significantly increase in PBMCs exposed to CBZ. In PBMCs exposed to 9-AC, increased activation of caspase was observed after the 2 hour exposure in a dose-dependent manner. Only for 200 µM was the caspase activation found to be at the same level as in the unexposed cells (see Fig. 2.12).

For the 24 hour exposure, the activation of caspase decreased with an increase in 9-AC concentration below the level of caspase activity observed in unexposed cells.

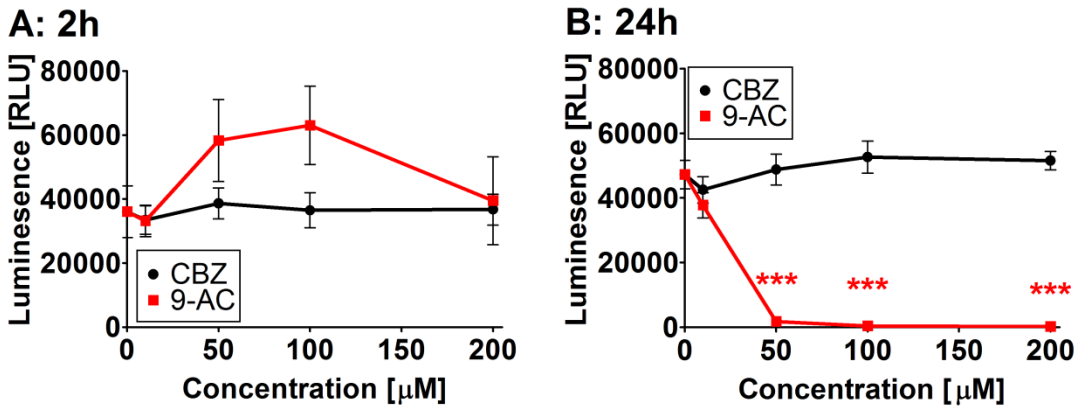

Figure 2.12: Caspase activity in PBMCs after exposure to compounds

PBMCs were exposed to different concentrations of compounds 2 (**A**) and 24 (**B**) hours. 24 hours after the start of the incubation, the assay was stopped by adding reagent and luminescence was measured (n=3, error bars: standard deviation of the mean, and p-value: *: <0.05-0.01, **: <0.01-0.001, ***: <0.001).

9-AC dependent caspase activation was observed in PBMCs exposed for 2 and 24 hours but was reduced by Z-VAD-FMK. This observation shows that 9-AC induces caspase-dependent cell death (see Fig. 2.13). The caspase activation in the 24 hour incubation was significantly higher than the caspase activation in the control. This contradicts the previous observation, where the caspase activation of the PBMCs treated with 9-AC was significantly lower than the control (see Fig. 2.12).

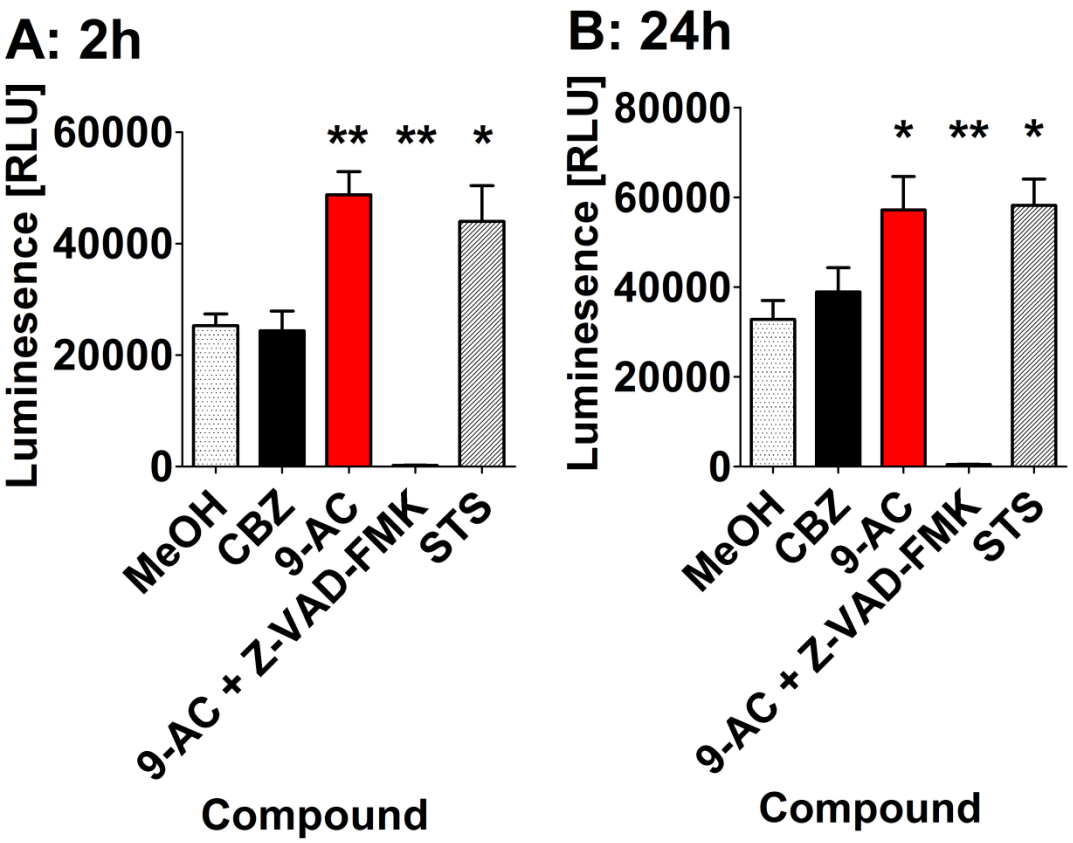

Figure 2.13: Caspase activity in PBMCs after exposure to single compound concentration

PBMCs were exposed to 50 µM of CBZ and 9-AC, 50 µM 9-AC plus 50 µM Z-VAD-FMK, and 4 µM of STS for 2 (**A**) and 24 (**B**) hours. 24 hours after the start of the incubation, the assay was stopped by adding reagent and luminescence was measured (n=3, error bars: standard deviation of the mean, and p-value: *: <0.05-0.01, **: <0.01-0.001, ***: <0.001).

2.3.2.1 Evaluation of interindividual variability

The variability in the outcome of the previous experiments with PBMCs suggested that there might be interindividual variability in susceptibility to the cytotoxic effect of 9-AC. Therefore PBMCs from 20 CBZ-naïve, healthy volunteers were isolated and exposed to a single dose (50 µM) of CBZ and 9-AC. The PBMCs were only exposed to the drug for 2 hours and replaced for the rest of the 24 hours with drug-free medium as this showed the strongest cytotoxic effect in previous experiments. Measurement of apoptotic and necrotic cells was not conducted as the data obtained in experiments were not interpretable and therefore provided no further information on apoptotic and necrotic cell death.

PBMCs from 20 healthy volunteers exposed to a single dose of CBZ showed no sign of cell death. The cell viability measured via the metabolic activity of the cells did not show a decrease. Additionally no increase of cells with MMP was observed nor was the activity of caspase significantly increased (see Fig. 2.14).

PBMCs exposed to 50 µM of 9-AC showed a decrease in their viability. Also the amount of cells exhibiting MMP increased in a statistically significant manner and caspase activation was seen after exposure to 9-AC when compared with control incubation.

The cytotoxic response to the single concentration of CBZ and 9-AC from different individuals showed variation. The strongest variation was observed in the caspase activation after exposure to the compounds.

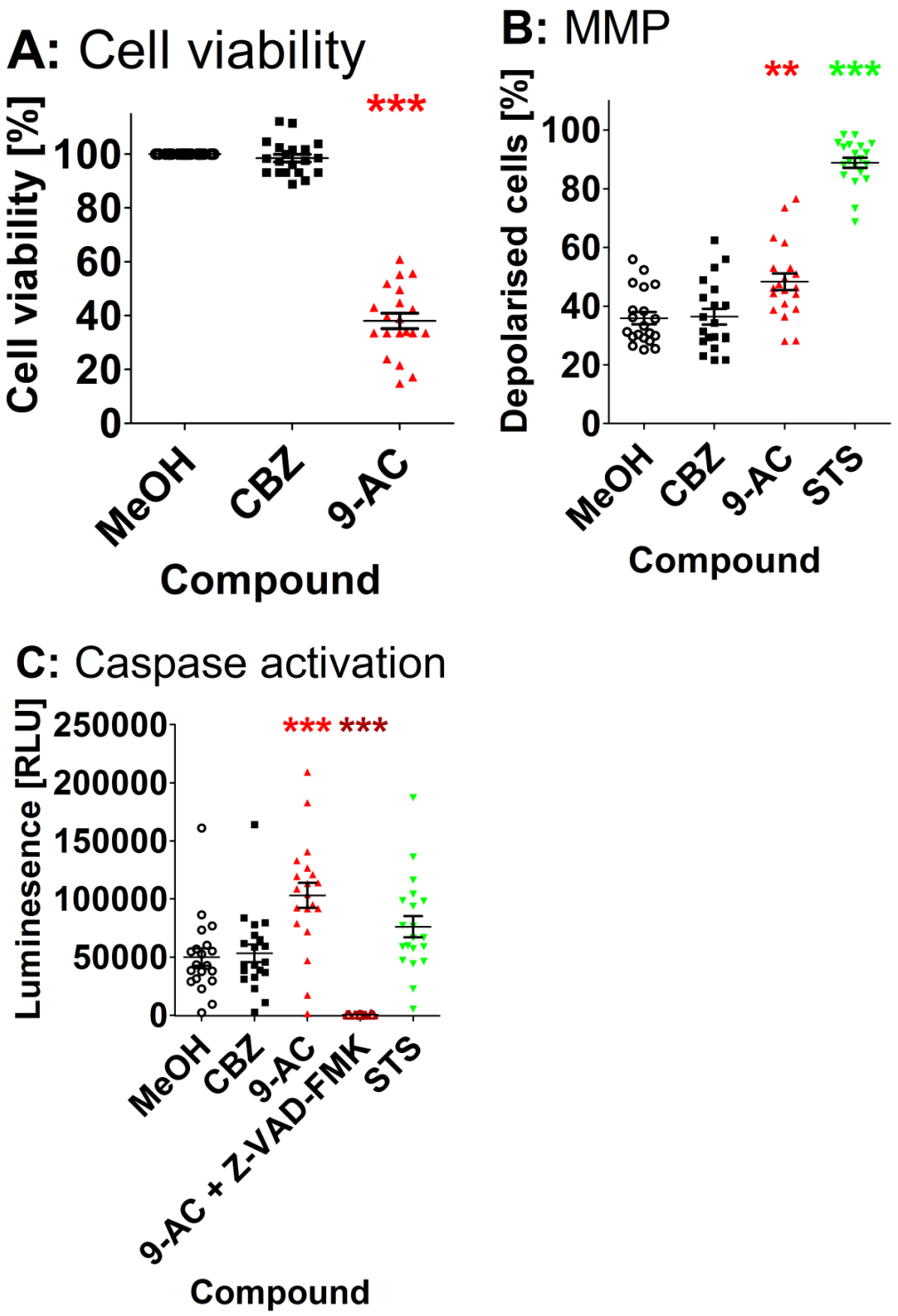

Figure 2.14: Cell viability (A), MMP (B), and caspase activity (C) in PBMCs after exposure to single compound concentration for 2 hours

PBMCs from 20 different individuals were exposed to 50 µM of CBZ, 9-AC, 9-AC plus the caspase inhibitor Z-VAD-FMK (for caspase activation) and STS (for MMP and caspase activation) for 2 hours. After 24 hours of incubation, reagent according to specific assay was added (error bars: standard deviation of the mean and p-value: *: <0.05-0.01, **: <0.01-0.001, ***: <0.001).

2.4 Discussion

CBZ is one of the most widely prescribed anticonvulsants for the treatment of partial seizures. 10% of patients treated with CBZ develop skin rashes [35]. These can develop further into more severe forms of CBZ-induced hypersensitivity reactions. An association between HLA-A*31:01 and CBZ-induced hypersensitivity reactions has been found and represents a prediction method for risk evaluation for the development of idiosyncratic reactions during treatment with CBZ [36]. It is therefore of utmost importance to understand the underlying mechanisms involved and through this, find other predictive markers for the development of CBZ-induced hypersensitivity reactions.

The underlying pathological mechanisms involved in the development of CBZ-induced adverse drug reactions are still unknown. Patients treated with CBZ can have antibodies against CBZ in their blood [37-40]. This was found for CBZ-tolerant as well as CBZ-hypersensitive patients. It has also been shown that T cells play a role in hypersensitivity reactions and can be found in cutaneous blisters [41, 42]. T cells are thought to be responsible for the cytotoxic effects observed. How these T cells are primed against CBZ is unclear.

The hypothesis behind the work in this chapter was based on the danger hypothesis, as described in the general introduction (see section 1.5.4). In brief, the danger hypothesis takes into consideration that T cell activation is not based on just one signal, non-self proteins, but on the presence of at least one additional signal, expressed by APCs in the presence of danger signals. Additionally, it was shown that certain drugs or their metabolites can damage cells and thus induce the presentation of costimulatory signals for T cell activation on APCs [43-45]. The leakage of cytosolic content, which would lead to the presentation of costimulatory signals, could be the result of cells undergoing necrosis after exposure to the compounds. Therefore the aim was to identify the type of cell death caused by the exposure of cells to

CBZ and one metabolite, 9-AC, thus testing the hypothesis that cell death can lead to danger signalling and to the activation of the immune system. To achieve this, different methods for assessing cell death and distinguishing between apoptosis and necrosis were utilised. The variation in cytotoxic response of PBMCs from CBZ-naïve healthy volunteers was also assessed. The assays utilised for this project were: cell viability assay, MMP assay, PS exposure combined with vital dye assay and caspase activation assay (for more details, including advantages and disadvantages of the assays used, see Tab. 2.1)

The results from the assays revealed that 9-AC causes the CCRF-CEM cell line to undergo apoptosis in a dose-dependent manner since the cytotoxic effect increases with the concentration of 9-AC. For the 2 hour exposure of cells to 9-AC, not all assays were able to detect signs of cell death. A more distinct apoptotic effect was found for cells that were exposed for 24 hours to 9-AC. The first statistically significant effect for all assays was observed for 50 µM of 9-AC and 24 hour exposure.

The results of the cell viability assay and the MMP assay of CCRF-CEM showed different sensitivity for cytotoxicity caused by 9-AC (Fig. 2.4 and 2.5). The cell viability measured through MTT transformation correlates the metabolic activity with viability of the cell [20]. This metabolic activity is generally attributed to the mitochondria [46-48]. Therefore, the depolarisation of the mitochondrial membrane should occur before the decrease in metabolic activity of the cell during cell death. However, the dehydrogenases which transform MTT are not only present in mitochondria but can also be found in the cytosol [49]. Furthermore, the conversion of MTT reflects metabolic alteration which can be influenced by other factors, e.g. medium overconsumption or excessive cell density [20]. This may explain the observed discrepancy between the metabolic activity and the MMP of the CCRF-CEM cells.

Table 2.1: Advantages and disadvantages of assays used in this project [17]

Method	Detection method	Advantages	Disadvantages
Cell viability assay Tetrazolium salt conversion (MTT)	Spectrophotometry	• Relatively inexpensive • Based on standard laboratory equipment	• Mitochondrial activity can be decreased in cell death-unrelated processes • MTT is converted into cytotoxic product • Requires optimisation
MMP assay $\Delta\psi_m$-sensitive dye (TMRE)	Cytoflowcytometry	• Quantitative • On living cells • Several dyes allow for co-staining	• MMP can occur in cell death-unrelated processes • Some fluorochromes exhibit self-quenching
PS exposure (Annexin V) and vital dye (PI) assay	Cytoflowcytometry	• Rapid (no fixation required) • Specific for early phase of apoptosis	• PS exposure can occur in apoptosis-unrelated processes
Caspase activation assay (Fluorogenic caspase substrate)	Photometry	• Allows large scale high-throughput utilisation • Based on standard laboratory equipment	• Caspase activation can occur in apoptosis-unrelated processes • Fluorogenic caspase substrates have very limited half-life

MTT: 3-(4,5-dimethylthiazol-2-yl)-2,5-diphenyltetrazolium bromide, TMRE: tetramethylrhodamine, ethyl ester, perchlorate, PS: phosphatidylserine, PI: Propidium iodide

In the PS exposure and vital dye assay, a large number of necrotic cells were observed after 24 hours of exposure at the highest concentration of 9-AC. A continuous increase in apoptotic and necrotic cells was observed, with the apoptotic cells representing the dominant population. The necrotic cells seen after exposure to 200 µM of 9-AC were probably a result of secondary necrosis [50]. Cells undergo complete apoptosis and after blebbing, the apoptotic bodies stay in the culture media. Due to the fact that there are no macrophages in the media, unlike the *in vivo* situation, apoptotic bodies are not cleared through phagocytosis. The apoptotic bodies are unable to maintain membrane integrity and start rupturing resulting in necrosis like spillage of the contents into the culture media [50]. In certain assays, this will be detected as cells that appear to have undergone necrosis. This assumption is supported by the caspase activation assay.

The activation of caspase increases with higher concentrations of 9-AC. For the highest dose, however, the activity of caspase drops even below the caspase activity level in untreated cells suggesting that the ATP content of the cells is completely depleted and apoptosis completed.

This decrease in caspase activation below the caspase activity of unexposed cells was also observed in cells that were exposed to 9-AC and the caspase inhibitor Z-VAD-FMK. It was reported that cells exposed to a toxin in the presence of a caspase inhibitor still undergo cell death as the caspase inhibitor only prevents apoptosis but not necrotic cell death [51]. Cells undergo apoptosis and the process stops at the point where the activation of caspase would start. As the process cannot continue, the cells become necrotic, meaning that the cell membrane integrity will not be upheld. Similar observations were made for cells with depleted ATP reservoirs. Also in this case, cells are not able to proceed with apoptosis until the formation of apoptotic bodies and therefore become necrotic [52].

CBZ did not show a cytotoxic effect in the T lymphoblastoid cell line for most of the concentrations used in the experiments. A statistically significant increase of cells displaying signs of cell death was detected after 24 hour

exposure to 200 µM of CBZ. However, these findings were not confirmed by all assays. Furthermore, it should be noted that this concentration also exceeds the therapeutic concentration by more than twofold [53].

The experiments conducted in this work showed that 9-AC also causes apoptosis in PBMCs of CBZ-naïve healthy volunteers. The apoptotic effect was found to increase with higher dose. The difference could not be shown to be statistically significant in all assays used, as the variability in the response of different individuals was too large. Signs of apoptosis were detectable in PBMCs after 2 hours of exposure to 9-AC, which suggests that PBMCs are more susceptible to the cytotoxic effect of 9-AC than CCRF-CEM cells, for which a significant increase of apoptotic signs were detected after 24 hours of exposure. The difference observed could be explained by the fact that the CCRF-CEM cell line is derived from blood of a patient with acute lymphoblastic leukaemia [54]. It is known that cancer cells develop mechanism to escape the elimination by the immune system through resistance against apoptosis [55]. It has been shown that both alleles of tumour suppressor gene p53 are mutated in CCRF-CEM cells, which leads to a defect of p53 inducing apoptosis [56, 57]. This reported impairment of apoptosis may explain the observed difference in viability between CCRF-CEM cells and PBMCs.

PBMCs did not show any signs of cytotoxicity when exposed to CBZ. This was expected, as it has been reported previously by Furst and Uetrecht that CBZ does not cause cell death [58]. In their experiments, it was observed that 9-AC but not CBZ caused cytotoxicity in human blood cells *in vitro*. The results presented in this chapter support these findings.

For the MMP assay, it was found that a large percentage (>20%) of cells showed signs of MMP without being exposed to any of the compounds. PBMCs consist of different cell types and these different cell types might occur at variable frequencies while being stained with TMRE. The different cell types could also possess varying sensitivities towards the process of purification. The assay still showed an increase in cells with MMP with higher concentrations of 9-AC.

In the PS exposure and vital dye assay, data form flow cytometry did not allow a distinction between the apoptotic and necrotic cell populations. Nevertheless, distinguishing between living and dead cells was possible. Here, again the reason could lie in the different cell types in the PMBC population. To overcome the issue of undistinguishable populations of necrotic and apoptotic cells, cells were triple stained, including a dye for $CD3^+$ T cells. This showed that less than 10% of cells in the samples were $CD3^+$ and the amount of $CD3^+$ cells decreased with higher concentration of 9-AC suggesting that this marker was lost during the process of cell death and therefore not suitable in solving the problem (Fig. A2.2 in appendix). Triple staining with annexin V, PI and $CD3^+$ of human PBMCs has been described for analysis of apoptosis and necrosis in freshly isolated PBMCs from patients but not for PBMCs in culture [59].

The assumption that the problems experienced during the flow cytometric assays is the result of different cell types making up the PBMC population is indirectly supported by the fact that no such difficulties were experienced with the viability assay and caspase activation assay, which are known to assess the signs of cell death in a cell type-independent manner [34].

Besides the problems experienced with the flow cytometry assays, the contradictory findings of the caspase activation assay revealed another limitation of the experiments. Due to the limited access to healthy volunteers and the complexity of the study design (four assays, two compounds, and four concentrations per compound), it was only possible to measure the viability of PBMCs from each individual once with each assay. A better approach would have been to obtain and measure PBMCs from each individual at least three times and use the mean of these results. This would have delivered more robust and reproducible data for each individual.

The experiments with PBMC samples of 20 healthy volunteers exposed for 2 hours to 50 µM CBZ or 9-AC showed that only 9-AC induces cell death in PBMCs. The difference between the untreated control and 9-AC was statistically significant. The extent of the cytotoxicity observed in the samples of the different individuals showed variability. This suggests that some

individuals are more susceptible to the cytotoxic effect of 9-AC. The low level of activated caspase in some PBMCs exposed to 9-AC suggests that the cell death in these samples might not be caspase dependent. It has been reported that the dose of cytotoxic drugs can determine the cell death pathway [60, 61]. At low doses, cells undergo apoptosis, while higher doses result in necrosis. Therefore, the susceptibility of cells to the cytotoxic effect of 9-AC might lead to different pathways of cell death, which could result in the release of danger signals. Further investigation of this mechanism in CBZ-induced hypersensitivity reactions is required.

Studies, using the lymphocyte toxicity assay after Spielberg, found that lymphocytes from patients [6], which had experienced CBZ-induced hypersensitivity reactions, were more susceptible to cytotoxicity of oxidative metabolites generated by hepatic microsomes than lymphocytes from CBZ-tolerant patients or CBZ-naïve volunteers [8, 9]. It was also suggested that *in vitro* cytotoxicity assays could be used before the treatment of patients to evaluate their risk [9]. The finding of inter-individual variability in cell viability in this chapter, however, was made in CBZ-naïve volunteers. Therefore, the extent of the variability between patients who had suffered from CBZ-induced hypersensitivity reactions and CBZ-tolerant patients would be an interesting point for further investigations.

In the experiments included in this chapter, only the parent drug, CBZ, and one metabolite, 9-AC, were used. However, more than 30 metabolites of CBZ have been found in patients treated with the drug. Furthermore, it has been speculated that a highly reactive arene oxide is generated during the metabolism of CBZ, which could lead to cellular damage [62]. Therefore, the cytotoxicity of other metabolites would need to be tested. The type of cell death caused by these toxic metabolites would then need to be examined to further investigate the possibility of CBZ metabolites causing danger signalling.

The focus of the experiments conducted for this work lay on differentiating between apoptosis and necrosis. As mentioned in the general introduction, a number of cell death pathways have been described, some of which are

controlled forms of cell death. However, not all of these controlled forms take place under maintenance of the outer cell membrane integrity. It has been shown that these pathways can play an important role in the cytotoxicity caused by xenobiotics [63]. Therefore, the involvement of other cell death pathways would need to be examined, as they could lead to costimulatory signalling by leakage of cytosolic content into the surrounding tissue, similar to the leakage of necrotic cells.

In conclusion, the results show that only the metabolite 9-AC causes cytotoxicity, while CBZ was not toxic in the concentration range used. Furthermore, it was found that 9-AC causes apoptotic cell death. Therefore, neither the parent drug CBZ nor its metabolite 9-AC would cause danger signalling as a result of cellular damage, which is necessary for T cell activation according to the danger hypothesis. However, danger signalling could be caused through other modalities, such as different forms of cell death or different metabolites. The inter-individual variability in cell viability observed in the experiments could indicate that cells exposed to 9-AC die via different cell death pathways, some of which might result in the release of danger signals. Additionally, an infection during the treatment with the drug could also induce the expression of costimulatory signals on APCs. These other possibilities need to be investigated before dismissing the danger hypothesis as an important mechanism during T cell activation in hypersensitivity reactions. Taken together, many factors which could explain danger signalling in the initiation of hypersensitivity reactions in patients remain unknown.

2.5 References

1. Furst, S.M. and J.P. Uetrecht, *Carbamazepine metabolism to a reactive intermediate by the myeloperoxidase system of activated neutrophils.* Biochem Pharmacol, 1993. **45**(6): p. 1267-75.
2. Cribb, A.E., et al., *Peroxidase-dependent oxidation of sulfonamides by monocytes and neutrophils from humans and dogs.* Mol Pharmacol, 1990. **38**(5): p. 744-51.
3. Uetrecht, J., et al., *Metabolism of dapsone to a hydroxylamine by human neutrophils and mononuclear cells.* J Pharmacol Exp Ther, 1988. **245**(1): p. 274-9.
4. Uetrecht, J. and N. Zahid, *N-chlorination of phenytoin by myeloperoxidase to a reactive metabolite.* Chem Res Toxicol, 1988. **1**(3): p. 148-51.
5. Siest, G., et al., *Transcription factor and drug-metabolizing enzyme gene expression in lymphocytes from healthy human subjects.* Drug Metab Dispos, 2008. **36**(1): p. 182-9.
6. Spielberg, S.P., et al., *Anticonvulsant toxicity in vitro: possible role of arene oxides.* J Pharmacol Exp Ther, 1981. **217**(2): p. 386-9.
7. Wolkenstein, P., et al., *Metabolic predisposition to cutaneous adverse drug reactions. Role in toxic epidermal necrolysis caused by sulfonamides and anticonvulsants.* Arch Dermatol, 1995. **131**(5): p. 544-51.
8. Pirmohamed, M., et al., *Carbamazepine-hypersensitivity: assessment of clinical and in vitro chemical cross-reactivity with phenytoin and oxcarbazepine.* Br J Clin Pharmacol, 1991. **32**(6): p. 741-9.
9. Shear, N.H. and S.P. Spielberg, *Anticonvulsant hypersensitivity syndrome. In vitro assessment of risk.* J Clin Invest, 1988. **82**(6): p. 1826-32.
10. Raffray, M. and G.M. Cohen, *Apoptosis and necrosis in toxicology: a continuum or distinct modes of cell death?* Pharmacol Ther, 1997. **75**(3): p. 153-77.
11. Coleman, M.L., et al., *Membrane blebbing during apoptosis results from caspase-mediated activation of ROCK I.* Nat Cell Biol, 2001. **3**(4): p. 339-45.
12. Kroemer, G., et al., *Classification of cell death: recommendations of the Nomenclature Committee on Cell Death 2009.* Cell Death Differ, 2009. **16**(1): p. 3-11.
13. Vandenabeele, P., et al., *Molecular mechanisms of necroptosis: an ordered cellular explosion.* Nat Rev Mol Cell Biol, 2010. **11**(10): p. 700-14.
14. Degterev, A., et al., *Chemical inhibitor of nonapoptotic cell death with therapeutic potential for ischemic brain injury.* Nat Chem Biol, 2005. **1**(2): p. 112-9.
15. Fischer, K., et al., *Antigen recognition induces phosphatidylserine exposure on the cell surface of human CD8+ T cells.* Blood, 2006. **108**(13): p. 4094-101.
16. Qu, X., et al., *Autophagy gene-dependent clearance of apoptotic cells during embryonic development.* Cell, 2007. **128**(5): p. 931-46.
17. Kroemer, G., L. Galluzzi, and C. Brenner, *Mitochondrial membrane permeabilization in cell death.* Physiol Rev, 2007. **87**(1): p. 99-163.
18. Maiuri, M.C., et al., *Self-eating and self-killing: crosstalk between autophagy and apoptosis.* Nat Rev Mol Cell Biol, 2007. **8**(9): p. 741-52.
19. Galluzzi, L., et al., *No death without life: vital functions of apoptotic effectors.* Cell Death Differ, 2008. **15**(7): p. 1113-23.
20. Galluzzi, L., et al., *Guidelines for the use and interpretation of assays for monitoring cell death in higher eukaryotes.* Cell Death Differ, 2009. **16**(8): p. 1093-107.

21. Lipinski, M.M., et al., *Genome-wide analysis reveals mechanisms modulating autophagy in normal brain aging and in Alzheimer's disease.* Proc Natl Acad Sci U S A, 2010. **107**(32): p. 14164-9.
22. Shi, J., S. Springer, and P. Escobar, *Coupling cytotoxicity biomarkers with DNA damage assessment in TK6 human lymphoblast cells.* Mutat Res, 2010. **696**(2): p. 167-78.
23. Martin, S.J., et al., *Early redistribution of plasma membrane phosphatidylserine is a general feature of apoptosis regardless of the initiating stimulus: inhibition by overexpression of Bcl-2 and Abl.* J Exp Med, 1995. **182**(5): p. 1545-56.
24. Galluzzi, L., et al., *Methods for the assessment of mitochondrial membrane permeabilization in apoptosis.* Apoptosis, 2007. **12**(5): p. 803-13.
25. Boyum, A., *Separation of leukocytes from blood and bone marrow. Introduction.* Scand J Clin Lab Invest Suppl, 1968. **97**: p. 7.
26. Schroder, J., *[Determination of resistance of leukocytes].* Blut, 1956. **2**(3): p. 203-10.
27. Mosmann, T., *Rapid colorimetric assay for cellular growth and survival: application to proliferation and cytotoxicity assays.* J Immunol Methods, 1983. **65**(1-2): p. 55-63.
28. Farkas, D.L., et al., *Simultaneous imaging of cell and mitochondrial membrane potentials.* Biophys J, 1989. **56**(6): p. 1053-69.
29. Tamaoki, T., et al., *Staurosporine, a potent inhibitor of phospholipid/Ca++dependent protein kinase.* Biochem Biophys Res Commun, 1986. **135**(2): p. 397-402.
30. Lecoeur, H., *Nuclear apoptosis detection by flow cytometry: influence of endogenous endonucleases.* Exp Cell Res, 2002. **277**(1): p. 1-14.
31. Theodoropoulos, P.A., et al., *Cytochalasin B may shorten actin filaments by a mechanism independent of barbed end capping.* Biochem Pharmacol, 1994. **47**(10): p. 1875-81.
32. Roche. *Annexin-V-FLUOS Staining Kit*. Available from: https://cssportal.roche.com/LFR_PublicDocs/ras/11858777001_en_09.pdf.
33. Garcia-Calvo, M., et al., *Inhibition of human caspases by peptide-based and macromolecular inhibitors.* J Biol Chem, 1998. **273**(49): p. 32608-13.
34. Choy, E., et al., *Genetic analysis of human traits in vitro: drug response and gene expression in lymphoblastoid cell lines.* PLoS Genet, 2008. **4**(11): p. e1000287.
35. Marson, A.G., et al., *The SANAD study of effectiveness of carbamazepine, gabapentin, lamotrigine, oxcarbazepine, or topiramate for treatment of partial epilepsy: an unblinded randomised controlled trial.* Lancet, 2007. **369**(9566): p. 1000-15.
36. McCormack, M., et al., *HLA-A*3101 and carbamazepine-induced hypersensitivity reactions in Europeans.* N Engl J Med, 2011. **364**(12): p. 1134-43.
37. Igarashi, M., et al., *Immunosuppressive factors detected during convalescence in a patient with severe serum sickness induced by carbamazepine.* Int Arch Allergy Immunol, 1993. **100**(4): p. 378-81.
38. Horneff, G., H.G. Lenard, and V. Wahn, *Severe adverse reaction to carbamazepine: significance of humoral and cellular reactions to the drug.* Neuropediatrics, 1992. **23**(5): p. 272-5.
39. Igarashi, M., et al., *An immunodominant haptenic epitope of carbamazepine detected in serum from patients given long-term treatment with carbamazepine without allergic reaction.* J Clin Immunol, 1992. **12**(5): p. 335-40.

40. Hosoda, N., et al., *Anticarbamazepine antibody induced by carbamazepine in a patient with severe serum sickness.* Arch Dis Child, 1991. **66**(6): p. 722-3.
41. Naisbitt, D.J., et al., *Hypersensitivity reactions to carbamazepine: characterization of the specificity, phenotype, and cytokine profile of drug-specific T cell clones.* Mol Pharmacol, 2003. **63**(3): p. 732-41.
42. Mauri-Hellweg, D., et al., *Activation of drug-specific CD4+ and CD8+ T cells in individuals allergic to sulfonamides, phenytoin, and carbamazepine.* J Immunol, 1995. **155**(1): p. 462-72.
43. Martin, A.M., et al., *Immune responses to abacavir in antigen-presenting cells from hypersensitive patients.* AIDS, 2007. **21**(10): p. 1233-44.
44. Sanderson, J.P., et al., *Sulfamethoxazole and its metabolite nitroso sulfamethoxazole stimulate dendritic cell costimulatory signaling.* J Immunol, 2007. **178**(9): p. 5533-42.
45. Rodriguez-Pena, R., et al., *Potential involvement of dendritic cells in delayed-type hypersensitivity reactions to beta-lactams.* J Allergy Clin Immunol, 2006. **118**(4): p. 949-56.
46. Tajeddine, N., et al., *Hierarchical involvement of Bak, VDAC1 and Bax in cisplatin-induced cell death.* Oncogene, 2008. **27**(30): p. 4221-32.
47. de La Motte Rouge, T., et al., *A novel epidermal growth factor receptor inhibitor promotes apoptosis in non-small cell lung cancer cells resistant to erlotinib.* Cancer Res, 2007. **67**(13): p. 6253-62.
48. Vitale, I., et al., *Inhibition of Chk1 kills tetraploid tumor cells through a p53-dependent pathway.* PLoS One, 2007. **2**(12): p. e1337.
49. Berridge, M.V., P.M. Herst, and A.S. Tan, *Tetrazolium dyes as tools in cell biology: new insights into their cellular reduction.* Biotechnol Annu Rev, 2005. **11**: p. 127-52.
50. Wyllie, A.H., J.F. Kerr, and A.R. Currie, *Cell death: the significance of apoptosis.* Int Rev Cytol, 1980. **68**: p. 251-306.
51. Hirsch, T., et al., *The apoptosis-necrosis paradox. Apoptogenic proteases activated after mitochondrial permeability transition determine the mode of cell death.* Oncogene, 1997. **15**(13): p. 1573-81.
52. Leist, M., et al., *Intracellular adenosine triphosphate (ATP) concentration: a switch in the decision between apoptosis and necrosis.* J Exp Med, 1997. **185**(8): p. 1481-6.
53. Ghannoum, M., et al., *Extracorporeal treatment for carbamazepine poisoning: Systematic review and recommendations from the EXTRIP workgroup.* Clin Toxicol (Phila), 2014: p. 1-12.
54. Foley, G.E., et al., *Continuous Culture of Human Lymphoblasts from Peripheral Blood of a Child with Acute Leukemia.* Cancer, 1965. **18**: p. 522-9.
55. Igney, F.H. and P.H. Krammer, *Immune escape of tumors: apoptosis resistance and tumor counterattack.* J Leukoc Biol, 2002. **71**(6): p. 907-20.
56. Geley, S., et al., *p53-induced apoptosis in the human T-ALL cell line CCRF-CEM.* Oncogene, 1997. **15**(20): p. 2429-37.
57. Cheng, J. and M. Haas, *Frequent mutations in the p53 tumor suppressor gene in human leukemia T-cell lines.* Mol Cell Biol, 1990. **10**(10): p. 5502-9.
58. Furst, S.M. and J.P. Uetrecht, *The effect of carbamazepine and its reactive metabolite, 9-acridine carboxaldehyde, on immune cell function in vitro.* Int J Immunopharmacol, 1995. **17**(5): p. 445-52.
59. Dhir, V., et al., *Increased T-lymphocyte apoptosis in lupus correlates with disease activity and may be responsible for reduced T-cell frequency: a cross-sectional and longitudinal study.* Lupus, 2009. **18**(9): p. 785-91.
60. Elmore, S., *Apoptosis: a review of programmed cell death.* Toxicol Pathol, 2007. **35**(4): p. 495-516.

61. Zeiss, C.J., *The apoptosis-necrosis continuum: insights from genetically altered mice.* Vet Pathol, 2003. **40**(5): p. 481-95.
62. Gerson, W.T., et al., *Anticonvulsant-induced aplastic anemia: increased susceptibility to toxic drug metabolites in vitro.* Blood, 1983. **61**(5): p. 889-93.
63. Aki, T., T. Funakoshi, and K. Uemura, *Regulated necrosis and its implications in toxicology.* Toxicology, 2015. **333**: p. 118-126.

Chapter 3

Mass spectrometric characterisation of covalent protein adducts from carbamazepine and its metabolites *in vitro*

3.1 Introduction

Carbamazepine (CBZ) is known to cause hypersensitivity reactions in up to 10% of patients treated with the drug [1]. As CBZ is extensively metabolised in the human body [2, 3], it is unclear whether the parent compound is causing these reactions or one of the more than 30 metabolites found *in vivo*.

Several studies showed that antibodies against CBZ can be found in sera from patients on CBZ treatment [4-7]. These antibodies were not only found in the sera of patients developing CBZ-induced ADRs but also in CBZ tolerant patients. The role of CBZ-specific antibodies in CBZ-induced hypersensitivity reactions is unknown. Generally, antibodies are secreted by B cells and bind to the surface of antigens, thus inducing the complement system or marking them for the clearance by phagocytic cells of the innate immune system [8, 9]. As CBZ-specific antibodies were found in CBZ hypersensitive as well as CBZ-tolerant patients this seems not to be the underlying mechanism. Other studies detected specific autoantibodies against human liver microsomal proteins in the blood of a patient that had suffered from CBZ-induced hepatotoxicity but it was not demonstrated whether these antibodies are immunogenic [10, 11].

The activation of the immune system can be caused through the production of reactive metabolites [12, 13]. The metabolites are predominantly generated by the cytochrome P450 CYP3A4 in the human liver. In the case of CBZ, a highly reactive arene oxide was hypothesised. Due to its high reactivity, the arene oxide has never been observed in humans but evidence of its existence was found in rat bile [14].

Pirmohamed and colleagues investigated the possibility of the formation of protein-reactive, unstable metabolites *in vitro* [15]. Following this investigation, Pearce and colleagues extensively assessed the role of different cytochrome P450 enzymes in the formation of different CBZ metabolites (see Fig. 3.1) [16-18].

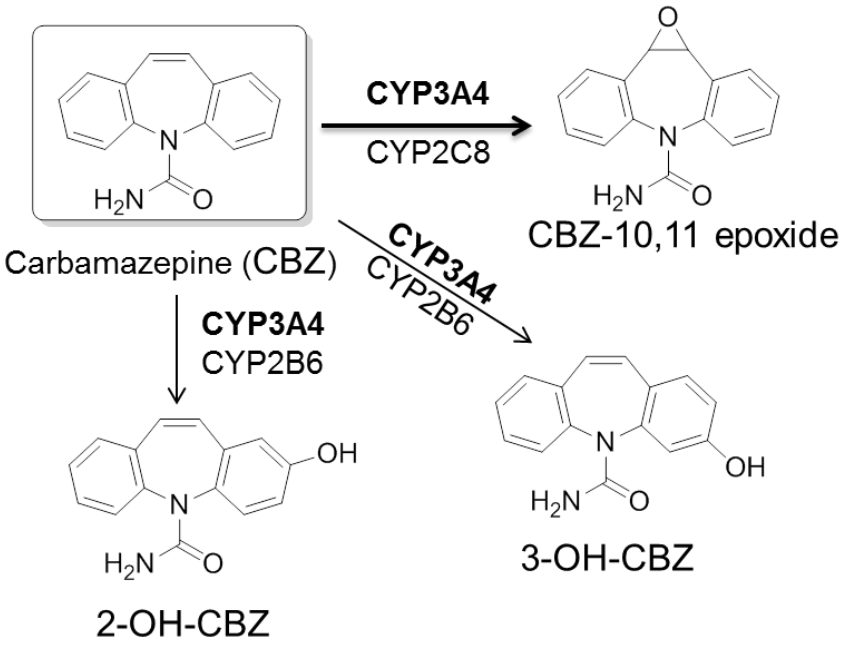

Figure 3.1: Isoforms of cytochrome P450 (CYP) responsible for metabolism of Carbamazepine (CBZ)

Furthermore, Furst and colleague showed that activated leukocytes can metabolise CBZ to reactive forms *in vitro*. The enzyme responsible for this metabolism was myeloperoxidase which can be also found in the skin. The postulated metabolites resulting from this metabolism included acridine derivatives such as 9-acridinecarboxaldehyde (9-AC) [19].

In the experiments for the previous chapter, lack of cytotoxicity from 9-AC, was observed when peripheral blood mononuclear cells were cultured in protein rich medium (Fig. A2.3-A2.5 in appendix). Furst and colleagues have reported that 9-AC can bind to proteins. Their experiments suggested that the binding occurs via a Schiff base [20]. In their experiments they used radiolabeled molecules for the detection of the binding. This approach does not allow the determination of the exact binding in the protein.

Liquid chromatography-tandem mass spectrometry (LC-MS/MS) platforms are a major tool in the identification of protein modification. LC-MS/MS allows the use of intact proteins or enzymatic digested proteins [21, 22]. The fragments of the digested peptide are first separated from each other using

HPLC. The eluted analytes are then ionised before the mass/charge ratio is detected. The resulting list can then be compared with a theoretical list of fragments that would be expected.

Ma and colleagues showed that reactive metabolites of drugs can be trapped and thus detected by MS. In their experiments, the parent drug or one metabolite was co-incubated with protein in the presence of metabolising enzymes [23, 24]. Due to its reactive cysteine residue, glutathione is used as a trapping agent [25]. Cysteine is the most common binding partner. Nevertheless compounds binding to other amino acids have been reported [26-29].

As mentioned above, drug-specific antibodies in the sera of hypersensitive patients, as well as in tolerant controls, were detected. For the production of antibodies by the immune system, the drug would need to modify proteins in the body. Therefore, the hypothesis in this chapter was that CBZ and its metabolites, carbamazepine-10,11 epoxide (CBZE) and 9-AC, bind covalently to proteins. Therefore, the aim of this work was to investigate the ability of the drug and its metabolites to modify proteins, as well as to identify the type of modification (covalent or non-covalent binding). Covalently modified proteins could play a role in the T cell activation according to the hapten hypothesis (see general introduction 1.5.1). The hapten hypothesis might not be sufficient to explain naïve T cell activation in hypersensitivity reactions but would still induce signal 1 as described in the danger hypothesis (see general introduction 1.5.4).

3.2 Material and Methods

3.2.1 Chemicals

CBZ (TOCRIS bioscience, Bristol, UK), CBZE (Toronto Research Chemicals Inc., Ontario, Canada) and 9-AC (Life Chemicals, Braunschweig, Germany) were investigated in the experiments. Dimethyl sulfoxide (DMSO) and methanol (MeOH, Sigma-Aldrich Co, Poole, UK) were used as solvents. Human serum albumin (HSA), N-α-acetyl-lysine, and N-ε-acetyl-lysine (NAL, Sigma-Aldrich Co) were used as protein or amino acids for the experiments. Sodium cyanoborohydride ($NaBH_3CN$, Sigma-Aldrich Co) was used to reduce the Schiff base that results from binding of 9-AC to terminal N groups of amino acids such as lysine.

Phosphate buffer was obtained by diluting 8 g NaCl, 0.2g KCl, 1.44 g Na_2HPO_4, and 0.24g KH_2PO_4 (Sigma-Aldrich Co) in 1 l distilled water. The pH was adjusted to 7.4 with HCl.

3.2.2 Bradford assay

Calibration dilutions (0.2, 0.25, 0.4, 0.5, 0.7, 0.8, 1.0, 1.2 mg/ml) were prepared in phosphate buffer using bovine serum albumin (BSA, Sigma-Aldrich). 5 µl of each dilution were plated into 4 wells of a 96 well plate. Samples were plated into 3 different wells of the plate. 250 µl of Bradford reagent (Bio-Rad Laboratories Ltd., Hertfordshire, UK) was added to each well. The content was mixed and air bubbles were removed. Absorbance was measured at 570 nm using a plate reader. The mean was calculated for the values obtained for the calibration dilutions. The mean was plotted and a standard curve was fitted. With the equation for the standard curve, the protein content of each sample was calculated using Excel.

3.2.3 Incubation of compounds with N-acetyl-lysine

A solution of 1 mM N-α-acetyl-lysine or N-ε-acetyl-lysine was made in phosphate buffer. 9-AC was dissolved in DMSO (100 µM final concentration) and incubated with N-α-acetyl-lysine or N-ε-acetyl-lysine (1 mM), in the presence of sodium cyanoborohydride (1 mM), in phosphate buffer at room temperature [20].

Aliquots of the incubation were removed immediately after mixing and analysed by LC-MS. The incubation time was approximately 10 minutes. Other aliquots were measured at 40 min, 2 h, 4 h and 6 h after the start of the incubation.

Aliquots of the solutions were chromatographed at room temperature on an Agilent 5-µm Zorbax Eclipse XDB-C8 column (150 mm x 4.6 mm; Agilent Technologies, Santa Clara, CA, USA). Analytes were eluted with an isocratic-gradient system of acetonitrile (ACN) in 0.05% formic acid: 15% for 5 min; 15% to 40% over 10 min; 40% to 15% over 0.1 min; 15% for 4.9 min. The eluent flow rate was 1.0 ml/min. The retention time of authentic 9-AC was 4 min.

Eluent was delivered by a PerkinElmer series 200 HPLC system (pump and autosampler; PerkinElmer, Norwalk, CT, USA). The column was connected to the Turbo V electrospray source of an API 4000 Qtrap hybrid quadrupole mass spectrometer (AB Sciex, Warrington, UK) via a Valco flow-splitting T-piece (Valco Instruments Co. Inc., Houston, TX, USA). The flow rate of eluate to the mass spectrometer was approximately 150 µl/min.

The standard operating parameters of the mass spectrometer (Q1 operation) were as follows: source temperature, 450 °C; ionspray (electrospray capillary) voltage, 4 500 V; desolvation potential (DP), 100 V; entrance potential (EP), 10 V; curtain gas setting, 15; spray gas (Gas-1) setting, 50; heater gas (Gas-2) setting, 50. To obtain greater in-source analyte fragmentation, the DP was uprated to 120 V. All of the source gas requirements were met by a nitrogen/zero-grade air generator. The instrument was set up for full-scanning acquisitions in the positive-ion mode

over a scan range of m/z 100-1 000 with a scan time of 5 s. Instrument management and data processing were accomplished through Analyst 1.5.1 software.

3.2.4 Isolation of His-tagged GSTPi on nickel beads

Hexahistidine-tagged human glutathione S-transferase π (GSTPi) was expressed in *Escherichia coli* [30]. His-Select nickel affinity gel (Sigma-Aldrich Co) was used for the purification of GSTPi [31]. The gel was suspended in 900 µl of phosphate buffer and 100 µl of lysate from GSTPi expressing *Escherichia coli* was added. The mixture was incubated for 10 min at room temperature with agitation. After that, beads were washed 5 times with phosphate buffer. The Bradford assay (Bio-Rad Laboratories Ltd.) was performed to determine the concentration of protein. According to the Bradford assay, protein compound ratios were created using the procedure as described below.

3.2.5 Incubation of protein with compounds

Different compound to protein mixtures were prepared using either CBZ, CBZE or 9-AC. For GSTPi, the used amount of protein depended on the yield from the isolation. For HSA, a 66 mg/ml solution was prepared.

For concentration-dependent experiments, the following compound to protein ratios were used: 1:1, 10:1, and 25:1. The incubations were carried out at 37°C for 24 h.

The time-dependent experiments were conducted using a 10:1 compound to protein ratio. The samples were incubated for 1, 4, and 24 hours at 37°C.

3.2.6 Incubation of 9-AC and HSA with $NaBH_3CN$

For the incubation of 9-AC with HSA in the presence of the reducing agent $NaBH_3CN$, the compound to protein ratios were: 10:1, 1:1, and 0.5:1. $NaBH_3CN$ (0.2 mM) was added after the samples were incubated at 37°C for 30 min and the samples were incubated at 37°C for 16 h.

3.2.7 Preparation of samples for LC-MS/MS analysis

At the end of the incubation, the protein was precipitated using 9 volumes of cold MeOH. The mixture was then centrifuged at 14 000 RPM for 20 min at 4°C. The supernatant was removed and the protein pellet was washed 3 times with ice cold MeOH before being resuspended in 80 µl of PBS. The protein was denatured by adding 8.8 µl of dithiothreitol (100 mM) and incubating the sample for 15 min at room temperature. After that, 11 µl of iodoacetamide (500 mM) was added and the sample incubated for 15 min at room temperature. The protein was then precipitated using MeOH as described before. The pellet was reconstituted in 50 µl of ammonium bicarbonate solution (50 mM) and the concentration was determined utilising the Bradford assay. The protein was digested by trypsin (200 µg protein per µg trypsin). Samples were incubated at 37°C overnight. The digestion was stopped by acidifying the samples with trifluoroacetic acid (TFA, 1%). To desalt the peptide mixture, C18 Zip-Tips (Millipore, Waterford, UK) were used according to specifications provided by the manufacturer. The bed of the C18 Zip-Tip was humidified with ACN and equilibrated with TFA (0.1%). The sample was then loaded on the column and washed with TFA (0.1%). After that the samples were eluted with a mixture of ACN (50%) and TFA (0.1%). After the elution, the samples were dried and stored at 4°C before being analysed in the LC-MS/MS.

For the LC-MS/MS analysis, the samples were reconstituted in 2% ACN/0.1% formic acid (FA, v/v). Samples of 2.4 to 5.0 pmol were delivered into a QTRAP 5500 mass spectrometer (AB Sciex, Framingham, MA, USA) fitted with a NanoSpray II source by automated in-line liquid chromatography

(U3000 HPLC System, 5 mm C18 nano-precolumn and 75 µm × 15 cm C18 PepMap column [Dionex, California, USA]) via a 10 µm inner diameter PicoTip (New Objective, Massachusetts, USA). A gradient from 2% ACN/0.1% FA (v/v) to 50% ACN/0.1% FA (v/v) in 60 min was applied at a flow rate of 300 nL/min. The ion spray potential was set to 2 200−3 500 V, the nebulizer gas to 19, and the interface heater to 150 °C. Spectra were acquired automatically in positive ion mode using information-dependent acquisition powered by Analyst 1.5 software, using mass ranges of 400−1 000 amu in MS and 100−1 000 amu in MS/MS. The 5 most intense ions were selected for MS/MS, using a threshold of 5 000 counts per second, with dynamic exclusion for 30 s and rolling collision energy. Data were analysed using PeakView 1.2.0.3 (AB Sciex) or ProteinPilotTM 4.2 beta.

The sequence and the theoretical mass of the the tryptic digestion were generated by the PeptideMass software, available on the ExPASy website, allowing for one cleavage site to be missed.

3.3 Results

3.3.1 Binding of 9-AC to N-acetyl-lysine

To detect the Schiff base formed between 9-AC and amine, 9-AC was reacted with N-α-acetyl-lysine in the presence of a reducing agent. A molecule with a mass of 380.20 amu was detected after 2.43 min. The intensity of that molecule increased over time up to 6 h after the start of the measurement (Fig. 3.3). The mass spectrometric analysis revealed the adduct as a reduced Schiff base from the reaction of 9-AC and N-α-acetyl-lysine (Fig. 3.2).

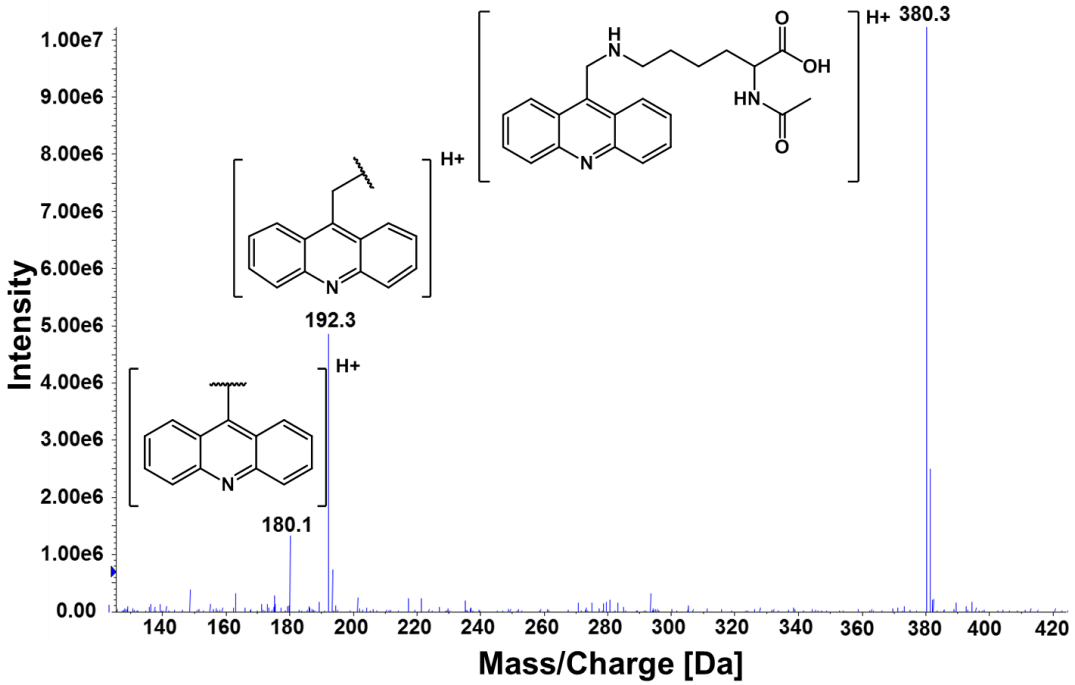

Figure 3.2: Mass spectrometric analysis of 9-AC-modified N-α-acetyl-lysine

An ion at m/z 380.20 corresponding to a reduced 9-AC-NAL adduct was detected and characteristic fragment ions were interpreted as the inserted structure.

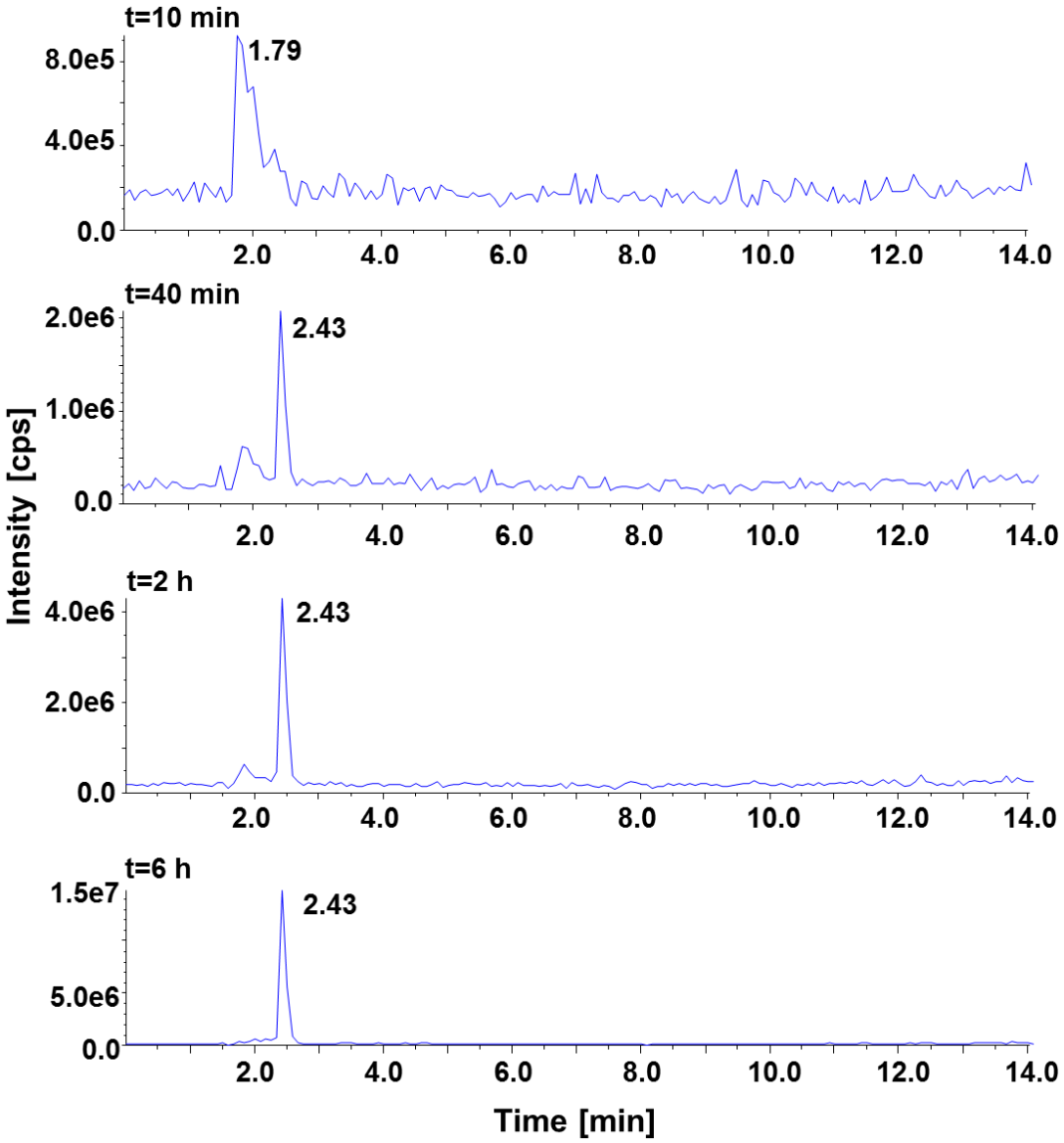

Figure 3.3: Liquid chromatographic spectrum for fragments with a mass of 380 amu

Spectrum shows increase in the intensity of product peak (2.43 min) over time. No internal standard was used. Identity of the product was confirmed using mass spectrometric analysis (Fig. 3.2).

The experiment was repeated with 9-AC and N-ε-acetyl-lysine. An experimental error resulted in an excessive amount of reducing agent (100 mM compared to 0.1 mM). The HPLC and the mass spectrometric analysis showed molecule with the mass of 382.20 amu, suggesting that two reductions occurred (see Fig. 3.4). The analyses of several mass peaks lead to the conclusion that the second reduction must have taken place in the N-acetyl-lysine. The results show the formation with the Schiff base with the α-nitrogen group of lysine.

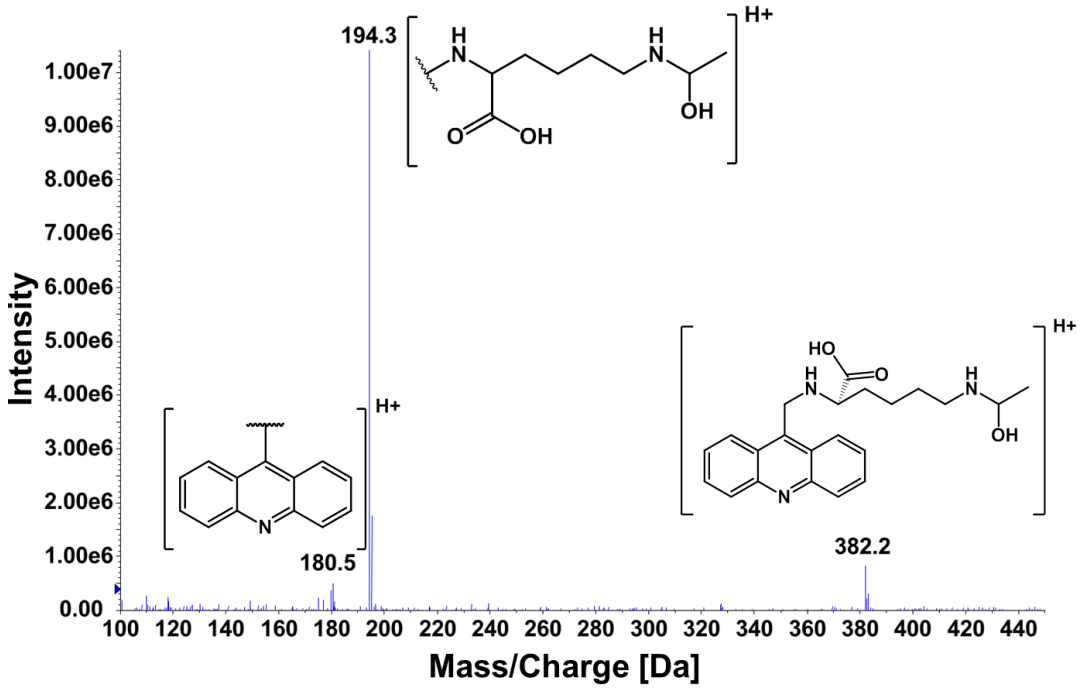

Figure 3.4: Mass spectrometric analysis of 9-AC-modified N-ε-acetyl-lysine

An ion at m/z 382.20 was detected and interpreted as an adduct of 9 acridinecarboxaldehyde and N-ε-acetyl-lysine that had under two reductions. Characteristic fragment ions were interpreted and as the structure found next to the peaks.

3.3.2 Characterisation of compound modified HSA

The most abundant protein in human blood, HSA, was used to observe possible covalent binding of CBZ and its metabolites through an addition in human blood. The mass spectrometric analysis of the tryptic digests of HSA in the presence of CBZ did not reveal any conjugates. The analysis detected only binding of 9-AC to the N-terminal α-amino group of HSA (Fig. A3.1 in appendix). The samples of HSA incubated with 9-AC exhibited lower protein coverage compared to all the other samples including HSA alone and HSA incubated with compounds.

For CBZE, the analysis revealed two modified peptides that both contained a histidine residue. The first one was found on His146-containing peptide ^{145}RHPYFYAPELLFFAK^{159}. The adduct was eluted at 37.78 min and identified as a triple charged ion at m/z 547.28, which had an additional mass of 253 amu to the parent peptide. The MS/MS analysis confirmed the identity of the peptide and the binding of CBZE to His146 (m/z 547.28) (Fig 3.5 A). The peptide sequence was confirmed by the observation of a series of b ions and y ions. The modification site was located at His146 by the observation of CBZE-modified b_2 ions. The presence of characteristic fragment ions derived from CBZE provided further evidence of the modification (see Fig. 3.6). The second adduct was found in the His338-containing fragment ^{337}RHPDYSVVLLLR^{348}. This peptide eluted after 28.25 min and was detected as a triple charged ion at m/z 574.22. Again the peptide sequence was confirmed by the observation of b and y ions. The modification site was found by the observation of CBZE-modified b_2 ions and the binding was supported by fragment ions of CBZE.

The peptide and the binding of CBZE to His338 were confirmed in the MS/MS analysis (Fig 3.5 B). Both fragments were found at a 10:1 drug: protein ratio and after a 24 hour incubation. The amount of additional mass corresponds to the expected amount of adduct from a nucleophilic addition of CBZE and HSA.

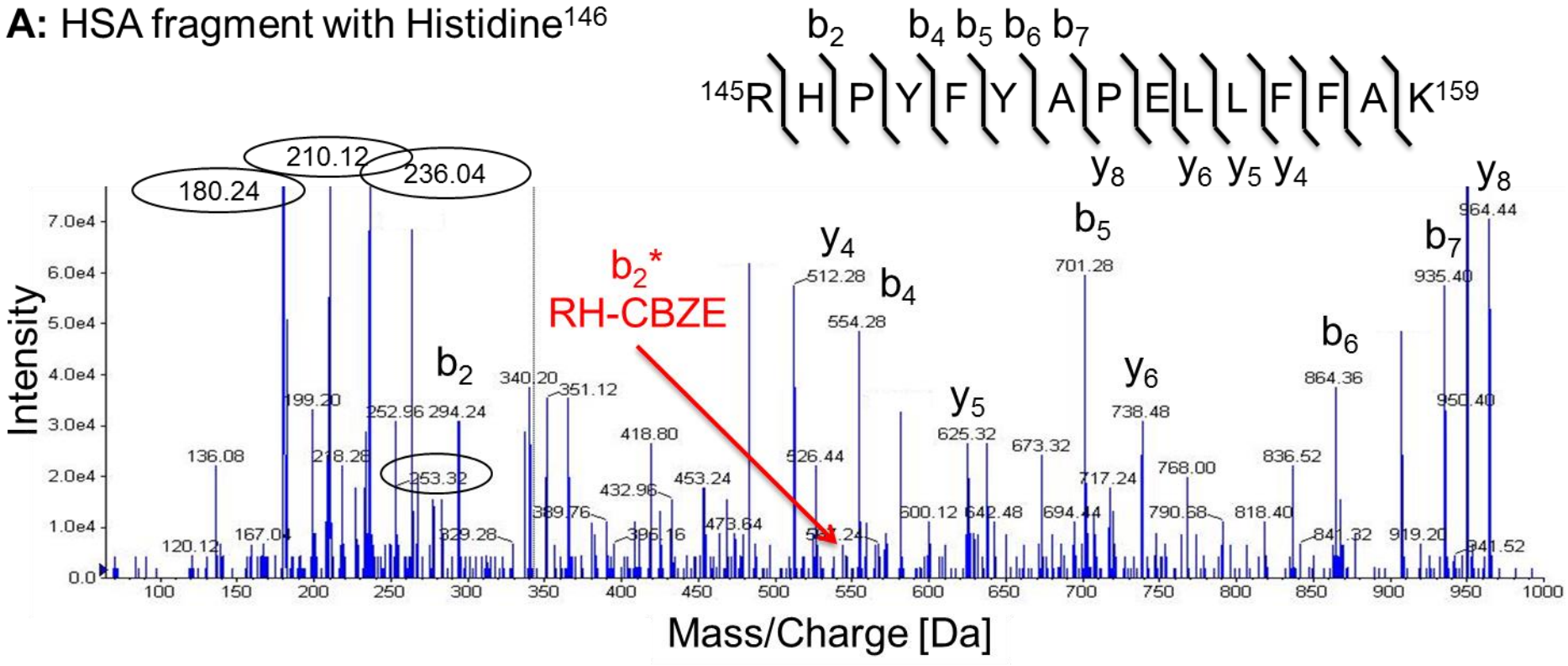

Figure 3.5 A: Identification of HSA residues modified by CBZE

MS/MS spectrum showing CBZE-modified tryptic peptide ^{145}AH*PYFYAPELLFFAK^{159} with adduct of His146 and CBZE and mass addition of 253 amu. HSA was reacted with CBZE in vitro with a 10:1 protein: compound ratio for 24 hours. The encircled mass peaks show fragments of CBZE (see Fig.3.6).

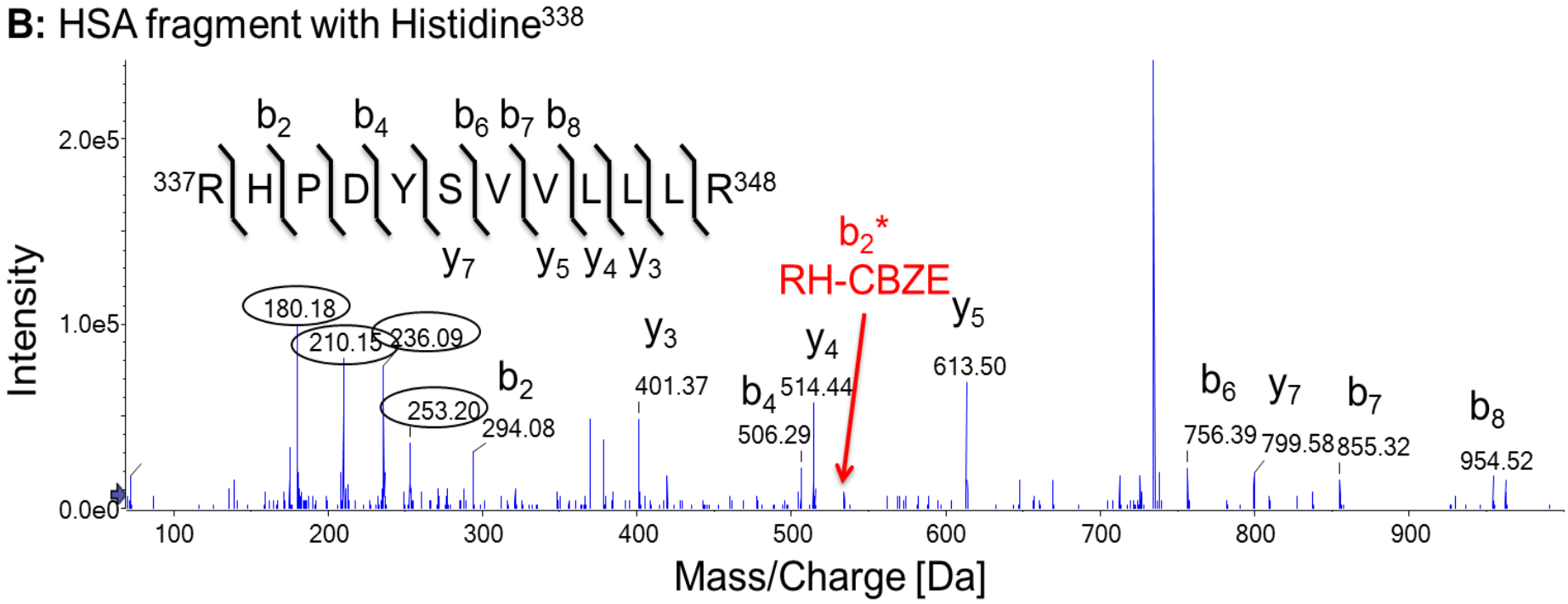

Figure 3.5 B: Identification of HSA residues modified by CBZE

MS/MS spectrum showing CBZE-modified tryptic peptide ^{337}RH*PDYSVVLLLR^{348} with adduct of His338 and CBZE and mass addition of 253 amu. HSA was reacted with CBZE in vitro with a 10:1 protein: compound ratio for 24 hours. The encircled mass peaks show fragments of CBZE (see Fig.3.6).

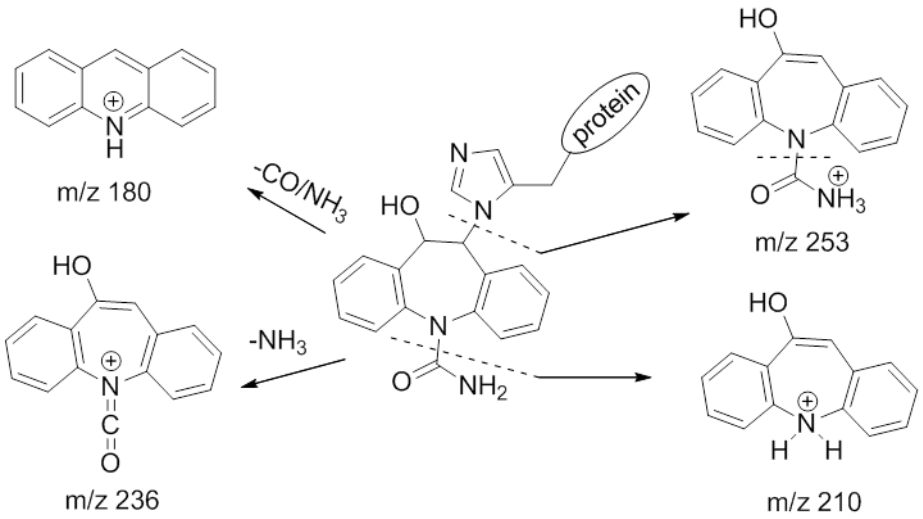

Figure 3.6: Fragmentation of CBZE adduct in MS/MS

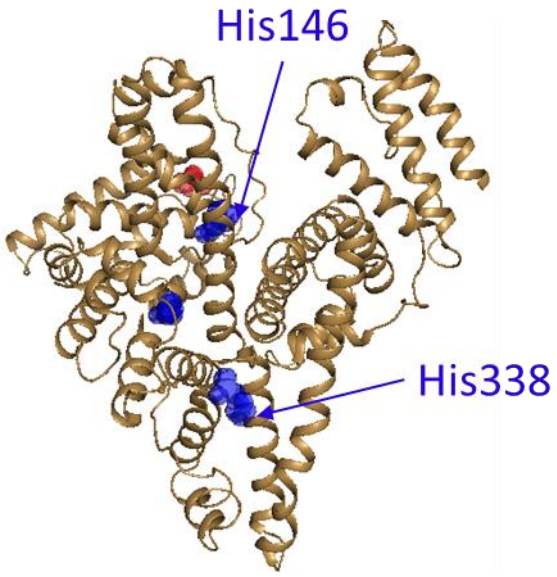

Figure 3.7: Tertiary structure of HSA showing CBZE binding sites detected *in vitro*

Protein was depicted as ribbons and the modified histidine residues shown as blue spheres.

3.3.3 Characterisation of compound modified GSTPi

GSTPi was used for the detection of protein binding, as it was shown to be a model protein for reactive metabolites due to the reactive cysteine residue it contains [25]. As for HSA there were no conjugates found in the mass spectrometric analysis of the tryptic digested peptide from GSTPi incubated with CBZ or 9-AC. The protein coverage for GSTPi samples incubated with 9-AC was again lower compared to the coverage of other samples.

For CBZE, the mass spectrometric analysis revealed a conjugation on Cys47 at the 10:1 ratio and after a 24 hour incubation. This cysteine is located in the peptide ^{45}ASCLYGQLPK^{54}. The CBZE-modified peptide was found as a double charged ion at m/z 542.21 and eluted at 37.66 min. This fragment showed a gain in mass of 253 amu compared to the mass of the parent peptide (Fig. 3.9). The peptide sequence was identified by observing b and y ions of the fragment. The binding of CBZE to Cys47 (m/z 542.21) was confirmed by the detection of the modified b_3 ion as well as characteristic CBZE fragment ions (see Fig. 3.7)

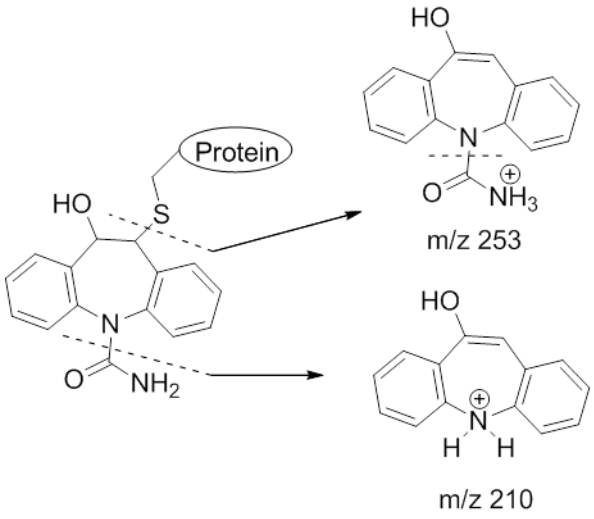

Figure 3.8: Fragmentation of CBZE adduct in MS/MS

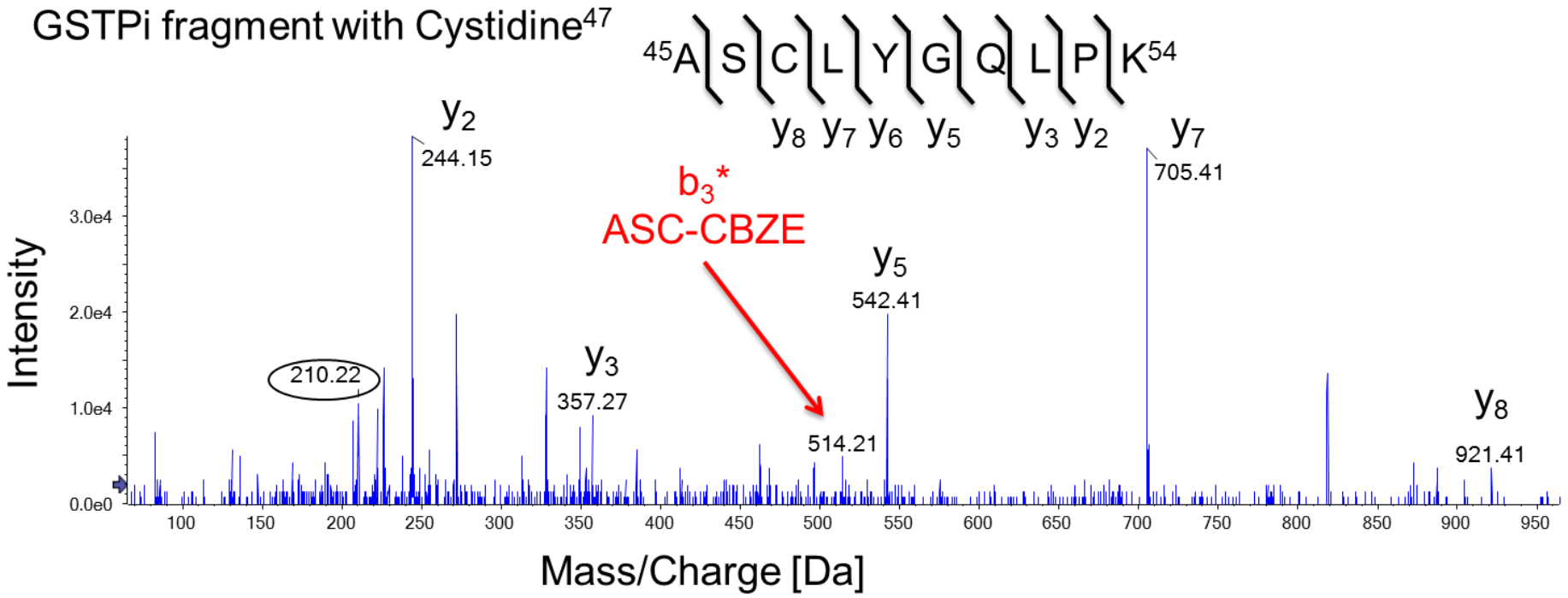

Figure 3.9: Identification of GSTPi residue modified by CBZE

MS/MS spectrum showing CBZE-modified tryptic peptide ^{45}ASC*LYGQLPK^{54} with adduct of Cys47 and CBZE and mass addition of 253 amu. GSTPi was reacted with CBZE *in vitro* with a 10:1 protein: compound ratio for 24 hours. The encircled mass peaks show fragments of CBZE (see Fig.3.8).

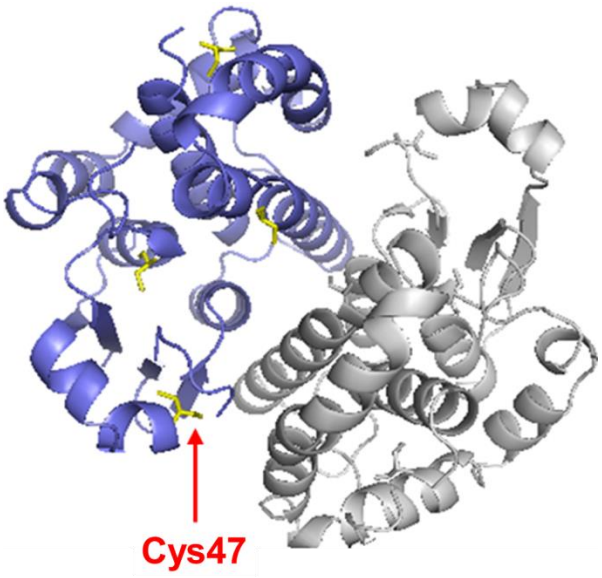

Figure 3.10: Tertiary structure of GSTPi showing CBZE binding site detected *in vitro*

Protein depicted as ribbons and the red arrow pointing at modified cysteine residue shown in yellow.

3.3.4 Binding of 9-AC with HSA in the presence of $NaBH_3CN$

To observe the possible Schiff base formation from 9-AC and HSA, the protein was reacted in the presence of $NaBH_3CN$. No conjugates were observed in the mass spectrometric analysis of the tryptic digests of HSA. The protein coverage, as in previous experiments, was low.

3.4 Discussion

The mechanism by which the immune system is activated in CBZ-induced hypersensitivity reactions is not clear. It has been proposed that the activation of the immune system results from the generation of reactive metabolites [32].

Biotransformation is crucial during the clearance of a drug. During the biotransformation, the less reactive parent drug is metabolised into intermediates that have a higher reactivity towards proteins. The drug-modified proteins may then potentially cause an immune response, in some cases resulting in a cutaneous idiosyncratic ADR [33]. The detection of antibodies against microsomal proteins in the blood of patients that had suffered from CBZ-induced liver injuries suggests that CBZ or one of its metabolites can bind to proteins and thus trigger an immune reaction [10].

The liver is the main site for drug metabolism but it is questionable that the highly reactive metabolites will be found outside the liver [34, 35]. Metabolism outside the liver, generating protein reactive intermediates, might be more important in the activation of the immune system known to occur in idiosyncratic ADRs [34, 36-38]. For CBZ, Furst and colleagues showed that 9-AC can be generated by activated human lymphocytes [19]. The binding of 9-AC and CBZE was shown using radiolabeled compounds [20, 39]. These experiments only found that protein modification was possible but were unable to determine the residue inside the protein.

Drugs are considered too small to be detected by the immune system. Therefore they would need to modify proteins in order to be immunogenic. In this chapter, the experiments were designed to assess protein modification of CBZ and its metabolites, CBZE and 9-AC. Covalent binding is described in the hapten hypothesis as a mechanism for drugs to become immunogenic (see general introduction 1.5.1). Therefore, an additional aim was to detect the exact binding site within the protein. For this assessment of the exact

protein binding site of CBZ and its metabolites CBZE and 9-AC, HSA and GSTPi were analysed by LC-MS/MS. HSA and GSTPi have been previously reported to bind drugs and drug metabolites and the modified proteins have been identified as activators of immune response, thus the proteins presented promising targets for this work [25, 40-44].

The results showed that no conjugates were observed in samples of HSA or GSTPi incubated with the parent drug CBZ. This was expected as in the literature covalent protein binding of CBZ was only reported in the presence of a metabolising enzyme [20]. This would suggest that CBZ acts as a pro-hapten and therefore cannot covalently bind to proteins (see general introduction 1.5.1). CBZ as a chemically inert drug can be transformed into a reactive structure through the drug's metabolism. This was also confirmed in the experiments of this chapter, where instead a metabolising system, selected metabolites were used.

In the samples of HSA and GSTPi, conjugates with CBZE were found and characterised for both proteins. It was shown that CBZE forms covalent bonds with histidines in HSA and the highly reactive cysteine in GSTPi.

Epoxides are considered hard electrophiles and therefore able to bind to histidine residues. This was observed in HSA. CBZE was found to bind to His146 and His338. Since both residues could be found at the same concentration and the same time point, no preference could be determined. Histidine is a nucleophilic side chain and was therefore expected to react with CBZE. His146 is also the most reactive of the histidine residues in HSA [40, 44].

Covalent binding of CBZE to a reactive cysteine residue (Cys47) was detected in GSTPi. This finding had been reported before [39]. No binding to a histidine residue was detected in GSTPi.

This different selectivity of binding in GSTPi and HSA could be caused by different parameters at the possible binding site within the protein. These parameters include intrinsic chemical reactivity of amino acids and non-covalent interaction between a molecule and the binding pocket of the

protein. Additionally, CBZE represents a bulky molecule. Due to this, the tertiary structure of the protein could influence the accessibility of potential binding sites. There is also only one cysteine in HSA that is not forming a disulphide bond (Cys34) [45]. After tryptic digestion this cysteine is located in a larger peptide. For further investigation of the binding of CBZE to this cysteine other digestion methods could be used.

These findings also indicate the difficulties in drug design. During the development of a new drug, attempts to predict the protein binding capabilities of the drug and its metabolites are undertaken with the aim of minimising adverse reaction for patients treated in clinical trials with the new drug. The findings for CBZE indicate that binding to particular residues within proteins can be missed depending on the protein chosen for the experiments. Ideally, all proteins of the human body should be screened during the development of a new drug. However, this would increase the costs of drug development severely and would be therefore not feasible.

Nevertheless, the conjugates of CBZE indicate a possible involvement of haptens formed by the main metabolite of CBZ. The immunogenicity of these modified proteins remains to be shown and would be a very interesting point for further studies. One possibility to determine whether these adducts are immunogenic would be the T cell proliferation assay. In this assay, the drug-specific T cells from CBZ hypersensitive patients would be incubated in the presence of peptides derived from the modified proteins and the proliferation of the T cells would be measured.

The binding of 9-AC and N-acetyl-lysine was proven to be a Schiff base. The adduct was only found to be covalent in the presence of a reducing agent transforming the imine into an amine, as it was reported before [20].

This formation of a Schiff base, in which the carbonyl carbon of the aldehyde group in 9-AC reacts with an amino group of a residue or the N-terminus to an unstable imine, should also be observable in proteins. No Schiff base adducts of 9-AC and an ε-amino group of a residue was observed even at high concentrations. The only conjugates observed resulted from unspecific

binding to the backbone of the proteins. No other conjugates were observed for either HSA or GSTPi. Also in the presence of a reducing agent, no covalent binding was observed in HSA. Higher concentrations of reducing agent should be used in further experiments to find the Schiff base products that were expected.

The protein coverage in the samples containing 9-AC was always lower compared to the coverage observed in all the other samples. The reason for the low coverage could lie in the solubility of 9-AC in methanol and the protein precipitation conducted in methanol. Conjugated proteins could have stayed in solution and were therefore not detected. To eliminate this possibility, the proteins could be isolated using other precipitation methods.

Another consideration for further studies could include the investigation of the immunogenicity of the non-covalent modification of peptides by 9-AC. In order to determine this, T cell proliferation could be examined by incubating T cells from CBZ hypersensitive patients with 9-AC in the presence of chemically fixed APCs, thus analysing the role of the p-i mechanism in the 9-AC mediated activation of T cells during hypersensitivity reactions.

In summary, CBZE was able to covalently modify proteins. This observation indicates that haptens could play a role in the pathogenesis of CBZ-induced hypersensitivity reactions. As all experiments were conducted *in vitro*, it is uncertain whether these modifications can also be observed *in vivo*. Therefore the presence of these adducts need to be investigated in patients undergoing CBZ treatment. The immunogenicity of these adducts would also need further investigation. Nevertheless, the role of the hapten hypothesis cannot be excluded and could offer an explanation for the first signal needed in the activation of naïve T cells according to the danger hypothesis. Additionally, the findings for 9-AC indicate that non-covalent binding to proteins might also occur during CBZ-induced hypersensitivity reactions. Therefore the T cell activation in patients suffering from CBZ-induced hypersensitivity reactions needs further investigation and should include methods for the detection of covalent as well as non-covalent modifications causing the activation.

3.5 References

1. Marson, A.G., et al., *The SANAD study of effectiveness of carbamazepine, gabapentin, lamotrigine, oxcarbazepine, or topiramate for treatment of partial epilepsy: an unblinded randomised controlled trial.* Lancet, 2007. **369**(9566): p. 1000-15.
2. Lertratanangkoon, K. and M.G. Horning, *Metabolism of carbamazepine.* Drug Metab Dispos, 1982. **10**(1): p. 1-10.
3. Leeder, J.S., *Mechanisms of idiosyncratic hypersensitivity reactions to antiepileptic drugs.* Epilepsia, 1998. **39 Suppl 7**: p. S8-16.
4. Horneff, G., H.G. Lenard, and V. Wahn, *Severe adverse reaction to carbamazepine: significance of humoral and cellular reactions to the drug.* Neuropediatrics, 1992. **23**(5): p. 272-5.
5. Hosoda, N., et al., *Anticarbamazepine antibody induced by carbamazepine in a patient with severe serum sickness.* Arch Dis Child, 1991. **66**(6): p. 722-3.
6. Igarashi, M., et al., *Immunosuppressive factors detected during convalescence in a patient with severe serum sickness induced by carbamazepine.* Int Arch Allergy Immunol, 1993. **100**(4): p. 378-81.
7. Igarashi, M., et al., *An immunodominant haptenic epitope of carbamazepine detected in serum from patients given long-term treatment with carbamazepine without allergic reaction.* J Clin Immunol, 1992. **12**(5): p. 335-40.
8. Borghesi, L. and C. Milcarek, *From B cell to plasma cell: regulation of V(D)J recombination and antibody secretion.* Immunol Res, 2006. **36**(1-3): p. 27-32.
9. Ravetch, J.V. and S. Bolland, *IgG Fc receptors.* Annu Rev Immunol, 2001. **19**: p. 275-90.
10. Pirmohamed, M., et al., *Detection of an autoantibody directed against human liver microsomal protein in a patient with carbamazepine hypersensitivity.* Br J Clin Pharmacol, 1992. **33**(2): p. 183-6.
11. Riley, R.J., et al., *Human anti-endoplasmic reticulum autoantibodies produced in aromatic anticonvulsant hypersensitivity reactions recognise rodent CYP3A proteins and a similarly regulated human P450 enzyme(s).* Biochem Biophys Res Commun, 1993. **191**(1): p. 32-40.
12. Park, B.K. and N.R. Kitteringham, *Drug-protein conjugation and its immunological consequences.* Drug Metab Rev, 1990. **22**(1): p. 87-144.
13. Nelson, S.D. and P.G. Pearson, *Covalent and noncovalent interactions in acute lethal cell injury caused by chemicals.* Annu Rev Pharmacol Toxicol, 1990. **30**: p. 169-95.
14. Madden, S., J.L. Maggs, and B.K. Park, *Bioactivation of carbamazepine in the rat in vivo. Evidence for the formation of reactive arene oxide(s).* Drug Metab Dispos, 1996. **24**(4): p. 469-79.
15. Pirmohamed, M., et al., *An investigation of the formation of cytotoxic, protein-reactive and stable metabolites from carbamazepine in vitro.* Biochem Pharmacol, 1992. **43**(8): p. 1675-82.
16. Pearce, R.E., et al., *Pathways of carbamazepine bioactivation in vitro. III. The role of human cytochrome P450 enzymes in the formation of 2,3-dihydroxycarbamazepine.* Drug Metab Dispos, 2008. **36**(8): p. 1637-49.
17. Pearce, R.E., J.P. Uetrecht, and J.S. Leeder, *Pathways of carbamazepine bioactivation in vitro: II. The role of human cytochrome P450 enzymes in the*

formation of 2-hydroxyiminostilbene. Drug Metab Dispos, 2005. **33**(12): p. 1819-26.
18. Pearce, R.E., G.R. Vakkalagadda, and J.S. Leeder, *Pathways of carbamazepine bioactivation in vitro I. Characterization of human cytochromes P450 responsible for the formation of 2- and 3-hydroxylated metabolites.* Drug Metab Dispos, 2002. **30**(11): p. 1170-9.
19. Furst, S.M. and J.P. Uetrecht, *Carbamazepine metabolism to a reactive intermediate by the myeloperoxidase system of activated neutrophils.* Biochem Pharmacol, 1993. **45**(6): p. 1267-75.
20. Furst, S.M., et al., *Covalent binding of carbamazepine oxidative metabolites to neutrophils.* Drug Metab Dispos, 1995. **23**(5): p. 590-4.
21. Sobott, F. and C.V. Robinson, *Protein complexes gain momentum.* Curr Opin Struct Biol, 2002. **12**(6): p. 729-34.
22. Kleno, T.G., et al., *MALDI MS peptide mapping performance by in-gel digestion on a probe with prestructured sample supports.* Anal Chem, 2004. **76**(13): p. 3576-83.
23. Ma, S. and M. Zhu, *Recent advances in applications of liquid chromatography-tandem mass spectrometry to the analysis of reactive drug metabolites.* Chem Biol Interact, 2009. **179**(1): p. 25-37.
24. Ma, S. and R. Subramanian, *Detecting and characterizing reactive metabolites by liquid chromatography/tandem mass spectrometry.* J Mass Spectrom, 2006. **41**(9): p. 1121-39.
25. Jenkins, R.E., et al., *Glutathione-S-transferase pi as a model protein for the characterisation of chemically reactive metabolites.* Proteomics, 2008. **8**(2): p. 301-15.
26. Ikehata, K., et al., *Protein targets of reactive metabolites of thiobenzamide in rat liver in vivo.* Chem Res Toxicol, 2008. **21**(7): p. 1432-42.
27. Helleberg, H. and M. Tornqvist, *A new approach for measuring protein adducts from benzo[a]pyrene diolepoxide by high performance liquid chromatography/tandem mass spectrometry.* Rapid Commun Mass Spectrom, 2000. **14**(18): p. 1644-53.
28. Bambal, R.B. and R.P. Hanzlik, *Bromobenzene 3,4-oxide alkylates histidine and lysine side chains of rat liver proteins in vivo.* Chem Res Toxicol, 1995. **8**(5): p. 729-35.
29. Ding, A., et al., *Reactivity of tolmetin glucuronide with human serum albumin. Identification of binding sites and mechanisms of reaction by tandem mass spectrometry.* Drug Metab Dispos, 1995. **23**(3): p. 369-76.
30. Chang, M., J.L. Bolton, and S.Y. Blond, *Expression and purification of hexahistidine-tagged human glutathione S-transferase P1-1 in Escherichia coli.* Protein Expr Purif, 1999. **17**(3): p. 443-8.
31. Jenkinson, C., et al., *A mechanistic investigation into the irreversible protein binding and antigenicity of p-phenylenediamine.* Chem Res Toxicol, 2009. **22**(6): p. 1172-80.
32. Shear, N.H. and S.P. Spielberg, *Anticonvulsant hypersensitivity syndrome. In vitro assessment of risk.* J Clin Invest, 1988. **82**(6): p. 1826-32.
33. Roychowdhury, S. and C.K. Svensson, *Mechanisms of drug-induced delayed-type hypersensitivity reactions in the skin.* AAPS J, 2005. **7**(4): p. E834-46.
34. Uetrecht, J.P., *The role of leukocyte-generated reactive metabolites in the pathogenesis of idiosyncratic drug reactions.* Drug Metab Rev, 1992. **24**(3): p. 299-366.
35. Reilly, T.P., et al., *A role for bioactivation and covalent binding within epidermal keratinocytes in sulfonamide-induced cutaneous drug reactions.* J Invest Dermatol, 2000. **114**(6): p. 1164-73.

36. Vyas, P.M., et al., *Enzyme-mediated protein haptenation of dapsone and sulfamethoxazole in human keratinocytes: II. Expression and role of flavin-containing monooxygenases and peroxidases.* J Pharmacol Exp Ther, 2006. **319**(1): p. 497-505.
37. Roychowdhury, S., P.M. Vyas, and C.K. Svensson, *Formation and uptake of arylhydroxylamine-haptenated proteins in human dendritic cells.* Drug Metab Dispos, 2007. **35**(4): p. 676-81.
38. Sharma, A.M. and J. Uetrecht, *Bioactivation of drugs in the skin: relationship to cutaneous adverse drug reactions.* Drug Metab Rev, 2014. **46**(1): p. 1-18.
39. Bu, H.Z., et al., *Human in vitro glutathionyl and protein adducts of carbamazepine-10,11-epoxide, a stable and pharmacologically active metabolite of carbamazepine.* Drug Metab Dispos, 2005. **33**(12): p. 1920-4.
40. Meng, X., et al., *Cyclization of the acyl glucuronide metabolite of a neutral endopeptidase inhibitor to an electrophilic glutarimide: synthesis, reactivity, and mechanistic analysis.* J Med Chem, 2007. **50**(24): p. 6165-76.
41. Jenkins, R.E., et al., *beta-Lactam antibiotics form distinct haptenic structures on albumin and activate drug-specific T-lymphocyte responses in multiallergic patients with cystic fibrosis.* Chem Res Toxicol, 2013. **26**(6): p. 963-75.
42. Jenkins, R.E., et al., *Characterisation of flucloxacillin and 5-hydroxymethyl flucloxacillin haptenated HSA in vitro and in vivo.* Proteomics Clin Appl, 2009. **3**(6): p. 720-9.
43. Rappaport, S.M., et al., *Adductomics: characterizing exposures to reactive electrophiles.* Toxicol Lett, 2012. **213**(1): p. 83-90.
44. Meng, X., et al., *Abacavir forms novel cross-linking abacavir protein adducts in patients.* Chem Res Toxicol, 2014. **27**(4): p. 524-35.
45. Sugio, S., et al., *Crystal structure of human serum albumin at 2.5 A resolution.* Protein Eng, 1999. **12**(6): p. 439-46.

Chapter 4

Genome-wide analysis of the inter-individual variability in *in vitro* cell viability on exposure to carbamazepine and its metabolites

4.1 Introduction

Various *in vivo* and *in vitro* analyses of skin lesions from patients with drug-induced hypersensitivity reactions have revealed the involvement of cytotoxic mechanisms mediated by drug-specific cytotoxic T cells [1-7]. The activation of those T cells can lead to widespread apoptosis [8]. It has been also shown that the severity of the drug-induced hypersensitivity is strongly associated with a high expression of cytotoxic markers [9]. The association of drug-induced cytotoxicity with the development of drug-induced hypersensitivity reactions is less well studied.

Computational toxicology is a rapidly expanding field. It combines methodologies from computer science bioinformatics, chemistry and molecular biology [10-12]. Classical experimental approaches in toxicology are based on *in vivo* testing in animal models. This approach, although delivering reliable results, is very time- and cost-intensive. It has also led to a huge backlog of chemicals to be tested. The amount of chemicals that require testing is growing rapidly with the discovery of new chemicals. The concept of computational toxicology lies in identifying chemicals that bear a hazard for individuals and prioritise these compounds for animal testing or even replace animal testing in the future [13, 14]. Utilising the *in vitro-in vivo* extrapolation paradigm, *in vitro* data for thousands of chemicals were generated by the Tox21 program which comprises several agencies in the United States of America including the National Toxicology Program, National Chemical Genomics Center, Environmental Protection Agency and Food and Drug Administration, to re-establish the field of predictive chemical toxicology [15].

Chemical mechanistic data provide information about the toxicity of a chemical based on its structure. Such information can be obtained by *in vivo* testing in animals, chemical structure-based prediction models or *in vitro* screening for endpoint toxicity.

Chemical structure-based prediction links the geometry and the electronic structure of a molecule to an activity, such as adverse health outcomes. This can be achieved either through statistical models, assigning scores according to structural similarities of a new compound or by expert systems utilising rules determined by scientific consensus. It has been shown that chemicals with ≥ 0.85 similarity (based on the Tanimoto coefficient) to active compounds were 30 times more likely to be active themselves compared to randomly chosen chemicals [16]. The Ashby-Tennant structural alerts for carcinogenicity are an example of an expert system incorporated in many software tools [17, 18]. Although both models are used for the prediction of toxic effects, it has been shown that they do not allow the prediction of complex biological phenotypes [10].

Recent advances in automated quantitative high-throughput screening (qHTS) allows the generation of vast amounts of biological data. These experiments range from short-term *in vitro* assays to various *in vivo* endpoints and allow the prediction of *in vivo* toxicity using statistical or machine learning approaches [19].

In the past, genetic studies, investigating disease-gene associations, were primarily focusing on one or a few target genes [20]. This approach required *a priori* information about the genes and pathways involved, meaning that a hypothesis of the involved mechanism needed to be generated [21]. In the last decade, extensive characterisation of the human genome through next-generation DNA sequencing has allowed a better understanding of the impact of single nucleotide polymorphisms (SNP) on phenotypes [22]. This allows investigation of the association of genetic variance to toxicity in an unbiased approach. As the genetic associations in idiosyncratic drug reactions are not related to the known pathological pathways of the drug, this novel method may be better suited for discovering associations.

Complex data generated, using the different methods described, can be integrated in different ways. These include consensus, hierarchical and hybrid approaches (see Fig. 4.1) [23-26]. It has been shown that these approaches allow a better prediction of *in vivo* toxicity and allow prioritisation of additional testing in classical animal testing or generation of testable hypotheses concerning the underlying mechanism of toxicity [14, 27, 28].

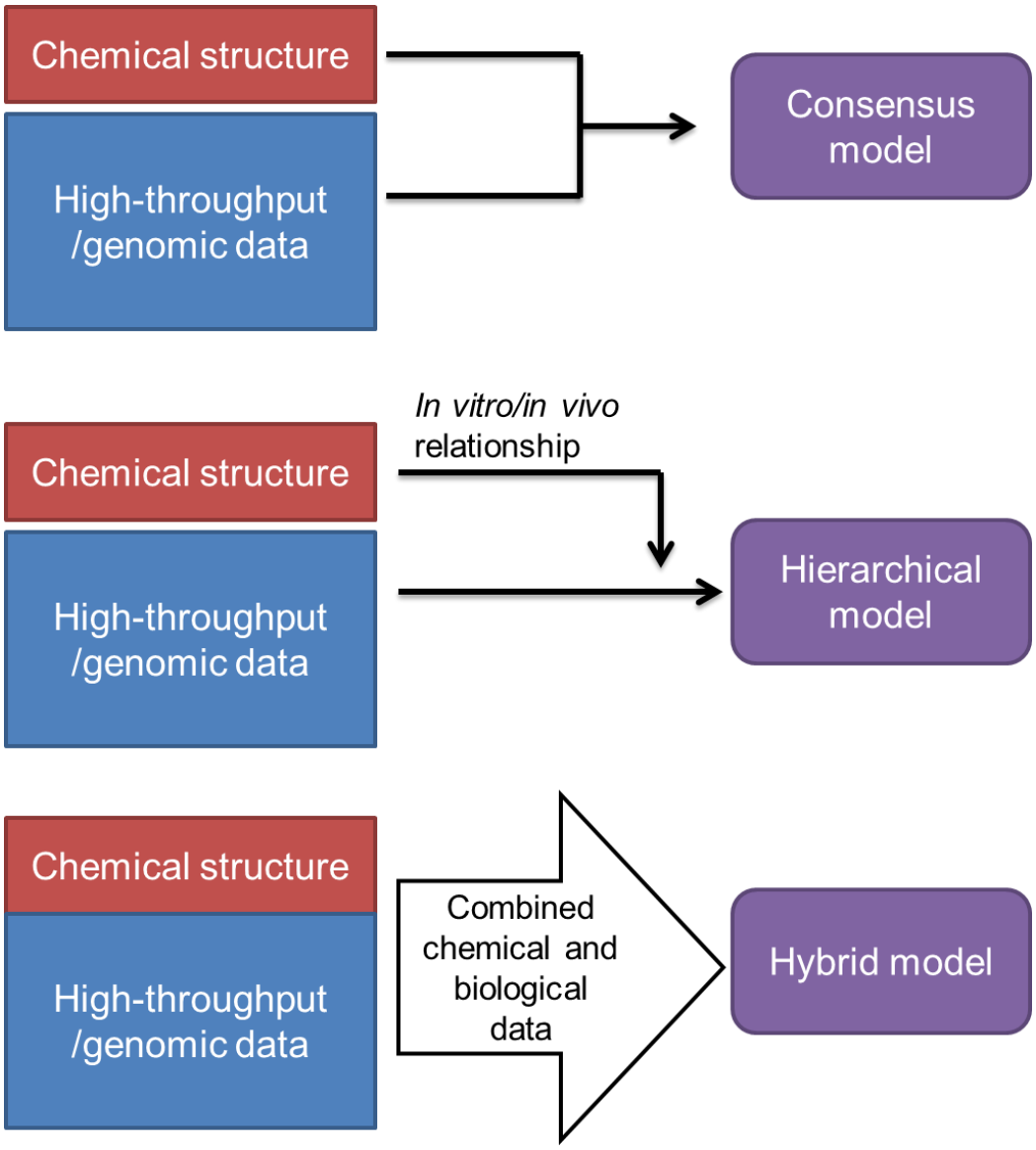

Figure 4.1: Approaches for integration of chemical and biological data for predictive models in computational toxicology (adapted from Rusyn *et al.*, 2012 [29])

The advanced knowledge about the genome combined with the *in vivo* studies in genetically diverse mice showed that polymorphisms can have a fundamental effect on disease risk after drug or toxin exposure [30]. In one study, it was observed that genetic variation in CD44 influenced liver injury caused by acetaminophen. These factors cannot be assessed or evaluated using established animal systems or cell lines as these are missing such genetic variation [31]. For the 1000 Genomes project, samples from healthy volunteers in 25 populations were collected and lymphoblast cell lines were generated (see Tab 4.1) [32]. These were generated by transforming B cells from participants with the Epstein-Barr virus into immortalised cell lines [33]. The lymphoblast cell lines were made commercially available to researchers. Such lymphoblasts enable *in vitro* testing at the population scale. The feasibility of the *in vitro* model was used to assess interindividual- and population-wide variability of chemically-induced toxicity phenotypes [34].

In chapter 2, inter-individual variability was observed in the viability of cells exposed to a metabolite of carbamazepine (CBZ), 9-acridinecarboxaldehyde (9-AC). Based on these findings, it was hypothesised, that the variability may be caused by genetic differences and could lead to the initiation of hypersensitivity reaction. Following the previous results, the aim of this chapter was to further investigate the inter-individual variability and inter-population differences in cell viability of 331 lymphoblastoid cell lines exposed to CBZ and its metabolites. For the detection of genetic association with lower tolerance of CBZ and its metabolites, a genome-wide association study (GWAS) was to be performed using the dose-response data from the screening and DNA sequencing data. Candidate SNPs were to be assessed for potential biological plausibility and the most plausible SNP was to be validated in patients with CBZ-induced hypersensitivity reactions and CBZ-tolerant controls.

This presents a novel approach for discovering SNPs involved in the development of CBZ-induced hypersensitivity reactions in patients. The findings could also unravel the underlying mechanisms involved in these reactions.

Table 4.1: Populations from the 1000 Genomes project [32]

Continent of origin	Population description
Africa	Esan in Nigeria
	Gambian in Western Davison, the Gambia
	Luhya in Webuye, Kenya
	Mende in Sierra Leone
	Yoruba in Ibadan, Nigeria
America	African Ancestry in Southwest US
	African Caribbean in Barbados
	Colombian in Medellin, Colombia
	Mexican Ancestry in Los Angeles, California
	Peruvian in Lima, Peru
	Puerto Rican in Puerto Rico
Asia	
East	Chinese Dai in Xishuangbanna, China
	Han Chinese in Beijing, China
	Han Chinese South
	Japanese in Tokyo, Japan
	Kinh in Ho Chi Minh City, Vietnam
South	Bengali in Bangladesh
	Gujarati Indian in Houston, Texas
	Indian Telugu in the UK
	Punjab in Lahore, Pakistan
	Sri Lankan Tamil in the UK
Europe	Britisch from England and Scotland
	Finnish in Finland
	Iberian populations in Spain
	Utah residence with northern and western European ancestry
	Toscani in Italy

4.2 Material and Methods

4.2.1 Chemicals

CBZ and its metabolites, CBZ-10,11 epoxide (CBZE, eMolecules Inc., Cambridge, USA) and 9-AC (Life Chemicals, Braunschweig, Germany), were used in these experiments. The compounds were dissolved in dimethyl sulfoxide (DMSO, eMolecules Inc.) and diluted into 12 different stock concentrations ranging from 20 000 to 10 µM (see Tab. 4.2).

Table 4.2: Serial dilution of stock concentrations

Concentration (µM)	µl added from dilution	µl of DMSO added	Final concentration (µM)
20 000	2 800 from stock	0	200
10 000	1 400 from stock	1 400	100
3 000	420 from stock	2 380	30
1 000	280 from 10 000	2 520	10
300	280 from 3 000	2 520	3
100	280 from 1 000	2 520	1
30	280 from 300	2 520	0.3
10	280 from 100	2 520	0.1

These dilutions were aliquoted into 96-well plates and stored at -80°C until use in the experiment. The final concentration ranged from 200 to 0.1 µM in the assay. DMSO was used as negative control (0.5% v/v final concentration). Tetraoctylammonium bromide (eMolecules) was used as a positive control for cytotoxicity as described by Cho and colleagues (46 µM final concentration) [35].

4.2.2 Cell lines and culturing

340 immortalised lymphoblastoid cell lines from participants of the 1000 Genome project were obtained from Coriell Cell Repositories (Camden, NJ, USA). These cell lines were chosen as their basal gene expression levels were known through RNA sequencing [36]. The cells were genotyped by exon targeting using NimbleGen 385K capture chip followed by Illumina Genome Analyzer I and II, AB SOLiD System 1.0 and 2.0 or 454 GS FLX for sequencing [32]. The cells were transformed into immortalised cell lines, using Epstein Bar viruses [33], for further scientific experiments. The cells were derived from 340 unrelated, healthy individuals representing four different populations. 78 cell lines (22.9%) were residents from Utah with northern and western European ancestry (CEU). 90 cell lines (26.5%) were Tuscan residents from Italy (TSI). 91 cell lines (26.8%) were from England and Scotland (GBR). 81 cell lines (23.8%) were from Nigerians, Yoruban from Ibadan (YRI). The cell lines were divided into 9 randomised batches for culturing and cytotoxic screening.

Cells were cultured at 37°C with 5% CO_2 in suspension in flasks oriented upright containing RPMI 1640 media (Gibco, Carlsbad, CA, USA) supplemented with 10% fetal calf serum (FCS, Gibco) and 0.1% penicillin-streptomycin (Gibco). The cells were counted and viability was measured on five consecutive days using the Trypan blue (Sigma-Aldrich Inc.) exclusion method and the Cellometer Auto T4 (Nexcelom, Bioscience, Lawrence, MA, USA). Daily measurements were conducted to account for differences in cytotoxicity of lymphoblast cell lines caused by differences in baseline growth rate and metabolic status [37].

4.2.3 Patients

DNA samples from 153 individuals from the DNA archive in Liverpool were used for the genotyping. 109 of these patients were recruited by researchers in Liverpool over the past two decades and 44 individuals have been recruited globally within the international Serious Adverse Events Consortium

(iSAEC). The iSAEC is a non-profit organization, comprising pharmaceutical companies, academic institutions and international regulatory bodies such as the Food and Drug Administration in the USA [38]. The main objective of the consortiums work is the identification of genetic variants responsible for severe, drug-induced reactions including severe skin rashes. The summary of ethnicities of the cohort used in this work can be found in table 4.3 (see Tab. A4.1 in appendix for individual genotype).

Table 4.3: Ethnicity of patients

Ethnicity	Number of individuals
African	1
Asian	5
Caribbean	1
White	127
Mixed	17
Not known	2

From the 109 patients who had suffered from hypersensitivity reactions: 39 of the 109 were patients with maculopapular exanthema (MPE), 1 patient with acute generalised exanthematous pustulosis (AGEP), 43 patients with drug reaction with eosinophilia and systemic syndromes (DRESS), and 26 patients with Steven Johnson syndrome and/or toxic epidermal necrolysis (SJS/TEN). The clinical phenotypes were defined as described by Pirmohamed and colleagues (see general introduction section 1.2.2) [39].

44 were CBZ tolerant patients defined as taking CBZ for a minimum of 6 months without any adverse effects (see Tab. 4.4).

Table 4.4: Patient phenotypes and number of patients used for genotyping

Clinical diagnosis	Number of patients
MPE	39
AGEP	1
DRESS	43
SJS/TEN	26
CBZ tolerant	44

AGEP: Acute generalised exanthematous pustulosis DRESS: Drug rash with eosinophilia and systemic symptoms, SJS: Steven Johnson Syndrome, TEN: toxic epidermal necrolysis, MPE: maculopapular exanthema

4.2.4 Cytotoxicity assay

The CellTiter-Glo Luminescent Cell viability assay (Promega Cooperation, Madison, WI, USA) was used to assess the intracellular adenosine triphosphate (ATP) concentration 23 hours after exposure of the cells to the compounds. ATP is a marker of the metabolic activity of cells and therefore a marker of cytotoxicity [40].The principle of the assay is similar to the MTT assay as described in chapter 2. The assay was selected based on its utility for *in vitro* screening of cytotoxicity in cell type- and individual-independent manner as shown in cross-cell line and cross-individual experiments [37, 41]. It has been demonstrated in different cell lines and individuals that the assay does not depend on cell type or individual and therefore is not introducing further limitations on the experiments.

The cells were counted and the viability measured using the Trypan blue exclusion method. Cell lines with a viability of 90% or higher were diluted to a concentration of $3x10^5$ cells/ml. The dilutions of cells, together with the master plate containing the dilutions of compounds were plated in duplicates

into white bottom 96 well plates using a liquid handling robotic for improved reproducibility (Biomek3000, Beckman Coulter Inc., Irving, TX, USA). Diluted cells (198 µl) and compounds (2 µl) were added to a well and split into two wells of different plates, so that each well contained 100 µl. The plates were incubated for 23 hours in an incubator at 37°C and 5% CO_2. After 23 hours the plates were taken out of the incubator and cooled down to room temperature before adding freshly prepared reagent. The content was mixed by a shaker. Plates were then incubated for 20 minutes at room temperature in the dark before measuring luminescence (DTX880 Multimode Detector, Beckman Coulter Inc.). The experiments were conducted in laboratory of Professor Rusyn's group at the University of North Carolina at Chapel Hill in USA.

4.2.5 Analysis of Single Nucleotide Polymorphism

14 SNPs were identified as top hits in the GWAS. The HaploReg v2 online database was used for the SNP analysis [42]. The database allows submission of queries by rs-ID number of the SNP. The data obtained from the database include the position of the SNP in the chromosome (intronic and exonic) the known function of the SNP as well as SNPs that are in linkage disequilibrium. The information in the database was generated by genotyping individuals included in the 1000 Genomes project [32].

4.2.6 Dual oxidase 1 genotyping

The genetic variants of the DUOX1 allele were genotyped using the rs16939743 TaqMan® SNP genotyping assay (Life Technologies Ltd., Paisley, UK).This SNP was selected for validation because it was the only potentially functunal SNP (missense mutation) and it was also found to be associated with the cytotoxicity in all three compounds tested.

The TaqMan® SNP genotyping assay is a PCR assay utilising the 5' exonuclease activity of AmpliTaq Gold® DNA polymerase [43, 44]. For the

PCR, two locus-specific primers flanking the SNP of interest and two allele-specific oligonucleotide TaqMan® probes are included. The probes are labeled with a fluorescent reporter dye at the 5' end and a non-fluorescent quencher with a minor groove binder at the 3' end [45]. Minimal fluorescence is emitted by an intact probe, due to the close proximity of the quencher [46]. A signal is generated by cleaving the fluorescent reporter dye from the 5' end of a probe hybridised to the target allele through the polymerase during each PCR cycle. The PCR primers amplify the specific locus of the DNA template. The cleavage of one or both dyes of the probes produces an exponentially increasing fluorescent signal. The use of two allele-specific probes labelled with two different fluorescent dyes, allows the detection of both alleles in a single PCR. The use of a minor groove binder enhances the allelic discrimination through stabilising the probe template hybridisation and reducing mismatch hybridisation [47].

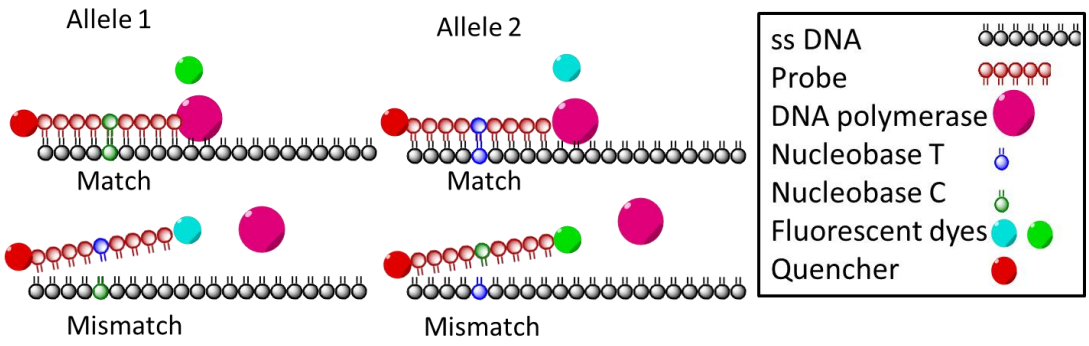

Figure 4.2: Schematic view of probe binding and generation of allele-specific florescent signal through cleavage of DNA polymerase

The PCR was conducted in accordance with the TaqMan® protocol using the dry-down DNA method. Briefly, the samples were prepared in 384-well optical reaction plates. 20ng of DNA were dispensed into each well and left to dry overnight. A master mix of the reagents for the PCR was prepared in a 5 µl volume as follows: TaqMan® universal PCR master mix (final concentration: 1X) and working stock of SNP genotyping assay (final concentration: 1X) were mixed and added up to the final volume with DNase-free water. The plate was then placed in the thermal cycler (7900HT Fast

Real-Time PCR System, Applied Biosystems, Life Technologies) and the PCR reaction was conducted. The PCR was initiated at 95°C for 10 min followed by 40 cycles of denaturing at 92°C for 15 sec and annealing and extending at 60°C for 1 min. The fluorescence was measured by the thermal cycler and analysed using the SDS 2.4 software.

4.2.7 Cytotoxicity assay data processing

The data from the cytotoxicity assay were normalised to the positive and negative control and expressed as percentage of viability compared to the negative control (DMSO) [41].

4.2.7.1 Curve fitting

A Hill equation was fitted to the normalised concentration-response titration points of each compound and the data from each cell line. The baseline (ceiling), 100% of living cells, was estimated from the lower concentration-responses. The maximum response (floor) is fixed to 100% dead cells (from positive control) unless another floor was observed for the cell line. Outliers of the data set from each cell line were removed if they lay more than 2 standard deviations from the estimated fit. The program also fitted a Hill equation to the normalised concentration-response titration points for each compound and the data sets of all cell lines.

4.2.7.2 Effective concentration 10

The effective concentration 10 (EC10) is the concentration at which the luminescence dropped to 90% of the fitted value for the lowest concentration used in the experiment. For estimation of EC10, a program was used, which had been developed in Professor Rusyn's group at the University of North Carolina at Chapel Hill. In case of the EC10 dose not being within the concentration range, the program estimated the EC10 at 251 µM. This

concentration is slightly higher than the highest concentration (200 µM) used in the experiments. This allows for the use of the data set in further analysis (such as the GWAS using the Plink software).

4.2.8 Statistical analysis

The statistical analysis was conducted by Prof. Rusyn's group using the R statistical software (2.10.0; R Development Core Team, Vienna, Austria).

4.2.8.1 Assessing reproducibility of assays

The Pearson correlation coefficient (ρ) between pairs of replicates was used to assess the reproducibility of the experiments. The two EC10 estimates for each cell line and each compound were used to calculate the Pearson correlation coefficient. In addition, ρ was calculated for each compound separately and for each compound against one of the other two compounds to investigate whether there was a correlation between them. A Kruskal-Wallis ANOVA [48] was performed to test for significant differences the EC10 estimates to check for batch effects. Batch effects were adjusted using the Combining Batches (ComBat) method developed by Johnson and colleagues [49]. Experimental variations without biological cause, also referred to as batch effects, are commonly observed in experiments that logistically require the sizing of different batches. These make the combination of data inappropriate without adjustment for these batch effects. The combination of data is necessary for increased statistical power. The ComBat method is based on parametric and nonparametric empirical Bayes frameworks to adjust the data for batch effects in small samples sizes and has proven robustness against outliers in such situations [49].

4.2.8.2 Group difference

A Kruskal-Wallis ANOVA [48] was performed to test for significant differences in the EC10 estimates for each compound, each compound in the different genders and also for each compound in different populations. These comparisons resulted in the multiple comparison problem. The false discovery rate is generally set at 0.05 level through the p-value. Through the screening of multiple hypothesis simultaneously, the probability of making a false discovery could increase far beyond the pre-set 0.05 level. Different approaches have been described of accounting for multiple comparisons in the false discovery rate. For the group differences, the Benjamini-Hochberg false discovery rate was used to correct for multiple comparison [50].

4.2.8.3 MAGWAS analysis

To measure the relationship of cytotoxicity and genotype, multivariate ANCOVA genome-wide association software (MAGWAS) was used [51]. This software provides analysis tools for association studies of single nucleotide polymorphisms (SNP) in genetic data having multivariate responses and possibly, multiple covariates. The software is based on the multivariate analysis of covariance (MANCOVA). MANCOVA combines the advantages of the analysis of covariance (ANCOVA) and the multivariate analysis of variance (MANOVA).

The core of all these analyses is the analysis of variance (ANOVA), which tests three or more groups for mean differences based on a continuous response variable (independent variable) measured in a scale or interval. For the comparison of the variance in the means of two groups, t-test can be utilised. Conducting multiple t-tests for the comparisons of more than two group means is not advisable as multiple testing would result in an inflation of the false discovery rate (Type I error). Therefore, ANOVA is used for such comparisons.

In comparison to ANOVA, ANCOVA includes one or more covariates. Covariates are variables that are not part of the experimental design but can

have an influence on the on the outcome (dependent variable). ANCOVA assesses the distribution of means in the outcome within different treatment groups (independent variables), while statistically monitoring the influence of covariates and adjusting for these. Therefore, ANCOVA separates variance in the outcome into three groups: variance accounted for by the treatment, variance caused by covariates, and residual variance. The variance caused by covariates (covariance) is measured as a linear association between the covariates and the outcome. Due to this adjustment, ANCOVA reduces the error variance within a group and also eliminates the possibility of confounds.

MANOVA is an extension of ANOVA and can be used for analysing multiple dependent variables. ANOVA can only analyse one association of one dependent variable. Similar to the situation of multiple t-tests, the conduction of multiple ANOVAs is inappropriate, as this would lead to an increase in the false discovery rate. Another advantage of using MANOVA over multiple ANOVAs is that MANOVA takes into account relationships between outcomes (dependent variables) by including them in one analysis.

Therefore, analysing the data with a MANCOVA software allows the use of the dose response data measured instead of EC10, as well as adjusting for various covariates. The screening for all cell lines used in the experiments could not be measured at the same time and might influence the means depending on these circumstances, such as the day on which the cells were measured.

“For covariates, responses were fit to the model using following formula:

$$Y_i = \alpha + X_i + E_i;$$

where Y_i is the vector of responses for the i-th cell lines, and X_i contains effects from covariates. This regression identifies overly influential observations that would be used in the association analysis.

For phenotype, responses were modelled using the following formula:

$$Y_{ij} = \alpha + X_{i,-j} + E_{ij};$$

where Y_{ij} is the j-th response from the i-th cell lines, and $Y_{i,-j}$ are vectors of responses, excluding j, from the i-th cell line. This regression identifies responses that do not match the rest of the dose-response curve.

For this the program uses following guidelines:

- Replace responses > 3:5 ɕ-hat away from their predicted value
- Use original ranked responses instead if replacement > 5%
- Use original ranked response also, if absolute skewness > 1 or kurtosis > 4.5”

The information was provided by Chad Brown, the developer of the MAGWAS.

For the MAGWAS, genotype data from each cell line comprising 1510701 SNPs was obtained from the 1000 genome project [32]. For the quality control of the genotyping data, the missingness test (GENO > 0.1), minor allele frequency test (MAF < 0.05) and Hardy-Weinberg test (p ≤ 0.001) were used. The missingness test determines the quality of a marker by assessing the call rate for a particular SNP. In this GWAS, it was set less than 10%, meaning that the lowest call rate for a SNP was above 90%. This excluded 48 SNPs. The minor allele frequency (MAF) test excludes very rare SNPs from the analysis. Because of their rare occurrence, these SNPs generally require larger sample sizes. In this GWAS, 481 379 SNPs with MAF below 5% were excluded. The Hardy-Weinberg equilibrium (HWE) assumes that all frequencies of alleles and genotypes can be estimated from one generation to the other in the absence of migration, mutation, natural selection and inbreeding [52]. The HWE test is a Chi-squared test assessing how good the

data fit the HWE [53]. 19 169 markers were excluded based on HWE test. After the quality control of the data, 1 015 304 SNPs were included in the GWAS. Phenotype was derived as the normalised and adjusted dose-response data for the cell lines in the MAGWAS analysis. For covariates, the first 10 principal components were used for to adjust for population stratification (see Fig. 4.3 and 4.4). Furthermore batch, gender, day, and batch and day were included in the model.

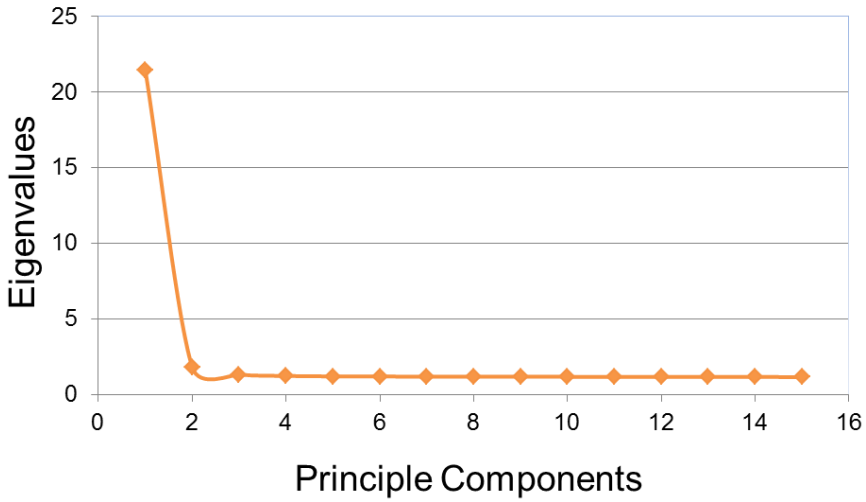

Figure 4.3: Eigenvalues of first 15 principal components

The x-axis shows the principle components and y-axis shows Eigenvalues. Eigenvalues represent how much variation is caused by principle component.

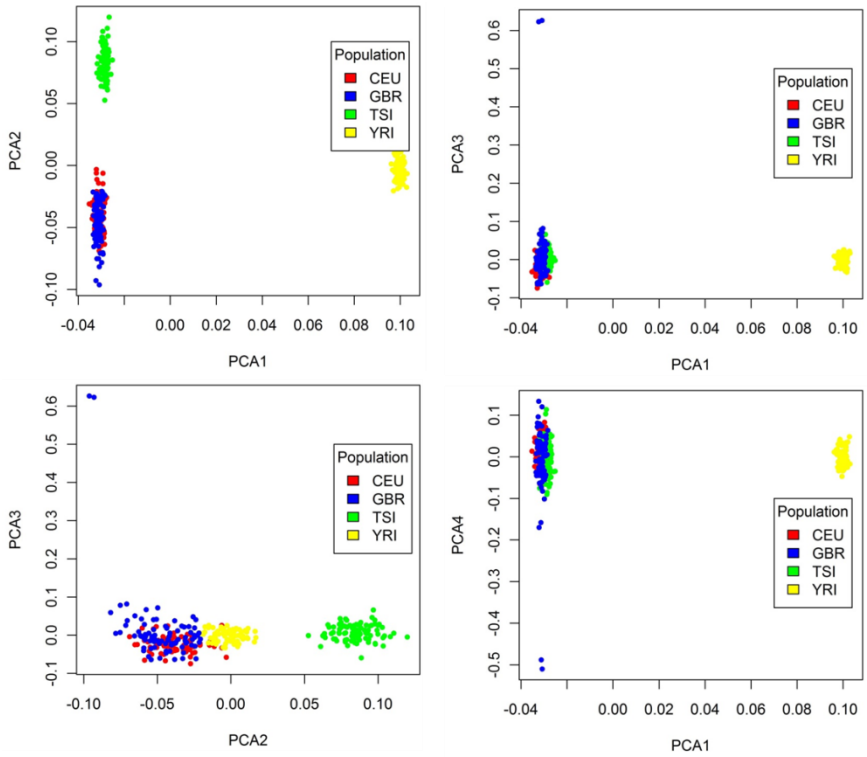

Figure 4.4: Principle component analysis

CEU: residents from Utah with northern and western European ancestry, TSI: Tuscan residents from Italy, GBR: British population from England and Scotland, YRI: Nigerians, Yoruban from Ibadan.

LocusZoom was used to visualise the genomic context for suggestive loci determined by MAGWAS [54].

P-values below 1 x 10^{-8} were considered genome-wide significant. This value derives from the Bonferroni correction [55]. Cut off of $p < 10^{-8}$ was also used in other GWASs [56-60]. The approach for this correction is conservative; and therefore, p-values between $1x10^{-5}$ and $1x10^{-8}$ were also taken into consideration but as genome-wide suggestive.

4.2.8.4 Fisher's exact test

The clinical outcome of the patients was compared against the DUOX1 genotyping data utilising the Fisher's exact test [61].

4.2.8.5 Power calculation for SNP validation

Based on the frequency of the rare variant of DUOX1 in European (0.01), to achieve 80% power with 5% alpha error and odds ratio of 5, approximately 144 cases and 175 controls in a 1:5 ratio would need to be included.

To determine whether the polymorphism in DUOX1 is associated with all hypersensitivity phenotypes, genotyping needs to be conducted in a large number of individuals with diverse clinical phenotypes. To assess a sample size for future studies to detect a statistical difference between case- and control group under the assumption that the frequency of the DUOX1 variant is 20% in patients with hypersensitivity reactions, a power calculation was performed with varying frequencies of the DUOX1 variant in the control group (see Tab. 4.5).

Table 4.5: Number of patients required to conduct a case control study with varying frequencies of DUOX1 variant in a control group (frequency of DUOX1 variant in cases: 20%, 5% Alpha error and 80% power)

		Frequency of DUOX1 variant in control group		
Case : Control ratio	Groups	8% (Worldwide)	14% (Asian)	19% (African)
		Numbers of individuals required		
1:1	Cases	131	615	24 641
	Controls	131	615	24 641
1:5	Cases	69	354	14 707
	Controls	345	1 770	73 535
1:10	Cases	61	321	13 465
	Controls	610	3 210	134 650

4.3 Results

The screening was conducted in a 96-well plate format using a robotic system. Out of the 340 cell lines that were chosen originally for the experiment, 9 had low viability (<90%), and therefore cells were not used for the screening. The number of cells and the percentage of cell lines from different populations utilised in the experiments are shown in Table 4.6.

Table 4.6: Screened cell lines after correction for cell viability and quality requirements

Population	Cell lines	Percentage
CEU	76	22.9
YRI	81	23.3
TSI	90	26.3
GBR	91	27.5
Total	**331**	

The remaining 331 cell lines were divided into random batches and screened against the 3 compounds. Each 96-well plate contained one cell line exposed to CBZ and its two metabolites, CBZE and 9-AC, together with the vehicle control DMSO and the positive control tetraoctylammonium bromide.

4.3.1 Interindividual variability

The cytotoxicity data from the ATP assay and the utilisation of strictly controlled conditions, allowed the investigation of variation in dose-response in 331 individuals of different ancestry [62]. The normalised data for each compound is shown in grey for each concentration and all individuals (Fig. 4.1). The data for each individual were pooled and a logistic curve was fitted

(red-dashed curve). From separately performed logistic curve fits, an EC10 was estimated for each individual cell line, shown as a histogram. In case of the EC10 dose not being within the concentration range, the EC10 was estimated at 251 µM to allow for inclusion of the data for further analysis.

For a better comparison, the EC10s for the 3 compounds were plotted as box plots (see Fig. 4.5). The plots showed that the average EC10 for 9-AC was much lower than the EC10s for CBZ and CBZE, showing that 9-AC was toxic in the concentration range used in this experiment, while CBZ and CBZE were non-toxic. The box plots also showed that for all three compounds, there were individuals with higher susceptibility to the cytotoxic effect of each compound.

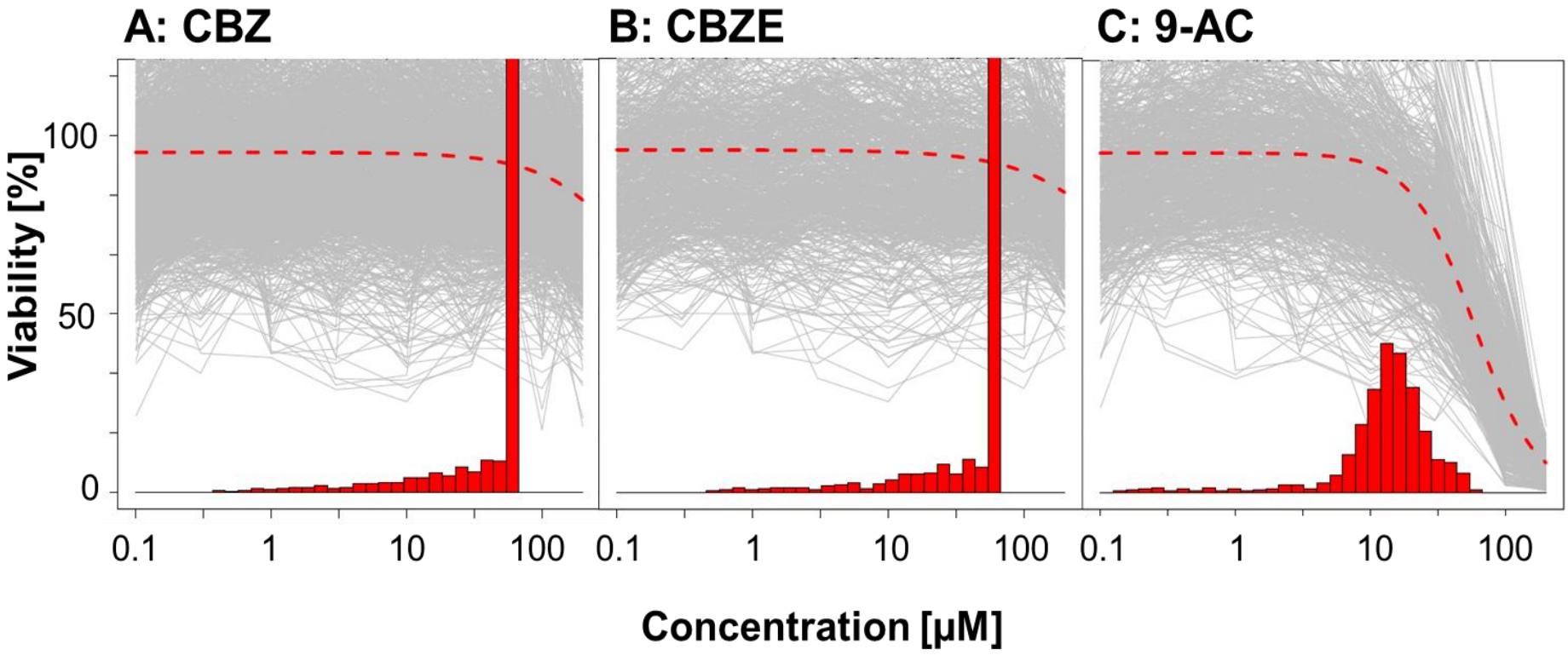

Figure 4.5: Dose response data of 331 screened cell lines

The diagrams show the modelled population concentration response using *in vitro* data from screening of compounds CBZ (**A**), CBZE (**B**), and 9-AC (**C**). The individual 10% effective concentration values (EC10) were provided from logistic dose-response modelling for the data of each individual (shown in grey). The EC10s obtained are shown as a histogram. The red dashes line represents the logistic dose-response modelling for all of the data combined.

4.3.2 Robustness and reproducibility of qHTS data

Each plate was prepared and measured in duplicate to increase the robustness of the data. For testing the reproducibility of the screening data, the two EC10 estimates from the duplicates were plotted against each other and pair-wise Pearson correlation among replicate plate pairs was performed (Fig. 4.6). For CBZ, the Pearson correlation coefficient ρ was 0.59. For CBZE, ρ was 0.60. This showed that there was no strong correlation between the EC10s of CBZ and CBZE. For 9-AC, ρ was 0.79 showing a much higher association between the EC10s of 9-AC.

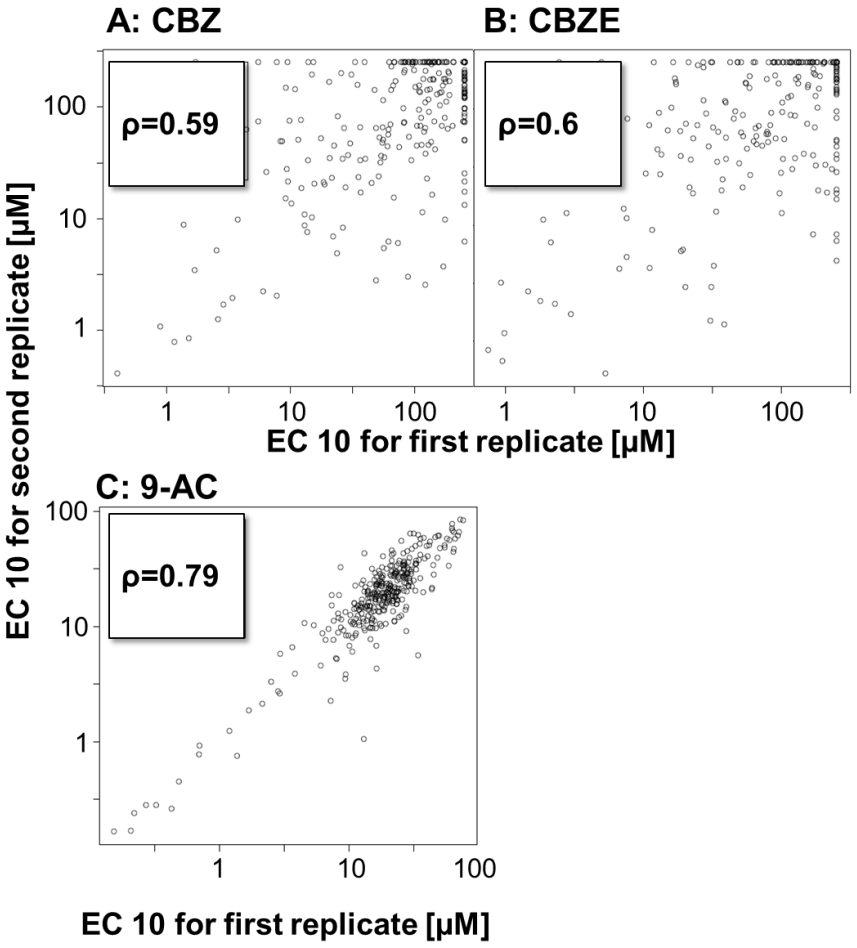

Figure 4.6: Intra-experimental reproducibility of EC10

The EC10s from the two replicates of each experiment were plotted against each other and a pair-wise Pearson correlation was performed to assess the reproducibility of the outcome.

4.3.3 Differences between genders and populations

The EC10s showed inter-individual variability. To investigate the nature of these differences further, the two genders as well as the four different populations were compared with each other. The EC10 were analysed using a Kruskal-Wallis ANOVA. No significant difference was observed for any of the three compounds (data for CBZ and CBZE not shown). Figure 4.7 shows the comparison of the EC10s from 9-AC for the different genders and figure 4.8 shows the comparison of EC10s from 9-AC for the four populations.

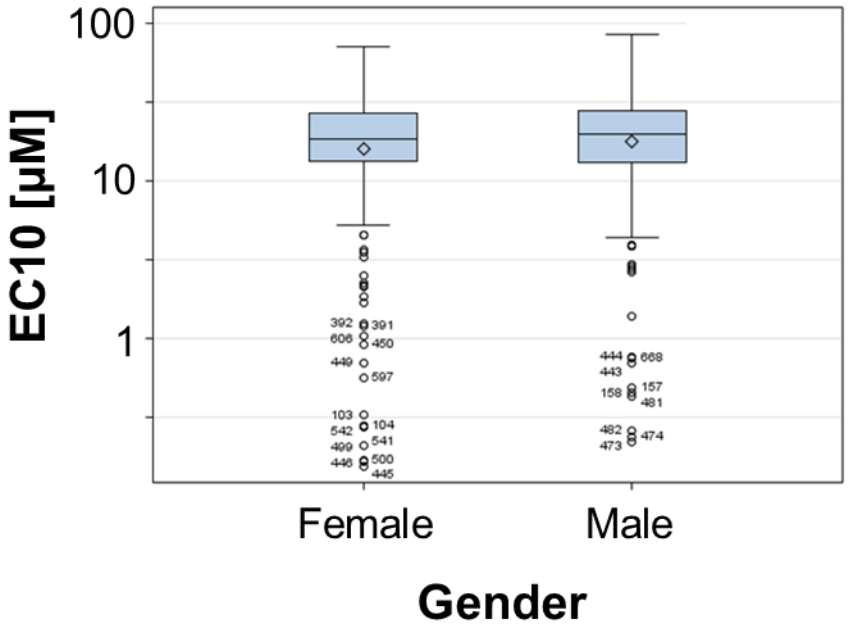

Figure 4.7: Comparison of EC10s from 9-AC for genders

The EC10s of the two different genders were visualised in a box plot. A Kruskal-Wallis ANOVA was performed to find significant differences between the EC10s of the genders.

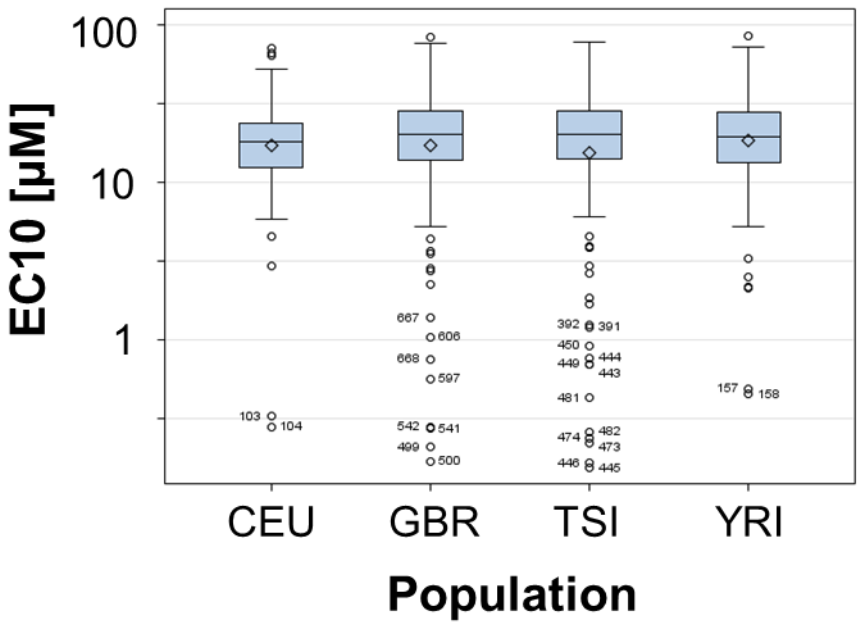

Figure 4.8: Comparison of EC10s from 9-AC for different populations

The EC10s of the four populations were visualised in a box plot. A Kruskal-Wallis ANOVA was performed to investigate whether differences exist between the EC10s of the four populations.

4.3.4 Evaluation between cytotoxicity and genotype

The observation that EC10s vary by up to 2 magnitudes between individuals for all three compounds raised the following question: could genetic loci be identified that are associated with the higher susceptibility for toxicity caused by CBZ and its metabolites? Publicly available genotypes from the 1000 Genomes project were used [32] and a MAGWAS was performed using the dose-response data as a phenotype.

The MAGWAS revealed SNPs that were associated with the higher susceptibility to the cytotoxic effect caused by the compounds (see Tab. 4.7).

Table 4.7: Number of SNPs associated with susceptibility to cytotoxic effect

Compound	SNPs with p-value below $1x10^{-4}$	SNPs with p-value below $1x10^{-5}$	SNPs with p-value below $1x10^{-6}$	Minimum p-value
CBZ	94	16	0	$2.5x10^{-6}$
CBZE	130	16	1	$2.0x10^{-8}$
9-AC	104	18	3	$2.5x10^{-7}$

For each compound MAGWAS revealed SNPs that were to varying significant degrees associated to the higher susceptibility of cell lines to the cytotoxic effect of compounds.

For CBZ, the GWAS revealed SNP rs4772593 on chromosome 13 with the lowest p-value in association with susceptibility to cytotoxicity in cell lines (see Fig. 4.9 A). Two SNPs, rs56303447 on chromosome 5 and rs2927299 on chromosome 16, had the lowest p-value, which indicates susceptibility to cytotoxicity of CBZE (see Fig. 4.10 A). Three SNPs revealed in the GWAS (see Fig. 4.11 A); SNP rs1624718 located on chromosome 16, rs7998181 located on chromosome 13 and rs6984950 located on chromosome 8 were associated with susceptibility to 9-AC cytotoxicity. Several locus zooms were presented in this chapter, which were derived from Manhattan plot analysis. The left y-axes in the LocusZooms show the p-values for the negative logarithm of the p-value for each SNP (see Fig. 4.9 to 4.11). The x-axis shows the position of each SNP on the chromosomes as well as known genes in the vicinity. The right y-axis shows the recombination rate on the chromosome and the depicted region. The dots and their colour show the linkage disequilibrium of the SNP and other polymorphisms in the region of the chromosome.

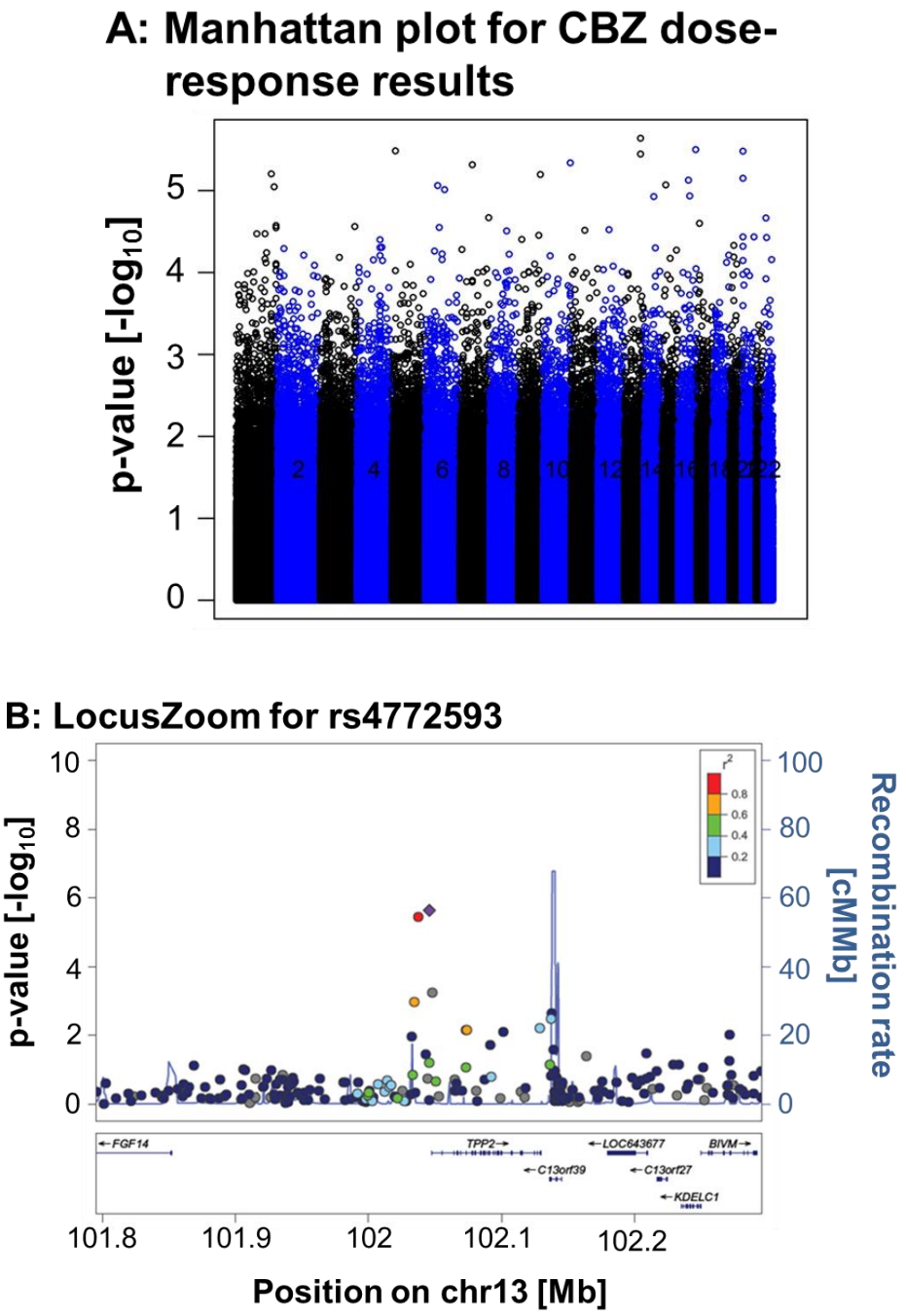

Figure 4.9: Results of Genome-wide Association Study of toxicity-genotype relationship for CBZ

A: Manhattan plot from GWAS for the dose response data of CBZ. SNP with lowest p-value was located on chromosome 13 **B:** Locus zoom for the region of chromosome (chr) 13 containing the most significant SNP, rs4772493. Left y-axis shows the p-value as the negative logarithm ($-\log_{10}$). Right y-axis shows the recombination rate of region 101 and 102 Mb on the chromosome 13. X-axis shows the position of rs4772493. The dots and their colour show other polymorphisms in the region and their linkage disequilibrium to rs4772493.

A: Manhattan plot for CBZE dose-response results

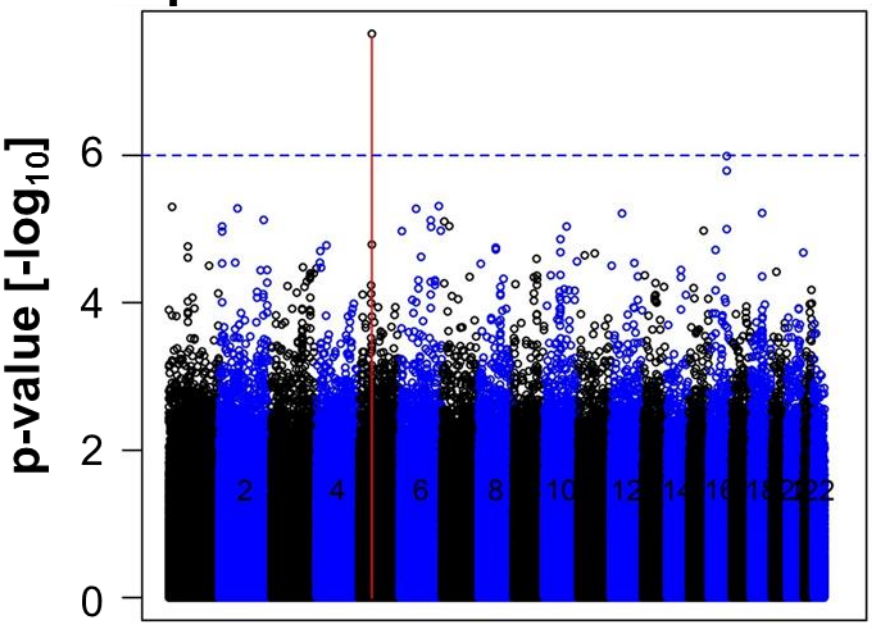

B: LocusZoom for rs56303447

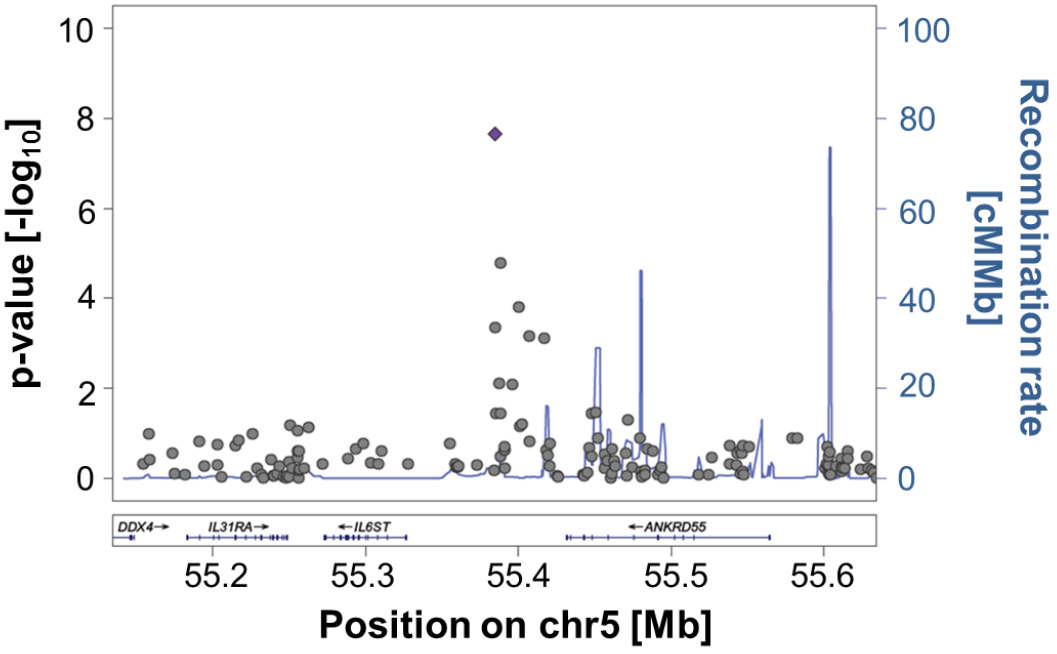

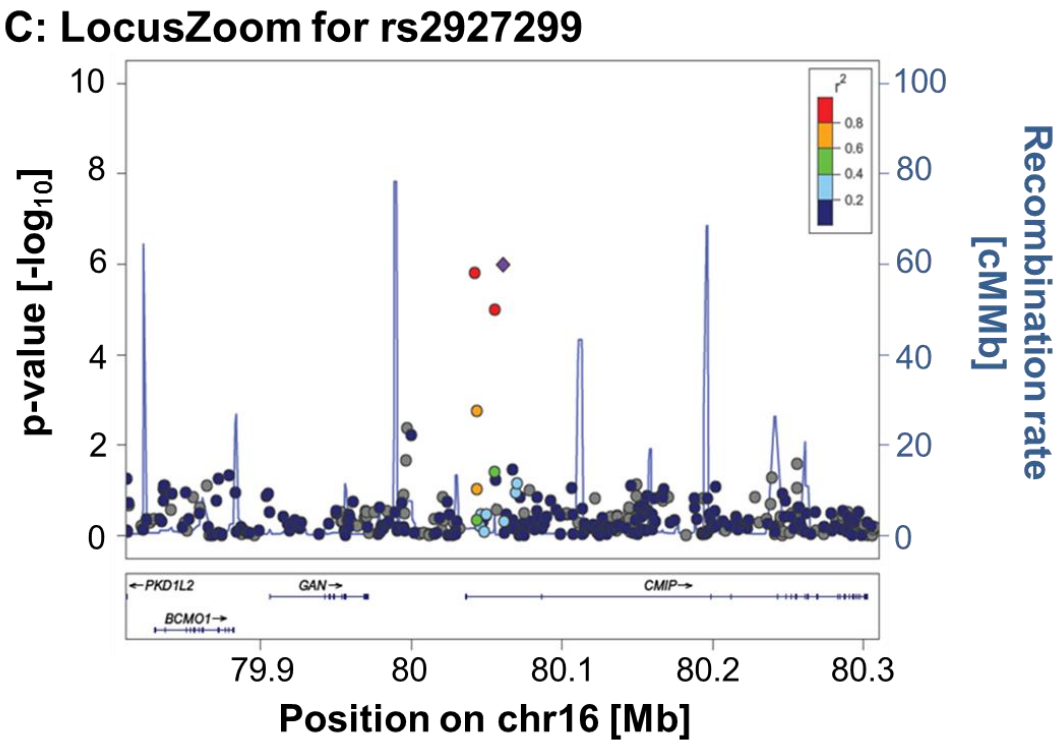

Figure 4.10: Results of Genome-wide Association Study of toxicity-genotype relationship for CBZE

A: Manhattan plot from GWAS for the dose response data of CBZE. SNPs with lowest p-value were located on chromosomes 5 and 16 **B:** Locus zoom for the region of chromosome (chr) 5 containing the most significant SNP, rs56303447, **C:** Locus zoom of region on chromosome 16 containing rs2927299. Left y-axis show p-values as the negative logarithm ($-\log_{10}$). Right y-axes show the recombination rate of regions on chromosomes. The x-axes show the position of SNP on chromosomes. The dots and their colour represent other polymorphisms in the region and their linkage disequilibrium to SNPs.

A: Manhattan plot for 9-AC dose-response results

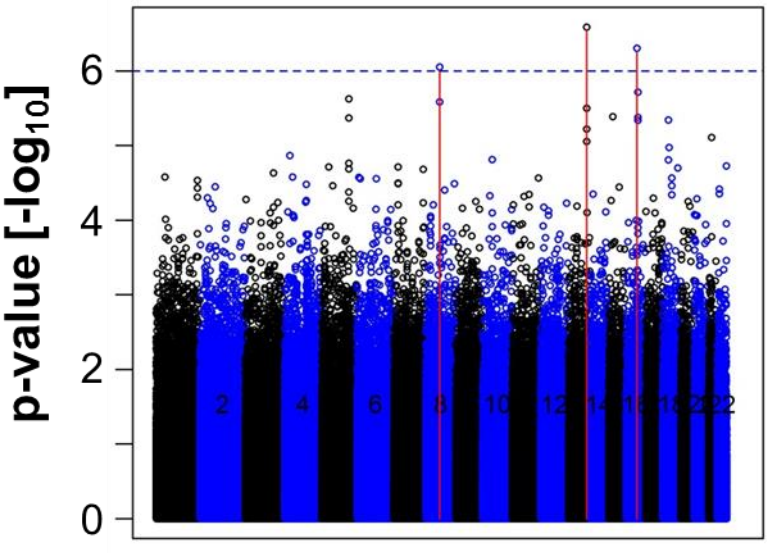

B: LocusZoom for rs1624718

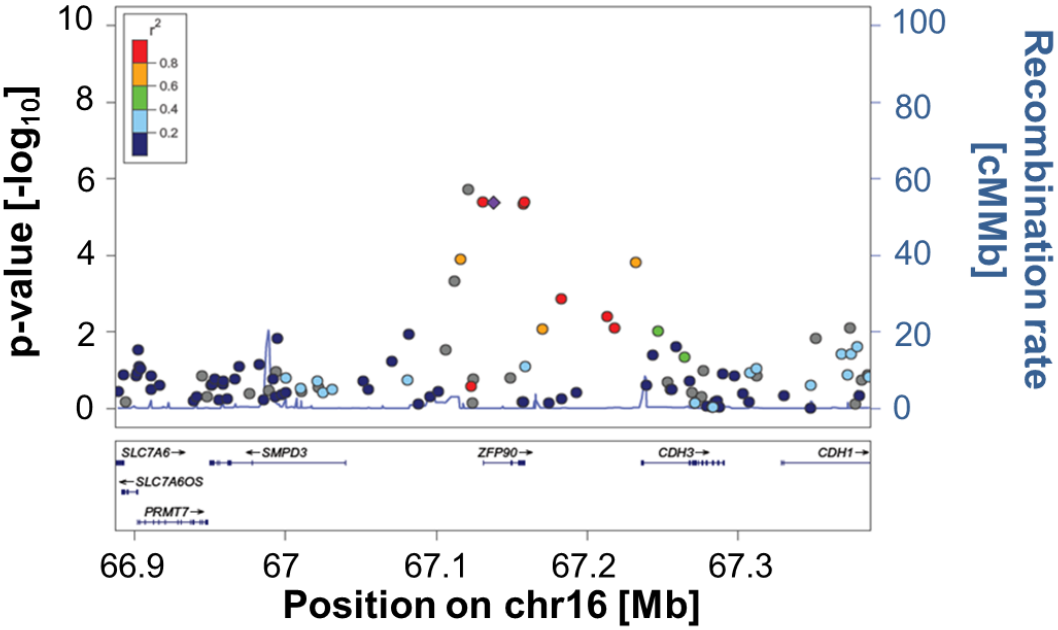

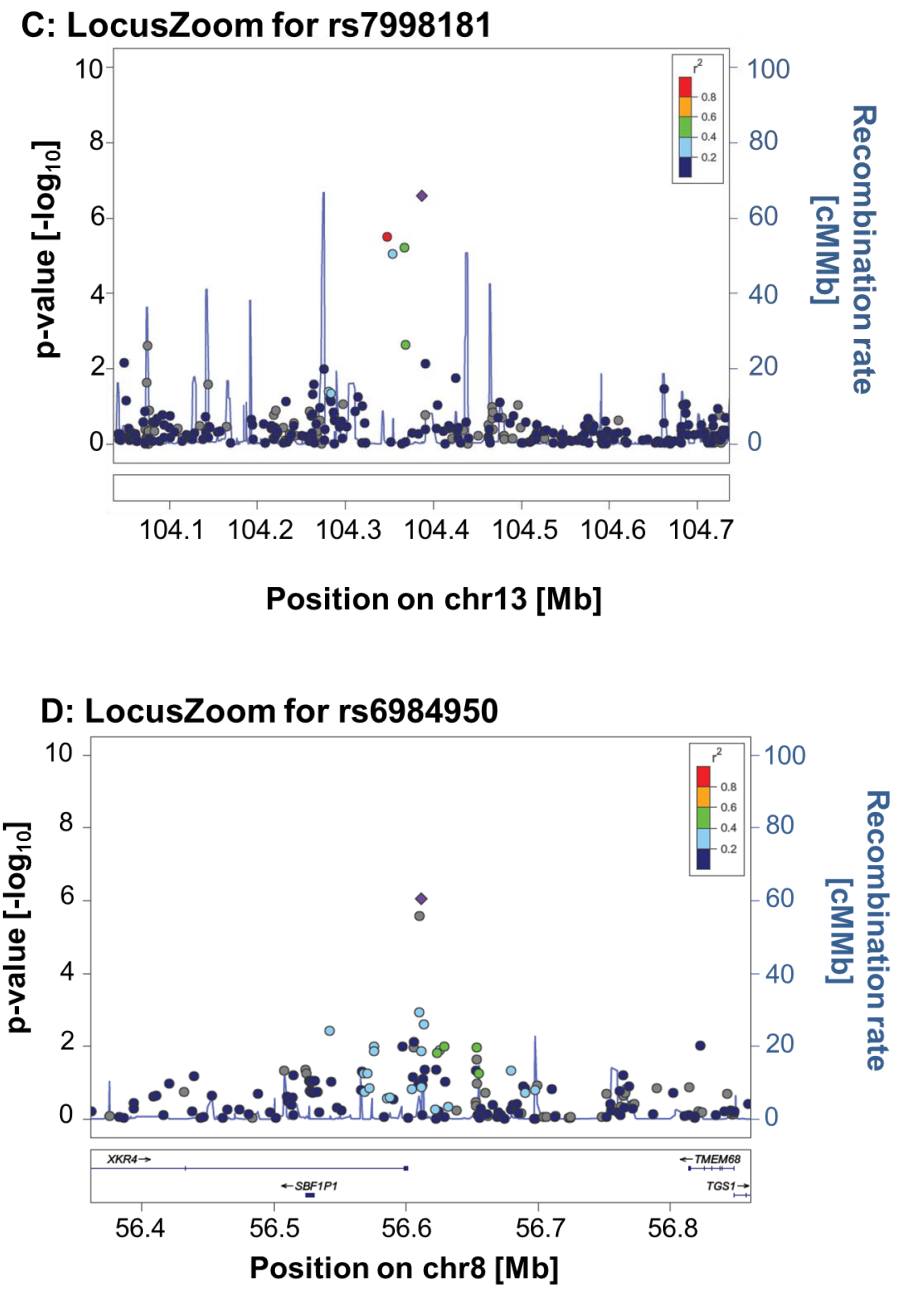

Figure 4.11: Results of Genome-wide Association Study of toxicity-genotype relationship for 9-AC

A: Manhattan plot from GWAS for the dose response data of CBZE. SNPs with lowest p-value were located on chromosomes 8, 13 and 16 **B:** Locus zoom for the region of chromosome (chr) 16 containing rs1624718, **C:** Locus zoom of region on chromosome 13 containing rs7998181. **D:** Locus zoom of region around rs6984950 on chromosome 8. Left y-axis show p-values as the negative logarithm ($-\log_{10}$). Right y-axes show the recombination rate of regions on chromosomes. The x-axes show the position of SNP on chromosomes. The dots and their colour represent other polymorphisms in the region and their linkage disequilibrium to SNPs.

Some SNPs were also found to have low p-values for the susceptibility to the cytotoxicity of all 3 compounds (see Tab. 4.8).

Table 4.8: SNPs associated with susceptibility to cytotoxicity found for more than one compound

SNP ID	p-value for CBZ	p-value for CBZE	p-value for 9-AC	Function
rs16939743	$8.5x10^{-6}$	$6.3x10^{-5}$	$4.1x10^{-6}$	missense
rs62048729	$7.4x10^{-6}$	$4.5x10^{-5}$	$5.0x10^{-7}$	-
SNP2-81896	$9.8x10^{-5}$	$9.3x10^{-6}$	-	-
rs73319053	$5.0x10^{-5}$	$4.6x10^{-5}$	-	intronic
rs7930391	$3.0x10^{-5}$	$2.1x10^{-5}$	-	intronic
rs4144233	$6.5x10^{-6}$	-	$7.1x10^{-5}$	intronic
rs7080371	$6.3x10^{-5}$	-	$4.7x10^{-5}$	intronic
rs56303447	-	$2.2x10^{-8}$	$3.5x10^{-5}$	5.9 kb 5' of gene
rs57831073	-	$2.0x10^{-5}$	$7.8x10^{-5}$	82 kb 5' of gene

The GWAS revealed 14 SNPs that were associated with the cytotoxic effects of the compounds; CBZ, CBZE, and 9-AC. 2 of these 14 SNPs were found to be associated with toxicity to all 3 compounds, 7 with 2 compounds, and 5 with 1 compound. None had reached the predefined genome-wide significant cut off ($1x10^{-8}$). SNPs located in biologically plausible genes were validated using samples from patients that had undergone CBZ treatment.

4.3.5 SNP analysis

The 14 SNPs, that were found genome-wide suggestive in the GWAS, were identified and analysed using HaploReg v2 online database (Tab. 4.9) [42].

From the 14 top hits found in the GWAS (see Tab 4.8), 5 were found to be in flanking regions of genes (rs56303447, rs57832073, rs4772493, rs6984950 and rs7998181), 6 SNPs were in introns of genes (rs73319053, rs7930391,

rs4144233, rs7080371, rs2927299 and rs1624718) and one SNP was inside the coding region of a gene and functionally significant (rs16939743).

It was shown that SNPs located in flanking regions of genes can have an influence on the transcriptional regulation [63-65]. For example, a SNP in the 5'-flanking region of the cytochrome P450 CYP2E1 gene was reported to enhance its expression [66]. SNPs located in introns of genes can result in different splice variants of certain genes [67]. Further investigation of the genes located next to the SNP or intronic SNPs found in the GWAS were excluded for different reasons.

In the variant of the DUOX1 gene, a thymine is exchanged with a cysteine. This exchange leads to the substitution of an isoleucine with a threonine in the DUOX1 (p.I962T) [68]. SNP rs16939743 has a minor allele frequency (MAF) below 1% in European populations. A MAF <1 is considered a mutation [69]. Because of low MAF, the GWAS chip used in the past did not include rs16939743 [70]. It was the only functional SNP revealed by the GWAS and also associated to a higher susceptibility to cytotoxicity for all three compounds. DUOX1 was shown to play a role in the activation of the immune system [71-73]. Unpublished data from lymphocyte toxicity assay conducted in our group suggested that during the exposure of peripheral blood mononuclear cells to CBZ, high levels of hydrogen peroxide might be generated in certain samples. This finding requires further investigation. DUOX1 could be responsible for these levels of hydrogen peroxide. Therefore it was decided to genotype the samples for their DUOX1 status.

Table 4.9: Analysis of 14 SNPs with lowest p-values identified by GWAS to be associated with cytotoxicity of compounds carbamazepine (CBZ), CBZ-10,11 epoxide (CBZE), and 9-acridinecarboxaldehyde (9-AC) (Chr. = Chromosome)

SNP ID	Gene	Chr	Position	p-value			Function
				CBZ	CBZE	9-AC	
rs16939743	DUOX1	15	45442896	$8.5x10^{-6}$	$6.3x10^{-5}$	$4.1x10^{-6}$	missense
rs62048720	RP11-354|13.2	16	60394885	$7.4x10^{-6}$	$4.5x10^{-5}$	$5.0x10^{-7}$	
SNP2-81896				$9.8x10^{-5}$	$9.3x10^{-6}$	-	
rs73319053	ISM2	14	77954853	$5.0x10^{-5}$	$4.6x10^{-5}$	-	intronic
rs7930391	MYO7A	11	76881925	$3.0x10^{-5}$	$2.1x10^{-5}$	-	intronic
rs4144233	LMX1B	9	129414169	$6.5x10^{-6}$	-	$7.1x10^{-5}$	intronic
rs7080371	ENKUR	10	25287916	$6.3x10^{-5}$	-	$4.7x10^{-5}$	intronic
rs56303447	5.9kb 5' CTD2227|181	5	55348941	-	$2.2x10^{-8}$	$3.5x10^{-5}$	
rs57831073	82kb 5' MIR572	4	11288684	-	$2.0x10^{-5}$	$7.8x10^{-5}$	
rs4772493	1.7kb 5' TPP2	13	103247692	$>1x10^{-5}$	-	-	
rs2927299	CMIP	16	81503403	-	$>1x10^{-6}$	-	intronic
rs1624718	ZFP90	16	68580385	-	-	$<1x10^{-6}$	intronic
rs6984950	2.4kb 3' RP11-628E19.3	8	56448940	-	-	$8.9x10^{-7}$	
rs7998181	522kb 3' DAOA-AS1	13	105588931	-	-	$2.6x10^{-7}$	

Table 4.10: Function of genes associated to SNPs found by GWAS (see Tab 4.9)

Gene code	Gene name	Function of encode gene product
DUOX1	Dual oxidase 1	Generation of peroxides, involved in antimicrobial defence
ISM2	Isthmin2	Contains motifs from complement system but also extracellular matrix proteins
MYO7A	Myosine VIIA	Intracellular transport
LIMX1B	LIM homebox transcription factor 1, beta	Transcription factor during development of body
ENKUR	Enkurin, TRPC channel interacting protein	Involved in calmodulin signal transduction
MIR572	microRNA 572	post-transcriptional regulation of gene expression (micro RNA in general)
TPP2	Tripeptidyl peptidase II	Peptidase involved in MHC class I peptide presentation
CMIP	c-Maf inducing protein	Involved in the T cell signalling pathway
ZFP90	Zinc finger protein 90	-
DAOA-AS1	D-Amino acid oxidase activator antisense RNA 1	Inhibition of activator for D-amino acid oxidase

4.3.6 SNP genotyping of DUOX1

From the 109 samples that were used, the genotyping did not work in 2 cases. 65 samples were from patients that had suffered ADRs during their CBZ treatment and 44 samples were from CBZ tolerant patients (Tab. 4.11). Only 3 patients were carriers of the rare variant of DUOX1. One was a CBZ tolerant patient. The other 2 were patients that had suffered from severe CBZ-induced hypersensitivity reactions. Interestingly enough, these two patients were not of European descent. One patient had Thai and English ancestry. The other patient had declared to be of European descent but principle component analysis, from previous genome-wide analysis, of the DNA clustered this sample with DNA samples of Indian ancestry.

Table 4.11: Assessment of DUOX1 status in CBZ-treated patient samples from Liverpool cohort

Clinical diagnosis	Number of patients	Number of carriers of the DUOX1 variant
MPE	39	0
DRESS	22	1
SJS/TEN	5	1
CBZ tolerant	44	1

DRESS: Drug rash with eosinophilia and systemic symptoms, SJS: Steven Johnson Syndrome, TEN: toxic epidermal necrolysis, MPE: maculopapular exanthema

From the 4 DNA samples of patients with non-European ancestry that suffered from CBZ-induced hypersensitivity reaction, 2 were carriers of the rs16939743 variant of DUOX1. 44 DNA samples from the ITCH study were genotyped to assess their DUOX1 status, including 23 samples from non-white patients. All patients had suffered from severe hypersensitivity reactions while treated with CBZ. The PCR did not work for 2 of the samples.

The genotyping showed that 5 patients, who had previously suffered from CBZ-induced ADRs, were carriers of the variant of DUOX1. From these 5 patients 4 were non-white. The other carrier of the DUOX1 variant was recruited in Brazil.

Due to the diversity of populations from which the DNA samples for the genotyping derived, there were only a few samples in each group. No DNA samples from non-white, CBZ tolerant patients were available to compare the results of the hypersensitive patients.

The overall outcome of the assessment of the genotyping of the DUOX1 status in patient samples can be found in table 4.12. The full list of DNA samples showing genotype, phenotype and ethnicity can be found in the appendix (Tab. A4.1).

Table 4.12: Overall outcome of genotyping of DUOX1 in patient samples

Clinical diagnosis	Number of patients	Number of carriers of the DUOX1 variant	Number of non-white samples	Number of DUOX1 variant in non-white
MPE	39	0	0	0
AGEP	1	0	0	0
DRESS	43	3	14	3
SJS/TEN	26	3	11	2
CBZ tolerant	44	1	0	0

DRESS: Drug rash with eosinophilia and systemic symptoms, SJS: Steven Johnson Syndrome, TEN: toxic epidermal necrolysis, MPE: maculopapular exanthema

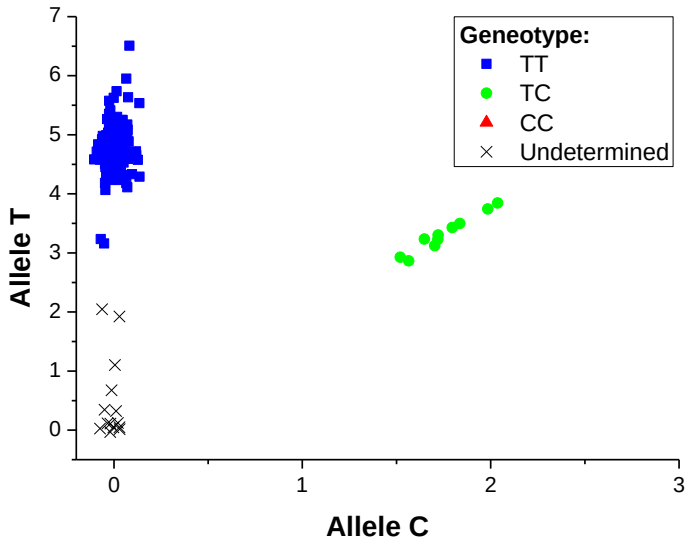

Figure 4.12: Results of real-time PCR genotyping for DUOX1

Scatter plot of fluorescence measured at the end of the real-time PCR for all 151 samples. Fluorescence was utilised to assess the genotype of SNP rs16939743 for each individual.

4.3.7 Statistical analysis of DUOX1 genotyping

The genotyping showed that overall 6.9% of the DRESS patients were carrying the rare variant of DUOX1. 11.5% of the SJS/TEN patients were carriers of the rare variant. The frequency for the combination of the severe, CBZ-induced hypersensitivity reactions (AGEP, DRESS and SJS/TEN) was 8.6%. The Fisher's exact test for the combined data of the genotyping delivered a p-value of 0.17 (one sided, 95% confidence interval: 0.46 – 190, see Tab. 4.13).

For non-white patients, genotyping for DUOX1 showed that 20% of the patients that had suffered from severe CBZ-induced hypersensitivity reactions (AGEP, DRESS and SJS/TEN) were carriers of the rare variant.

Table 4.13: Comparison of clinical outcome against DUOX1 status

		Pathological phenotype	
		Patient with severe DHRs	Tolerant individual
Genotyping	Carrier of DUOX1 variant	6	1
	Non-carrier of DUOX1 variant	64	43

4.4 Discussion

Studying drug-induced hypersensitivity reactions *in vitro* is difficult as there are only a few animal models available. The incidence rate of hypersensitivity in patients is low, making the collection of samples difficult. Hypersensitivity reactions result from genetic variability in pathways not involved in the pharmacological characteristics of the drug [74]. Toxicological studies such as the prediction of toxicity based on the structure of the compound, qHTS for endpoint toxicity and *in vivo* animal testing are currently used during the development of a new drug [75, 76]. The increased number of black box warnings and an increase in drug withdrawal show that these current methods would need to be improved to predict the occurrence of adverse drug reactions in general and hypersensitivity reactions in particular [77, 78].

Utilizing GWASs for *in vitro* toxicity testing allows high-throughput risk assessment compared to the traditional low-throughput screening used in animal testing. The challenge for developing computational toxicity testing methods is to detect the varying susceptibility of different individuals. Lock and colleagues established such a new method using a population-based cell culture model [34]. The method was capable of finding inter-individual variation in toxicity and also associations between the toxicity and genetic differences.

In the experiments conducted for the work of chapter 2, inter-individual variability in viability of PBMCs from CBZ-naïve healthy volunteers was observed. The hypothesis of the experiments conducted in this chapter was that this inter-individual variability is caused by genetic differences in the individuals. Additionally, it was assumed that these differences in the susceptibility to the toxic effect of the drug and its metabolites could play a vital role in the induction of hypersensitivity reactions. Therefore, the work in this chapter was performed to identify genetic association with the difference in viability and also to determine the role of these associations in

hypersensitive patients. The cytotoxicity caused by compounds and the resulting damage of cells could lead to the activation of naïve T cells through danger signals as described in the general introduction (see 1.5.4).

In the study by Furst and Uetrecht, it has been shown that CBZ and CBZE show no toxic effect, while 9-AC has been reported to cause toxicity *in vitro* [79]. The comparison of the EC10 from 2 replicates of the same cell line showed better reproducibility for 9-AC than CBZ and CBZE. Nevertheless for all 3 compounds used, cell lines more susceptible to the cytotoxic effect were found for each compound.

The comparison of the different groups in relation to gender or ethnicity did not reveal significant differences. This shows that the susceptibility to cytotoxicity of certain individuals is not gender or population specific. Rates for CBZ-induced hypersensitivity reactions are also the same in different populations and indeed different genders.

The advantage of immortalised lymphoblast cell lines is their expression of metabolising enzymes. Their expression of genes encoding metabolic enzymes is not as high as in liver cells but lymphoblastoid cell lines still contain most phase I and II enzymes [80]. In comparison with primary cells, which may derive from the tissue of interest, the use of immortalised lymphoblast cell lines comes with certain limitations. These include the inability to detect organ specific adverse effects, the lack of other environmental factors such as diet or co-exposure of other drugs, and cell-cell interactions including triggering of immune response. It was demonstrated however by Lock and colleagues that genotyping of lymphoblastoid cell lines in combination with qHTS strategies can predict the cytotoxicity of a compound *in vitro* and even accurately predict toxicity of toxins with similar cytotoxic mechanisms [34].

The GWAS revealed 14 SNPs with low p-values for higher susceptibility to the toxicity of the compounds. Some of these SNPs were found to be associated to a higher susceptibility to all 3 compounds used. None of the SNPs reached the predefined genome-wide significance level of $p < 1x10^{-8}$. Nevertheless, SNPs were found that reached the pre-set genome-wide

suggestive level ($p < 1x10^{-5}$). These SNPs therefore needed further investigation. The SNPs associated with a higher susceptibility to toxicity for more than one compound represent an interesting opportunity for further investigation.

Although a large number of lymphoblastoid cell lines (N=331) were screened, none of the SNPs investigated reached the predefined cut-off for genome-wide significance. A post hoc power analysis was performed using the G*Power software to estimate the power of the GWAS undertaken in this chapter [81]. The 331 samples gave an estimated power of 98% with $5x10^{-7}$ α error probability (corrected for multiple comparisons of 1 015 304 SNPs using the Bonferroni approach [55]), and was able to detect a 25% difference in cell viability between the lowest and highest end of the spectrum, which presents a medium sized effect based on Cohen's criteria (Fig. 4.13) [82]. Thus, our GWAS sample size of 331 was adequate to detect associations between SNPs and medium sized effects in viability. Considering that the variability in the cell viability might be a complex trait, it was estimated that approximately 1 818 cell lines would give a statistical power of 95% ($5x10^{-7}$ α error) to detect an approximate 10% difference in cell viability. Therefore, more lymphoblastoid cell lines from the 1000 genomes project and other sources could be screened to find associations between genetic makers and small variance in viability.

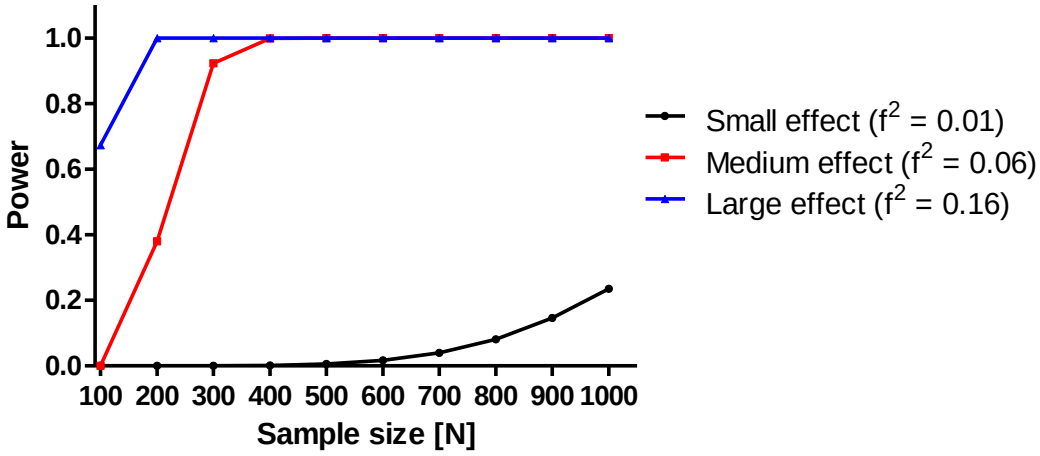

Figure 4.13: Post hoc power analysis for achieved power of GWAS

Power (1-β error probability; β error probability: not rejecting H_0 when H_0 is false) is shown as a function of the number of samples for small ($f^2 = 0.01 = 0.1^2$), medium ($f^2 = 0.06$), and large ($f^2 = 0.16$) effect size according to Cohen's criteria [82]. The f statistic for MANOVA was chosen and the sum of the concentrations (8) and covariates (14) was used as groups in the power calculation to allow the power estimation for MANCOVA [83]. The α error probability (rejection of H_0 when H_0 is true) was adjusted for multiple comparisons of 1 015 304 SNPs following the Bonferroni correction ($5x10^{-7}$) [55]; (number of predictors: 14, response variables 7).

Of the 14 SNPs found in the GWAS, rs16939743 the only functional SNP and also appeared plausible, therefore it was further investigated. The SNP was found to be associated with a higher rate of the cytotoxic effect of all three compounds. The MAF is reported by the 1000 Genome project to be 8% worldwide, but varies greatly amongst different ethnicities (19% Africa, 2% America, 14% Asia, and 1% Europe) [32]. It is located in the dual oxidase 1 (DUOX1) gene [68, 84], located on the long arm of chromosome 15 (15q15.3). The variant causes an amino acid exchange which leads to the missense mutation and gene product (p.I962T) [68]. DUOX1 is a member of the NADPH oxidase family [85]. It was shown that DUOX1 regulates the amount of reactive oxygen species in cells and thereby modulates cell signalling [86]. It can also generate hydrogen peroxide and by that plays a role in the activation of peroxidases involved in immune response [71, 72]. It

was shown that the redox signalling during the response of the innate immune system is DUOX1-mediated and that upon the detection of bacterial ligands such as lipopolysaccharides, stimulates the production of DUOX1. One study showed the involvement of DUOX1 in T cell signalling [73]. During the activation of T cell receptor (TCR), DUOX1 was found to mediate the signal. DUOX1 knockdown with small interfering RNA and small hairpin RNA led to the inhibition of TCR signalling and the production of cytokines.

The SNP rs16939743 has variable MAF across populations and was included in the GWAS as the worldwide MAF is 8%. Due to the low MAF in European populations, the SNP has not been included into the list of interrogated genetic markers for different GWAS chips. Therefore it was decided to validate this SNP in the samples of patients with CBZ-hypersensitivity from the Liverpool archive for several reasons:

- The population of patients is of diverse ethnic background, including patients from populations with relative high MAF (African and Asian).
- The SNP has potentially relevant functional significance, due to the role of DUOX1 in the immune response.
- Unpublished data from our group showed that certain samples generated high levels of hydrogen peroxide during the exposure to CBZ.

For validation of the finding from the GWAS, samples of CBZ treated patients were genotyped in order to assess their DUOX1 rs16939743 status.

The variant of DUOX1 was only found in one CBZ tolerant patient with European ancestry. In non-white patients that had developed CBZ-induced hypersensitivity syndromes, a higher percentage of carriers of the DUOX1 variant was found. 21.4% of the non-white patients that had suffered from DRESS and 18.2% of the patients that had suffered from SJS/TEN during their treatment with CBZ were carriers of the DUOX1 variant. Taken together, the frequency of DUOX1 in non-European with severe hypersensitivity is 20%, which is slightly higher than the MAF found in African populations (19%) [32]. The frequency for the combination of the severe,

CBZ-induced hypersensitivity reactions of all genotyped samples was 8.6% and the Fisher's exact test delivered a p-value of 0.17.

One of the limitations of the experiments conducted is that they lack the statistical power to detect the differences in SNP frequency among groups of patients of diverse ethnicity. For the different ethnicities the data had to be pooled as there were fewer samples included for each ethnicity. For further investigation, larger number of patients from non-European populations would be needed and ideally include CBZ-tolerant patients from the corresponding cohort.

In conclusion, the role of individual susceptibility to the toxicity of CBZ and two of its metabolites in drug hypersensitive patients has been analysed. Genetic association with the susceptibility was assessed utilising a novel approach derived from computational toxicology. This new approach combined the dose-response data from *in vitro* cytotoxicity screening with the genotyping data from the lymphoblastoid cell lines in a GWAS. Following this approach, possible genetic markers were discovered. To analyse the role of inter-individual variability in the viability of cells after exposure to the compounds during CBZ-induced hypersensitivity reactions, the genetic markers were assessed for biological plausibility and the most promising candidate, rs16939743, was analysed by genotyping hypersensitive patients. This new approach represents a promising model for further investigations of genetic associations in hypersensitivity reaction. It was also found that the analysed SNP rs16939743 could play an important role in non-European hypersensitive patients. In European patients who had suffered from CBZ-induced hypersensitivity, SNP rs16939743 was not detected. However, at this stage the role of the SNP in European patients cannot be excluded. Further investigations by genotyping more patients from various populations would need to be conducted.

4.5 References

1. Le Cleach, L., et al., *Blister fluid T lymphocytes during toxic epidermal necrolysis are functional cytotoxic cells which express human natural killer (NK) inhibitory receptors.* Clin Exp Immunol, 2000. **119**(1): p. 225-30.
2. Yawalkar, N., et al., *Infiltration of cytotoxic T cells in drug-induced cutaneous eruptions.* Clin Exp Allergy, 2000. **30**(6): p. 847-55.
3. Schmid, S., et al., *Acute generalized exanthematous pustulosis: role of cytotoxic T cells in pustule formation.* Am J Pathol, 2002. **161**(6): p. 2079-86.
4. Nassif, A., et al., *Toxic epidermal necrolysis: effector cells are drug-specific cytotoxic T cells.* J Allergy Clin Immunol, 2004. **114**(5): p. 1209-15.
5. Chung, W.H., et al., *Granulysin is a key mediator for disseminated keratinocyte death in Stevens-Johnson syndrome and toxic epidermal necrolysis.* Nat Med, 2008. **14**(12): p. 1343-50.
6. Nassif, A., et al., *Drug specific cytotoxic T-cells in the skin lesions of a patient with toxic epidermal necrolysis.* J Invest Dermatol, 2002. **118**(4): p. 728-33.
7. Kuechler, P.C., et al., *Cytotoxic mechanisms in different forms of T-cell-mediated drug allergies.* Allergy, 2004. **59**(6): p. 613-22.
8. Viard, I., et al., *Inhibition of toxic epidermal necrolysis by blockade of CD95 with human intravenous immunoglobulin.* Science, 1998. **282**(5388): p. 490-3.
9. Posadas, S.J., et al., *Delayed reactions to drugs show levels of perforin, granzyme B, and Fas-L to be related to disease severity.* J Allergy Clin Immunol, 2002. **109**(1): p. 155-61.
10. Rusyn, I. and G.P. Daston, *Computational toxicology: realizing the promise of the toxicity testing in the 21st century.* Environ Health Perspect, 2010. **118**(8): p. 1047-50.
11. Nigsch, F., et al., *Computational toxicology: an overview of the sources of data and of modelling methods.* Expert Opin Drug Metab Toxicol, 2009. **5**(1): p. 1-14.
12. Kavlock, R.J., et al., *Computational toxicology--a state of the science mini review.* Toxicol Sci, 2008. **103**(1): p. 14-27.
13. Gibb, S., *Toxicity testing in the 21st century: a vision and a strategy.* Reprod Toxicol, 2008. **25**(1): p. 136-8.
14. Reif, D.M., et al., *Endocrine profiling and prioritization of environmental chemicals using ToxCast data.* Environ Health Perspect, 2010. **118**(12): p. 1714-20.
15. Collins, F.S., G.M. Gray, and J.R. Bucher, *Toxicology. Transforming environmental health protection.* Science, 2008. **319**(5865): p. 906-7.
16. Martin, Y.C., J.L. Kofron, and L.M. Traphagen, *Do structurally similar molecules have similar biological activity?* J Med Chem, 2002. **45**(19): p. 4350-8.
17. Ashby, J. and R.W. Tennant, *Prediction of rodent carcinogenicity for 44 chemicals: results.* Mutagenesis, 1994. **9**(1): p. 7-15.
18. Marchant, C.A., K.A. Briggs, and A. Long, *In silico tools for sharing data and knowledge on toxicity and metabolism: derek for windows, meteor, and vitic.* Toxicol Mech Methods, 2008. **18**(2-3): p. 177-87.
19. Shukla, S.J., et al., *The future of toxicity testing: a focus on in vitro methods using a quantitative high-throughput screening platform.* Drug Discov Today, 2010. **15**(23-24): p. 997-1007.

20. Spitz, M.R. and M.L. Bondy, *The evolving discipline of molecular epidemiology of cancer.* Carcinogenesis, 2010. **31**(1): p. 127-34.
21. Risch, N. and K. Merikangas, *The future of genetic studies of complex human diseases.* Science, 1996. **273**(5281): p. 1516-7.
22. Livingston, R.J., et al., *Pattern of sequence variation across 213 environmental response genes.* Genome Res, 2004. **14**(10A): p. 1821-31.
23. Sedykh, A., et al., *Use of in vitro HTS-derived concentration-response data as biological descriptors improves the accuracy of QSAR models of in vivo toxicity.* Environ Health Perspect, 2011. **119**(3): p. 364-70.
24. Zhu, H., et al., *A novel two-step hierarchical quantitative structure-activity relationship modeling work flow for predicting acute toxicity of chemicals in rodents.* Environ Health Perspect, 2009. **117**(8): p. 1257-64.
25. Zhu, H., et al., *Use of cell viability assay data improves the prediction accuracy of conventional quantitative structure-activity relationship models of animal carcinogenicity.* Environ Health Perspect, 2008. **116**(4): p. 506-13.
26. Tong, W., et al., *Gaining Confidence on Molecular Classification through Consensus Modeling and Validation.* Toxicol Mech Methods, 2006. **16**(2-3): p. 59-68.
27. Martin, M.T., et al., *Impact of environmental chemicals on key transcription regulators and correlation to toxicity end points within EPA's ToxCast program.* Chem Res Toxicol, 2010. **23**(3): p. 578-90.
28. Xia, M., et al., *Identification of compounds that potentiate CREB signaling as possible enhancers of long-term memory.* Proc Natl Acad Sci U S A, 2009. **106**(7): p. 2412-7.
29. Rusyn, I., et al., *Predictive modeling of chemical hazard by integrating numerical descriptors of chemical structures and short-term toxicity assay data.* Toxicol Sci, 2012. **127**(1): p. 1-9.
30. Harrill, A.H., et al., *Mouse population-guided resequencing reveals that variants in CD44 contribute to acetaminophen-induced liver injury in humans.* Genome Res, 2009. **19**(9): p. 1507-15.
31. Rusyn, I., et al., *Toxicogenetics: population-based testing of drug and chemical safety in mouse models.* Pharmacogenomics, 2010. **11**(8): p. 1127-36.
32. Genomes Project, C., et al., *A map of human genome variation from population-scale sequencing.* Nature, 2010. **467**(7319): p. 1061-73.
33. Tosato, G. and J.I. Cohen, *Generation of Epstein-Barr Virus (EBV)-immortalized B cell lines.* Curr Protoc Immunol, 2007. **Chapter 7**: p. Unit 7 22.
34. Lock, E.F., et al., *Quantitative high-throughput screening for chemical toxicity in a population-based in vitro model.* Toxicol Sci, 2012. **126**(2): p. 578-88.
35. Cho, M.H., et al., *A bioluminescent cytotoxicity assay for assessment of membrane integrity using a proteolytic biomarker.* Toxicol In Vitro, 2008. **22**(4): p. 1099-106.
36. Lappalainen, T., et al., *Transcriptome and genome sequencing uncovers functional variation in humans.* Nature, 2013. **501**(7468): p. 506-11.
37. Choy, E., et al., *Genetic analysis of human traits in vitro: drug response and gene expression in lymphoblastoid cell lines.* PLoS Genet, 2008. **4**(11): p. e1000287.
38. Behr, E.R., et al., *The International Serious Adverse Events Consortium (iSAEC) phenotype standardization project for drug-induced torsades de pointes.* Eur Heart J, 2013. **34**(26): p. 1958-63.
39. Pirmohamed, M., et al., *Phenotype standardization for immune-mediated drug-induced skin injury.* Clin Pharmacol Ther, 2011. **89**(6): p. 896-901.

40. Leist, M., et al., *Intracellular adenosine triphosphate (ATP) concentration: a switch in the decision between apoptosis and necrosis.* J Exp Med, 1997. **185**(8): p. 1481-6.
41. Xia, M., et al., *Compound cytotoxicity profiling using quantitative high-throughput screening.* Environ Health Perspect, 2008. **116**(3): p. 284-91.
42. Ward, L.D. and M. Kellis, *HaploReg: a resource for exploring chromatin states, conservation, and regulatory motif alterations within sets of genetically linked variants.* Nucleic Acids Res, 2012. **40**(Database issue): p. D930-4.
43. Livak, K.J., *Allelic discrimination using fluorogenic probes and the 5' nuclease assay.* Genet Anal, 1999. **14**(5-6): p. 143-9.
44. McGuigan, F.E. and S.H. Ralston, *Single nucleotide polymorphism detection: allelic discrimination using TaqMan.* Psychiatr Genet, 2002. **12**(3): p. 133-6.
45. Afonina, I., et al., *Efficient priming of PCR with short oligonucleotides conjugated to a minor groove binder.* Nucleic Acids Res, 1997. **25**(13): p. 2657-60.
46. Livak, K.J., et al., *Oligonucleotides with fluorescent dyes at opposite ends provide a quenched probe system useful for detecting PCR product and nucleic acid hybridization.* PCR Methods Appl, 1995. **4**(6): p. 357-62.
47. Kutyavin, I.V., et al., *3'-minor groove binder-DNA probes increase sequence specificity at PCR extension temperatures.* Nucleic Acids Res, 2000. **28**(2): p. 655-61.
48. Kruskal, W.H. and W.A. Wallis, *Use of Ranks in One-Criterion Variance Analysis.* Journal of the American Statistical Association, 1952. **47**(260): p. 583-621.
49. Johnson, W.E., C. Li, and A. Rabinovic, *Adjusting batch effects in microarray expression data using empirical Bayes methods.* Biostatistics, 2007. **8**(1): p. 118-27.
50. Benjamini, Y. and D. Yekutieli, *The control of the false discovery rate in multiple testing under dependency.* Annals of Statistics, 2001. **29**(4): p. 1165-1188.
51. Brown, C.C., et al., *Multivariate methods and software for association mapping in dose-response genome-wide association studies.* BioData Min, 2012. **5**(1): p. 21.
52. Crow, J.F., *Eighty years ago: the beginnings of population genetics.* Genetics, 1988. **119**(3): p. 473-6.
53. Wellek, S., *Tests for establishing compatibility of an observed genotype distribution with Hardy-Weinberg equilibrium in the case of a biallelic locus.* Biometrics, 2004. **60**(3): p. 694-703.
54. Pruim, R.J., et al., *LocusZoom: regional visualization of genome-wide association scan results.* Bioinformatics, 2010. **26**(18): p. 2336-7.
55. Dunn, O.J., *Multiple Comparisons among Means.* Journal of the American Statistical Association, 1961. **56**(293): p. 52-&.
56. International HapMap, C., *A haplotype map of the human genome.* Nature, 2005. **437**(7063): p. 1299-320.
57. Dudbridge, F. and A. Gusnanto, *Estimation of significance thresholds for genomewide association scans.* Genet Epidemiol, 2008. **32**(3): p. 227-34.
58. Bishop, D.T., et al., *Genome-wide association study identifies three loci associated with melanoma risk.* Nat Genet, 2009. **41**(8): p. 920-5.
59. Sabatti, C., et al., *Genome-wide association analysis of metabolic traits in a birth cohort from a founder population.* Nat Genet, 2009. **41**(1): p. 35-46.
60. Vasan, R.S., et al., *Genetic variants associated with cardiac structure and function: a meta-analysis and replication of genome-wide association data.* JAMA, 2009. **302**(2): p. 168-78.

61. Fisher, R.A., *On the interpretation of x(2) from contingency tables, and the calculation of P.* Journal of the Royal Statistical Society, 1922. **85**: p. 87-94.
62. National Research Council Committee on Improving Risk Analysis Approaches Used by the, U.S.E., in *Science and Decisions: Advancing Risk Assessment*. 2009, National Academies Press (US)

63. Feng, Q., et al., *Human S-adenosylhomocysteine hydrolase: common gene sequence variation and functional genomic characterization.* J Neurochem, 2009. **110**(6): p. 1806-17.
64. Bayerer, B., et al., *Genomic variations and transcriptional regulation of the human mu-opioid receptor gene.* Eur J Pain, 2007. **11**(4): p. 421-7.
65. Fishman, D., et al., *The effect of novel polymorphisms in the interleukin-6 (IL-6) gene on IL-6 transcription and plasma IL-6 levels, and an association with systemic-onset juvenile chronic arthritis.* J Clin Invest, 1998. **102**(7): p. 1369-76.
66. Hayashi, S., J. Watanabe, and K. Kawajiri, *Genetic polymorphisms in the 5'-flanking region change transcriptional regulation of the human cytochrome P450IIE1 gene.* J Biochem, 1991. **110**(4): p. 559-65.
67. Wang, G.S. and T.A. Cooper, *Splicing in disease: disruption of the splicing code and the decoding machinery.* Nat Rev Genet, 2007. **8**(10): p. 749-61.
68. Rigutto, S., et al., *Activation of dual oxidases Duox1 and Duox2: differential regulation mediated by camp-dependent protein kinase and protein kinase C-dependent phosphorylation.* J Biol Chem, 2009. **284**(11): p. 6725-34.
69. Strachan, T. and A.P. Read, *Human Molecular Genetics*. 2nd ed. 1999, New York: Wiley-Liss.
70. McCormack, M., et al., *HLA-A*3101 and carbamazepine-induced hypersensitivity reactions in Europeans.* N Engl J Med, 2011. **364**(12): p. 1134-43.
71. Wang, L., et al., *Lipid raft-dependent activation of dual oxidase 1/H2O2/NF-kappaB pathway in bronchial epithelial cells.* Am J Physiol Cell Physiol, 2011. **301**(1): p. C171-80.
72. Rada, B. and T.L. Leto, *Characterization of hydrogen peroxide production by Duox in bronchial epithelial cells exposed to Pseudomonas aeruginosa.* FEBS Lett, 2010. **584**(5): p. 917-22.
73. Kwon, J., et al., *The nonphagocytic NADPH oxidase Duox1 mediates a positive feedback loop during T cell receptor signaling.* Sci Signal, 2010. **3**(133): p. ra59.
74. Park, B.K., M. Pirmohamed, and N.R. Kitteringham, *Idiosyncratic drug reactions: a mechanistic evaluation of risk factors.* Br J Clin Pharmacol, 1992. **34**(5): p. 377-95.
75. Cui, Y. and R.S. Paules, *Use of transcriptomics in understanding mechanisms of drug-induced toxicity.* Pharmacogenomics, 2010. **11**(4): p. 573-85.
76. Ekins, S., Y. Nikolsky, and T. Nikolskaya, *Techniques: application of systems biology to absorption, distribution, metabolism, excretion and toxicity.* Trends Pharmacol Sci, 2005. **26**(4): p. 202-9.
77. Lasser, K.E., et al., *Timing of new black box warnings and withdrawals for prescription medications.* JAMA, 2002. **287**(17): p. 2215-20.
78. Adkinson, N.F., Jr., et al., *Task force report: future research needs for the prevention and management of immune-mediated drug hypersensitivity reactions.* J Allergy Clin Immunol, 2002. **109**(3): p. S461-78.

79. Furst, S.M. and J.P. Uetrecht, *The effect of carbamazepine and its reactive metabolite, 9-acridine carboxaldehyde, on immune cell function in vitro.* Int J Immunopharmacol, 1995. **17**(5): p. 445-52.
80. Siest, G., et al., *Transcription factor and drug-metabolizing enzyme gene expression in lymphocytes from healthy human subjects.* Drug Metab Dispos, 2008. **36**(1): p. 182-9.
81. Faul, F., et al., *G*Power 3: a flexible statistical power analysis program for the social, behavioral, and biomedical sciences.* Behav Res Methods, 2007. **39**(2): p. 175-91.
82. Cohen, J., *Statistical power analysis for the behavioral sciences*. 2nd ed. 1988, Hillsdale, N.J.: L. Erlbaum Associates. xxi, 567 p.
83. Dattalo, P., *Determining sample size : balancing power, precision, and practicality*. Pocket guides to social work research methods. 2008, Oxford ; New York: Oxford University Press. 167 p.
84. Zody, M.C., et al., *Analysis of the DNA sequence and duplication history of human chromosome 15.* Nature, 2006. **440**(7084): p. 671-5.
85. De Deken, X., et al., *Cloning of two human thyroid cDNAs encoding new members of the NADPH oxidase family.* J Biol Chem, 2000. **275**(30): p. 23227-33.
86. Pettigrew, C.A., J.S. Clerkin, and T.G. Cotter, *DUOX enzyme activity promotes AKT signalling in prostate cancer cells.* Anticancer Res, 2012. **32**(12): p. 5175-81.

Chapter 5
Validation of new SSP-PCR HLA-A*31:01 typing methods

5.1 Introduction

Human leucocyte antigens (HLAs) play an important role in the predisposing to diseases caused by the immune system. For example certain drug-induced hypersensitivity reactions are also associated with particular HLA alleles [1, 2].

As mentioned in the general introduction (see section 1.4), the MHC is located on chromosome 6, a highly polymorphic region of the human genome. Through efforts from various research groups, this part of the genome was amongst the first genomic regions to be fully sequenced. The MHC spans over 3.6 megabase pairs accommodating 224 gene loci. About 60% of those are considered to be expressed and 40% are estimated to play a role in the immune system. A large number of HLA alleles have been characterised [3].

Initially, HLA typing was performed using serological typing [5]. Since then the typing methods have evolved dramatically. The first vast improvement was the application of PCR methods for typing. The development of next generation sequencing technologies was the second breakthrough, introducing the possibility of sequence-based HLA typing. Following these advances, the number of known HLA alleles has increased exponentially (see Fig. 5.1).

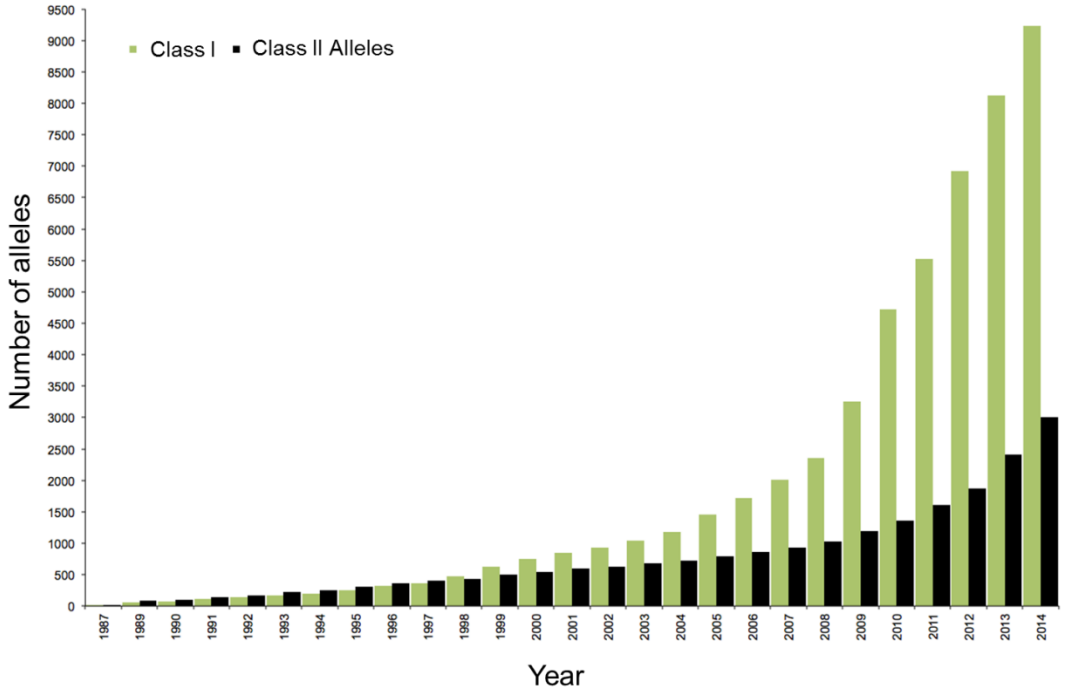

Figure 5.1: Known HLA alleles by year [6]

The three most commonly used PCR-based HLA typing methods are:

1. PCR utilising sequence base typing (SBT-PCR)
2. PCR utilising sequence-specific oligonucleotides (SSO-PCR)
3. PCR utilising sequence-specific primers (SSP-PCR)

SBT-PCR for HLA typing gives the highest possible resolution compared to the other two methods, for which resolution is limited by the oligonucleotides or primers used. It also allows for the detection of undiscovered HLA alleles. PCR sequencing HLA typing methods have been described using a generic PCR amplification system [7-9]. Advances in next generation sequencing for DNA have made this method the current gold standard for HLA typing [10-12]. This method is very labour and time intensive and requires special equipment, and specially trained personnel. Therefore such HLA typing is generally performed by specialised laboratories.

SSO-PCR HLA typing involves PCR to amplify the sequence from the HLA locus to be tested. This PCR product is then hybridised against a panel of oligonucleotide probes, which have complementary sequences of stretches containing known polymorphisms of the HLA alleles in question [13]. It is a good method for high-throughput HLA typing as many samples can be processed in parallel. SSO-PCR HLA typing is quite labour and time intensive.

The most commonly used method in clinical immunology laboratories for HLA typing is the SSP-PCR approach. SSP-PCR HLA typing uses multiple PCR primer pairs that target only specific DNA sequences. This annealing therefore requires the presence of certain SNPs [14, 15]. This is achieved by designing the primers that are complementary to the sequence for the SNP at the 3' end of the primer. The method is the fastest HLA typing method available with gel electrophoresis being the rate-limiting step. It utilises standard equipment found in a biological laboratories, such as thermal cyclers, gel electrophoresis facilities and ultraviolet (UV) transilluminator. The costs for the assay can be kept low with self-designed and optimised primers. The limitation of this SSP-PCR HLA typing is that the first PCR can only provide low- to medium-resolution results, depending on the number of different primers used. The second PCR can then achieve high-resolution to 8 digits for some HLA alleles.

The underlying molecular mechanism of HLA-associated hypersensitivity reactions are complex. The association of abacavir-induced hypersensitivity reactions and HLA-B*57:01 was first reported 2002 [1, 16] but the exact molecular mechanism was only discovered about a decade later [17-20]. Abacavir interacts with residues of amino acids within the binding groove of HLA-B*57:01 and thus changes the configuration of the grove, resulting in the presentation of altered self-peptides by HLA-B*57:01. This presentation of altered self-peptides leads to the activation of T cells (see general introduction 1.5.3). HLA screening before prescription of abacavir significantly reduces the incidence of hypersensitivity reactions [21, 22].

For CBZ, recent studies have demonstrated an association between an increased risk of severe ADRs and HLA alleles [23, 24]. In Asian populations a strong association was found between HLA-B*15:02 and SJS/TEN [25-30]. In Caucasian and Japanese populations, a similar association between HLA-A*31:01 and CBZ-induced hypersensitivity has been found [31, 32]. Other known associations of CBZ-induced hypersensitivity reactions and HLA alleles can be found in table 5.1.

As most of these severe ADRs are otherwise unpredictable, the information about the HLA status is the only risk marker for patients treated with CBZ. The FDA and the UK regulatory agency recommend screening patients with Asian ancestry for HLA-B*15:02 statues before administering the CBZ [33, 34], while the association with HLA-A*31:01 is provided for information in the label.

It is therefore important to develop new reliable assays, which can be used in clinical practice before the start of CBZ treatment. Such assays need to improve the safety of the patient, be cost-effective and have a short turnaround time for the results. For the reduction of the time to result, assays which are easy to use and robust would be preferable as this allows testing in hospitals.

The aim of this chapter was to validate two new SSP-PCR HLA typing methods. Both methods utilise one pair of specific primers to assess whether or not the individual is a carrier of the HLA-A*31:01 allele.

Table 5.1: Overview of HLA alleles found associated with CBZ-induced hypersensitivity reaction

HLA allele	Ethnicity	Clinical manifestation	Reference
B*15:02	Han Chinese	SJS/TEN	[26]
	Malaysian, Chinese	SJS/TEN	[30]
	Thai	SJS/TEN	[27]
	Diverse	SJS/TEN	[35]
A*31:01	European	MPE, DRESS, SJS/TEN	[31, 35]
	Han Chinese	MPE	[26]
	Japanese	DRESS, SJS/TEN	[36]
	Korean	DRESS	[29]
	Diverse	MPE, DRESS	[35]
A*02:01	Han Chinese	MPE	[37]
B*15:11	Korean	SJS	[29]
B*58:01	Han Chinese	MPE	[37]
DRB*03:01	Han Chinese	MPE	[37]
DRB*14:05	Han Chinese	MPE	[37]

DRESS: Drug rash with eosinophilia and systemic symptoms, SJS: Steven Johnson Syndrome, TEN: toxic epidermal necrolysis, MPE: maculopapular exanthema

5.2 Material and Methods

5.2.1 Samples

347 DNA samples from the DNA archive in Liverpool, obtained from patients that had received CBZ treatment were used in these experiments. The samples were obtained from 62 patients that had developed CBZ-induced hypersensitivity reactions and from 285 healthy volunteers.

5.2.2 HLA typing

For the validation of the two new methods, the HLA type of the samples used had to be determined by the currently most reliable methods. Therefore the current gold standard, high-resolution, SBT-PCR HLA typing as well as the proxy SNP typing were compared with the newly developed methods to be validated.

5.2.2.1 HLA high-resolution genotyping

The DNA of 280 patients was isolated from 10 ml venous blood using magnetic separation (Chemagen, Baesweiler, Germany). The DNA was genotyped using high-resolution, sequence based HLA-A typing performed in the Histogenetics laboratory (Histogenetics, New York, USA). The typing was performed using SBT-PCR. The sequencing primers were produced for locus- and group-specific amplification, especially for exon 2 and 3 of HLA-A [38]. 24 of these samples were from patients that had developed hypersensitivity reactions and 256 were from healthy volunteers [39].

5.2.2.2 Proxy SNP HLA typing

Genotyping for the rs1061235 SNP for 73 samples was performed by KBioscience. Complete linkage disequilibrium (r^2=1) for this SNP and HLA-A*31:01 allele had been shown previously in individuals with European ancestry [40]. The genotyping was performed by KBioscience utilising the SSP-PCR method. The primers used for the PCR are labelled with fluorescence resonant energy transfer (FRET) molecules, allowing the discrimination between two alleles in the same sample [41]. 44 of the 73 DNA samples were obtained from patients that had suffered CBZ-induced hypersensitivity reactions and 29 derived from healthy volunteers.

*5.2.2.3 SSPGo HLA-A*31 Identification kit from Biofortuna*

The primers for the SSP-PCR were designed to align only at the specific sequence. It is based on the principle that only a complete match at the 3' terminals leads to the amplification while the mismatch does not yield amplification products [42]. This approach is also referred to as Allele Specific Amplification as the reaction only occurs when the DNA material includes that particular SNP.

The SSPGo HLA-A*31 Identification kit from Biofortuna was designed to assess the HLA-A*31:01 status in patients. The design of the primer was not revealed by the company. The kit comes in 96 well plates. Each well contains the dried mix of lyophilised primers, polymerase, dNTPs and buffer. Two sets of primers were included necessary for HLA typing as well as primers for an internal control gene. The internal control allows for detection of intrinsic problems with the DNA sample.

The experiments were performed following the manufacturers protocol [43].

The SSP-PCR was performed in a thermal cycler (Veriti 96 Well Thermal Cycler, Applied Biosystems, Paisley, UK). 10 ng of sample DNA were added to each well containing the dried mix for the SSP-PCR.

The SSP-PCR was initiated at 94°C for 5 min. Following this, 10 cycles with the following parameters were performed: denaturing at 96°C for 15 s, annealing at 66°C for 50 s, and extending at 72°C for 30s. These 10 cycles were followed by 20 cycles with the setting: denaturing at 96°C for 15s, annealing at 64°C for 50 s, and extending at 72°C for 30 s. The samples were cooled to 15°C.

The SSP-PCR product was loaded on 2% agarose (Sigma Aldrich Co, Poole, UK) gel containing 0.5 µg/ml ethidium bromide (Sigma Aldrich). The electrophoresis was done for 20 min at 10 V/cm (PowerPac^{TM} Basic, Bio-Rad Laboratories Ltd., Hertfordshire, UK). Pictures of the gel were taken under UV light (GelVue, Syngene, Cambridge, UK) and interpreted.

*5.2.2.4 HLA-A*31:01 SSP genotyping*

An HLA typing method developed in the laboratory of Mary Carrington of the National Cancer Institute in Frederick (Maryland, USA) was also validated. This is a wet lab technique using side specific primers for the amplification of genomic DNA (SSP-PCR HLA typing method) [31].

Primer design:

Forward primer: gatagagcaggagaggcct

Reverse primer: agcgcaggtcctcgttcaa

The PCR was performed according to an optimised protocol. The difference between the original and the optimised protocol were: 4 µl of DNA were used instead of 2 µl, 0.5 µl instead of 0.2 µl of the dNTP mix and 0.5 µl instead of 0.125 µl of polymerase were used for the master mix of each sample. Because of the resulting additional volume, the amount of DNase-free water added was reduced to 13.5 µl instead of 16.175µl. In addition the last set of cycles was increased from 4 cycles to 9 cycles.

The SSP-PCR was performed in 96-well plate format.

A PCR master mix for all samples was prepared (see Tab. 5.2).

Table 5.2: Master mix for HLA*A-31:01 SSP genotyping

		per sample [µl]:
GoTaq buffer	1x	2.5
$MgCl_2$	25 mM	1.5
dNTPs	10 mM / dNTP	0.5
Forward primer	20 µM	1.25
Reverse primer	20 µM	1.25
Polymerase	1 u	0.5
DNase-free water	add to 21 µl	13.5

To 4µl of the DNA sample (20 ng/µl), master mix (21µl) was added, giving a reaction volume of 25 µl. The PCR was conducted in a thermal cycler (Veriti 96 Well Thermal Cycler).

The PCR was initiated at 95°C for 3 min. 5 cycles with the following parameters were performed: denaturing at 95°C for 15 s, annealing at 70°C for 15 s, and extending at 72°C for 30s. These 5 cycles were followed by 21 cycles with the setting: denaturing at 95°C for 15s, annealing at 65°C for 15 s, and extending at 72°C for 30 s. The last 9 cycles had the following settings: denaturing at 95°C for 15s, annealing at 55°C for 1 min, and extending at 72°C for 2 min. After the last cycles the samples were kept at 72°C for 7 min before being cooled to 4°C.

After the SSP-PCR, the product was loaded on 1.5% agarose gel containing 0.5 µg/ml ethidium bromide. The electrophoresis was conducted at 120 V (PowerPac™ Basic). Pictures of the gel were taken under transilluminator (GelVue) and interpreted.

5.2.3 Statistical analysis

HLA genotyping data from the different methods were compared using the Fisher's exact test [44].

The positive predictive value was calculated with the following formula:

$$\text{Positive predictive value} = \frac{\sum \text{True positive}}{\sum \text{Test outcome positive}}$$

The negative predictive value was calculated using following formula:

$$\text{Negative predictive value} = \frac{\sum \text{True negative}}{\sum \text{Test outcome negative}}$$

The accuracy was determined according to the following formula:

$$\text{Accuracy} = \frac{\sum \text{True positive} + \sum \text{True negative}}{\sum \text{Total population}}$$

5.3 Results

In these experiments the accuracy of different SSP-PCR methods was validated. To achieve this, DNA samples from 347 individuals, were used. Before the utilisation of the samples, the HLA-A*31:01 status had to be determined, using the current gold standard.

High-resolution HLA typing by Histogenetics was performed for 280 participants. Of those, 32 (11.4%) individuals were positive for the HLA-A*31:01 allele. For one sample the HLA typing failed. The remaining 247 (88.2%) samples were found to be negative for HLA-A*31:01.

The proxy SNP genotyping by KBioscience was performed for 73 individuals. Out of these, 9 (12.3%) individuals were carriers of the HLA-A*31:01 allele while the remaining 64 (87.7%) were from individuals not carrying this allele.

The HLA types for 6 samples had been determined by both methods. The results of these samples were compared to each other (see Tab. 5.3). The false negative result was from a patient with one parent of Thai origin who carried the HLA-A*11:33, one of the two HLA alleles with high similarity to A*31:01 (see Fig. 5.3).

Table 5.3: Comparison of the high-resolution HLA typing against proxy SNP genotyping

		High-resolution HLA typing	
		Carrier of HLA-A*31:01 allele	Non-carrier of HLA-A*31:01 allele
Proxy SNP genotyping	Carrier of HLA-A*31:01 allele	3	1
	Non-carrier of HLA-A*31:01 allele	0	2

```
A*31:01:02 GCTCCCA CTCCATGAGG TATTTCACCA CATCCGTGTC CCGGCCCGGC CGCGGGGAGC CCCGCTTCAT CGCCGTGGGC TACGTGGACG ACACGCAGTT
A*02:32N   ----T-- ---------- ------TT-- ---------- ---------- ---------- ---------- ---A------ ---------- ----------
A*11:33:02 ------- ---------- ------TA-- -C-------- ---------- ---------- ---------- ---------- ---------- ----------

A*31:01:02 CGTGCGGTTC GACAGCGACG CCGCGAGCCA GAGGATGGAG CCGCGGGCGC CGTGGATAGA GCAGGAGAGG CCTGAGTATT GGGACCAGGA GACACGGAAT
A*02:32N   ---------- ---------- ---------- ---------- ---------- ---------- -------G-T --G------- -----GG--- ---------A
A*11:33:02 ---------- ---------- ---------- ---------- ---------- ---------- -------G-- --G------- ---------- ----------

A*31:01:02 GTGAAGGCCC ACTCACAGAT TGACCGAGTG GACCTGGGGA CCCTGCGCGG CTACTACAAC CAGAGCGAGG CCG|GTTCTCA CACCATCCAG ATGATGTATG
A*02:32N   ---------- ---------C -C-------- ---------- ---------- ---------- ---------- ---|------- ----G----- -G--------
A*11:33:02 ---------- -G-------C ---------- ---------- ---------- ---------- ---------- A--|------- ---------- --A-------

A*31:01:02 GCTGCGACGT GGGGTCGGAC GGGCGCTTCC TCCGCGGGTA CCAGCAGGAC GCCTACGACG GCAAGGATTA CATCGCCTTG AACGAGGACC TGCGCTCTTG
A*02:32N   ---------- ---------- T--------- ---------- ---C---T-- ---------- ---------- -------C-- --A------- ----------
A*11:33:02 ---------- ----C----- ---------- ---------- --G------- ---------- ---------- -------C-- ---------- ----------

A*31:01:02 GACCGCGGCG GACATGGCGG CTCAGATCAC CCAGCGCAAG TGGGAGGCGG CCCGTGTGGC GGAGCAGTTG AGAGCCTACC TGGAGGGCAC GTGCGTGGAG
A*02:32N   ---------- --------A- --T---C--- -A---A---- ---------- ---A------ ---------- ---------- ---------- ----------
A*11:33:02 ---------- --------A- ---------- ---------- ---------- ---A--C--- -------CA- ---------- --------CG ----------

A*31:01:02 TGGCTCCGCA GATACCTGGA GAACGGGAAG GAGACGCTGC AGCGCACGG
A*02:32N   ---------- ---------- ---------- ---------- ---------
A*11:33:02 ---------- ---------- ---------- ---------- ---------
```

Figure 5.3: Sequence alignment of HLA*A-31:01:02, HLA*A-02:32N and HLA*A-11:33:01

The HLA typing showed that in total out of the 347 genotyped individuals, 37 (10.7%) were carriers of HLA*A-31:01 allele.

5.3.1 Validation of SSPGo HLA-A*31 Identification kit

For the validation of the SSP-PCR kit from Biofortuna 347 samples were utilised. Two plates were excluded because of the poor call rate; in one plate, 94 (98%) and in the other 64 (67%) samples could not be genotyped because the intrinsic controls did not work. Because of the high failure rate, systematic issues were assumed to be the underlying reason.

272 samples were included for further analysis. The internal control of the SSPGo HLA-A*31 identification kit from Biofortuna showed that the PCR had not worked for 35 (13.1%) samples. All 35 samples were from patients not carrying the HLA*A-31:01 allele.

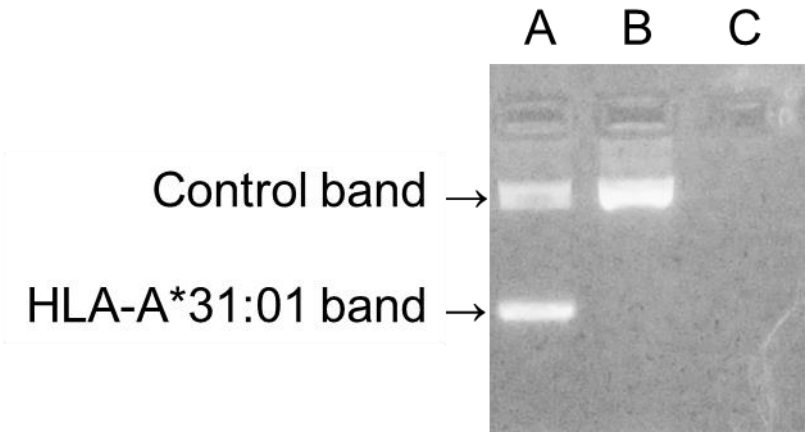

Figure 5.4: Outcome of SSPGo HLA-A*31 Identification kit from Biofortuna

The picture shows an agarose gel under UV light after electrophoresis. The direction of the electrophoresis was from the top down. The sample **A** is from an individual carrying the HLA-A*31:01 allele. The PCR product shows two distinct bands. The upper one is the control band and the lower one shows the presence of the HLA-A*31:01 allele in the DNA sample. Sample **B** is from an individual negative for the HLA-A*31:01 allele. The sample shows only one distinct band, the control band. The PCR for sample **C** did not work. Therefore no bands are visible under the UV light.

To evaluate the reliability, the results obtained from the SSPGo HLA-A*31 Identification kit were compared to the results from the high-resolution, sequence based HLA typing and HLA-A*31:01 proxy SNP genotyping. The 35 samples, for which the SSP-PCR failed, were excluded from this analysis.

For the 193 samples that were typed with the high-resolution, sequence based typing and included in the evaluation, the assay was in exact accordance with the current gold standard (see Tab. 5.4). The positive predictive value, the negative predictive value, and the accuracy of the kit from Biofortuna were found to be 100%.

Table 5.4: Comparison of the high-resolution HLA typing against SSPGo HLA-A*31 Identification kit

		High-resolution HLA typing	
		Carrier of HLA-A*31:01 allele	Non-carrier of HLA-A*31:01 allele
Kit from Biofortuna	Carrier of HLA-A*31:01 allele	31	0
	Non-carrier of HLA-A*31:01 allele	0	162

For the 44 samples typed with proxy SNP genotyping, the SSPGo kit produced two false negative results (see Tab. 5.5). The positive predictive value was 100% but the negative predictive value was 95%.

Table 5.5: Comparison of the results from proxy SNP genotyping against the SSPGo kit

		Proxy SNP genotyping	
		Carrier of HLA-A*31:01 allele	Non-carrier of HLA-A*31:01 allele
Kit from Biofortuna	Carrier of HLA-A*31:01 allele	7	0
	Non-carrier of HLA-A*31:01 allele	2	35

5.3.2 Validation of HLA-A*31:01 SSP genotyping

For the validation of the HLA-A*31:01 SSP genotyping following the Mary Carrington's protocol, 77 samples were used. 3 were excluded as the data obtained for the samples were inconclusive. These samples showed a band for the HLA-A*31:01 allele in one experiment, but failed to replicate in a duplicate or vice versa.

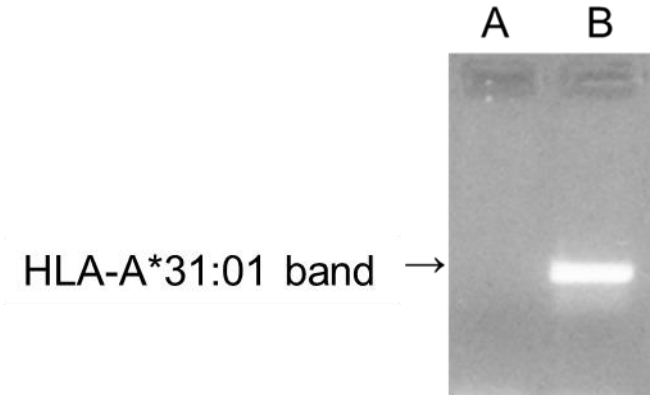

Figure 5.5: Outcome of HLA-A*31:01 SSP genotyping

The picture shows an example of an agarose gel under UV light after electrophoresis. The direction of the electrophoresis was from top down. The sample **A** is from a patient not carrying the HLA-A*31:01 allele. No band can be visualised. Sample **B** is from a patient carrying the HLA-A*31:01 allele. The PCR product shows one distinct band for the HLA-A*31:01 allele PCR product.

The results obtained from SSP-PCR HLA-A*31:01 typing were compared with the results from the high-resolution, sequence based HLA typing.

For the 73 samples that were typed with the high-resolution, sequence based typing, 3 (4.1%) true positives and 60 (82.2%) true negatives were found by the SSP-PCR. The SSP-PCR also gave one (1.4%) false negative and 9 (12.3%) false positive results (see Tab. 5.6). The positive predictive value was 25% and the negative predictive value was 98% for the HLA-A*31:01 SSP genotyping. Therefore the accuracy of the SSP-PCR was 86.3%.

Table 5.6: Comparison of the high-resolution HLA typing against SSP-PCR HLA-A typing after Mary Carrington

		High-resolution HLA typing	
		Carrier of HLA-A*31:01 allele	Non-carrier of HLA-A*31:01 allele
SSP-PCR after Mary Carrington	Carrier of HLA-A*31:01 allele	3	9
	Non-carrier of HLA-A*31:01 allele	1	60

For the comparison of the SSP-PCR against the proxy SNP genotyping, there was only one sample available. This sample was found HLA-A*31:01 positive from both SSP-PCR HLA typing and proxy SNP HLA typing.

5.4 Discussion

An increasing number of studies show associations between HLA alleles and immune-mediated drug-induced hypersensitivity reactions [2, 16, 25, 45]. The most renowned example is the association of HLA-B*57:01 with hypersensitivity to abacavir, an antiretroviral drug used for the treatment of human immunodeficiency virus infection (HIV) [1, 22, 46]. It is recommended by FDA guidelines to test for HLA-B*57:01 before prescription. This proved to be cost-effective and reduced the incidence of abacavir-induced hypersensitivity [21, 47].

Information on the association between CBZ-induced hypersensitivity reactions and HLA-A*31:01 in Europeans [31] and Japanese [32] is included in the label of the drug. For the association between HLA-B*15:02 and CBZ-induced hypersensitivity reactions in Asians [25, 26], the FDA and the UK regulatory agency recommend screening patients with Asian ancestry for their HLA-B*15:02 status before administering CBZ [33, 34].

HLA genes are the most polymorphic genes in the human genome. Different HLA types can share similarities and only differ in one SNP. For an exact assessment of the HLA type, high-resolution, sequence based HLA typing methods are required. These methods are expensive and require specialised laboratories with specially trained personnel. The methods are also time intensive. The time until the results are obtained and the treatment of a patient can be started can take up to several days. Therefore their utilisation in clinical practice is currently not feasible. In the attempt to tackle these issues, assays have been developed for the HLA-A*31:01 and HLA-B*15:02 typing [48, 49]. These assays determine whether or not the patient is a carrier of the HLA risk allele. Therefore they utilise one set of primers in addition to a set of primers for a housekeeping gene.

The SSPGo HLA-A*31 Identification kit from Biofortuna and the SSP-PCR protocol developed by the group of Mary Carrington follow similar approaches as described for B*15:02. These assays were validated to

assess their accuracy compared with the current gold standard and their practicality for clinical practice.

The SSPGo HLA-A*31 Identification kit from Biofortuna showed results that were as reliable as the current gold standard. It even distinguished between HLA-A*31:01 and the two very similar alleles, HLA-A*02:32 and HLA-A*11:33. This distinction can currently be only achieved using high-resolution sequence based HLA typing.

The SSPGo HLA-A*31 Identification kit produced two false negatives when compared with the proxy SNP genotyping. Proxy SNP genotyping is not 100% accurate, although this SNP has been reported to be in complete linkage disequilibrium with HLA-A*31:01 in Europeans [40]. One of the “false negatives” found in the comparison between SSPGo HLA-A*31 and the proxy SNP genotyping has been actually incorrectly assigned A*31:01 genotype by the proxy SNP genotyping compared to the HLA high-resolution genotyping (see Tab 5.3). The sample was from a patient with one parent of Thai origin. The second sample with discordant results is of white ethnicity and should undergo genotyping using the HLA high-resolution sequence based typing to ascertain the HLA type.

Using the Biofortuna kit was user friendly and fast, but two 96 well plates had to be excluded as the PCR for the housekeeping gene failed in a large percentage of samples (98% and 67%). The only two samples that worked on the plate with 98% failure rate were from one carrier of HLA-A*31:01 genotyped in a duplicate. Such a high error rate could have been caused by the way in which the experiment was conducted (human error) or a result of some problems with the equipment, such as the UV light in the transilluminator or the sensitivity of the camera. In addition to the high error rate, there were also some issues with the positive control of the housekeeping gene. The PCR assay from Biofortuna did not work for 35 (13.1%) samples. All of these samples were from patients not carrying the HLA-A*31:01 allele. This taken together with the previous observations would suggest that the primers for the control gene are not as robust as the SSP-PCR primer. This would need to be further investigated.

The validation of the SSP-PCR protocol developed by Carrington's group was less accurate (positive predictive value: 25%, and negative predictive value: 98.4%) in comparison to the gold standard or the kit from Biofortuna. Another disadvantage of the method is that it does not contain a pair of primers for a housekeeping gene. Therefore it was not possible to determine whether or not the PCR worked. Further optimisation should include the use of an appropriate pair of primers for a housekeeping gene.

Overall, the validation of the two newly developed methods for HLA-A*31:01 typing found that the SSP-PCR approach presents a cheaper possibility for assessing the HLA type of a patient before the start of treatment. Even though both methods tested in this chapter would need further optimisation, the validation showed promising results for potential clinical application. One of the methods was even as accurate as the gold standard, HLA high-resolution genotyping. However, the reliability would need to be improved. The methods were also more user-friendly compared to current typing methods, reducing the turnover time significantly and thus allow prompt results. The case of abacavir, demonstrates that assessing the HLA-B*57:02 statues of a patient before drug treatment can improve the safety of patients [1]. The first successful method to assess a patients HLA type before the start of treatment was a SSP-PCR, which proved accurate, fast and reliable [50]. Further successful attempts to improve the turnover time included allele-specific PCR, real-time PCR, and flow cytometric detection using fluorescence coupled antibodies [51-53]. Similar approaches could be followed to further reduce the turnover time in assessing the HLA-A*31:01 status of Caucasian patients before the start of CBZ therapy. The clinical use of HLA typing before the treatment of CBZ would vastly improve the patient's safety and allow clinicians to treat their patients based on their genotype in a more personalised approach.

5.5 References

1. Mallal, S., et al., *Association between presence of HLA-B*5701, HLA-DR7, and HLA-DQ3 and hypersensitivity to HIV-1 reverse-transcriptase inhibitor abacavir.* Lancet, 2002. **359**(9308): p. 727-32.
2. Daly, A.K., et al., *HLA-B*5701 genotype is a major determinant of drug-induced liver injury due to flucloxacillin.* Nat Genet, 2009. **41**(7): p. 816-9.
3. Robinson, J., et al., *The IMGT/HLA database.* Nucleic Acids Res, 2013. **41**(Database issue): p. D1222-7.
4. Vandiedonck, C. and J.C. Knight, *The human Major Histocompatibility Complex as a paradigm in genomics research.* Brief Funct Genomic Proteomic, 2009. **8**(5): p. 379-94.
5. McCluskey, J., C. Kanaan, and M. Diviney, *Nomenclature and serology of HLA class I and class II alleles.* Curr Protoc Immunol, 2003. **Appendix 1**: p. Appendix 1S.
6. HLA Informatics Group. *HLA Nomenclature*. 28.10.2014]; Available from: http://hla.alleles.org/.
7. van der Vlies, S.A., C.E. Voorter, and E.M. van den Berg-Loonen, *A reliable and efficient high resolution typing method for HLA-C using sequence-based typing.* Tissue Antigens, 1998. **52**(6): p. 558-68.
8. Turner, S., et al., *Sequence-based typing provides a new look at HLA-C diversity.* J Immunol, 1998. **161**(3): p. 1406-13.
9. Swelsen, W.T., C.E. Voorter, and E.M. van den Berg-Loonen, *Sequence-based typing of the HLA-A10/A19 group and confirmation of a pseudogene coamplified with A*3401.* Hum Immunol, 2005. **66**(5): p. 535-42.
10. Gabriel, C., et al., *Rapid high-throughput human leukocyte antigen typing by massively parallel pyrosequencing for high-resolution allele identification.* Hum Immunol, 2009. **70**(11): p. 960-4.
11. Lind, C., et al., *Next-generation sequencing: the solution for high-resolution, unambiguous human leukocyte antigen typing.* Hum Immunol, 2010. **71**(10): p. 1033-42.
12. Erlich, R.L., et al., *Next-generation sequencing for HLA typing of class I loci.* BMC Genomics, 2011. **12**: p. 42.
13. Balazs, I., et al., *Molecular typing of HLA-A, -B, and DRB using a high throughput micro array format.* Hum Immunol, 2001. **62**(8): p. 850-7.
14. Olerup, O. and H. Zetterquist, *HLA-DR typing by PCR amplification with sequence-specific primers (PCR-SSP) in 2 hours: an alternative to serological DR typing in clinical practice including donor-recipient matching in cadaveric transplantation.* Tissue Antigens, 1992. **39**(5): p. 225-35.
15. Bunce, M., et al., *Phototyping: comprehensive DNA typing for HLA-A, B, C, DRB1, DRB3, DRB4, DRB5 & DQB1 by PCR with 144 primer mixes utilizing sequence-specific primers (PCR-SSP).* Tissue Antigens, 1995. **46**(5): p. 355-67.
16. Hetherington, S., et al., *Genetic variations in HLA-B region and hypersensitivity reactions to abacavir.* Lancet, 2002. **359**(9312): p. 1121-2.
17. Adam, J., et al., *Avidity determines T-cell reactivity in abacavir hypersensitivity.* Eur J Immunol, 2012. **42**(7): p. 1706-16.
18. Illing, P.T., et al., *Immune self-reactivity triggered by drug-modified HLA-peptide repertoire.* Nature, 2012. **486**(7404): p. 554-8.
19. Norcross, M.A., et al., *Abacavir induces loading of novel self-peptides into HLA-B*57: 01: an autoimmune model for HLA-associated drug hypersensitivity.* AIDS, 2012. **26**(11): p. F21-9.

20. Ostrov, D.A., et al., *Drug hypersensitivity caused by alteration of the MHC-presented self-peptide repertoire.* Proc Natl Acad Sci U S A, 2012. **109**(25): p. 9959-64.
21. Hughes, D.A., et al., *Cost-effectiveness analysis of HLA B*5701 genotyping in preventing abacavir hypersensitivity.* Pharmacogenetics, 2004. **14**(6): p. 335-42.
22. Mallal, S., et al., *HLA-B*5701 screening for hypersensitivity to abacavir.* N Engl J Med, 2008. **358**(6): p. 568-79.
23. Apanius, V., et al., *The nature of selection on the major histocompatibility complex.* Crit Rev Immunol, 1997. **17**(2): p. 179-224.
24. Chung, W.H., S.I. Hung, and Y.T. Chen, *Human leukocyte antigens and drug hypersensitivity.* Curr Opin Allergy Clin Immunol, 2007. **7**(4): p. 317-23.
25. Chung, W.H., et al., *Medical genetics: a marker for Stevens-Johnson syndrome.* Nature, 2004. **428**(6982): p. 486.
26. Hung, S.I., et al., *Genetic susceptibility to carbamazepine-induced cutaneous adverse drug reactions.* Pharmacogenet Genomics, 2006. **16**(4): p. 297-306.
27. Locharernkul, C., et al., *Carbamazepine and phenytoin induced Stevens-Johnson syndrome is associated with HLA-B*1502 allele in Thai population.* Epilepsia, 2008. **49**(12): p. 2087-91.
28. Mehta, T.Y., et al., *Association of HLA-B*1502 allele and carbamazepine-induced Stevens-Johnson syndrome among Indians.* Indian J Dermatol Venereol Leprol, 2009. **75**(6): p. 579-82.
29. Kim, S.H., et al., *Carbamazepine-induced severe cutaneous adverse reactions and HLA genotypes in Koreans.* Epilepsy Res, 2011. **97**(1-2): p. 190-7.
30. Then, S.M., et al., *Frequency of the HLA-B*1502 allele contributing to carbamazepine-induced hypersensitivity reactions in a cohort of Malaysian epilepsy patients.* Asian Pac J Allergy Immunol, 2011. **29**(3): p. 290-3.
31. McCormack, M., et al., *HLA-A*3101 and carbamazepine-induced hypersensitivity reactions in Europeans.* N Engl J Med, 2011. **364**(12): p. 1134-43.
32. Kashiwagi, M., et al., *Human leukocyte antigen genotypes in carbamazepine-induced severe cutaneous adverse drug response in Japanese patients.* J Dermatol, 2008. **35**(10): p. 683-5.
33. U.S. Food and Drug Administration. *Carbamazepine*. July, 2014 31.07.2014]; Available from: http://www.fda.gov/Drugs/DrugSafety/PostmarketDrugSafetyInformationforPatientsandProviders/ucm124718.htm.
34. The Medicines and Healthcare Products Regulatory Agency. *Carbamazepine, oxcarbazepine and eslicarbazepine: potential risk of serious skin reactions associated with the HLA-A* 3101 allele.* July, 2014 31.07.2014]; Available from: http://www.mhra.gov.uk/Safetyinformation/DrugSafetyUpdate/CON214944.
35. Amstutz, U., et al., *HLA-A 31:01 and HLA-B 15:02 as genetic markers for carbamazepine hypersensitivity in children.* Clin Pharmacol Ther, 2013. **94**(1): p. 142-9.
36. Ozeki, T., et al., *Genome-wide association study identifies HLA-A*3101 allele as a genetic risk factor for carbamazepine-induced cutaneous adverse drug reactions in Japanese population.* Hum Mol Genet, 2011. **20**(5): p. 1034-41.
37. Li, L.J., et al., *Predictive markers for carbamazepine and lamotrigine-induced maculopapular exanthema in Han Chinese.* Epilepsy Res, 2013. **106**(1-2): p. 296-300.
38. Histogenetics. Available from: http://www.histogenetics.com/resolutions.

39. Alfirevic, A., et al., *In silico analysis of HLA associations with drug-induced liver injury: use of a HLA-genotyped DNA archive from healthy volunteers.* Genome Med, 2012. **4**(6): p. 51.
40. de Bakker, P.I., et al., *A high-resolution HLA and SNP haplotype map for disease association studies in the extended human MHC.* Nat Genet, 2006. **38**(10): p. 1166-72.
41. LGC Group. Available from: http://www.lgcgroup.com/LGCGroup/media/PDFs/Products/Genotyping/kasp-explanation-fact-sheet.pdf?ext=.pdf.
42. Saiki, R.K., et al., *Analysis of enzymatically amplified beta-globin and HLA-DQ alpha DNA with allele-specific oligonucleotide probes.* Nature, 1986. **324**(6093): p. 163-6.
43. Biofortuna. *SSPGo Instructions for Use*. Available from: http://www.biofortuna.com/index.php/products/ssp-go/.
44. Fisher, R.A., *On the interpretation of x(2) from contingency tables, and the calculation of P.* Journal of the Royal Statistical Society, 1922. **85**: p. 87-94.
45. Donaldson, P.T., et al., *Human leucocyte antigen class II genotype in susceptibility and resistance to co-amoxiclav-induced liver injury.* J Hepatol, 2010. **53**(6): p. 1049-53.
46. Saag, M., et al., *High sensitivity of human leukocyte antigen-b*5701 as a marker for immunologically confirmed abacavir hypersensitivity in white and black patients.* Clin Infect Dis, 2008. **46**(7): p. 1111-8.
47. Schackman, B.R., et al., *The cost-effectiveness of HLA-B*5701 genetic screening to guide initial antiretroviral therapy for HIV.* AIDS, 2008. **22**(15): p. 2025-33.
48. Cheng, S.H., et al., *New testing approach in HLA genotyping helps overcome barriers in effective clinical practice.* Clin Chem, 2009. **55**(8): p. 1568-72.
49. Aoki, M., et al., *New pharmacogenetic test for detecting an HLA-A*31: 01 allele using the InvaderPlus assay.* Pharmacogenet Genomics, 2012. **22**(6): p. 441-6.
50. Martin, A.M., D. Nolan, and S. Mallal, *HLA-B*5701 typing by sequence-specific amplification: validation and comparison with sequence-based typing.* Tissue Antigens, 2005. **65**(6): p. 571-4.
51. Rodriguez-Sainz, C., et al., *Flow cytometry analysis with a new FITC-conjugated monoclonal antibody-3E12 for HLA-B*57:01 rapid screening in prevention of abacavir hypersensitivity in HIV-1-infected patients.* HIV Clin Trials, 2013. **14**(4): p. 160-4.
52. Dello Russo, C., et al., *Novel sensitive, specific and rapid pharmacogenomic test for the prediction of abacavir hypersensitivity reaction: HLA-B*57:01 detection by real-time PCR.* Pharmacogenomics, 2011. **12**(4): p. 567-76.
53. Hammond, E., et al., *HLA-B*5701 typing: evaluation of an allele-specific polymerase chain reaction melting assay.* Tissue Antigens, 2007. **70**(1): p. 58-61.

Chapter 6
Final Discussion

Drug-induced hypersensitivity reactions (DHRs) or Type B adverse drug reactions (ADRs) are not related to the known pharmacological characteristics of the drug. They are rare, but cause approximately 20% of all hospital admissions related to ADRs [1]. Although only a minority of patients treated with the drug suffer from DHRs, they are a major clinical issue due to the often high severity and mortality [2].

Carbamazepine (CBZ) is one of the most commonly prescribed anticonvulsants used to treat patients with partial seizures, trigeminal neuralgia and bipolar disorder. Although only a small number of patients treated with CBZ develop severe ADRs, skin rashes are fairly common affecting up to 10% of patients [3]. This requires discontinuation of therapy to prevent more severe DHRs. The most severe types of CBZ-induced hypersensitivity reactions are Steven Johnson syndrome (SJS), toxic epidermal necrolysis (TEN) and drug reactions with eosinophilia and systemic symptoms (DRESS). These reactions are not limited to the skin; they lead to organ dysfunction, for example in the liver. Patients suffering from these severe reactions are sometimes treated in intensive care units. The mortality rate is approximately 10% for SJS and DRESS, and 30% for TEN [4].

Despite intensive research in this field, the underlying pathophysiological mechanisms of DHRs still remain mostly unknown. Immunogenetic T cell-mediated mechanisms have been postulated for hypersensitivity reactions to several aromatic antiepileptic drugs. It has been possible to isolate drug-specific T cells from the blood and other tissues of patients with CBZ and lamotrigine-induced hypersensitivity reactions [5-9]. T cell phenotypes and effector functions have been studied and characterised, but molecular

mechanisms of T cell activation in DHRs is still poorly understood. It has been demonstrated in *in vitro* studies that CBZ metabolism is not necessary for the activation of T cells [10]. The lack of T cell activation by dendritic cells presenting CBZ-modified peptides suggests non-covalent protein binding of stable metabolites of CBZ [10, 11]. In a study by Furst and colleagues it was shown that a toxic metabolite binds in a non-covalent way to peptides *in vitro* [12]. They reported that 9-acridinecarboxaldehyde (9-AC) binds to nucleophiles but that adduct formation was reversible under physiological pH. They were able to show that the adduct becomes irreversible in the presence of a mild reducing agent. They therefore hypothesised that the reversible binding of 9-AC to protein occurs via a Schiff base which is then reduced to the stable adduct.

To follow on from these findings, in chapter 3, protein binding of CBZ, CBZE, and 9-AC was assessed, utilising mass-spectrometric methods to determine the binding site of the compounds. In these experiments, covalent protein binding was only shown for CBZE with glutathione S-transferase π (GSTPi) and human serum albumin (HSA). With GSTPi, CBZE was found to bind to the cysteine at position 47 while in HSA, CBZE was found to bind to the histidine at position 146 and the histidine at position 338. This represents a novel finding as only the binding of CBZE in GSTPi has previously been reported in the literature [13]. Surprisingly, the binding was found on different amino acids. It would be expected that the binding affinity would be to the same amino acids. Different positions within each protein structure as well as neighbouring amino acids could lead to the differences in preference.

For 9-AC no covalent binding was observed with protein, which confirms the previous study by Furst and colleagues [12]. A similar approach as in the study, using reducing agent to transform the Schiff base into a stable product, was attempted for HSA but did not yield any measurable amount of adduct. A higher dose of reducing agent could overcome the problem and should be further investigated. The mass spectrometric analysis revealed nonspecific binding to the N-terminus of the protein backbone, which had not been reported previously (see Fig. A3.1 in appendix). This could indirectly show that a non-covalent adduct was present in the full length protein.

Further experiments are necessary to assess the protein binding capability of 9-AC.

It has been shown previously that the formation of haptens is not required to trigger T cell activation in CBZ-induced hypersensitivity reactions [10, 11, 14]. A better approach for the assessment of protein binding during the induction of CBZ-induced ADRs could include the use of protein fragments mounted on HLA and thus determine the capability of CBZ or its metabolites to interact with proteins.

An increasing number of studies have demonstrated a strong link between several drug-induced hypersensitivity reactions and specific HLA alleles [15-17]. These findings provided a new insight into the mechanism of DHRs and for the first time allowed the prediction of individual patient's risk for developing DHRs. The best known examples include the association between abacavir-induced hypersensitivity reactions and HLA-B*57:01 in all ethnicities [18] and CBZ-induced SJS and HLA-B*15:02 in Asian populations [19].

In Caucasians with CBZ-induced hypersensitivity reactions, two independent genome-wide association studies (GWAS) showed an association with HLA-A*31:01 [20]. Unlike HLA-B15:02, HLA-A*31:01 has been associated with multiple phenotypes in several ethnicities. These two alleles can be used to predict the increased risk for developing severe hypersensitivity reactions [20-24]. Given the strong evidence, the FDA and UK regulatory agency recommend genotyping for HLA-B*15:02 before the start of CBZ treatment [25, 26].

DNA sequencing is the most reliable method for high resolution HLA typing. This technique is labour and time intensive and requires specialised facilities with trained personnel. To overcome this, several existing methods have been optimised to achieve rapid and simple HLA typing that can be utilised in general clinical laboratories [27, 28]. Biofortuna [29], a small biotechnology company, as well as the Carrington group [20] developed new methods for clinical HLA typing based on SSP-PCR. For the validation of these methods, clinical samples were HLA typed and the results compared to the gold

standard, sequence based typing. For HLA-A*31:01 carriers the Biofortuna kit proved to be as reliable as the current gold standard. However, a very high proportion of DNA samples from patients that were not carrying the HLA-A*31:01 allele failed to amplify. This observation may represent a chance finding because HLA-A*31:01 is a rare allele and only 32 out of the 347 patients carried that allele. However, if there is such a high failure rate, one has to question the reliability of the method.

The SSP-PCR HLA typing from Carrington's group was less accurate. The lack of primers for a housekeeping gene made it hard to distinguish between samples for which the PCR did not work and samples of patients not carrying the HLA-A*31:01 allele. The method would therefore benefit from further optimisation before it can be considered for clinical use.

Although there is strong evidence for an association between the HLA-A*31:01 allele and CBZ-induced hypersensitivity reactions in Europeans, the pathogenesis is poorly understood and other genetic and non-genetic factors might also play a role. For example in Asians, it has been found that the interaction of CBZ with HLA-B*15:02 results in the stimulation of a subset of T cells ($CD8^+$) [11, 19, 20]. A similar investigation of the interaction of CBZ with HLA-A*31:01 failed to show such stimulation [30]. It is possible that for Europeans at least, several rare not yet discovered genetic variants may be involved in CBZ-induced hypersensitivity reactions.

CBZ is extensively metabolised *in vivo*. Over 30 metabolites of CBZ have been discovered (for more details, see metabolism of CBZ in general introduction 1.7.1) [31-34]. It is unknown whether the parent drug or one of its metabolites causes CBZ-induced adverse reactions. Therefore, the metabolism of CBZ could play an important role in the onset of DHRs. Phase I metabolism takes place mainly in the liver. Highly unstable metabolites, such as the hypothesised CBZ arene oxide, would react with proteins in close vicinity within the liver but may not be detectable outside the liver [35]. This would explain hypersensitivity reactions involving the liver but would not explain other reactions such as the cutaneous ADRs.

Leukocytes in particular monocytes and neutrophils, possess strong oxidizing properties because they contain myeloperoxidase. Myeloperoxidase together with hydrogen peroxide and chloride is able to form hypochlorous acid [36]. It was shown that drugs, such as dapson, sulfamethoxazole and phenytoin, can be oxidised to reactive intermediates [37-39]. Furst and Uetrecht found that similar metabolism for CBZ could take place in human blood [40]. In their *in vitro* studies they observed a ring contraction of CBZ. Although several intermediates were not detected, it was shown that myeloperoxidase was the metabolising enzyme. This study also showed that the same metabolism can occur in neutrophils but to a lesser extent (500-fold less) than with myeloperoxidase. Such metabolism could explain the occurrence of hypersensitivity reactions outside of the liver as reactive species were found to be bound covalently to blood cells. The cell damage caused by the metabolites could result in the release of danger signals that lead to the activation of the immune system as described in the danger hypothesis for T cell activation (see general introduction 1.5.4) [41].

In computational toxicology, a new concept for determining individual susceptibility to toxicity has been developed by linking toxic phenotypes to genetics [42]. The methodology is sensitive enough for the detection of inter-individual variability. This new concept was utilized in chapter 4 and is a novel approach to detect biomarkers for risk assessment of CBZ treatment in patients.

As a preliminary step towards the new approach, a T lymphoblastoid cell line (CCRF-CEM) and peripheral blood mononuclear cells (PBMC) from healthy volunteers were exposed to CBZ and its toxic metabolite 9-AC *in vitro*. Four different assays; cell viability, mitochondrial membrane permeabilisation, phosphatidylserine exposure and membrane integrity, and caspase activation assay were used to assess the cell death pathways.

Typical characteristics of apoptosis are activation of caspases, the mitochondrial membrane permeabilisation and exposure of phosphatidylserine on the cell surface [43]. These pathological characteristics can be observed during other processes in the cell, including

other modes of cell death but also in situations that do not lead to the death of the cell [44-46]. Because of these findings, it is necessary to observe cell death with a minimum of two different assays [47, 48]. Four assays were used in the experiments to find the best working and feasible method for quantitative high-throughput screening (qHTS). For the CCRF-CEM cells all assays worked well and they showed that the cells exposed to 9-AC died via an apoptotic pathway. As expected, CBZ showed no toxic effect in the range of concentrations used for the experiments. Experiments using primary cells (PBMCs) were more difficult to perform and problems with flow cytometry, namely indistinct populations of living and dead cells, were encountered. However, similar to the results observed in T lymphoblastoid cells, the assays showed that the PBMCs also die via an apoptotic pathway when exposed to 9-AC. No toxicity of the parent drug was observed.

In chapter 2, the inter-individual variability to cytotoxicity caused by CBZ and 9-AC was assessed. Since the data obtained from the double staining were inconclusive, only the three assays measuring the viability, mitochondrial depolarisation, and activation of caspase, were used for the preliminary screening of inter-individual variability in response to CBZ and its metabolites in PBMCs from 20 CBZ-naïve healthy volunteers. The PMBCs showed variation in response to the cytotoxic effect of 9-AC. The observation of inter-individual viability presented an interesting finding for further investigation by quantitative high-throughput screening (qHTS).

It has been shown that lymphocytes from CBZ hypersensitive patients are more sensitive to the cytotoxicity of CBZ metabolite using a lymphocyte toxicity assay that included a metabolising system [49, 50]. This has led to the hypothesis that hypersensitivity reactions are the result of an imbalance between the generation and detoxification of reactive metabolites [50]. In order to understand the inter-individual variability in patient responses to drugs and prove the hypothesis, polymorphisms in various genes including drug metabolising enzymes, drug transporters and receptors, have been analysed [51-53]. These studies were unable to find associations between hypersensitivity reactions and an imbalance in the metabolism.

The findings for the flow cytometric assays of chapter 2 showed that cells of a single cell type would be preferable compared to a mixture of cells, especially with the assays relying on flow cytometry. This approach was not chosen for this work as cell-cell interactions, possibly occurring in the human blood, would be missed and therefore not fully represent the situation found in patients.

As the incidence rate of CBZ-induced hypersensitivity reactions is low and therefore the patient samples are rare, the qHTS was conducted in immortalised lymphoblastoid cell lines. These cells were generated as part of the 1000 genome project to allow scientists to conduct experiments with a defined genetic diversity. It has been shown previously that lymphoblastoid cell lines express enzymes responsible for drug metabolism [54]. In their study, Siest and colleagues measured the expression of 16 drug metabolising enzymes as well as 13 known transcription factors in PBMCs of 20 healthy volunteers. The drug metabolising enzymes included a variety of cytochrome P450s as well as GSTs. The highest expression of cytochrome P450s was found in T cells but was still considerably lower compared to liver tissue (20 to 2000 times). GST was also found to be expressed in the PBMCs. GST is responsible for the conjugation of reactive species during metabolism and leads to the renal clearance of the conjugate, which offers protection against toxic metabolites. This study showed that PBMCs can be used as a model system to study inter-individual differences in metabolism.

In toxicology, new *in vitro* based assays have been tested for classifying the cytotoxic profile of chemicals. The current backlog of toxicity testing for chemicals is of great concern for regulatory committees worldwide. Traditional animal testing is time consuming and costly, as it requires a large number of laboratory animals. In addition, animal models are lacking interindividual variability due to their inbred nature. Recently, a program was formed by several governmental agencies in the United States to assess the implementation of qHTS using *in vitro* toxicity assays in the field of computational toxicology [55, 56]. These qHTS combined with the recent advances in genome sequencing, allow the consideration of interindividual biological variability in human health hazard. Genetic variability may have a

role in individual susceptibility to ADRs after exposure to toxins or drugs [57]. The availability of well-defined genetically diverse renewable sources of human cells, derived from the International HapMap and 1000 Genomes project allows *in vitro* screening on a population scale [58, 59].

In chapter 4, immortalised lymphoblastoid cell lines were exposed to CBZ, its main metabolite CBZE and one toxic metabolite 9-AC. The overall dose-response to CBZ and CBZE demonstrated that there was no cytotoxic effect for the two compounds. The concentration range included the clinically relevant concentrations. More interesting, the individual dose-response revealed variability and several cell lines showed more pronounced cytotoxic effects from these compounds then the majority of cells. The overall dose-response data for 9-AC showed that this metabolite is cytotoxic to all cell lines that were exposed to it. Some individuals were more susceptible to the cytotoxic effect than others. Due to the plating of cells and compounds being undertaken using robotics, the experimental error was minimised and therefore, even small differences in viability could be detected and included in the analysis. The screening of cell viability has been successfully used in the past for the prediction of cytotoxicity for known toxins and had shown promising results for the association of cytotoxic genotypes with observed phenotypes [42].

Following these findings, a GWAS was performed to reveal genetic variants that might be associated with the higher susceptibility to toxic effects. This GWAS revealed 14 biologically plausible SNPs with low p-values, however none of the SNPs reached genome-wide significance ($1x10^{-8}$). Therefore further validation was necessary. The experiments were conducted in cell lines derived from CBZ-naïve individuals. To optimise the outcome, cells could be primed before the start of the assay. Primed T cells have a lower activation threshold in comparison with naïve T cells. This can be achieved by culturing T cells in the presence of antigen-presenting cells and repeatedly stimulating them with the drug of interest [60, 61]. A series of experiments from our department using flucloxacillin and sulfamethoxazole, have demonstrated that primed cells could have similar outcomes as cells from drug-induced hypersensitive patients [62, 63]. Furthermore, PBMCs

from CBZ-naïve carriers of HLA-B*15:02 were stimulated using the priming method and exhibited similar response to CBZ as T cells from patients that had suffered from CBZ-induced hypersensitivity [64]. Including primed and non-primed T lymphoblastoid cell lines for qHTS might allow the exploration of underlying changes in the cell during hypersensitivity reaction. Another possibility could be the inclusion of metabolising systems in the screening as described for the lymphocyte toxicity assay by Spielberg and colleagues [65]. This assay has been successfully used in the past and it was found that cells derived from hypersensitive patients showed higher susceptibility to toxic effects of the generated metabolites than the tolerant controls [49, 50].

The SNPs from the GWAS conducted for this work were characterised and it was found that only one SNP (rs16939743) in the DUOX1 gene was functionally relevant. This SNP was found at p-values $8.5x10^{-6}$ for CBZ, $6.3x10^{-5}$ for CBZE, and $4.1x10^{-6}$ for 9-AC, which suggests that carriers may be at higher risk to develop CBZ-induced hypersensitivity reactions than non-carriers. The SNP is a missense variation within DUOX1. DUOX1 plays a role in both innate and adaptive immune responses.

Samples from CBZ-tolerant as well as from CBZ-hypersensitive patients were used to validate this finding and were genotyped to determine their DUOX1 status. The genotyping suggests that the rare minor allele variant of DUOX1 does not play an important role in the initiation of CBZ-induced hypersensitivity reactions in Europeans. Because of the low minor allele frequency (MAF) in Europeans (below 1%), the statistical power of the genotyping in patients was not sufficient to detect the difference. The variant of DUOX1 was only found in individuals of non-European ancestry. The frequency of the minor DUOX1 allele in CBZ hypersensitive patients detected through the genotyping conducted in the experiments of this thesis was similar to the highest MAF reported in 1000 Genomes project, which was found in populations of African ancestry.

Because severe CBZ-induced hypersensitivity reactions are so rare even after two decades of recruiting patients, the number of samples from Caucasians in the DNA archive of the University of Liverpool was limited.

Furthermore, the patient cohort was heterogeneous comprising samples from many different ethnicities as well as different clinical phenotypes. To validate the effect of rare DUOX1 variants in non-Europeans, populations from homogeneous ethnic background would need to be genotyped together with ethnicity matched treated controls.

In addition to the SNP in DUOX1 found by the GWAS conducted for this work, several other SNPs in close proximity of genes or in introns of several genes were found at increased frequency. It has been shown that SNPs in such locations can have an effect on gene expression or gene variant splicing [66, 67]. This requires further investigation.

Following the experiments in chapter 4, another analysis of the data will be conducted in the future using a different software [68]. In this analysis the concentration of CBZ and its metabolites, at which a 10% decrease in viability was observed, will be utilised to determine whether there is a correlation with higher cytotoxicity during exposure to compounds, compared to the dose-response data used in the described analysis (chapter 4). This 10% difference in viability was shown to be sufficient as the starting point of cytotoxicity [42]. The results of both analyses will be compared for verification of results from the first analysis. The cell material, which was collected during the experiments, will be used in future proteomic experiments to assess differences in protein abundance before and after the exposure of the compounds and to validate previous findings.

The bridging of cytotoxic effects *in vitro* to the onset of CBZ-induced hypersensitivity reactions through danger signals leading to an immune response *in vivo* remains to be established. In the novel approach, which applied computational toxicology to personalised pharmacology, a possible new genetic marker for predicting risk for ADRs was found. This marker was investigated in a retrospective cohort of CBZ hypersensitive patients and tolerant controls. However, the majority of experiments in this thesis were conducted using cells from CBZ-naïve volunteers. The best approach would be to collect samples from patients before they receive CBZ treatment and store them. In case patients developed hypersensitivity reactions on

exposure to CBZ, new samples can be collected and compared with the pre-treatment one. This approach however, would not be feasible because of the cost, logistics, ethical, and societal difficulties with sample and information storage. Therefore, alternative strategies should be explored. One of them would be to prime cells from CBZ-naïve volunteers [64]. Following this approach cells could be tested before and after priming, allowing the detection of changes in RNA expression and dose-response changes due to the priming.

The cell work in this thesis was conducted in PBMCs or lymphoblastoid cell lines. Although they offer certain advantages including the expression of drug metabolising enzymes and easy withdrawal from individuals with minimally invasive procedures, there are also disadvantages such as the cells lacking organ specific properties. To overcome this absence and better understand the mechanisms occurring during drug-induced hypersensitivity reactions, samples from different tissues or model systems affected during hypersensitivity including the skin and liver, could be used in further investigations. Due to the ethical and practical issues in tissue sampling from healthy volunteers, model systems or engineered tissue should be used to produce such tissue [69]. Model systems allow further investigations as the example of the rat model of nevarapine-caused skin rash demonstrated [70]. Through this animal model researchers were able to show that nevirapine-induced skin rashes were immune mediated and that T cells played an important role [71]. It was also possible to show that a sub-set of T cells is sensitised and through their transfer into unexposed animals, the susceptibility for reactions increased.

Further work could also include investigation of the role of danger signals derived from simultaneous viral infections such as reactivation of herpes virus (HHV) infection during the occurrence of DRESS [72, 73]. The role of HHV reactivation in the development of DRESS is well recognised [74, 75]. HHV-6 reactivation has been proposed by a Japanese consensus group for the diagnosis of DRESS [76]. Viral reactivation by a limited number of drugs has been detected in DRESS, but how these drugs induce HHV reactivation is not yet understood. It is still uncertain whether virus infection triggers

DRESS or DRESS triggers the virus reactivation [72, 75]. Findings supporting both hypotheses have been made [72, 77]. Further investigations would need to clarify the underlying mechanism and thus the role in hypersensitivity reactions.

Environmental factors may also play an important role in hypersensitivity reactions, but these however, have not been investigated in this thesis. Increased knowledge of metagenomics of the human gut showed that different diets influence the microbiota composition [78-81]. Nermes and colleagues investigated the interaction of bacteria (*Lactobacillus rhamnosus* GG) with gut microbiota and the influence on humoral immunity in infants with atopic dermatitis for period of three months [82]. The immunoglobulin (Ig)-secreting cells were measured as well as the proportion of memory B cells in blood. In their study they were able to show that the proportion of memory B cells increased significantly while the number of Ig-secreting cells decreased. They concluded that the gut barrier function might be enhanced through certain probiotics, which supports the development of immune response and thus provides control for further infections. Further investigation in hypersensitivity could therefore include information on gut microbiome in patients and thus add some information about their lifestyle.

Novel high-throughput technologies have made it possible to simultaneously examine millions of genes, transcripts, proteins, metabolites and microbiomes in an unbiased approach. This approach may hold a key to understand the mechanisms of hypersensitivity and to identify clinically useful prediction biomarkers [83-89]. Already, these methods, which require interdisciplinary collaboration, have improved the insight and understanding of human disease and therefore, they could also be applied for studying CBZ-induced hypersensitivity reactions [90]. Through these high-throughput technologies, vast amounts of complex and multifarious data, ranging from molecular to clinical, can be generated and system biology methods could be applied for the analysis. Several systems have been developed to overcome the problems of data integration [91-93]. These systems improve the analysis of data but there is no single standard. In a global open source partnership community, tranSMART was developed to establish the use of similar

standards for big data processing and integration [94]. The approach chosen by transSMART is based on the sharing of data on a cloud platform and allows the use of informatics-based translation of science into clinics, big data resource, newest and best suited analytic tools as well as experts opinions from all over the world.

In conclusion, inter-individual variability in the cytotoxic response to CBZ and its metabolites was detected *in vitro* in primary cells and lymphoblastoid cell lines from CBZ-naïve, healthy volunteers. There is a large variability in susceptibility to cell death with the doses at which cytotoxicity can be observed varying up to 100 fold for CBZ and its two metabolites investigated in this work. The GWAS revealed genetic polymorphisms, which could be associated with the observed variability. The frequency of the candidate SNP in DUOX1 was not increased in European patients suffering from CBZ-induced hypersensitivity reactions, but a higher frequency of this SNP could not be excluded for non-European patients. New conjugates for CBZE and HSA and evidence for non-covalent conjugation of 9-AC and HSA were found. These findings need further validation in patients that experienced CBZ-induced hypersensitivity reactions. Finally, new HLA typing methods were utilised and showed promising results but also require optimisation (see Fig. 6.1).

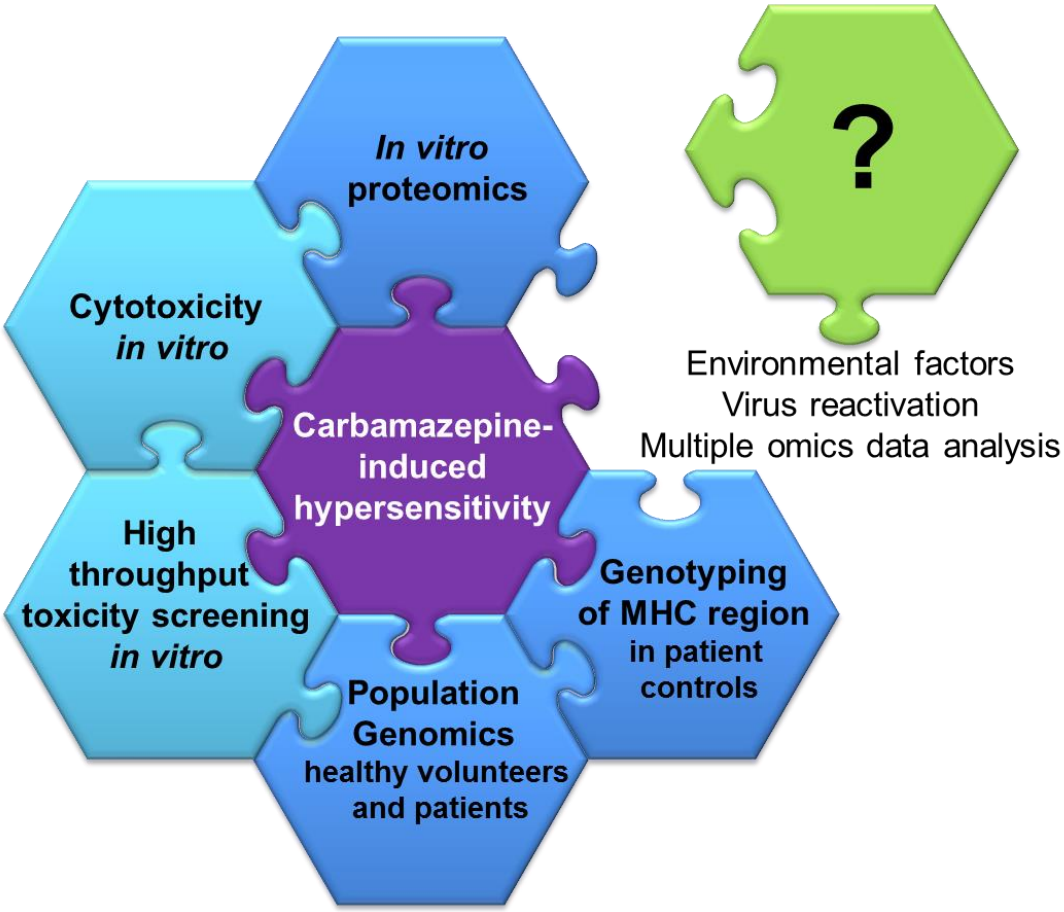

Figure 6.1: Contribution of present work to the field of Carbamazepine-induced hypersensitivity reaction

Recent discoveries in the field, such as the finding of HLA associations to hypersensitivity reactions and uncovering the exact mechanism of drug binding to HLA molecule in the case of abacavir, greatly improved our understanding of hypersensitivity reactions. Nevertheless, further investigations of the approaches undertaken in this study are necessary to confirm the association between cytotoxic susceptibility to drugs and the development of hypersensitivity reactions. The ultimate aim is to develop predictive testing to determine risk of hypersensitivity reactions in patients to prevent these reactions in the future and through that, to improve drug safety.

References

1. Routledge, P.A., M.S. O'Mahony, and K.W. Woodhouse, *Adverse drug reactions in elderly patients.* Br J Clin Pharmacol, 2004. **57**(2): p. 121-6.
2. Lazarou, J., B.H. Pomeranz, and P.N. Corey, *Incidence of adverse drug reactions in hospitalized patients: a meta-analysis of prospective studies.* JAMA, 1998. **279**(15): p. 1200-5.
3. Marson, A.G., et al., *The SANAD study of effectiveness of carbamazepine, gabapentin, lamotrigine, oxcarbazepine, or topiramate for treatment of partial epilepsy: an unblinded randomised controlled trial.* Lancet, 2007. **369**(9566): p. 1000-15.
4. Hausmann, O., B. Schnyder, and W.J. Pichler, *Drug hypersensitivity reactions involving skin.* Handb Exp Pharmacol, 2010(196): p. 29-55.
5. Nassif, A., et al., *Toxic epidermal necrolysis: effector cells are drug-specific cytotoxic T cells.* J Allergy Clin Immunol, 2004. **114**(5): p. 1209-15.
6. Naisbitt, D.J., et al., *Characterization of drug-specific T cells in lamotrigine hypersensitivity.* J Allergy Clin Immunol, 2003. **111**(6): p. 1393-403.
7. Naisbitt, D.J., et al., *Hypersensitivity reactions to carbamazepine: characterization of the specificity, phenotype, and cytokine profile of drug-specific T cell clones.* Mol Pharmacol, 2003. **63**(3): p. 732-41.
8. Schnyder, B., et al., *Recognition of sulfamethoxazole and its reactive metabolites by drug-specific CD4+ T cells from allergic individuals.* J Immunol, 2000. **164**(12): p. 6647-54.
9. Zanni, M.P., et al., *Recognition of local anesthetics by alphabeta+ T cells.* J Invest Dermatol, 1999. **112**(2): p. 197-204.
10. Wu, Y., et al., *Activation of T cells by carbamazepine and carbamazepine metabolites.* J Allergy Clin Immunol, 2006. **118**(1): p. 233-41.
11. Wei, C.Y., et al., *Direct interaction between HLA-B and carbamazepine activates T cells in patients with Stevens-Johnson syndrome.* J Allergy Clin Immunol, 2012. **129**(6): p. 1562-9 e5.
12. Furst, S.M., et al., *Covalent binding of carbamazepine oxidative metabolites to neutrophils.* Drug Metab Dispos, 1995. **23**(5): p. 590-4.
13. Bu, H.Z., et al., *Human in vitro glutathionyl and protein adducts of carbamazepine-10,11-epoxide, a stable and pharmacologically active metabolite of carbamazepine.* Drug Metab Dispos, 2005. **33**(12): p. 1920-4.
14. Wu, Y., et al., *Generation and characterization of antigen-specific CD4+, CD8+, and CD4+CD8+ T-cell clones from patients with carbamazepine hypersensitivity.* J Allergy Clin Immunol, 2007. **119**(4): p. 973-81.
15. Kim, S.H., et al., *Genetic and ethnic risk factors associated with drug hypersensitivity.* Curr Opin Allergy Clin Immunol, 2010. **10**(4): p. 280-90.
16. Torres, M.J., et al., *Diagnosis of immediate allergic reactions to beta-lactam antibiotics.* Allergy, 2003. **58**(10): p. 961-72.
17. Mallal, S., et al., *Association between presence of HLA-B*5701, HLA-DR7, and HLA-DQ3 and hypersensitivity to HIV-1 reverse-transcriptase inhibitor abacavir.* Lancet, 2002. **359**(9308): p. 727-32.
18. Hetherington, S., et al., *Genetic variations in HLA-B region and hypersensitivity reactions to abacavir.* Lancet, 2002. **359**(9312): p. 1121-2.
19. Chung, W.H., et al., *Medical genetics: a marker for Stevens-Johnson syndrome.* Nature, 2004. **428**(6982): p. 486.
20. McCormack, M., et al., *HLA-A*3101 and carbamazepine-induced hypersensitivity reactions in Europeans.* N Engl J Med, 2011. **364**(12): p. 1134-43.

21. Amstutz, U., et al., *HLA-A 31:01 and HLA-B 15:02 as genetic markers for carbamazepine hypersensitivity in children.* Clin Pharmacol Ther, 2013. **94**(1): p. 142-9.
22. Kim, S.H., et al., *Carbamazepine-induced severe cutaneous adverse reactions and HLA genotypes in Koreans.* Epilepsy Res, 2011. **97**(1-2): p. 190-7.
23. Ozeki, T., et al., *Genome-wide association study identifies HLA-A*3101 allele as a genetic risk factor for carbamazepine-induced cutaneous adverse drug reactions in Japanese population.* Hum Mol Genet, 2011. **20**(5): p. 1034-41.
24. Hung, S.I., et al., *Genetic susceptibility to carbamazepine-induced cutaneous adverse drug reactions.* Pharmacogenet Genomics, 2006. **16**(4): p. 297-306.
25. The Medicines and Healthcare Products Regulatory Agency. *Carbamazepine, oxcarbazepine and eslicarbazepine: potential risk of serious skin reactions associated with the HLA-A* 3101 allele.* July, 2014 31.07.2014]; Available from: http://www.mhra.gov.uk/Safetyinformation/DrugSafetyUpdate/CON214944.
26. U.S. Food and Drug Administration. *Carbamazepine*. July, 2014 31.07.2014]; Available from: http://www.fda.gov/Drugs/DrugSafety/PostmarketDrugSafetyInformationforPatientsandProviders/ucm124718.htm.
27. Aoki, M., et al., *New pharmacogenetic test for detecting an HLA-A*31: 01 allele using the InvaderPlus assay.* Pharmacogenet Genomics, 2012. **22**(6): p. 441-6.
28. Cheng, S.H., et al., *New testing approach in HLA genotyping helps overcome barriers in effective clinical practice.* Clin Chem, 2009. **55**(8): p. 1568-72.
29. Bunce, M. and B. Passey, *HLA typing by sequence-specific primers.* Methods Mol Biol, 2013. **1034**: p. 147-59.
30. Lichtenfels, M., et al., *HLA restriction of carbamazepine-specific T-Cell clones from an HLA-A*31:01-positive hypersensitive patient.* Chem Res Toxicol, 2014. **27**(2): p. 175-7.
31. Leeder, J.S., *Mechanisms of idiosyncratic hypersensitivity reactions to antiepileptic drugs.* Epilepsia, 1998. **39 Suppl 7**: p. S8-16.
32. Lertratanangkoon, K. and M.G. Horning, *Metabolism of carbamazepine.* Drug Metab Dispos, 1982. **10**(1): p. 1-10.
33. Frigerio, A. and P.L. Morselli, *Carbamazepine: biotransformation.* Adv Neurol, 1975. **11**: p. 295-308.
34. Eichelbaum, M., et al., *Plasma kinetics of carbamazepine and its epoxide metabolite in man after single and multiple doses.* Eur J Clin Pharmacol, 1975. **8**(5): p. 337-41.
35. Pirmohamed, M., et al., *Detection of an autoantibody directed against human liver microsomal protein in a patient with carbamazepine hypersensitivity.* Br J Clin Pharmacol, 1992. **33**(2): p. 183-6.
36. Weiss, S.J., *Tissue destruction by neutrophils.* N Engl J Med, 1989. **320**(6): p. 365-76.
37. Cribb, A.E., et al., *Peroxidase-dependent oxidation of sulfonamides by monocytes and neutrophils from humans and dogs.* Mol Pharmacol, 1990. **38**(5): p. 744-51.
38. Uetrecht, J., et al., *Metabolism of dapsone to a hydroxylamine by human neutrophils and mononuclear cells.* J Pharmacol Exp Ther, 1988. **245**(1): p. 274-9.
39. Uetrecht, J. and N. Zahid, *N-chlorination of phenytoin by myeloperoxidase to a reactive metabolite.* Chem Res Toxicol, 1988. **1**(3): p. 148-51.

40. Furst, S.M. and J.P. Uetrecht, *Carbamazepine metabolism to a reactive intermediate by the myeloperoxidase system of activated neutrophils.* Biochem Pharmacol, 1993. **45**(6): p. 1267-75.
41. Matzinger, P., *Tolerance, danger, and the extended family.* Annu Rev Immunol, 1994. **12**: p. 991-1045.
42. Lock, E.F., et al., *Quantitative high-throughput screening for chemical toxicity in a population-based in vitro model.* Toxicol Sci, 2012. **126**(2): p. 578-88.
43. Kroemer, G., et al., *Classification of cell death: recommendations of the Nomenclature Committee on Cell Death 2009.* Cell Death Differ, 2009. **16**(1): p. 3-11.
44. Galluzzi, L., et al., *Guidelines for the use and interpretation of assays for monitoring cell death in higher eukaryotes.* Cell Death Differ, 2009. **16**(8): p. 1093-107.
45. Kroemer, G., L. Galluzzi, and C. Brenner, *Mitochondrial membrane permeabilization in cell death.* Physiol Rev, 2007. **87**(1): p. 99-163.
46. Fischer, K., et al., *Antigen recognition induces phosphatidylserine exposure on the cell surface of human CD8+ T cells.* Blood, 2006. **108**(13): p. 4094-101.
47. Shi, J., S. Springer, and P. Escobar, *Coupling cytotoxicity biomarkers with DNA damage assessment in TK6 human lymphoblast cells.* Mutat Res, 2010. **696**(2): p. 167-78.
48. Raffray, M. and G.M. Cohen, *Apoptosis and necrosis in toxicology: a continuum or distinct modes of cell death?* Pharmacol Ther, 1997. **75**(3): p. 153-77.
49. Pirmohamed, M., et al., *Carbamazepine-hypersensitivity: assessment of clinical and in vitro chemical cross-reactivity with phenytoin and oxcarbazepine.* Br J Clin Pharmacol, 1991. **32**(6): p. 741-9.
50. Shear, N.H. and S.P. Spielberg, *Anticonvulsant hypersensitivity syndrome. In vitro assessment of risk.* J Clin Invest, 1988. **82**(6): p. 1826-32.
51. Taur, S.R., et al., *Association of polymorphisms of CYP2C9, CYP2C19, and ABCB1, and activity of P-glycoprotein with response to anti-epileptic drugs.* J Postgrad Med, 2014. **60**(3): p. 265-9.
52. Jaramillo, N.M., et al., *Pharmacogenetic potential biomarkers for carbamazepine adverse drug reactions and clinical response.* Drug Metabol Drug Interact, 2014. **29**(2): p. 67-79.
53. Park, P.W., et al., *Effect of CYP3A5*3 genotype on serum carbamazepine concentrations at steady-state in Korean epileptic patients.* J Clin Pharm Ther, 2009. **34**(5): p. 569-74.
54. Siest, G., et al., *Transcription factor and drug-metabolizing enzyme gene expression in lymphocytes from healthy human subjects.* Drug Metab Dispos, 2008. **36**(1): p. 182-9.
55. Xia, M., et al., *Compound cytotoxicity profiling using quantitative high-throughput screening.* Environ Health Perspect, 2008. **116**(3): p. 284-91.
56. Inglese, J., et al., *Quantitative high-throughput screening: a titration-based approach that efficiently identifies biological activities in large chemical libraries.* Proc Natl Acad Sci U S A, 2006. **103**(31): p. 11473-8.
57. Harrill, A.H., et al., *Mouse population-guided resequencing reveals that variants in CD44 contribute to acetaminophen-induced liver injury in humans.* Genome Res, 2009. **19**(9): p. 1507-15.
58. International HapMap, C., *A haplotype map of the human genome.* Nature, 2005. **437**(7063): p. 1299-320.
59. Genomes Project, C., et al., *A map of human genome variation from population-scale sequencing.* Nature, 2010. **467**(7319): p. 1061-73.

60. Dietz, L., et al., *Tracking human contact allergens: from mass spectrometric identification of peptide-bound reactive small chemicals to chemical-specific naive human T-cell priming.* Toxicol Sci, 2010. **117**(2): p. 336-47.
61. Engler, O.B., et al., *A chemically inert drug can stimulate T cells in vitro by their T cell receptor in non-sensitised individuals.* Toxicology, 2004. **197**(1): p. 47-56.
62. Wuillemin, N., et al., *HLA haplotype determines hapten or p-i T cell reactivity to flucloxacillin.* J Immunol, 2013. **190**(10): p. 4956-64.
63. Faulkner, L., et al., *The development of in vitro culture methods to characterize primary T-cell responses to drugs.* Toxicol Sci, 2012. **127**(1): p. 150-8.
64. Ko, T.M., et al., *Shared and restricted T-cell receptor use is crucial for carbamazepine-induced Stevens-Johnson syndrome.* J Allergy Clin Immunol, 2011. **128**(6): p. 1266-1276 e11.
65. Spielberg, S.P., et al., *Anticonvulsant toxicity in vitro: possible role of arene oxides.* J Pharmacol Exp Ther, 1981. **217**(2): p. 386-9.
66. Wang, G.S. and T.A. Cooper, *Splicing in disease: disruption of the splicing code and the decoding machinery.* Nat Rev Genet, 2007. **8**(10): p. 749-61.
67. Hayashi, S., J. Watanabe, and K. Kawajiri, *Genetic polymorphisms in the 5'-flanking region change transcriptional regulation of the human cytochrome P450IIE1 gene.* J Biochem, 1991. **110**(4): p. 559-65.
68. Purcell, S., et al., *PLINK: a tool set for whole-genome association and population-based linkage analyses.* Am J Hum Genet, 2007. **81**(3): p. 559-75.
69. Vrana, N.E., et al., *Engineering functional epithelium for regenerative medicine and in vitro organ models: a review.* Tissue Eng Part B Rev, 2013. **19**(6): p. 529-43.
70. Shenton, J.M., et al., *Characterization of a potential animal model of an idiosyncratic drug reaction: nevirapine-induced skin rash in the rat.* Chem Res Toxicol, 2003. **16**(9): p. 1078-89.
71. Shenton, J.M., et al., *Evidence of an immune-mediated mechanism for an idiosyncratic nevirapine-induced reaction in the female Brown Norway rat.* Chem Res Toxicol, 2005. **18**(12): p. 1799-813.
72. An, J., et al., *Drug rash with eosinophilia and systemic symptoms syndrome following cholestatic hepatitis A: a case report.* Korean J Hepatol, 2012. **18**(1): p. 84-8.
73. Tohyama, M., et al., *Association of human herpesvirus 6 reactivation with the flaring and severity of drug-induced hypersensitivity syndrome.* Br J Dermatol, 2007. **157**(5): p. 934-40.
74. Shiohara, T., et al., *Drug-induced hypersensitivity syndrome: recent advances in the diagnosis, pathogenesis and management.* Chem Immunol Allergy, 2012. **97**: p. 122-38.
75. Criado, P.R., et al., *Drug reaction with eosinophilia and systemic symptoms (DRESS): a complex interaction of drugs, viruses and the immune system.* Isr Med Assoc J, 2012. **14**(9): p. 577-82.
76. Shiohara, T., et al., *The diagnosis of a DRESS syndrome has been sufficiently established on the basis of typical clinical features and viral reactivations.* Br J Dermatol, 2007. **156**(5): p. 1083-4.
77. Barbaud, A., et al., *Comparison of cytokine gene polymorphism in drug-induced maculopapular eruption, urticaria and drug reaction with eosinophilia and systemic symptoms (DRESS).* J Eur Acad Dermatol Venereol, 2014. **28**(4): p. 491-9.
78. Power, S.E., et al., *Intestinal microbiota, diet and health.* Br J Nutr, 2014. **111**(3): p. 387-402.

79. David, L.A., et al., *Diet rapidly and reproducibly alters the human gut microbiome.* Nature, 2014. **505**(7484): p. 559-63.
80. Zimmer, J., et al., *A vegan or vegetarian diet substantially alters the human colonic faecal microbiota.* Eur J Clin Nutr, 2012. **66**(1): p. 53-60.
81. Walker, A.W., et al., *Dominant and diet-responsive groups of bacteria within the human colonic microbiota.* ISME J, 2011. **5**(2): p. 220-30.
82. Nermes, M., et al., *Interaction of orally administered Lactobacillus rhamnosus GG with skin and gut microbiota and humoral immunity in infants with atopic dermatitis.* Clin Exp Allergy, 2011. **41**(3): p. 370-7.
83. Laird, P.W., *Principles and challenges of genomewide DNA methylation analysis.* Nat Rev Genet, 2010. **11**(3): p. 191-203.
84. Licatalosi, D.D. and R.B. Darnell, *RNA processing and its regulation: global insights into biological networks.* Nat Rev Genet, 2010. **11**(1): p. 75-87.
85. Metzker, M.L., *Sequencing technologies - the next generation.* Nat Rev Genet, 2010. **11**(1): p. 31-46.
86. Farnham, P.J., *Insights from genomic profiling of transcription factors.* Nat Rev Genet, 2009. **10**(9): p. 605-16.
87. Park, P.J., *ChIP-seq: advantages and challenges of a maturing technology.* Nat Rev Genet, 2009. **10**(10): p. 669-80.
88. Wang, Z., M. Gerstein, and M. Snyder, *RNA-Seq: a revolutionary tool for transcriptomics.* Nat Rev Genet, 2009. **10**(1): p. 57-63.
89. Beyer, A., S. Bandyopadhyay, and T. Ideker, *Integrating physical and genetic maps: from genomes to interaction networks.* Nat Rev Genet, 2007. **8**(9): p. 699-710.
90. Hawkins, R.D., G.C. Hon, and B. Ren, *Next-generation genomics: an integrative approach.* Nat Rev Genet, 2010. **11**(7): p. 476-86.
91. Parkinson, H., et al., *ArrayExpress update--an archive of microarray and high-throughput sequencing-based functional genomics experiments.* Nucleic Acids Res, 2011. **39**(Database issue): p. D1002-4.
92. Barrett, T., et al., *NCBI GEO: mining tens of millions of expression profiles--database and tools update.* Nucleic Acids Res, 2007. **35**(Database issue): p. D760-5.
93. Martens, L., et al., *PRIDE: the proteomics identifications database.* Proteomics, 2005. **5**(13): p. 3537-45.
94. Athey, B.D., et al., *tranSMART: An Open Source and Community-Driven Informatics and Data Sharing Platform for Clinical and Translational Research.* AMIA Jt Summits Transl Sci Proc, 2013. **2013**: p. 6-8.

Appendix

Plots show the staining of PBMCs with Annexin V and PI:

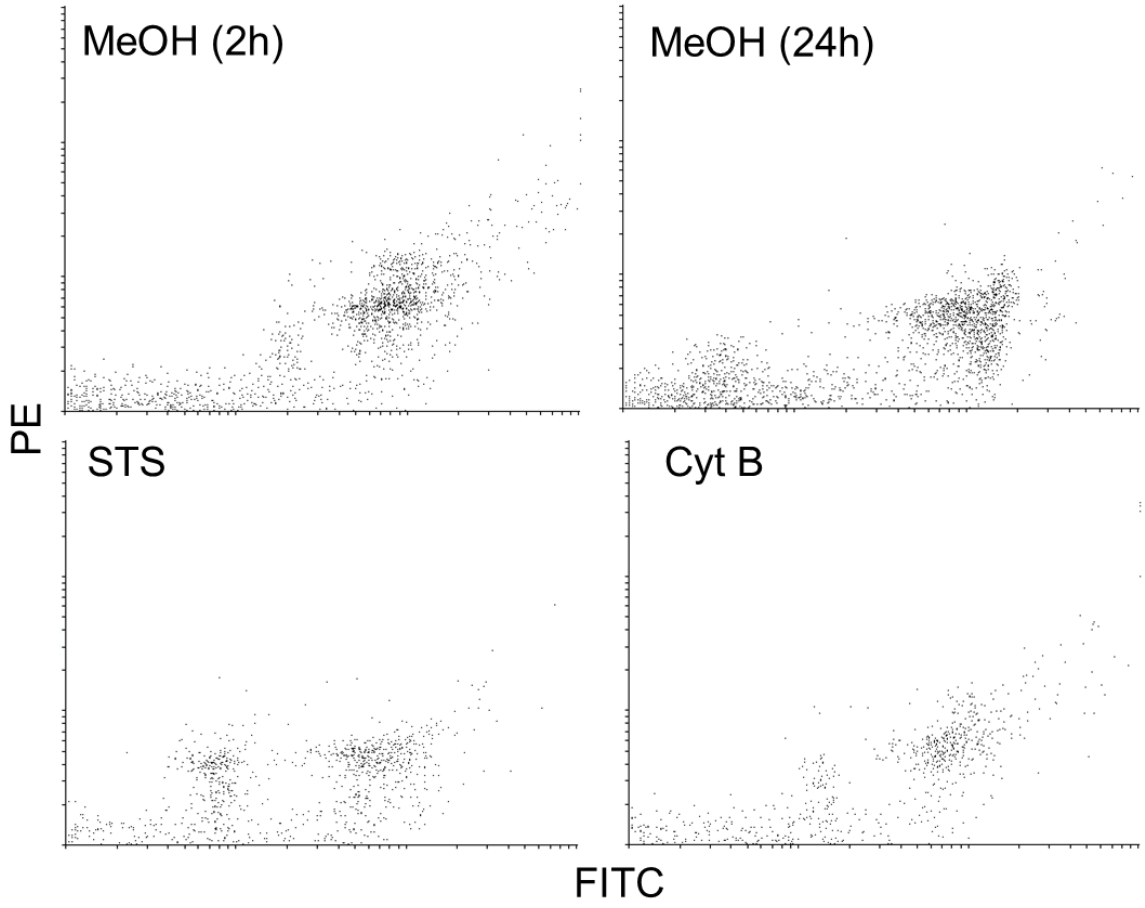

Figure A2.1: Staining of PBMCs with Annexin V and PI

The experiment was performed using PBMCs from one individual. PBMCs were exposed to Methanol (MeOH) 9-AC (50 µM) Staurosporine (STS, 4 µM), and Cytochalasin B (CytB, 50 µM) for 2 or 24 h. Samples were measured in flow cytometer.

Plots show the triple staining of PBMCs with Annexin V, PI, and a $CD3^+$ specific, florescent antibody:

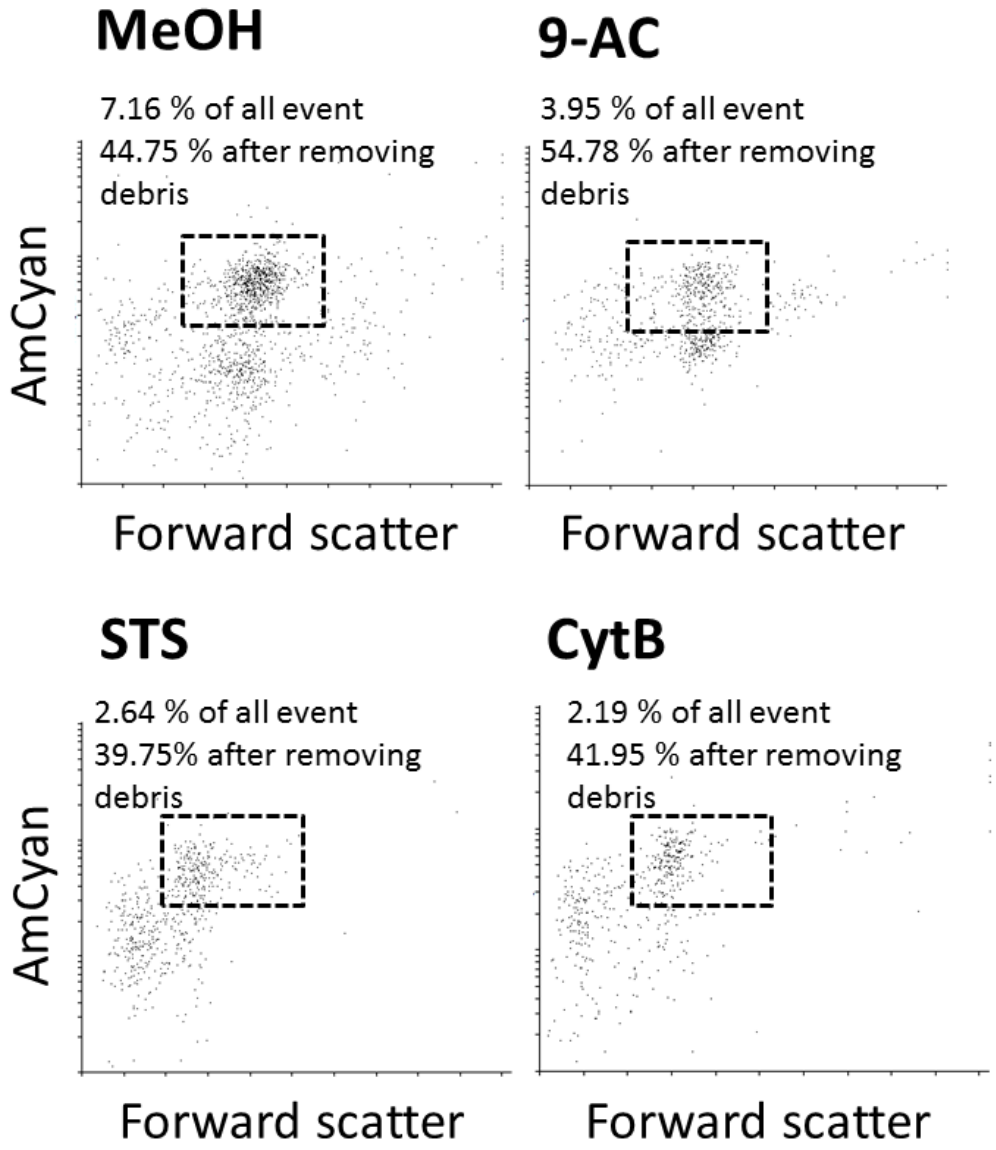

Figure A2.2: Triple staining of PBMCs with Annexin V, PI, and T-cell specific, fluorescent antibody $CD3^+$

The experiment was performed using PBMCs from one individual. PBMCs were exposed to Methanol (MeOH) 9-AC (50 µM) Staurosporine (STS, 4 µM), and Cytochalasin B (CytB, 50 µM) for 2 hours. The medium was replaced after 2 hours with fresh, drug-free medium for the rest of the 24 hours. After 24 hours of incubation, cells were stained with Annexin V and PI and the T-cell antibody. Samples were measured in flow cytometer.

Exposure of PBMCs to CBZ and 9-AC in RPMI-1640 media containing 10% foetal calve serum and 2 mM L-glutamine obtained from Invitrogen Ltd (Paisley, UK). For further description of the experimental setup see chapter 2.

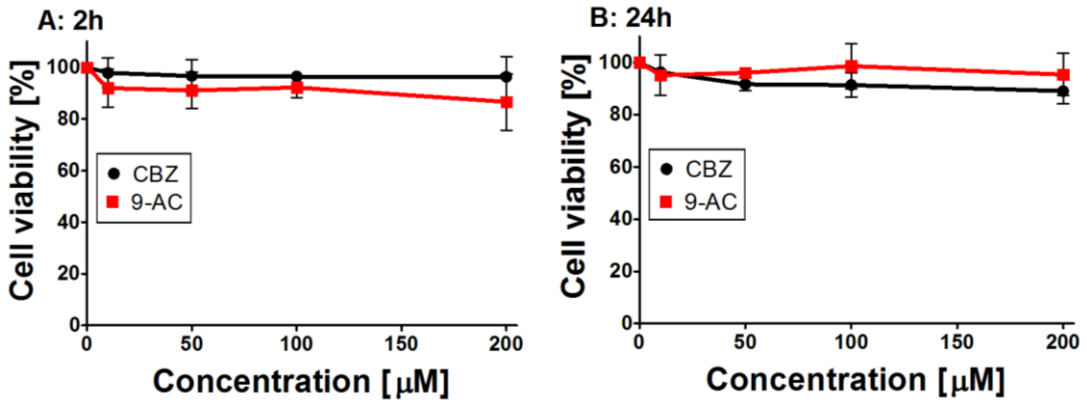

Figure A2.3: Cell viability of PBMCs exposed to CBZ and 9-AC in RPMI-1640

PBMCs were exposed to different concentrations of CBZ and 9-AC for 2 hours (**A**) and 24 hours (**B**).

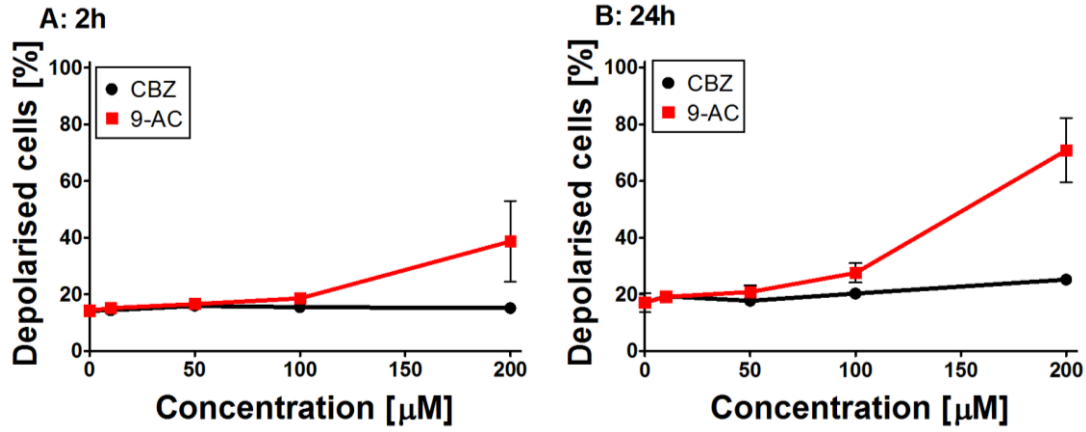

Figure A2.4: Mitochondrial depolarisation of PBMCs exposed to CBZ and 9-AC in RPMI-1640

PBMCs were exposed to different concentrations of CBZ and 9-AC for 2 hours (**A**) and 24 hours (**B**).

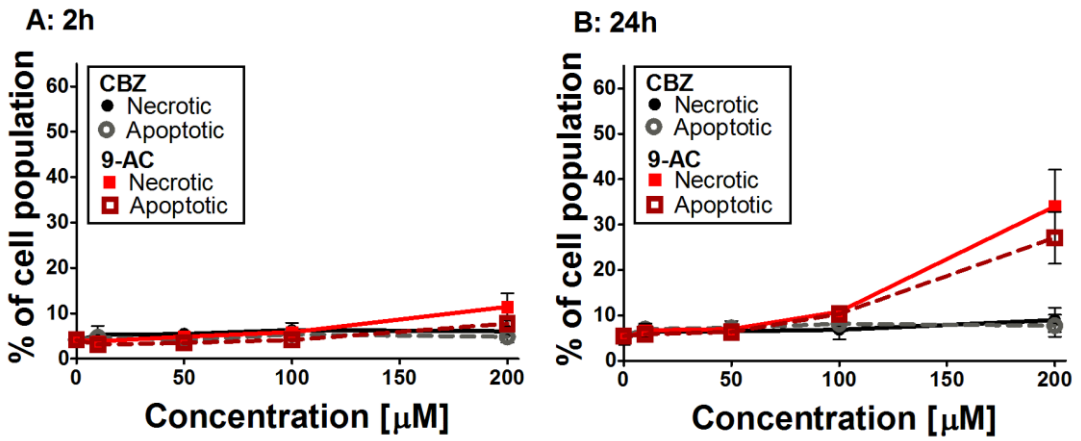

Figure A2.5: Measuring and apoptotic and necrotic cells of PBMCs exposed to CBZ and 9-AC in RPMI-1640

PBMCs were exposed to different concentrations of CBZ and 9-AC for 2 hours (**A**) and 24 hours (**B**).

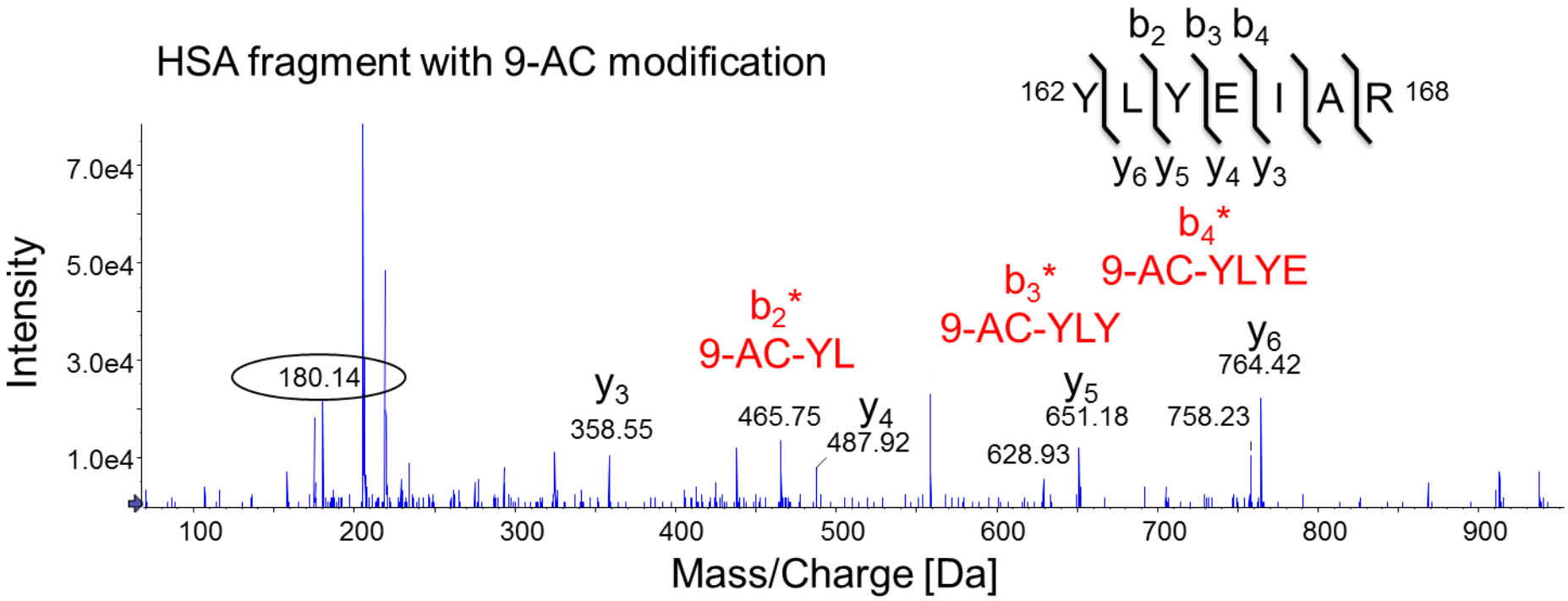

Figure A3.1: Identification of HSA residue modified by 9-AC

MS/MS spectrum showing 9-AC-modified tryptic peptide Y*LYEIAR with adduct of Tyr162 and 9-AC. HSA was reacted with CBZE i*n vitro* with a 25:1 protein: compound ratio for 24 hours. The encircled mass peak shows a characteristic fragment ion of 9-AC.

Table A4.1: Samples used for DUOX1 rs16939743 genotyping

Ctrl: control, MPE: maculopapular exanthema, AGEP: acute generalised exanthematous pustulosis, DRESS: drug reaction with eosinophilia and systemic syndromes SJS/TEN: Stevens-Johnson syndrome and/or toxic epidermal necrolysis, NK: not known

Sample ID	DUOX1 allele	Phenotype	Ethnicity
C001	TT	exposed ctrl	WHITE
C002	TT	exposed ctrl	WHITE
C003	TT	exposed ctrl	WHITE
C004	TT	exposed ctrl	WHITE
C005	TT	exposed ctrl	WHITE
C006	TT	exposed ctrl	WHITE
C007	TT	exposed ctrl	WHITE
C008	TT	exposed ctrl	WHITE
C009	TT	exposed ctrl	WHITE
C010	TT	exposed ctrl	WHITE
C011	TT	exposed ctrl	WHITE
C012	TT	exposed ctrl	WHITE
C013	TT	exposed ctrl	WHITE
C014	TT	exposed ctrl	WHITE
C015	TT	exposed ctrl	WHITE
C016	TT	exposed ctrl	WHITE
C017	TT	exposed ctrl	WHITE
C018	TT	exposed ctrl	WHITE
C019	TT	exposed ctrl	WHITE
C020	TT	exposed ctrl	WHITE
C021	TT	exposed ctrl	WHITE
C022	TT	exposed ctrl	WHITE
C023	TT	exposed ctrl	WHITE
C024	TT	exposed ctrl	WHITE
C025	TT	exposed ctrl	WHITE
C026	TT	exposed ctrl	WHITE
C027	TT	exposed ctrl	WHITE
C028	TT	exposed ctrl	WHITE
C029	TT	exposed ctrl	WHITE
C030	TT	exposed ctrl	WHITE
C031	TC	exposed ctrl	WHITE
C032	TT	exposed ctrl	WHITE
C033	TT	exposed ctrl	WHITE
C034	TT	exposed ctrl	WHITE
C035	TT	exposed ctrl	WHITE
C036	TT	exposed ctrl	WHITE
C037	TT	exposed ctrl	WHITE
C038	TT	exposed ctrl	WHITE
C039	TT	exposed ctrl	WHITE

C040	TT	exposed ctrl	WHITE
C041	TT	exposed ctrl	WHITE
C042	TT	exposed ctrl	WHITE
C043	TT	exposed ctrl	WHITE
C044	TT	exposed ctrl	WHITE
Greek	TT	SJS/TEN	WHITE
H001	TC	DRESS	White, but outlier in WGS
H002	TT	SJS	WHITE
H004	TT	DRESS	WHITE
H005	TT	MPE	WHITE
H006	TT	DRESS	WHITE
H010	TT	MPE	WHITE
H011	TT	MPE	WHITE
H017	TT	MPE	WHITE
H020	TT	DRESS	WHITE
H021	TT	DRESS	WHITE
H022	TT	MPE	WHITE
H023	TT	MPE	WHITE
H025	TT	DRESS	WHITE
H026	TT	MPE	WHITE
H027	TT	MPE	WHITE
H028	TT	MPE	WHITE
H029	TT	MPE	WHITE
H031	TT	MPE	WHITE
H033	TT	MPE	WHITE
H034	TT	MPE	WHITE
H035	TT	MPE	WHITE
H036	TT	MPE	WHITE
H037	TT	MPE	WHITE
H038	TT	MPE	WHITE
H039	TT	MPE	WHITE
H040	TT	DRESS	WHITE
H041	TT	MPE	WHITE
H042	TT	MPE	WHITE
H043	TT	MPE	WHITE
H044	TT	MPE	WHITE
H046	TT	MPE	WHITE
H047	TT	DRESS	WHITE
H048	TT	MPE	WHITE
H049	TT	DRESS	WHITE
H050	TT	MPE	WHITE
H051	TT	MPE	WHITE
H052	TT	MPE	WHITE
H053	TT	MPE	WHITE
H054	TT	DRESS	WHITE
H055	TT	HSS/DRESS/DIHS	INDIAN

H056	TT	MPE	WHITE
H057	TT	MPE	WHITE
H058	TT	MPE	WHITE
H062	TT	MPE	WHITE
H063	TT	DRESS	WHITE
H064	TT	MPE	WHITE
H065	TT	MPE	WHITE
H066	TT	HSS/DRESS/DIHS	ASIAN - YEMENI
H068	TT	MPE	WHITE
H069	TT	MPE	WHITE
H070	TT	MPE	WHITE
H071	TT	DRESS	WHITE
H072	TT	DRESS	WHITE
H073	TT	TEN	WHITE
H074	TT	MPE	WHITE
H075	TT	MPE	WHITE
H076	TT	DRESS	WHITE
H077	TT	DRESS	WHITE
H080	TT	DRESS	WHITE
HUC_0002	TT	HSS/DRESS/DIHS	WHITE
HUC_0005	undetermined	HSS/DRESS/DIHS	WHITE
IUB_0012	undetermined	SJS	BLACK AFRICAN
LSC_0020	TT	SJS/TEN	WHITE
LSC_0034	TT	SJS	WHITE
LSC_0073	TT	SJS/TEN	PAKISTANI
LSC_0092	TT	SJS/TEN	WHITE
LSC_0093	TT	HSS/DRESS/DIHS	WHITE
LSC_0094	TT	SJS/TEN	WHITE
LSC_0095	TT	HSS/DRESS/DIHS	WHITE
N002a	TT	DRESS	WHITE
N006a	TT	DRESS	WHITE
N008a	TT	DRESS	WHITE
N011a	TT	DRESS	WHITE
N012a	TC	SJS	THAI-WHITE
RPH_0012	TC	TEN	THAI
RPH_0013	TT	TEN	VIETNAMESE
RPH_0046	undetermined	SJS	BLACK CARIBBEAN
ULP_0121	TT	SJS/TEN	WHITE
ULP_0125	TT	SJS/TEN	WHITE
UPP_0015	TT	AGEP	WHITE
UPP_0019	TT	SJS	WHITE
USP_0001	TT	SJS/TEN	MIXED: BLACK/WHITE/NK
USP_0002	TC	HSS/DRESS/DIHS	MIXED: WHITE/BLACK/BRAZILIAN INDIAN
USP_0003	TT	SJS/TEN	MIXED: BLACK/WHITE/NK

USP_0005	TT	HSS/DRESS/DIHS	MIXED: WHITE/BLACK/BRAZILIAN INDIAN
USP_0006	TT	HSS/DRESS/DIHS	WHITE
USP_0010	TT	HSS/DRESS/DIHS	WHITE
USP_0011	TT	HSS/DRESS/DIHS	MIXED: BLACK/WHITE/NK
USP_0012	TT	HSS/DRESS/DIHS	WHITE
USP_0013	TT	SJS/TEN	MIXED: WHITE/BLACK/BRAZILIAN INDIAN
USP_0014	TT	HSS/DRESS/DIHS	MIXED: WHITE/BRAZILIAN INDIAN
USP_0015	TT	SJS/TEN	WHITE
USP_0016	TT	SJS/TEN	WHITE
USP_0017	TT	HSS/DRESS/DIHS	WHITE
USP_0018	TT	HSS/DRESS/DIHS	MIXED: BLACK/WHITE
USP_0022	TT	HSS/DRESS/DIHS	MIXED: WHITE/BLACK/BRAZILIAN INDIAN
USP_0029	TT	SJS/TEN	WHITE
USP_0030	TT	SJS/TEN	MIXED: WHITE/NK
USP_0031	TT	HSS/DRESS/DIHS	MIXED: WHITE/NK
USP_0034	undetermined	HSS/DRESS/DIHS	MIXED: WHITE/BRAZILIAN INDIAN/NK
USP_0035	TC	SJS/TEN	WHITE
USP_0036	TT	SJS/TEN	WHITE/NK
USP_0037	TC	HSS/DRESS/DIHS	WHITE/BLACK/NK
USP_0040	TT	HSS/DRESS/DIHS	NK
USP_0044	TT	SJS/TEN	WHITE
USP_0045	TT	HSS/DRESS/DIHS	NK
USP_0046	TT	HSS/DRESS/DIHS	MIXED: WHITE/BLACK/BRAZILIAN INDIAN
USP_0048	TT	HSS/DRESS/DIHS	MIXED: BLACK/WHITE